Redox regulation of an AP-1-like transcription factor, YapA, in the fungal symbiont *Epichloë festucae*

A thesis presented in partial fulfilment of the requirements for the degree of

Doctor of Philosophy (PhD) in

Genetics

at Massey University, Manawatu,

New Zealand.

Gemma Maree Cartwright

2013

Abstract

Reactive oxygen species (ROS) are emerging as important regulators required for the successful establishment and maintenance of the mutualistic association between the fungal endophyte *Epichloë festucae* and its grass host *Lolium perenne* (perennial ryegrass). The generation of reactive oxygen species (ROS) by the fungal NADPH oxidase, NoxA, has previously been shown to regulate hyphal growth of *E. festucae in planta*, a result that has led to the hypothesis that fungal-produced ROS are key second messengers in the symbiosis. However, the highly reactive nature of these molecules dictates that cells possess efficient redox sensing mechanisms to maintain ROS homeostasis and prevent oxidative damage to cellular components such as DNA, lipids and proteins. The *Saccharomyces cerevisiae* Gpx3-Yap1 and *Schizosaccharomyces pombe* Tpx1-Pap1, two-component H_2O_2 sensors, serve as model redox relays for coordinating the cellular response to ROS. While proteins related to the Yap1 and Pap1 basic-leucine zipper (bZIP) transcription factors have been identified in a number of filamentous fungi, the components involved in the upstream regulation remain unclear. This thesis presents an investigation into the role of the *E. festucae* Yap1 homologue, YapA, and putative upstream activators GpxC and TpxA, homologues of Gpx3 and Tpx1, respectively, in responding to ROS. YapA is involved in responding to ROS generated at the wound site following inoculation into ryegrass seedlings. However, deletion of *yapA* did not impair fungal colonisation of the host, indicating functional redundancy in systems used by *E. festucae* to sense and respond to plant-produced ROS. In culture, deletion of *E. festucae yapA* renders the mutants sensitive to only a subset of ROS and this sensitivity is influenced by the stage of fungal development. In contrast to the H_2O_2-sensitive phenotype widely reported for fungi lacking the Yap1-like protein, the *E. festucae yapA* mutant maintains wild-type mycelial resistance to H_2O_2 but conidia of the *yapA* mutant are sensitive to H_2O_2. Using a degron-tagged GFP-CL1 as a reporter, we found YapA is required for the expression of the spore-specific catalase, *catA*. Moreover, YapA is activated by H_2O_2, through disulfide bond formation, independently of both GpxC and TpxA, suggesting a novel mechanism of regulation exists in *E. festucae*. This work provides a comprehensive analysis of the role and regulation of the AP-1 transcription factor pathway in a filamentous fungal species

Acknowledgements

In many ways a PhD is like running a marathon. At the beginning the task seems huge and the finish line an unimaginable distance away. With sheer determination and perseverance and most importantly a great support crew, the road to a doctoral degree becomes a challenging and rewarding journey.

Firstly thank you to my supervisor Prof. Barry Scott, who was there every step of the way, guiding and supporting. I am in awe of your depth of knowledge and seemingly limitless enthusiasm for my project. Thank you also to my co-supervisor Dr. Rosie Bradshaw for your encouragement and advice.

Ruth, you were the whole package. Your impeccable organisation and guidance got me off to a flying start in the lab. With your friendship and support I was able to enjoy, rather than endure, my PhD years. Arvina, thank you for keeping everything in the lab running so smoothly and always with a smile on your face.

To the post-docs in Scottbase lab, past and present, Yvonne, Tetsuya, Sarah, Carla, Conni, Matt and Sanjay. Thank you for always having time to answer my questions, discuss results and share the occasional moment of mirth. Sarah Brown, I must single you out for imparting the wisest words of all "It'll be fine". To the rest of you docs, pre-docs, under-docs and maybe someday-docs in the lab, Emma, Milena, Daniel, Will, Rola, Alex, Pip, Chris, Leonie and Yonathan. Thank you for the engaging discussions, friendship and fun. Thank you for always eating the cupcakes so dutifully, without complaint, even when the cupcake influx reached an all-time high in the later stages of the PhD.

To Doug, Jianyu and Jordan, at the MMIC (my second home). Thank you not only for your technical assistance and advice, but also for all the good times and laughter shared. To Ann, Cynthia, Katrina, Tara and Paul, thank you for keeping everything running like a well-oiled machine. To Dr. Andrew Sutherland-Smith, who assisted with the protein modelling and Dr. Murray Cox who assisted with the statistical analysis. Thank you for allowing me to explore subject areas I hadn't encountered since my undergraduate papers. To Carlene Starck, thank you for your mentoring and counseling. Talking to someone who had 'been there, done that' helped to get me through.

Thanks to the many of you who took the time to review and comment on this work. Your input has been invaluable.

To my non-science friends and running buddies, especially Andrena, thank you for keeping the balance.

To my Mum and Dad, I am incredibly thankful for all of the love, support and encouragement you have given me throughout the years. I want you to realise just how important you have been in getting me to where I am today.

To Iain, my rock, my role model, my number one. Thank you for being so awesome.

This research was supported by a Top Achiever Doctoral Scholarship from the Tertiary Education Commission and funding from the Lincoln Bio-Protection Centre of Research Excellence (CoRE).

Table of Contents

List of Figures

List of Tables

Abbreviations

aa	Amino acid
Aa	*Alternaria alternata*
Amp	Ampicillin
Amp^R	Ampicillin resistant
Ao	*Aspergillus oryzae*
Bc	*Botrytis cinerea*
BLAST	Basic local alignment search tool
BLASTn	Nucleotide database search using a nucleotide query
BLASTp	Protein database search using a protein query
bp	Base pair(s)
C	Cysteine
Ca	*Candida albicans*
c-CRD	C-terminal cysteine-rich domain
cDNA	Complementary DNA
CDS	Coding DNA sequence
CFW	Calcofluor white
Ch	*Cochliobolus heterostrophus*
CIAP	Calf intestinal phosphatase
C_P	Peroxidatic cysteine
Cp	*Claviceps purpurea*
C_R	Resolving cysteine
CRD	Cysteine-rich domain
Cys	Cysteine
DAPI	4′,6-diamidino-2-phenylindole
dATP	Deoxyadenine triphosphate
DEPC	Diethylpyrocarbonate
DIC	Differential interference contrast

DIG	Digoxigenin
DNA	Deoxyribonucleic acid
dNTP	Deoxynucleotide triphosphate
dpi	Days post inoculation
DsRed	Discosoma red fluorescent protein
EDTA	Ethylene diamine tetra-acetic acid
EGFP	Enhanced green fluorescent protein
EMSA	Electrophoretic mobility shift assays
Fg	*Fusarium graminearum*
FGI	Fungal Genome Initiative
Fo	*Fusarium oxysporum*
FS	Flanking sequence
g	Gram
gDNA	Genomic DNA
Gen^R	Geneticin resistant
GFP	Green fluorescent protein
GPx	Glutathione peroxidase
Grx	Glutaredoxin
GSH	Glutathione
GST	Glutathione S-transferase
h	Hour(s)
H_2O_2	Hydrogen peroxide
HK	Histidine kinase
Hph	Hygromycin phosphotransferase
Hpt	Histidine-containing phosphotransfer
HRP	Horse radish peroxidase
Hyg^R	Hygromycin resistant
IAA	Iodoacetamide
kb	Kilobase(s)

Kl	*Kluyveromyces lactis*
KO	Knock-out
LB	Luria-Bertani broth
µg	Microgram
µm	Micrometre
µM	Micromolar
µL	Microlitre
M	Molar
MAPK	Mitogen activated protein kinase
min	Minute(s)
mg	Milligram
Mg	*Magnaporthe grisea*
mL	Millilitre
mm	Millimeter
mM	Millimolar
Mo	*Magnaporthe oryzae*
mRNA	Messenger ribonucleic acid
NA	Numerical aperture
NADH	Nicotinamide adenine dinucleotide (reduced form)
NADPH	Nicotinamide adenine dinucleotide phosphate (reduced form)
NBT	Nitroblue tetrazolium
Nc	*Neurospora crassa*
NCBI	National Centre for Biotechnology Information
n-CRD	N-terminal cysteine-rich domain
ng	Nanogram
NO	Nitric oxide
Nox	NADPH oxidase
OM	Osmotic medium
OSR	Oxidative stress response

Pa	*Podospora anserina*
PAMP	Pathogen-associated molecular pattern
PCR	Polymerase chain reaction
PD	Potato dextrose
PEG	Polyethylene glycol
Phox	Phagocyte oxidase
pmol	Picomole
PMSF	Phenylmethylsulfonyl fluoride
Prx	Peroxiredoxin
PTP	Protein tyrosine phosphatase
RG	Regeneration
RNA	Ribonucleic acid
RNase	Ribonuclease
ROS	Reactive oxygen species
rpm	Revolutions per minute
RR	Response regulator
RT	Reverse transcriptase
RT-PCR	Reverse transcriptase-polymerase chain reaction
Sak	Stress-activated kinase
Sc	*Saccharomyces cerevisiae*
SC	Synthetic complete
SD	Synthetic defined
SDS	Sodium dodecyl sulfate
SDS-PAGE	Sodium dodecyl sulfate-polyacrylamide gel electrophoresis
SEM	Scanning electron microscopy
SLS	Sodium lauroyl sarcosine
SOD	Superoxide dismutase
Sp	*Schizosaccharomyces pombe*
Ss	*Sclerotinia sclerotiurum*

TBE	Tris-boric acid-EDTA
tBLASTn	Translated nucleotide database search using a protein query
TEF	Translation elongation factor
TEM	Transmission electron microscopy
Tpx	Thiol peroxidase
Trx	Thioredoxin
U	Unit
Um	*Ustilago maydis*
UTR	Untranslated region
UV	Ultraviolet
V	Volts
v/v	Volume/volume ratio
WGD	Whole genome duplication
WT	Wild-type
w/v	Weight/volume ratio
YE	Yeast extract
YRE	Yap1 response element
°C	Degrees Celsius

1 Introduction

1.1 Plant-fungal symbioses

Associations between plants and fungi are extremely common in nature and of great importance in both agriculture and natural ecosystems. A broad range of vascular plants, including grasses, harbour endophytic fungi which grow inter- or intracellularly, most commonly within aerial plant tissues (Saikkonen *et al*., 1998). Fungi of the family Clavicipitaceae (Ascomycota) are an important group of endophytes that colonise the intercellular spaces of grasses of the family Poaceae (Schardl *et al*., 2004). Clavicipitaceous endophytes colonise a broad range of host plants and these interactions may range from mutualistic through neutral to antagonistic. In an antagonistic relationship host seed production is completely suppressed, referred to as 'choke', whereas in mutualistic relationships endophytes remain asymptomatic and are seed-transmitted. The nature of the interaction varies depending on the endophyte-host genetic combination, and particular endophyte-host combinations may also vary spatially and temporally. In mutualistic symbioses the endophyte is disseminated through the seed, whereas in more antagonistic symbioses meiotic ascospores produced in external sexual reproductive structures (stromata) are responsible for the contagious dispersal to uninfected plants (Scott & Schardl, 1993). Interestingly, infection by *Epichloë festucae* symbionts can be pleiotropic, producing endophyte infected seeds and stromata on different tillers of the same host plant (Schardl *et al*., 2004).

1.1.1 Taxonomy

The *Epichloë* species and their close relatives, the *Neotyphodium* species, are members of the fungal phylum Ascomycota, order Hypocreales, family Clavicipitaceae, genus *Epichloë* (Schardl, 2010). Ascomycota is the largest phylum in the fungal kingdom and contains diverse members such as model yeast species, *Saccharomyces cerevisiae* and *Schizosaccharomyces pombe*, model filamentous species, *Aspergillus nidulans* and *Neurospora crassa,* as well as many plant pathogens including *Magnaporthe oryzae* and *Fusarium oxysporum.* The defining feature of the Ascomycota is the 'ascus', a microscopic saclike structure in which sexual spores called ascospores are formed (James *et al*., 2006). However, some species of the Ascomycota (e.g. *Neotyphodium lolii*) are asexual and thus do not form asci or ascospores. The formation of asci around meiotic spores distinguishes Ascomycetes from the Basidiomycetes, the second largest phylum of fungi, where members characteristically produce spores externally, on the end of specialised cells called basidia (James *et al*., 2006). The Clavicipitaceae contain numerous species that are mutualistic or pathogenic symbionts of plants or pathogens of insects or other fungi

(Kuldau *et al.*, 1997). Within the Clavicipitaceous family of fungi is the grass-associated subfamily Clavicipitoideae, which includes *Claviceps*, *Balansia*, and *Epichloë* species (Sung *et al.*, 2007). *Epichloë* species are symbiotic with grasses of the subfamily *Poöideae* within the Poaceae grass family. Molecular phylogenetic analysis groups the ten known *Epichloë* species into two distinct clades: the main clade, containing *E. festucae, E. amarillans, E. baconii, E. bromicola, E. elymi, E. glyceriae* and *E. brachyelytri,* and a second clade, designated the *Epichloë typhina* complex, containing *E. typina*, *E. clarkii* and *E. sylvatica* (Clay & Schardl, 2002). *Epichloë* endophytes only infect grasses of the subfamily *Poöideae.* However, there is much variation in host-endophyte specificity within these groupings. *Epichloë festucae* mainly associates with *Festuca* and *Lolium* species and similarly, other *Epichloë* species display a relatively limited host range. In contrast, *E. typhina* has a broad host range that includes several grasses that belong to the Poeae and Brachypodieae tribes of the Pooideae subfamily (Schardl, 2010).

1.1.2 Lifecycle

The symbiotic interaction between *E. festucae* and its grass host shifts along the mutualism-antagonism continuum depending on the particular grass host and its physiological state and stage of development (Michalakis *et al.*, 1992). *E. festucae* naturally colonises *Festuca rubra* (red fescue) but the existence of isolates from different *Festucae* and *Lolium* grasses indicates a relatively wide host range within the subfamily Pooideae (Figure 1.1; (Christensen *et al.*, 2002, Leuchtmann *et al.*, 1994, Moon *et al.*, 1999, Schardl *et al.*, 1994). When the grass host is in the vegetative state, endophytic hyphae asymptomatically colonise the intercellular spaces of aerial plant tissues such as the leaf sheaths and blades. As the plant enters the reproductive phase of growth, the endophyte can grow into the developing seed head and colonise the new seeds and is thus transmitted vertically to the next generation of host (asexual life cycle).

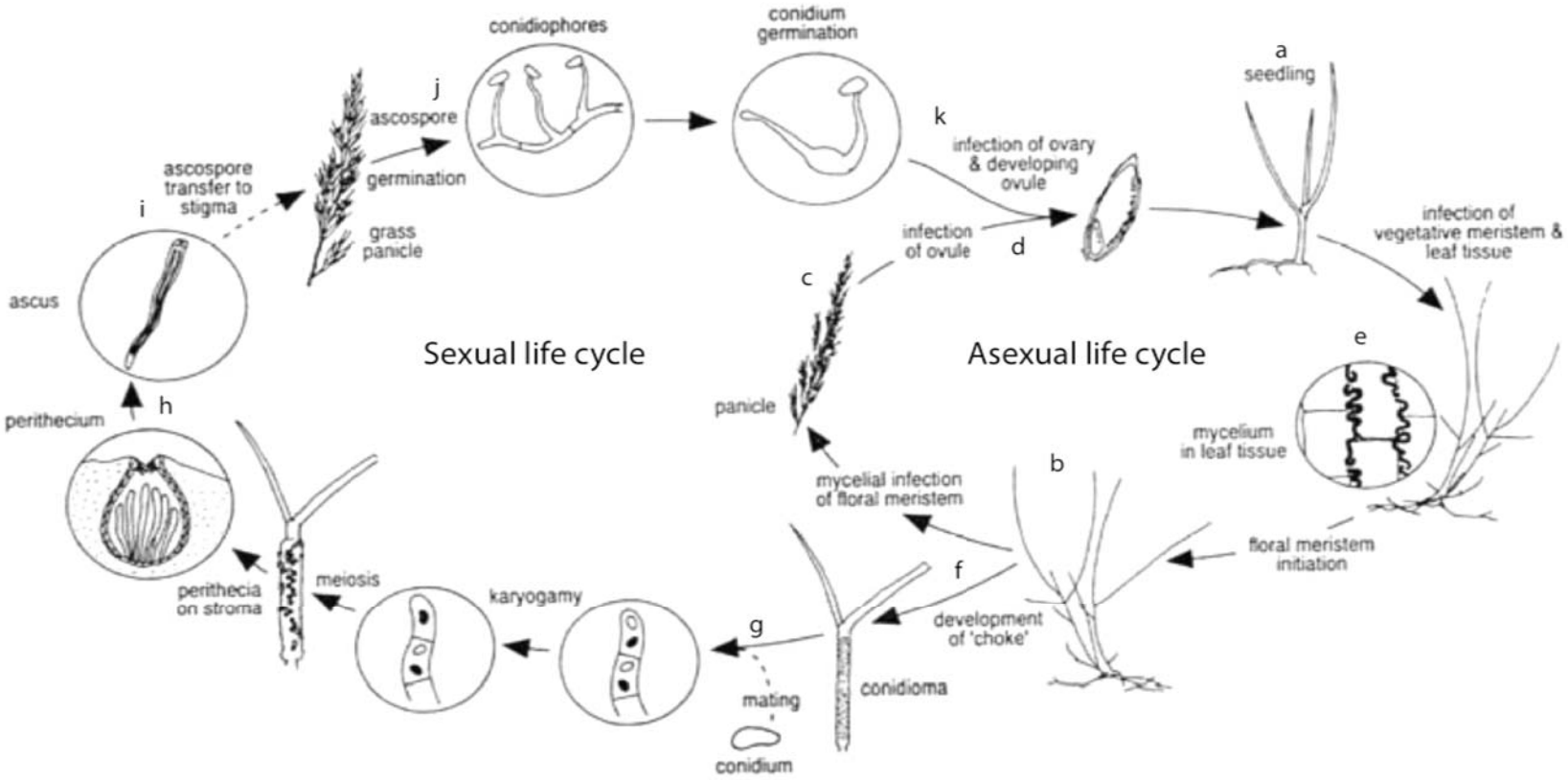

Figure 1.1 The *Epichloë* endophyte lifecycle. Fungal structures are shown in circles. In the asexual cycle hyphae grow intercellularly in leaf sheaths (a), floral meristems (b), and in the ovules of the florets (c) such that the fungus is transmitted by seeds to the next generation of the host (d). In the sexual cycle the fungus also grows asymptomatically within the vegetative leaf sheaths (e), but then produces mycelial stromata that develop on emerging inflorescences, preventing seed production (a process known as "choke disease") (f). Fertilisation is achieved when spermatia from one stroma are transferred to another of the opposite mating type (g). Fertilised stromata produce perithecia containing ascospores that are ejected (h) and may infect uninfected plants (i). Germinating ascospores on host florets (j) cause new infections of developing seeds (k). Diagram prepared by L. Grant.

Alternatively, in some tillers the endophyte exits its internal environment and proliferates externally forming stromata. On the stromata, the sexual stage is initiated. Meiotic ascospores, which are formed in perithecia after stroma fertilisation by conidia of the opposite mating type, serve as a means for horizontal transmission to new host plants (Figure 1.1; (Chung & Schardl, 1997, Clay & Schardl, 2002). *Neotyphodium lolii*, the asexual derivate of *E. festucae,* does not produce stromata and can only be vertically transmitted within the seeds of its host. Vertical transmission is also the predominant mode of infection by *E. festucae*. Only rarely do *E. festucae*-infected *F. rubra* plants develop choke stromata and, to date, there have been no reports of choke in associations between *E. festucae* and perennial ryegrass. During host flowering, fungi in the asexual state grow from the vegetative apex into the inflorescence primordium and floral apices to infect the ovules and seeds. After fertilisation, the ovule enlarges and develops into a mature seed containing the embryo. The endophyte enters the embryo and, as it matures, the fungus proliferates, resulting in colonisation of the embryo and associated tissues including the plumule apex, embryo axis, the aleurone layer, and between the scutellum and the endosperm. During seed germination, hyphae colonise the developing shoot apex. Hyphae also extend from the shoot apical meristem (SAM) of the vegetative apex into the leaf primordium, colonizing the leaf sheaths and blades as they develop (May *et al.*, 2008).

1.1.3 The Epichloë endophyte-grass symbiosis

Phylogenetic analysis has revealed that most *Neotyphodium* spp. are interspecific hybrids arising from two, or rarely, more parental *Epichloë* or *Neotyphodium* species. While most of the asexual *Neotyphodium spp.* are inter-specific hybrids, *N. lolii* is one of the few exceptions that appears to be a direct haploid derivative of *E. festucae* (Moon *et al.*, 2004). *E. festucae* and *N. lolii* interact mutualistically with their hosts; the host provides the fungus with shelter and access to nutrients and, in return, the fungus confers tolerance to both biotic (insect and mammalian herbivory) and abiotic (drought) stresses (Schardl *et al*., 2004). The most well documented benefit for the grass host is protection from insect herbivory by *E. festucae* through synthesis of peramine, a novel pyrrolopyrazine metabolite (Rowan *et al*., 1990, Tanaka *et al*., 2005a, Schardl *et al*., 2007, Wilkinson *et al*., 2000), or lolines, which are saturated pyrrolizidines (Schardl *et al*., 2007, Wilkinson *et al*., 2000). *E. festucae* naturally colonises fine (*F. rubra*) and hard (*F. longifolia*) fescues but is also capable of forming stable mutualistic interactions with perennial ryegrass, *Lolium perenne* (Christensen *et al*., 2002, Moon *et al*., 1999, Schardl *et al*., 2009). The comparative ease with which *L. perenne* plants can be inoculated and grown has led to the adoption of the *E. festucae – L. perenne* partnership as a model experimental system for studying fungal-grass symbioses (Schardl *et al*., 2007).

E. festucae and *N. lolii* systemically colonise the vegetative and reproductive aerial tissues of grasses but do not infect the roots. The growth of these fungi in the intercellular spaces of the leaves is highly coordinated and the hyphae are intimately associated with the host plant cells, suggesting biochemical communication between the endophyte and host. Thus it is a superb system in which to explore the signalling mechanisms and cellular pathways involved in host-symbiont communication and growth regulation.

Involvement of an NADPH oxidase in the E. festucae-L. perenne symbiosis

In recent years molecular genetic techniques have enabled researchers to identify and characterise *E. festucae* genes involved in establishing and maintaining this highly restricted association with its grass host, *L. perenne*. A plasmid insertional mutagenesis screen performed by Tanaka *et al*. (2006) identified an *E. festucae* mutant with a disruption in the *noxA* gene encoding an NADPH oxidase. Disruption of this single fungal gene has a profound effect on the endophyte-host plant interaction; ryegrass plants infected with the *noxA* mutant become stunted and undergo premature senescence (Tanaka *et al*., 2006). Within infected plants the *noxA* mutant shows proliferative hyphal growth contrasting with the highly restricted growth usually observed in wild-type *E. festucae-L. perenne* associations.

NADPH oxidases are multi-subunit membrane-bound enzyme complexes, which primarily function to catalyse the transfer of electrons from NADPH to molecular oxygen (O_2) resulting in the generation of the reactive oxygen species superoxide ($O_2^{\bullet-}$). Other ROS are derived from $O_2^{\bullet-}$ through its sequential detoxification (Figure 1.2). Disruption of a NADPH oxidase enzyme would be expected to impair ROS production, and indeed the *noxA* mutant shows a defect in the production of ROS in culture and *in planta*. This strongly indicates a role for ROS in regulating the symbiotic association between *E. festucae* and perennial ryegrass and is in line with recent research which demonstrates unequivocally that ROS are not only toxic byproducts of aerobic metabolism but also central players in cell signalling (Finkel, 2011, Tanaka *et al*., 2006).

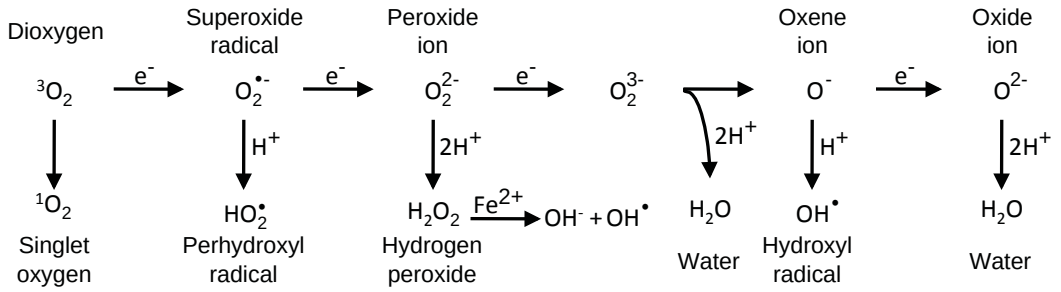

Figure 1.2. Generation of ROS from oxygen. Energy transfer or sequential univalent reduction of ground state triplet oxygen leads to formation of various ROS. In the presence of ferrous iron (Fe^{2+}) H_2O_2 forms the hydroxyl radical ($OH^{\bullet}$) via the Fenton reaction. Adapted from Apel & Hirt (2004).

1.1.4 ROS production in plant-fungal interactions

Fungal production of ROS

The involvement of NADPH oxidase-generated ROS in both mutualistic and antagonistic plant-fungal associations is a widespread occurrence. When *Botrytis cinerea,* a necrotrophic fungus, infects its host plant, an accumulation of ROS, thought to be of fungal origin, is observed within and surrounding fungal hyphae. Although both *bcnoxA* and *bcnoxB* mutants are impaired in pathogenicity, ROS production is not compromised in either mutant suggesting alternative ROS generating systems may compensate (Segmuller *et al.*, 2008). Deletion of either *nox1* or *nox2* in the rice blast fungus *Magnaporthe grisea* results in an even more severe pathogenicity defect with the apathogenicity of the mutants attributed to an impairment of appressorium-mediated cuticle penetration. Surprisingly, ROS levels in these mutants are elevated in culture, again suggesting a compensatory mechanism (Egan *et al.*, 2007). Deletion of the *cpnox1* gene in the biotrophic fungus *Claviceps purpurea* impairs infection of its plant host, however, deletion of the second *nox* gene, *cpnox2*, conversely results in an enhanced plant infection phenotype (Giesbert *et al.*, 2008). These studies highlight the central and complex involvement of NADPH oxidase-catalysed ROS in fungal-plant interactions. The contribution of ROS from the plant host must also be given important consideration, particularly in pathogenic interactions. Both pathogen-associated molecular pattern (PAMP) recognition and wounding responses result in plant production of ROS at the infection site.

Plant production of ROS

ROS of plant origin plays a key role in host defence against pathogens. Mechanical damage, such as that caused by insects and grazing herbivores, has been shown to stimulate the production of H_2O_2 in plants. This rapid and transient overproduction of ROS is referred to as the 'oxidative burst', and the ensuing localised host cell death contributes to the limitation of pathogen spread (Doke, 1983). While this defence response is effective towards biotrophs, which depend on living plant cells for development of disease, it may not impede necrotrophs, which grow by utilizing dead plant tissue (Govrin & Levine, 2000, Levine *et al.*, 1994). Furthermore, the wound-induced ROS is directly toxic to microbial invaders including bacteria, fungi and viral pathogens, which may infect through the wounded plant tissues.

Several enzymes have been implicated in plant ROS production following successful pathogen recognition and wounding, including NADPH oxidases, peroxidases and other oxidase enzymes (Le Deunff *et al.*, 2004, Torres *et al.*, 2006). Using chemical inhibitors of the NADPH oxidase complex, this enzyme complex has been shown to be implicated in the production of ROS and the induction of expression of several defence genes in response to mechanical wounding of tomato leaves. The presence of H_2O_2 in wounded as well as distal unwounded leaves supports a role for H_2O_2 as a signalling molecule. However the targets of H_2O_2 remain unclear. H_2O_2 also exerts a protective effect in response to wounding by mediating oxidative cross-linking of cell wall structural proteins, thus strengthening the cell wall and imposing a physical barrier against attempted pathogen penetration (Bradley *et al.*, 1992). Physical wounding of *L. perenne* leaf blades results in biphasic H_2O_2 production. An initial, transient and intense burst of ROS occurs almost immediately after wounding and is comprised of both $O_2^{\bullet -}$ and superoxide dismutase-generated H_2O_2. A second wave of H_2O_2 is observed several hours later and is most likely formed by the action of germin oxalate oxidase (G-OXO) enzymes which generate H_2O_2 from the oxidative breakdown of oxalate (Le Deunff *et al.*, 2004, Berna & Bernier, 1999, Zhang *et al.*, 1995). Increased activity of oxalate oxidase in response to pathogen attack has also been reported in wheat and barley, and thus, through the production of H_2O_2, oxalate oxidase represents another class of enzymes involved in the plant defence response (Berna & Bernier, 1999, Zhang *et al.*, 1995). From a biological perspective, the two-stage production of H_2O_2 in response to physical injury is a strategy employed by the plant to cope with wounding effectively, first providing a defence system against the damaging agent, i.e. herbivorous predators, and secondly allowing the plant to prepare for subsequent pathogen attack. Biphasic ROS accumulation is also observed in plants challenged by pathogens (Lamb & Dixon, 1997). The first phase of ROS production is

non-specific and occurs immediately after an attack by a virulent or avirulent pathogen. The second, greatly heightened phase of ROS accumulation, is associated only with avirulent pathogens and, given the delay in the response, may involve specific changes in gene expression of ROS-generating enzymes.

When investigating the role of ROS in the mutualistic *E. festucae-L. perenne* interaction the contribution from both the endophyte and the plant host must be considered. Furthermore, it is important to appreciate that ROS is an all-encompassing term for a wide range of oxygen-derived molecules and also that ROS are not only generated enzymatically but also produced non-enzymatically as a byproduct of aerobic metabolism.

1.2 Reactive Oxygen Species (ROS): production and detoxification

Reactive oxygen species (ROS), as their name suggests, are highly reactive molecules derived from oxygen. While O_2 is a relatively stable molecule, it is also a free radical, because it has two unpaired electrons with parallel spins in its outer p orbital. This electronic configuration makes oxygen susceptible to one e^- transfer reactions and leads to the formation of oxygen radicals or ROS, including superoxide ($O_2^{\bullet -}$), hydrogen peroxide (H_2O_2) and hydroxyl radicals (Figure 1.2). Additionally, energetic excitation of ground state oxygen ($^3O_2$) generates singlet oxygen ($^1O_2$), a highly reactive, non-radical form of oxygen. Ferrous iron (Fe^{2+}) catalyzes hydroxyl radical ($OH^{\bullet}$) formation from hydrogen peroxide. (Figure 1.2) (Apel & Hirt, 2004, Cadenas, 1989)

1.2.1 The Species

Oxyradicals

Oxygen-derived radicals or 'oxyradicals' are generally considered highly reactive and therefore short-lived due to the presence of unpaired electrons. However, more stable radicals include molecular dioxygen (O_2) and nitric oxide (NO). The hydroxyl radical is so reactive it will typically react indiscriminately with cellular components very close to its site of formation (Winterbourn & Hampton, 2008).

Superoxide

$O_2^{\bullet-}$ is the first reduction product of ground state oxygen and the primary species generated by the NADPH oxidase (Nox) and electron leakage from the mitochondrial electron transport chain. Although $O_2^{\bullet-}$ reacts with thiols, particularly low molecular weight thiols such as glutathione and cysteine, these reactions are typically out-competed by the reaction of $O_2^{\bullet-}$ with the superoxide-quenching superoxide dismutase and ascorbic acid (Winterbourn & Hampton, 2008). A signalling role for $O_2^{\bullet-}$ has been shown in both eukaryotes and prokaryotes. Hawkins *et al*. (2007) demonstrated that extracellular $O_2^{\bullet-}$ flux across pulmonary endothelial cell membranes is mediated by the chloride channel-3 (ClC-3) and stimulates intracellular signalling events including Ca^{2+} release and mitochondrial $O_2^{\bullet-}$ generation, further propagating the redox signal leading to apoptosis. In prokaryotes, $O_2^{\bullet-}$ has been shown to have a second messenger role, targeting the 2Fe-2S iron-sulfur clusters of the *E. coli* SoxR transcriptional regulator. Upon reversible reduction of the cluster, SoxR loses its transcriptional activity, thereby reversibly modulating gene expression (Hidalgo & Demple, 1994, Hidalgo *et al.*, 1997, Timmermann *et al.*, 2010, Winterbourn & Hampton, 2008).

Hydrogen peroxide

H_2O_2 is the dismutation product of $O_2^{\bullet-}$ and, unlike $O_2^{\bullet-}$, is neutral and membrane-permeable. Thus it is particularly suited to serve as a signalling molecule. In mammalian cells, the transport of H_2O_2 across the plasma membrane is mediated by specific aquaporin channels. However, this does not appear to be a universal mechanism regulating H_2O_2 uptake as inhibition of aquaporin channels in *S. cerevisiae* cells did not affect H_2O_2 permeability (Folmer *et al.*, 2008, Miller *et al.*, 2010). H_2O_2 is not a free radical as it has no unpaired electrons, in contrast to $O_2^{\bullet-}$ and the hydroxyl radical, and so is comparatively a less reactive and less damaging species. H_2O_2 does, however, readily react with thiols. Thiol peroxidases Gpx3 of *S. cerevisiae* and Tpx1 of *S. pombe* are two well-characterised H_2O_2 targets, which directly sense H_2O_2 via specific cysteine thiol groups and, in response to H_2O_2, activate downstream signalling components (Delaunay *et al.*, 2002, Vivancos *et al.*, 2005). Additionally, in the presence of iron H_2O_2 can further form hydroxyl radicals via the Fenton reaction (Halliwell & Gutteridge, 1992).

Reactive nitrogen species (RNS)

NO is a short-lived and membrane-permeable molecule generated from O_2 and L-arginine by specialised NO synthases (Guzik *et al.*, 2003). NO can produce different

protein modifications, including nitrosylation of metal and thiol groups and nitration of tyrosine residues, and is therefore capable of mediating redox-sensitive signal transduction. Like superoxide, nitric oxide appears to play a signalling role in vascular endothelial cells in mammalian systems. Superoxide and nitric oxide react rapidly *in vivo* to form peroxynitrite ($ONOO^-$) (Guzik *et al*., 2003). Peroxynitrite readily reacts with thiol groups of proteins, particularly cysteine thiols, and Ogusucu *et al*. (2007) demonstrated that *in vitro, S. cerevisiae* peroxiredoxins Tsa1 and Tsa2 react with peroxynitrite, which may permit signalling in much the same way as H_2O_2-mediated signalling by thiol peroxidases.

1.2.2 Cellular effects of ROS

ROS, as the name implies, are highly reactive and inherently indiscriminate and thus potentially damaging to cellular components such as DNA, RNA, proteins, and lipids. ROS can attack both the nucleic acid bases and sugar phosphate backbone of DNA and RNA. This has multiple consequences for the DNA, including single- and double-strand breaks, DNA cross-linking, base modifications and formation of DNA-protein adducts. If not repaired, these changes can lead to mutations and block key processes such as replication and transcription. Similarly, ROS can also damage RNA affecting processes such as protein synthesis as well as interfering with the functions of non-coding RNA molecules (Cabiscol *et al.*, 2000). ROS can react with various lipid components in cellular and organellar membranes causing lipid peroxidation (Avery, 2011). Peroxidised membranes display altered fluidity and permeability and a disruption in membrane-associated proteins (Avery, 2011). The effect of ROS on proteins is primarily due to the various modifications of amino acid side chains. Sulfur-containing residues, cysteine and methionine, are particularly susceptible to oxidation by ROS. Oxidation of cysteine sulfhydryl groups (SH) leads to the formation of disulfide bonds (SS) producing either intramolecular (P_1SSP_1) or intermolecular (P_1SSP_2) protein cross-linked derivatives. These modifications ultimately alter protein structure and function, which can have serious consequences for the cell (Avery, 2011). However, mildly oxidised proteins are very susceptible to proteolytic degradation, a property that offers the cell a 'second chance' at coping with the oxidative damage that occurs to protein substrates (Cabiscol *et al*., 2000).

Generation of ROS

Incidental ROS generation

Inherent to their aerobic lifestyles, both prokaryotic and eukaryotic organisms generate ROS intracellularly. Typically, mitochondria are considered a major source of cellular ROS due to the leakage of electrons from complexes in the mitochondrial electron transport chain to oxygen to form $O_2^{\bullet-}$. Often overlooked, peroxisomes, in most eukaryotic organisms, and chloroplasts, in photosynthetic organisms, also play a significant role in the generation of ROS. H_2O_2 is produced by a number of peroxisomal oxidases and, more recently, it has been demonstrated that $O_2^{\bullet-}$ and nitric oxide (NO) radicals are also produced in peroxisomes (del Rio *et al*., 2002). In plants, a proportion of photosynthesis-derived oxygen is reduced by electrons passing through the photosystems generating $O_2^{\bullet-}$, which is then converted to H_2O_2 by a CuZn superoxide dismutase enzyme (Apel & Hirt, 2004).

Enzyme-generated ROS

In addition to the ROS produced as by-products of cellular metabolic pathways, ROS can be derived from a number of enzymes including xanthine oxidase, oxygenases, peroxidases, NO synthase and NADPH oxidases (Apel & Hirt, 2004), with the latter being arguably the most important system for regulated ROS production. Members of the NADPH oxidase superfamily are widely distributed amongst all eukaryotic kingdoms: animals, plants, fungi and protists (Sumimoto, 2008). The well-characterised mammalian Nox complex responsible for the phagocytic oxidative burst is comprised of a catalytic subunit gp91phox (Nox2) and regulatory subunits p22phox, p40phox, p47phox, p67phox and GTPase Rac. In addition to $gp91^{phox}$, mammals also possess six other NADPH oxidases including Nox1, Nox3-5 and Duox1-2. Similarly, plants possess multiple Nox enzymes. The genome of *Arabidopsis thaliana* contains ten respiratory burst oxidase homologues (Rboh) (Foreman *et al*., 2003). Three distinct subfamilies (NoxA, NoxB and NoxC) are present within the fungi, with most filamentous fungi, including *E. festucae,* possessing a NoxA and NoxB isoform (Lara-Ortiz *et al*., 2003, Tanaka *et al*., 2006). As discussed above, *E. festucae noxA* is required to maintain a mutualistic interaction with perennial ryegrass whereas *noxB* does not appear to play a role in the symbiosis (Tanaka *et al*., 2006).

1.2.3 ROS detoxification

The potential damage to DNA, lipids and proteins by ROS necessitates the restoration of ROS levels back to basal levels to maintain cellular redox homeostasis. The diversity in the chemistry and cellular targets of ROS necessitated the evolution of multiple strategies to mitigate the damaging effects of ROS. Thus, cells possess a number of enzymatic and nonenzymatic antioxidant defences that function to detoxify these species.

Nonenzymatic ROS scavenging mechanisms

A large number of low molecular weight compounds have demonstrated antioxidant function in cells, including glutathione, ascorbate (vitamin C), α-tocopherol (vitamin E), coenzyme Q_{10}, proline, melatonin, flavonoids, carotenoids and alkaloids (Belozerskaia & Gessler, 2007, Halliwell, 2006). Mammals are unable to endogenously synthesise some antioxidants, such as vitamins C and E, in sufficient quantity and must acquire them through the plant component of their diet (Halliwell, 2006). Together, glutathione and ascorbate are considered the primary cellular redox buffer and control levels of hydrogen peroxide and protein thiol status. Reduced glutathione (GSH) is oxidised by ROS to GSSG, consisting of two GSHs linked by a disulfide bridge. Ascorbate is oxidised to monodehydroascorbate (MDA) and dehydroascorbate (DHA). The redox buffering pools of ascorbate and glutathione are intimately linked via the ascorbate-glutathione cycle (Apel & Hirt, 2004). Ascorbate is regenerated from dehydroascorbate through the ascorbate-glutathione cycle at the expense of GSH. GSH is also used as the reductant to regenerate seleno-glutathione peroxidases and some 1-Cys peroxiredoxins. α-tocopherol is the major liposoluble antioxidant and protects cellular membranes from lipid peroxidation by scavenging lipid peroxyl radicals and lipid-oxidising ROS, such as singlet oxygen, in cooperation with carotenoids. However, the fine balance between antioxidant and pro-oxidant functions was highlighted in a recent study by Lam *et al.* (2010), where treatment of an *S. cerevisiae* strain (K6001) with antioxidants α-tocopherol or coenzyme Q_{10} counterintuitively led to increased cellular ROS levels. The K6001 strain is resistant to multiple oxidants and was shown to express a dominant form of the peroxiredoxin Tsa1, one of the major enzymes involved in antioxidant enzymatic defences that will be discussed in more detail below (Timmermann *et al.*, 2010). Exogenously supplying antioxidants to this strain, in which endogenous antioxidant defences are heightened, increases oxidative stress, highlighting the complex interplay between ROS and both enzymatic and non-enzymatic ROS detoxification systems (Lam *et al.*, 2010).

Enzymatic ROS Scavenging Mechanisms

In addition to nonenzymatic antioxidant defence strategies, cells possess a number of ROS-detoxifying enzymes. The thioredoxin system, comprising thioredoxin (Trx), thioredoxin reductase (TrxR) and NADPH is a major enzymatic antioxidant system implicated in the modulation of ROS levels and redox regulation. Trx exerts its antioxidant function both directly by quenching singlet oxygen and scavenging hydroxyl radicals (Das & Das, 2000) and indirectly by reducing oxidised ROS target proteins (Powis & Montfort, 2001). The glutathione-glutaredoxin system consisting of glutaredoxin (Grx), glutathione (GSH) and glutathione reductase (GR) facilitates the non-enzymatic antioxidant function of GSH by converting GSSG back into GSH with the reducing agent NADPH. Substantial overlap and interplay between these two systems is thought to occur as in *S. cerevisiae* just a single Grx or Trx gene is sufficient for cell viability, whereas deletion of all four (*GRX1, GRX2, TRX1, TRX2*) is lethal (Draculic *et al.*, 2000).

Intimately linked with the thioredoxin- and glutathione- reduction systems are the peroxiredoxin (Prx) or thioredoxin peroxidase and glutathione peroxidase enzymes. Glutathione peroxidases (GPxs) catalyze the reduction of H_2O_2 to water with electrons typically supplied by glutathione (GSH). The oxidised glutathione (GSSG) can be converted back to GSH by glutathione reductase. Peroxiredoxins have garnered much attention in recent times, and it is now thought they may be the most important H_2O_2-removal system in most aerobic organisms. Peroxiredoxins, like GPxs, convert H_2O_2 to H_2O. However, the cellular reductant is typically thioredoxin and while catalytic rates of Prxs are slower, this is compensated for by the generally high abundance of these proteins (Halliwell, 2006, Winterbourn & Hampton, 2008).

Other antioxidant and detoxifying enzymes include superoxide dismutase (SOD), catalase (CAT) and NADPH:quinone oxidoreductase 1 (NQO). These enzymes cooperate in interconnected reactions to eliminate various forms of ROS. NADPH:quinone oxidoreductase 1 (NQO) catalyses the two-electron reduction of quinones, such as menadione, to hydroquinones, thereby preventing the one-electron reduction of quinones that results in the production of radical species such as the superoxide anion $O_2^{\bullet-}$ (Kim *et al.*, 2003). Superoxide that is formed in the cell is rapidly converted to H_2O_2 by superoxide dismutases. H_2O_2 is then detoxified to water and oxygen by Prxs, GPxs and catalases. Glutathione *S*-transferases (GSTs) provide protection from membrane lipid peroxidation through their Se-independent glutathione peroxidase activity and also detoxify lipid peroxidation end products such as 4-hydroxynonenal (4-HNE) (Sharma *et al.*, 2004).

As highlighted in the review by Foyer *et al*. (2005) antioxidant buffering and redox signalling are intimately linked and modulation of antioxidant activity in the cell may facilitate redox signalling. The quenching of ROS levels by the redox buffering systems in the cell would effectively reduce the redox flux through the signalling pathways. However, other antioxidant functions may in fact facilitate redox signalling i.e. elevated SOD levels contribute to increases in H_2O_2, a key signalling molecule in pathways such as the Gpx3/Yap1 transcription factor pathway of *S. cerevisiae* (Delaunay *et al*., 2002). The overlap between antioxidants and redox signalling compounds is exemplified by the thiol peroxidases, Gpx3 and Tpx1 of *S. cerevisiae* and *S. pombe,* respectively, which possess dual functions in H_2O_2 scavenging and signalling (Foyer & Noctor, 2005).

1.3 Pathways regulating the oxidative stress response in fungi

The cellular responses to oxidative stress in filamentous fungi and yeast are mediated by interconnected pathways including histidine kinase-based phosphorelays, stress-activated MAPK cascades and AP-1-like transcription factors. A number of key components of these pathways in a range of fungi have been characterised by mutational analysis (Toone *et al*., 1998, Temme & Tudzynski, 2009, Takahashi *et al*., 2010, Singh *et al*., 2004, Schnell *et al*., 1992, Qiao *et al*., 2008, Oide *et al*., 2010, Mutoh *et al*., 2005, Motoyama *et al*., 2008, Lin *et al*., 2009, Lev *et al*., 2005, Lamarre *et al*., 2007, Kuge *et al*., 1998, Hagiwara *et al*., 2008, Guo *et al*., 2011, Banno *et al*., 2007, Asano *et al*., 2007, Alarco & Raymond, 1999, Kuge & Jones, 1994). The sensitivities of each mutant to various oxidative stress-inducing compounds, including H_2O_2, *tert*-butyl hydroperoxide (t-BOOH), potassium superoxide (KO_2), menadione and diamide are summarised in Table 1.1 and will be discussed in further detail throughout Section 1.3.

Species	Strain	*Sp*/*Sc* orthologue	Form tested	H_2O_2	*t*-BOOH	KO_2	MD	D	Reference
S. pombe	Δ*pap1*	*PAP1*/*YAP1*	-	S	S	-	S	S	Toone *et al.*, 1998, Mutoh *et al.*, 2005
	Δ*prr1*	*PRR1*/*SKN7*	-	S	-	-	S	-	Mutoh *et al.*, 2005
	Δ*spc1*	*SPC1*/*HOG1*	-	S	S	-	-	S	Toone *et al.*, 1998
	Δ*atf1*	*ATF1*/*SKO1*	-	S	R	-	S	-	Mutoh *et al.*, 2005
S. cerevisiae	Δ*yap1*	*PAP1*/*YAP1*	-	S	S	-	S	S	Schnell *et al.*, 1992, Kuge & Jones, 1994
	Δ*skn7*	*PRR1*/*SKN7*	-	S	S	-	S	R	Morgan *et al.*, 1997
A. nidulans	Δ*atfA*	*ATF1*/*SKO1*	hyphae	R	R	-	R	-	Hagiwara *et al.*, 2008
	Δ*napA*	*PAP1*/*YAP1*	hyphae	S	S	-	S	-	Hagiwara *et al.*, 2008
	Δ*atfA*	*ATF1*/*SKO1*	conidia	S	-	-	-	-	Hagiwara *et al.*, 2008
	Δ*sskA*	*MCS4*/*SSK1*	conidia	S	S	R	R	R	Hagiwara *et al.*, 2007
	Δ*srrA*	*PRR1*/*SKN7*	conidia	S	S	R	R	R	Hagiwara *et al.*, 2007
	Δ*napA*	*PAP1*/*YAP1*	conidia	S	S	-	S	R	Asano *et al.*, 2007
C. albicans	Δ*cap1*	*PAP1*/*YAP1*	-	S	R	-	S	-	Alarco & Raymond, 1999
	Δ*skn7*	*PRR1*/*SKN7*	-	S	-	-	-	R	Singh *et al.*, 2004
A. fumigatus	Δ*yap1*	*PAP1*/*YAP1*	conidia	S	-	-	S	R	Qiao *et al.*, 2008
	Δ*skn7*	*PRR1*/*SKN7*	conidia	S	S	-	-	-	Lamarre *et al.*, 2007
C. heterostrophus	Δ*chap1*	*PAP1*/*YAP1*	conidia	S	-	-	S	-	Lev *et al.*, 2005
	Δ*skn7*	*PRR1*/*SKN7*	hyphae	S	S	S	-	-	Oide *et al.*, 2010
	Δ*ssk1*	*MCS4*/*SSK1*	hyphae	S	S	R	-	-	Oide *et al.*, 2010
A. alternata	Δ*aaap1*	*PAP1*/*YAP1*	hyphae	S	S	S	S	-	Lin *et al.*, 2009
B. cinerea	Δ*bap1*	*PAP1*/*YAP1*	hyphae	S	-	-	S	-	(Temme & Tudzynski, 2009
N. crassa	Δ*ncap1*	*PAP1*/*YAP1*	hyphae	S	S	-	S	-	Takahashi *et al.*, 2010
	Δ*skn7*	*PRR1*/*SKN7*	hyphae	-	S	-	-	-	Banno *et al.*, 2007
M. oryzae	Δ*moap1*	*PAP1*/*YAP1*	hyphae	S	-	-	-	-	Guo *et al.*, 2011
	Δ*moskn7*	*PRR1*/*SKN7*	hyphae	R	-	-	-	-	Motoyama *et al.*, 2008
U. maydis	Δ*yap1*	*PAP1*/*YAP1*	conidia	S	-	-	-	-	Molina & Kahmann, 2007

Table 1.1 Oxidative stress sensitivity of fungal mutants. Summary of sensitive (S) and resistant (R) phenotypes of fungal strains lacking orthologues of *S. pombe* and *S. cerevisiae* (*Sp*/*Sc*) oxidative stress response genes towards various oxidative stress-inducing compounds: H_2O_2, Hydrogen peroxide; *t*-BOOH, *tert*-butyl hydroperoxide; KO_2, potassium superoxide; MD, menadione; D, diamide. – unspecified/untested.

1.3.1 Multistep phosphorelays

S. pombe two-component His-Asp phosphorelay systems

Two-component related proteins play a major role in regulating the oxidative stress response in *S. pombe*. *S. pombe* possesses three hybrid histidine kinases (HK): two closely related proteins Mak2 and Mak3, and one more distantly related kinase Mak1; a single phosphorelay protein (HPt) Mpr1, and two response regulators (RR) Mcs4 and Prr1 which comprise two interrelated phosphorelay pathways (Figure 1.3) (Quinn *et al.*, 2011). Mak2 and Mak3 sense peroxide stress via sensory PAS and GAF domains, triggering autophosphorylation of a conserved histidine residue. In accordance with other yeast phosphorelay systems the phosphate is presumably transferred, in a series of steps, to a conserved aspartic acid residue in the receiver domain of Mak2/Mak3, and in turn passed on to a histidine residue in Mpr1 and finally to an aspartic acid residue in the receiver domain of Mcs4. Mcs4 can then transmit the stress signal to the Spc1 (Sty1) mitogen-activated protein kinase (MAPK) pathway which orchestrates appropriate changes in gene expression in response to peroxide stress (Quinn *et al.*, 2011). The Prr1 response regulator is a constitutively nuclear-localised transcription factor required for the activation of oxidative stress-responsive genes, including *trr1* and *ctt1 (*Ohmiya *et al.,* 2000*)*. However, regulation of Prr1 by two-component signalling is somewhat unclear and may be activated either by the Mak2/Mak3 HKs or the Mak1 HK via the common phosphorelay protein Mpr1 (Aguirre *et al.*, 2006, Buck *et al.*, 2001, Quinn *et al.*, 2011). The recruitment of Prr1 to promoters of antioxidant genes (*trr1, srx1* and *ctt1*) is dependent on the transcription factor Pap1; oxidised Pap1 appears to recruit Prr1 to the DNA and together they activate the expression of antioxidant genes (Calvo *et al.*, 2012). However, a subset of antioxidant genes only requires Prr1 for expression and conversely, a subset only depends on Pap1 for expression (Nguyen *et al.*, 2000).

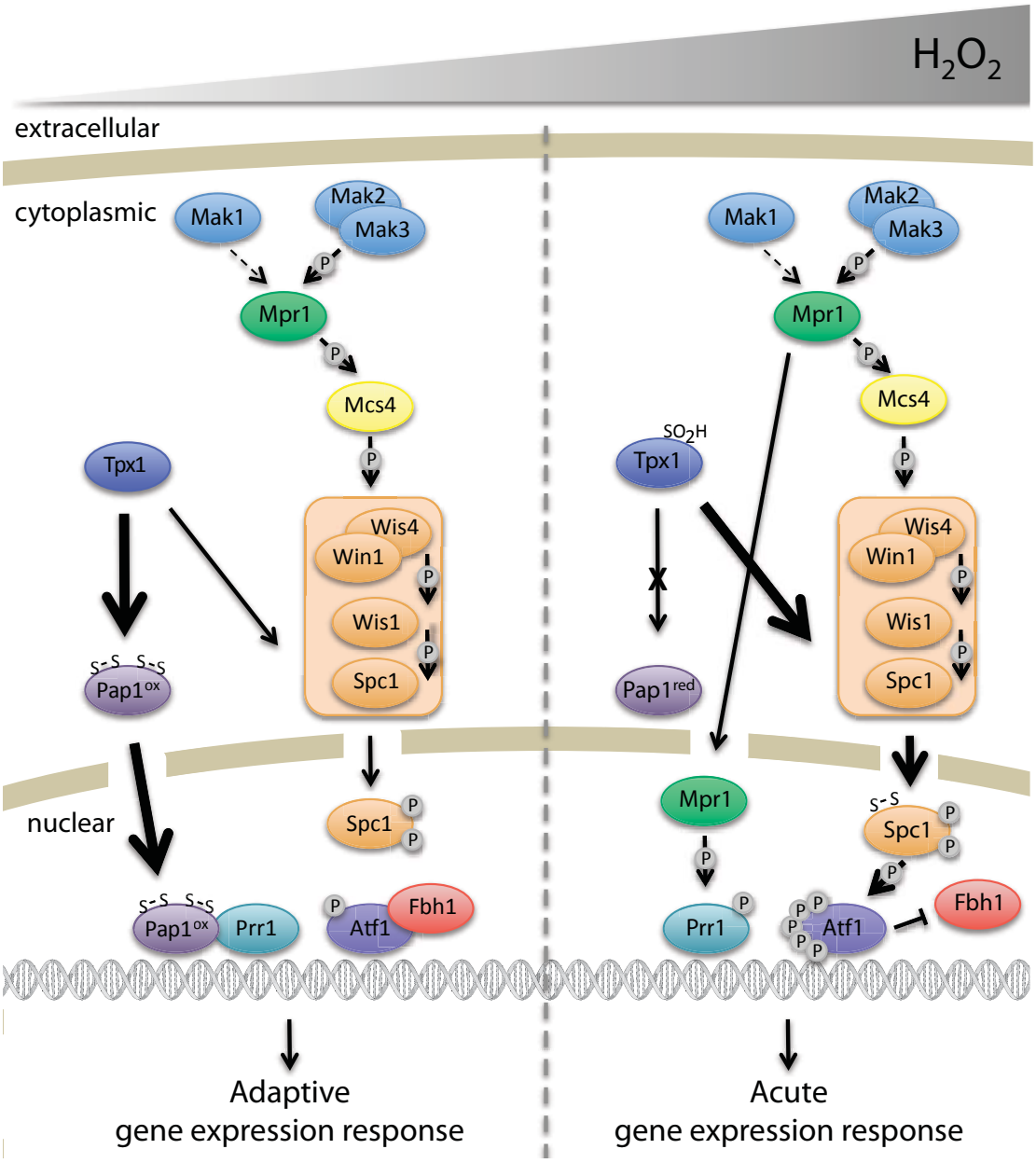

Figure 1.3 *S. pombe* stress-sensing pathways. *S. pombe* possesses two alternative pathways to respond to H_2O_2. Low levels of H_2O_2 are sensed via the Tpx1-Pap1 redox relay in which Tpx1 senses and transmits the H_2O_2 signal to Pap1 resulting in the activation of oxidative stress response genes for an adaptive response. Oxidised Pap1 interacts with the response regulator Prr1 in the nucleus and together they regulate a subset of the Pap1-dependent genes. At higher levels of H_2O_2, Tpx1 becomes hyperoxidised and the thioredoxin peroxidase-dependent activation of Pap1 is inhibited. Elevated H_2O_2 stabilises the transcription factor Atf1 by disrupting its interaction with the ubiquitin E3 ligase, Fbh1. Thus, higher levels of H_2O_2 are sensed via the Spc1 (Sty1) MAPK pathway. The initial H_2O_2 signal is perceived by cytoplasmic histidine kinases, Mak2 and Mak3, which transmit the signal via a phosphorelay system, involving the phosphotransfer protein Mpr1 and response regulator Msc4, to the MAPK pathway comprised of Win1 and Wis4 (MAPKKKs), Wis1 (MAPKK) and Spc1 (Sty1) (MAPK), and finally to Atf1 resulting in the activation of oxidative stress response genes for an acute

response. Tpx1 is also required for the hydrogen peroxide-induced activation of the Spc1 (Sty1) MAPK pathway, however, as Tpx1 regulates Spc1 by a thioredoxin peroxidase-independent mechanism this activation still occurs at high levels of H_2O_2. Mak1 appears to mediate the oxidative stress response through Prr1 in an Spc1-independent manner.

Oxidative signalling through these pathways is dose-dependent; *S. pombe* has developed sophisticated mechanisms that discriminate between low and high levels of H_2O_2. While Spc1 is required for gene expression over a wide range of H_2O_2 concentrations, at low-intermediate levels of H_2O_2, Spc1 is activated primarily via Mcs4 activation of the MAPK pathway, whereas at high levels of H_2O_2, a significant level of Spc1 activation occurs independently of the phosphorelay system via a Tpx1 redox relay (Quinn *et al.*, 2002). Furthermore, the Spc1-MAPK pathway and the downstream transcription factor Atf1 play a more significant role in sensing high rather than low levels of peroxide. Higher levels of H_2O_2 increase Spc1-phosphorylation of Atf1, which disrupts its interaction with the ubiquitin E3 ligase, Fbh1 diverting it from the ubiquitin-proteasome pathway. More recently, Quinn *et al*. (2011) showed Prr1 regulates gene expression in response to intermediate and high levels of H_2O_2, but only at high levels of peroxide stress was Prr1 activation dependent on the phosphorelay pathway.

S. cerevisiae two-component His-Asp phosphorelay system

In contrast to *S. pombe, S. cerevisiae* contains just a single HK, Sln1, acting upstream of the Mpr1-orthologous HPt protein, Ypd1, and the two RRs, Ssk1 and Skn7 (Figure 1.4). The Sln1 HK is a transmembrane protein with an extracellular domain, which senses osmotic and cell wall stress, and a cytoplasmic histidine kinase domain. In contrast, the HKs of *S. pombe* are entirely cytoplasmic and perceive oxidative stress signals (Quinn *et al*., 2011). Despite these differences, both the *S. cerevisiae* and *S. pombe* phosphorelays dually activate a stress-activated MAPK cascade and a response regulator with DNA-binding activity. Osmotic stress causes a reduction in Sln1 kinase activity and, consequently, a reduction in phosphorylation of Ypd1, Ssk1 and Skn7. Unphosphorylated Ssk1 stimulates the Hog1 MAPK leading to a derepression of Sko1-regulated osmoinducible genes. In contrast, cell wall stress induces an increase in Sln1 kinase activity and renders the Hog1 MAPK pathway inactive (Fassler & West, 2011, Ikner & Shiozaki, 2005). The Skn7 response regulator, like the *S. pombe* Prr1 homologue, is under the regulation of a His-Asp phosphorelay, but oxidative stress appears to activate Skn7 independently of the phosphorelay system. Phosphorylation of Skn7 by the HPt protein Ypd1 leads to activation of genes involved in cell cycle control and cell wall stress-responsive genes, whereas oxidative activation of Skn7 leads to activation of genes involved in the oxidative stress response (OSR) including *TRX2, TSA1, GPX2, AHP1, CCP1* and *CTT1*. Many of the oxidative stress response genes contain not only Skn7 binding sites, but also Yap1 binding sites (Yap1 response elements; YRE) and indeed it has been shown that these two factors coordinately regulate a large set of genes, including *CTT1, SOD1, SOD2, TRR1, TRX2* and *TSA1* in

the OSR regulon. A substantial number of OSR genes, including *GLR1*, *GSH1* and *CYS3*, depend on Yap1 alone for expression, however, evidence for Skn7 dependent/Yap1 independent OSR gene expression is lacking (Lee *et al.*, 1999, Mulford & Fassler, 2011). In response to oxidative stress, Yap1 binds weakly to unphosphorylated DNA-bound Skn7. A Skn7 kinase, yet to be identified, is then recruited to the Skn7-Yap1 complex, leading to the phosphorylation of Skn7, which in turn stabilises the complex (He *et al.*, 2009).

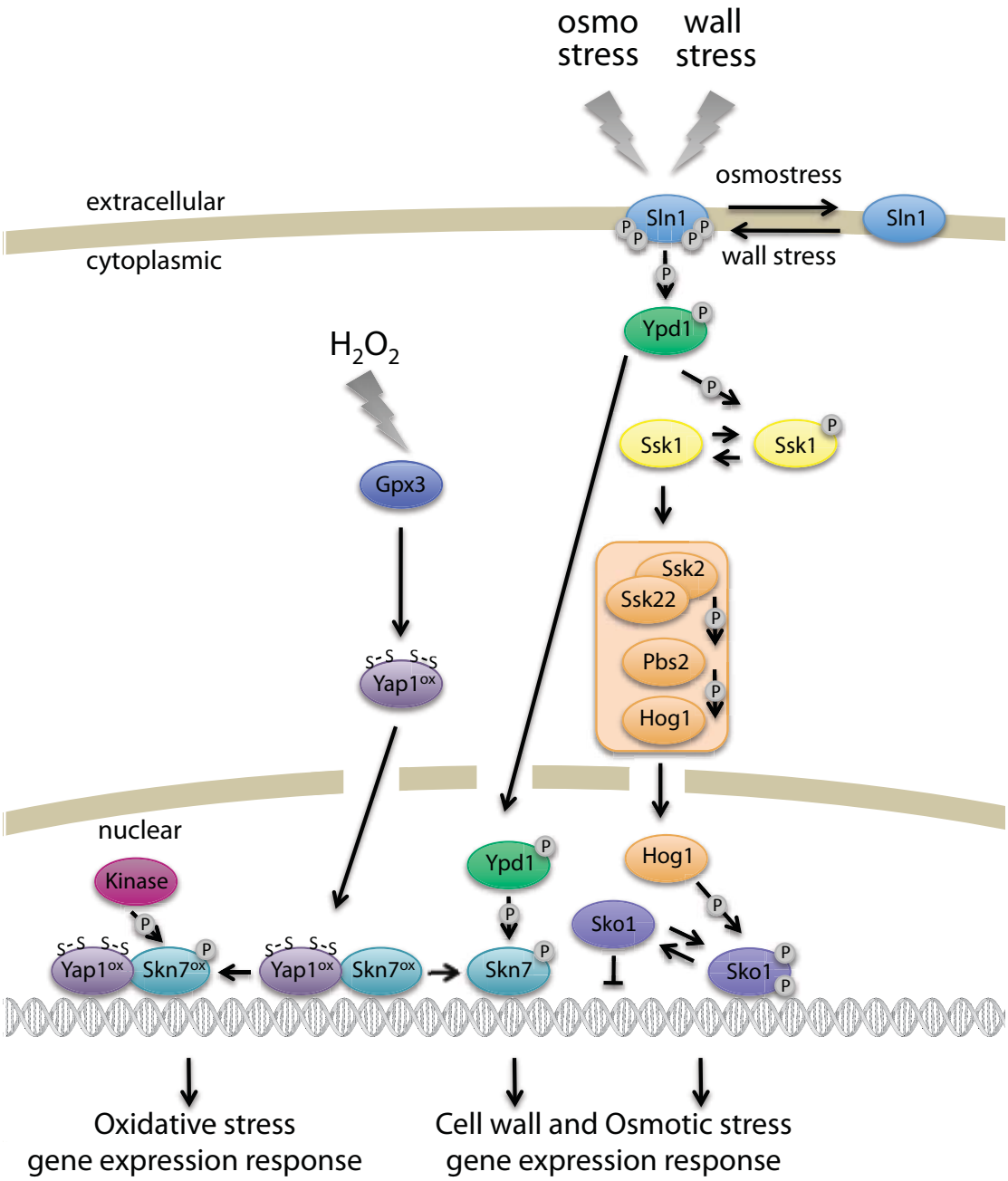

Figure 1.4 ***S. cerevisiae*** **stress-sensing pathways.** The major oxidative stress response pathway in *S. cerevisiae* involves the transcription factor Yap1. The thiol peroxidase Gpx3 senses and transmits the H_2O_2 signal to Yap1 resulting in the activation of oxidative stress response genes. Thiol reactive compounds also activate Yap1 via a Gpx3-independent mechanism (See Figure 1.5). Yap1 interacts with the response regulator Skn7 and the Yap1-Skn7 complex recruits a yet to be identified kinase, that phosphorylates Skn7 reinforcing the Skn7-Yap1 interaction resulting in the activation of gene expression. Yap1 also activates a subset of oxidative stress response genes independently of Skn7. The transmembrane histidine kinase Sln1 is autophosphorylated under normal growth conditions. Cell wall stress, induced by cell-wall perturbing agents such as calcofluor white (CFW) and sodium dodecyl sulfate (SDS) induces hyperactivation of the pathway and an accumulation of Ssk1 in a phosphorylated and

inactive state. Osmotic stress, induced by high NaCl and other conditions causing reduced turgor, lead to a reduction in Sln1 kinase activity and a consequential reduction in phosphotransfer to the phosphorelay intermediate Ypd1 and response regulators Ssk1 and Skn7. Accumulation of the unphosphorylated form of Ssk1 activates the Ssk2 and Ssk22 MAP kinase kinase kinases (MAPKKKs) which, in turn, activate the Pbs2-Hog1 MAPKK-MAPK pathway. Hog1 induces gene expression by inactivating the Sko1 transcriptional repressor. Cell wall stress also activates Skn7 via the Sln1-Ypd1 phosphorelay.

Phosphorelay systems in filamentous fungi

The fungal HK and HPt gene families appear to have expanded in filamentous fungi with 15 HK- and 4 RR-encoding genes identified in the *A. nidulans* genome along with a single HPt gene (Hagiwara *et al*., 2007). This is possibly a reflection of the more diverse environmental stresses encountered by these multicellular fungi. The response regulators SskA, a homologue of *S. cerevisiae* Ssk1 and *S. pombe* Mcs4, and SrrA, a homologue of *S. cerevisiae* Skn7 and *S. pombe* Prr1, have been implicated in oxidative stress and, to a lesser degree, osmotic stress resistance. Conidial germination and hyphal growth of the Δ*sskA* and Δ*srrA* mutants are sensitive to peroxide stress induced by *tert*-butyl hydroperoxide and H_2O_2 but tolerate oxidative stress generated by thiol-reactive compounds, menadione and diamide. Furthermore, Δ*sskA* (but not Δ*srrA*) conidia are inherently less viable than wild-type conidia. The finding that genes involved in conidial stress-tolerance (catalase A, *catA*; glycerol-3-phosphate dehydrogenase, *gfdB*; and trehalose-6-phosphate synthase, *tpsA*) are downregulated in the Δ*sskA* mutant supports the notion that this two-component pathway relays signals from receptor to nucleus (Furukawa *et al*., 2005). While SskA acts upstream of the HogA MAPK cascade, SrrA is thought to be a DNA-binding transcription factor (Furukawa *et al*., 2005).

1.3.2 Stress-activated MAPK cascades

Mitogen-activated protein kinase (MAPK) cascades constitute a fundamental signalling system universally employed by eukaryotes to regulate responses to various stimuli including pheromones, nitrogen and nutrient starvation, cell wall, osmotic and oxidative stress (Chen & Thorner, 2007). Such cascades consist of a three-tiered hierarchical organisation of sequentially acting kinases: a MAPK kinase kinase (MAPKKK), a MAPK kinase (MAPKK) and a MAPK. Additional upstream and downstream components are also required to initiate MAPKKK phosphorylation and translate the phosphorylation signal from the MAPK to a biological response (Chen & Thorner, 2007).

S. pombe Spc1 pathway

Operating downstream of the *S. pombe* Mak2/Mak3 phosphorelay previously described is the stress-activated MAP kinase cascade (Figure 1.3). This pathway consists of the MAPK Spc1 (Sty1), which is activated by the MAPKK Wis1, which is in turn activated by the two MAPKKKs, Win1 and Wis4. After phosphorylation by Wis1, Spc1 translocates to the nucleus where it activates the Atf1 transcription factor

resulting in the transcriptional induction of many stress-response genes. The target genes of Atf1 are varied but many have a general stress-response function, which is a reflection of the many different forms of stress, including high osmolarity, oxidative stress, heat shock, UV irradiation and nutrient limitation that activate the pathway (Quinn *et al.*, 2002). The involvement of Atf1 in oxidative stress signalling is H_2O_2 dose-dependent and, while Atf1 is constitutively nuclear, expression of Atf1 targets such as *gpx1* is primarily induced at high H_2O_2 concentrations. The response to lower levels of peroxide in *S. pombe* is mediated by the Pap1 transcription factor (Quinn *et al.*, 2002).

S. cerevisiae Hog1 pathway

The high osmolarity glycerol (Hog1) pathway of *S. cerevisiae* was initially characterised as a key pathway mediating adaptation of yeast cells to osmotic stress (Brewster *et al.*, 1993) but has since been implicated in responses to a variety of stresses including citric acid-, methylglyoxal-, temperature- and arsenite-induced stress (Aguilera *et al.*, 2005, Lawrence *et al.*, 2004, Panadero *et al.*, 2006, Thorsen *et al.*, 2006). It does not, however, appear to be involved in oxidative stress signalling. The *S. cerevisiae* Hog1 MAPK shares >80% amino acid sequence identity with the *S. pombe* homologue Spc1 and components upstream of Hog1. MAPKK Pbs2 and MAPKKKs Ssk2 and Ssk22 also demonstrate a high degree of similarity to their counterparts in fission yeast, MAPKK Wis1 and MAPKKKs Wis4 and Win1. However, rather than activating a transcription factor to induce gene expression, Hog1 facilitates gene expression by inactivating the transcriptional repressor, Sko1.

SakA MAPK pathways in filamentous fungi

Stress-activated MAPK signalling pathways, very similar to the fission and yeast pathways described above, have also been identified in filamentous fungi. Furukawa *et al.* (2005) showed that the *A. nidulans* HogA MAPK pathway operates downstream of the phosphorelay pathway involving SskA, analogous to the phosphorelay-MAPK coupling mechanism established in *S. cerevisiae* and *S. pombe* (Furukawa *et al.*, 2005). Much like *S. pombe* Spc1, the SakA MAPK of *Aspergillus nidulans* is involved in transducing various stress signals including oxidative, osmotic and heat shock stress. Downstream changes in gene expression are mediated by the transcription factor AtfA, a homologue of *S. pombe* Atf1 (Hagiwara *et al.*, 2007, Hagiwara *et al.*, 2008). While only the conidia of Δ*sakA* and Δ*atfA* mutants are sensitive to H_2O_2, both mycelia and conidia of upstream response regulator mutants, Δ*sskA* and Δ*srrA*, were sensitive to H_2O_2. AtfA is indispensible for the induction of the conidia-specific catalase, *catA*, whereas induction of the mycelia-specific catalase, *catB*, is largely unaffected by inactivation of

atfA (Hagiwara *et al*., 2008, Lara-Rojas *et al*., 2011). This indicates that the SskA-AtfA signalling cascade differentially regulates antioxidant responses in spores versus mycelia, in part through differential regulation of catalase enzymes (Hagiwara *et al*., 2008).

The *E. festucae* Δ*sakA* mutant in its vegetative mycelial form is sensitive to various stresses, including temperature and osmotic stresses, but not oxidative stress. Conidial stress-sensitivity was not tested as the Δ*sakA* mutant is defective in conidia formation. This does, however, suggest that SakA is involved in conidial stress-tolerance and viability (Eaton *et al*., 2008). This is in line with the decreased conidiation and reduction in conidial viability observed in the Δ*sakA* mutant of *A. nidulans* (Kawasaki *et al*., 2002, Lara-Rojas *et al*., 2011). Sensing stress by the *E. festucae* SakA MAPK translates to a role in regulating its association with perennial ryegrass. Deletion of *sakA* causes abnormal growth of the fungal hyphae, both in culture and *in planta,* and results in stunting of colonised host plants (Eaton *et al*., 2010).

1.3.3 AP-1-like transcription factors

One of the most well-studied targets of MAP kinase signal transduction cascades is the mammalian activator protein 1 (AP-1), a basic leucine zipper (bZIP) transcriptional regulator composed of members of the Fos and Jun families of DNA binding proteins (Whitmarsh & Davis, 1996). There is also evidence that AP-1 activation is regulated by changes in the intracellular redox status involving the redox factor-1 (Ref-1) protein (Xanthoudakis & Curran, 1992). AP-1 modulates gene expression in response to a variety of stimuli, including growth factors, cytokines, neurotransmitters and cellular stress (Angel & Karin, 1991). The Yap1 (yeast AP-1) and Pap1 (*pombe* AP-1) transcription factors are functional homologues of mammalian AP-1 in *S. cerevisiae* and S. *pombe,* respectively, and they too have been extensively studied. In addition to Yap1, *S. cerevisiae* possesses seven other AP-1 homologues, Yap2-Yap8, thought to be result of at least six duplication events (Kellis *et al.,* 2004). Yap1 and Pap1, the sole AP-1 homologue in *S. pombe* are the major contributors towards the oxidative stress response in yeast (Fernandes *et al.,* 1997).

S. cerevisiae Yap1 transcription factor

The Yap1 bZIP transcription factor contains two cysteine-rich domains, the N-terminus (n-CRD) and the C-terminus (c-CRD), that are fundamental to its activation. The nuclear localisation signal (NLS) and the nuclear export signal (NES) dictate transport into or out of the nucleus, respectively. In the absence of oxidative stress, the

S. cerevisiae Yap1 transcription factor is continuously exported out of the nucleus, mediated by the interaction of its NES with the Crm1 exportin. In cells exposed to oxidative stress, two disulfide bonds are formed between cysteines 303-598 and 310-629 (Wood *et al.*, 2004) (Figure 1.5A).

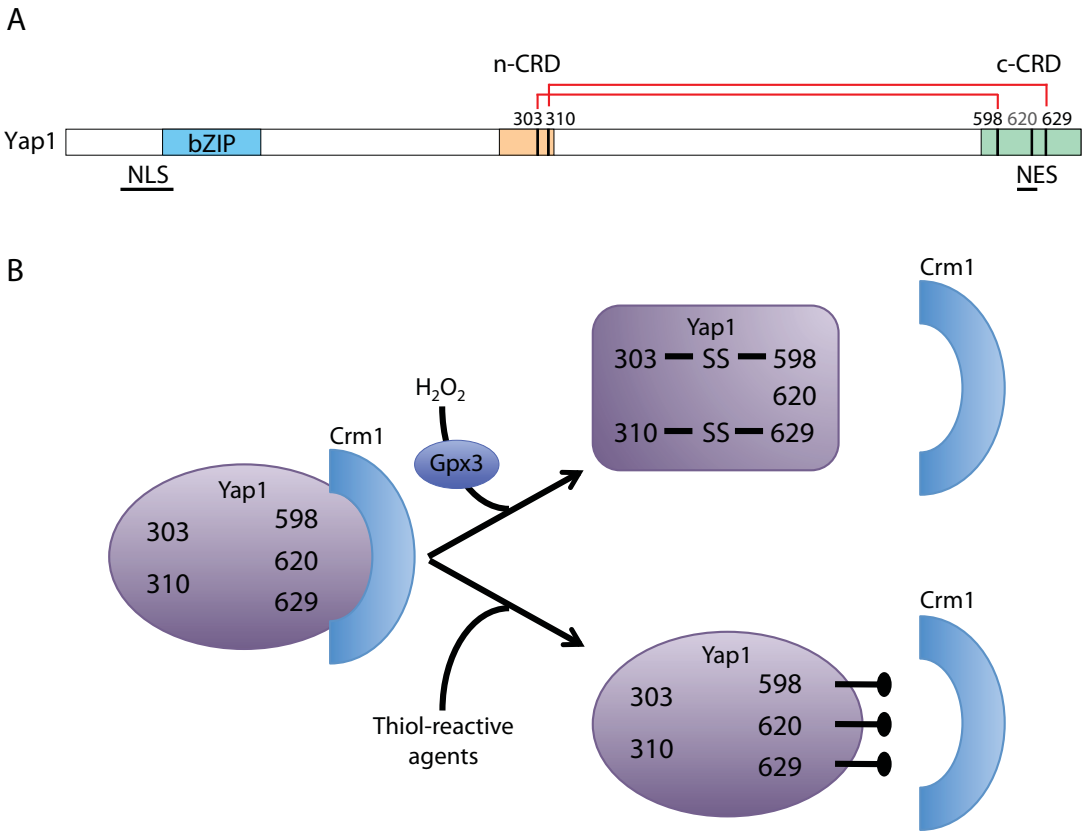

Figure 1.5 Redox regulation of *S. cerevisiae* Yap1. (A) H_2O_2-induced disulfide bond formation in Yap1. Cys residues 303 and 310 within the N-terminal cysteine-rich domain (n-CRD), shaded orange, and 598, 620 and 629 within the C-terminal cysteine-rich domain (c-CRD), shaded green, are indicated by vertical black lines. The Cys303-Cys598 and Cys310-Cys629 disulfide bonds are indicated with red lines. The nuclear localisation signal (NLS) and nuclear export sequence (NES) are located at the N- and C-termini, respectively. Figure adapted from Wood *et al.* (2004) (B) Distinct mechanisms of Yap1 activation by H_2O_2 or thiol-reactive agents. H_2O_2-induced Cys303-Cys598 and Cys310-Cys629 disulfide bond formation, mediated by Gpx3, causes a conformational change and activation of Yap1. Thiol-reactive agents activate Yap1 through modification of Cys598, Cys620 and Cys629 residues in the c-CRD without the involvement of the Gpx3 sensor or n-CRD Cys residues. Both modes of activation disrupt the association of Yap1 with the nuclear export receptor Crm1 leading to retention in the nucleus. Figure adapted from Azevedo *et al*. (2003).

These long-range disulfides link the n-CRD and c-CRDs and produce a conformational change that conceals the Crm1-nuclear export signal (NES) embedded in the c-CRD (Wood *et al.*, 2003a) (Figure 1.5A & B). As a result, oxidised Yap1 is retained in the nucleus and activates the expression of a large regulon including genes involved in antioxidant defence, heat shock response, amino acid, carbohydrate and glycerol metabolism (Lee *et al.*, 1999). The formation of the Cys303-Cys598 and Cys310-Cys629 disulfide bonds in Yap1 after exposure to H_2O_2 is by far the most commonly recognised mechanism of Yap1 activation, however, Yap1 is also activated by thiol-reactive electrophiles, such as diamide and *N*-ethylmaleimide. Flattery-O'Brien *et al.* (1993) demonstrated two distinct modes of Yap1 activation, one triggered by ROS (H_2O_2) and the other by compounds with thiol-reactivity such as menadione (MD). Pre-treatment of *S. cerevisiae* cells with a sublethal dose of menadione (MD) was unable to provide cross-resistance to subsequent higher doses of H_2O_2, whereas pre-treatment with sublethal doses of either MD or H_2O_2 induces an adaptive response to subsequent doses of MD and H_2O_2, respectively. Furthermore, unlike the H_2O_2-induced response, the MD response strictly requires the synthesis of new proteins (Flattery-O'Brien *et al.*, 1993). Yap1 activation by thiol-reactive compounds involves covalent modification of the Cys residues in the c-CRD. Thiol modification of the three cysteines in c-CRD (Cys598, Cys620 and Cys629), without the formation of Cys303-Cys598 and Cys310-Cys629 inter-domain disulfide bonds, seems sufficient to disrupt interaction between Yap1 and Crm1 and to promote the nuclear accumulation of Yap1 (Azevedo *et al.*, 2003, Kuge *et al.*, 2001) (Figure 1.5B). Menadione, both a thiol-oxidising agent and a superoxide generator, can unsurprisingly activate Yap1 through formation of disulfide bridges linking the n- and c-CRD and also through covalent modification of Cys residues in the c-CRD (Azevedo *et al.*, 2003). The activation of Yap1 by ROS (hydroperoxides and superoxides) is dependent on the Gpx3 oxidant sensor whereas sensing of thiol-reactive compounds bypasses Gpx3, directly targeting Yap1 through cysteine adduct formation (Figure 1.5B & 1.6) (Azevedo *et al.*, 2003). This alternative mode of activation has also been observed for the *S. pombe* Pap1 homologue, whereby diethylmaleate (DEM)-mediated activation is suggested to operate through covalent cysteine adduct formation (Castillo *et al.*, 2002).

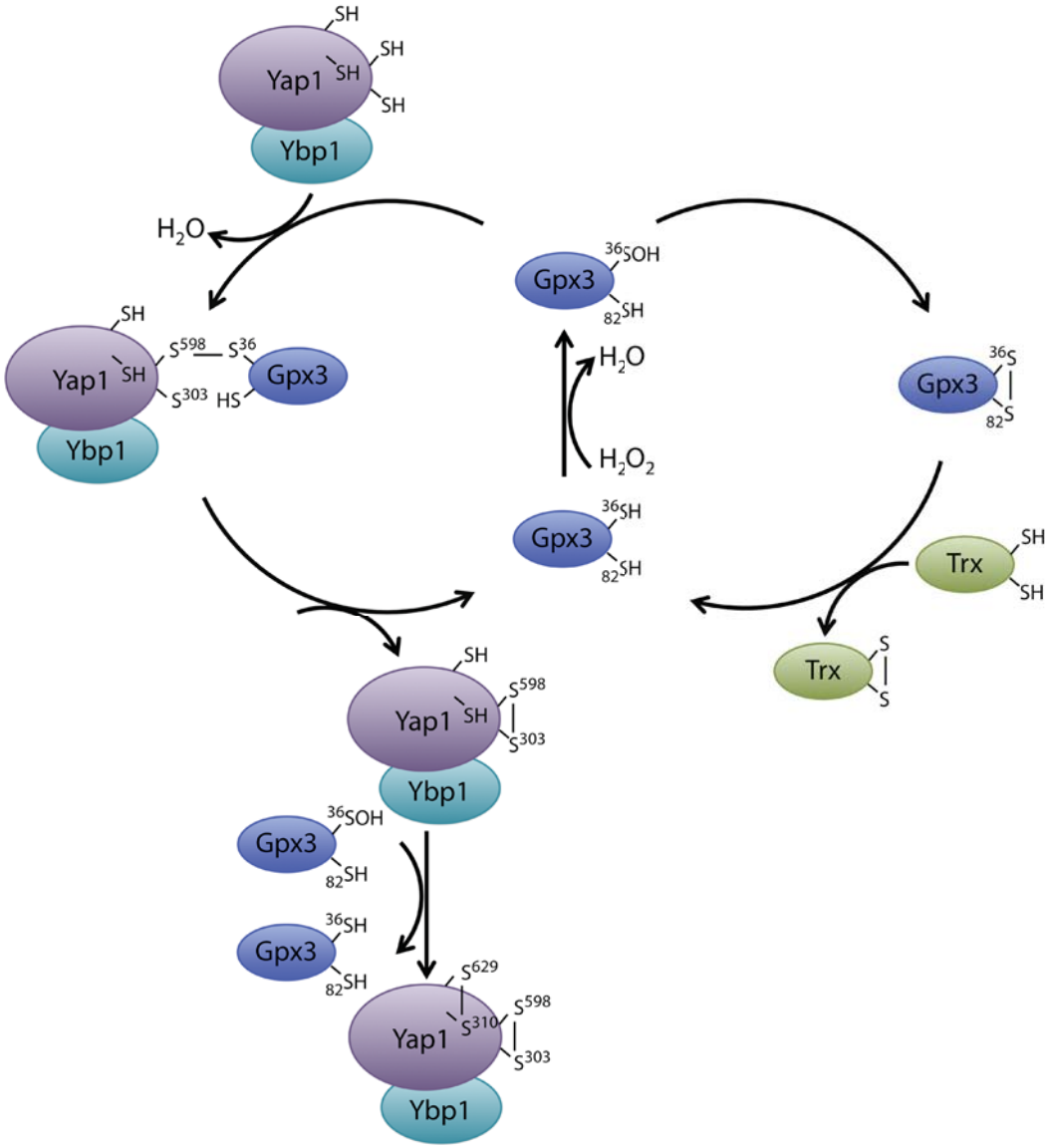

Figure 1.6 The Gpx3-Yap1 redox relay. Gpx3 reacts with H_2O_2 at its catalytic Cys36, which oxidises to a sulfenic acid (SOH). The Cys36-SOH reacts with the Yap1 Cys598 to form an intermolecular disulfide bond that is then resolved to an intramolecular Cys303–Cys598 disulfide bond within Yap1. This cycle is repeated to form the second Cys310-Cys629 disulfide bond within Yap1. Ybp1 acts as a scaffold to facilitate the Gpx3-Yap1 redox interaction and prevent the alternative glutathione peroxidase cycle occurring, in which condensation of Gpx3 Cys36-SOH with Gpx3 Cys82 results in formation of an intramolecular Gpx3 Cys36-Cys82 disulfide, which is then reduced by thioredoxin (Trx). Figure adapted from D'Autreaux & Toledano (2007).

In addition to Gpx3, H_2O_2 activation and nuclear localisation of Yap1 also requires the Yap1-binding protein Ybp1 (Figure 1.6). Ybp1 forms a peroxide-induced complex with Yap1 and appears to serve as a scaffold to facilitate oxidative folding of Yap1 (Gulshan *et al.*, 2011, Veal *et al.*, 2003). The requirement for Ybp1 appears to be peroxide specific. In Δ*ybp1* cells, a GFP-tagged Yap1 fails to localise to nuclei in response to H_2O_2, whereas nuclear localisation in response to diamide is unaffected (Veal *et al.*, 2003). In the nucleus, activated Yap1 binds the Yap1 response element (YRE) in the promoter of Yap1-regulated genes. Fernandes *et al*. (1997) showed that Yap1 preferentially recognises the conserved TTACTAA motif, consisting of a pair of inverted TTA half-sites. The promoter of *TRX2*, one of the first identified Yap1 targets, contains two such elements and Trx2 deactivates the pathway by reducing both the Gpx3 sensor and Yap1, demonstrating the cyclic nature of redox signalling (Delaunay *et al.*, 2002, Kuge & Jones, 1994). However, not all Yap1-regulated genes contain the conserved YRE motif (Krems *et al.*, 1996, Toone *et al.*, 1998). He & Fassler (2005) identified alternative Yap1 recognition motifs, capable of binding Yap1 and mediating the oxidative stress response, to explain the lack of canonical YRE motifs in *YAP1*-dependent genes such as *CCP1, CTT1*, *TSA1* and *AHP1* (He & Fassler, 2005, Mulford & Fassler, 2011).

S. pombe Pap1 transcription factor

S. pombe Pap1 is the homologue of *S. cerevisiae* Yap1 and also plays a central role in activating gene expression in response to oxidative stress. While the overall degree of sequence conservation between Yap1 and Pap1 is relatively low (20% identity and 34% similarity), they do share considerable sequence similarity within the bZIP and CRD domains (Toone *et al.*, 1998). This extends to functional homology as, similar to Yap1, H_2O_2 triggers formation of disulfide bridges between the n- and c-CRD, and the c-CRD is sufficient for sensing thiol-reactive compounds such as diethylmaleate. Like Yap1, Pap1 is regulated by changes in its subcellular localisation with redistribution from the cytoplasm to the nucleus in response to oxidative stress (Vivancos *et al.*, 2004). Nuclear-localised Pap1 binds response elements very similar to the canonical YRE (TTACGTAA and TTAGTAA) (Fujii *et al.*, 2000). A point of difference to the Gpx3-Yap1 pathway is that Tpx1, a peroxiredoxin, serves as the H_2O_2 sensor for Pap1. The inherent susceptibility of peroxiredoxins to hyperoxidation and inactivation restricts this pathway to sensing low levels of peroxide stress (Vivancos 2005). Furthermore, unlike *S. cerevisiae*, *S. pombe* does not appear to possess a gene encoding a Ybp1-like protein. Interestingly, in an *S. cerevisiae* strain containing a nonsense mutation in *YBP1*, Tsa1, the homologue of *S. pombe* Tpx1, rather than Gpx3 is then required for Yap1 activation

(Okazaki *et al.*, 2005). This suggests that the presence or absence of a functional Ybp1 protein influences whether a GPx or Prx activates the AP-1 transcription factor.

AP-1 transcription factors in filamentous fungi

AP-1 homologues have been identified in a range of other fungi including *Candida albicans* CAP1 (Alarco & Raymond, 1999), *Aspergillus fumigatus* AfYAP1 (Qiao *et al.*, 2008), *Cochliobolus heterostrophus* CHAP1 (Lev *et al.*, 2005), *Alternaria alternata* AaAP1 (Lin *et al.*, 2009), *Botrytis cinerea*, BcAP1 (Temme & Tudzynski, 2009), *Neurospora crassa* NcAP1 (Tian *et al.*, 2011), *Magnaporthe oryzae* MoAP1 (Guo *et al.*, 2011) and *Ustilago maydis* Yap1 (Molina & Kahmann, 2007). Disruption of these transcription factors commonly results in conidial or hyphal sensitivity to H_2O_2 and may be accompanied by sensitivity to other oxidative stress-inducing compounds such as *t*-BOOH, potassium superoxide, menadione and diamide, as summarised in Table 1.1. Functional studies have shown that regulation through control of nuclear import and export is a common feature shared by these AP-1-like proteins. Functional domains and motifs characteristic of AP-1 proteins (bZIP, n-CRD, c-CRD, NES and NLS) are found in these proteins, however, the domain structure of the n-CRD varies between yeast and filamentous fungal species. Specifically the number, spacing and conservation of the cysteine residues within the n-CRD differs between yeast and filamentous fungi. This is reflected in their phylogenetic relationships, which indicate AP-1 proteins of filamentous fungi and unicellular yeast have diverged into two separate clades (Lin *et al.*, 2009). Additionally, *YAP*-like genes more closely related to *S. cerevisiae* Yap3, Yap4, Yap6 and Yap8 are also present in filamentous fungi including *N. crassa, M. grisea* and *A. nidulans*. However, the role of these homologues in relation to stress protection remains largely unexplored (Tian *et al.*, 2011).

1.3.4 Role of AP-1-like transcription factors in fungal-plant interactions

The role of these bZIP transcription factors in phytopathogenic fungi has received much attention given their recurring involvement in detoxification of host-generated ROS and therefore virulence. As mentioned previously, plant-derived ROS produced in the oxidative burst is a defence strategy only effective against biotrophic pathogens. Necrotrophic pathogens, which thrive on dead plant tissue, may exploit this host defence strategy for their pathogenicity (Govrin & Levine, 2000). In line with this, AP-1 deletion mutants of biotrophic fungi *U. maydis* and *M. oryzae* display hypersensitivity to H_2O_2 and impaired virulence (Guo *et al.*, 2011, Molina & Kahmann, 2007). Following this rationale it would be expected that deletion of the AP-1 homologue in a

necrotrophic fungus would not impair virulence of the fungus and indeed this is observed for such fungi as *C. heterostrophus* and *B. cinerea* (Lev *et al*., 2005, Temme & Tudzynski, 2009). However, there are exceptions to this generalisation, as the AP-1 mutant of *A. alternata,* despite its necrotrophic lifestyle, is unable to successfully colonise its plant host. The effect on fungal virulence resulting from the deletion of the AP-1-encoding gene in various plant pathogenic fungi is summarised in Table 1.2.

Table 1.2 Virulence phenotype of phytopathogenic *AP-1* mutants

Species	Lifestyle	Virulence of AP-1 mutant	Reference
C. heterostrophus	necrotrophic	virulent	Lev *et al*., 2005
U. maydis	biotrophic	avirulent	Molina & Kahmann, 2007
A. alternata	necrotrophic	avirulent	Lin *et al*., 2009
B. cinerea	necrotrophic	virulent	Temme & Tudzynski, 2009
M. oryzae	biotrophic	avirulent	Guo *et al*., 2011

1.3.5 Role of AP-1-like transcription factors in plant infection

Visualisation of the subcellular localisation of GFP-tagged Yap1 proteins during infection has revealed they play a role in early stages of plant infection in both biotrophic and necrotrophic fungal pathogens. Immediately after the penetration of maize leaves by *U. maydis,* Yap1-GFP relocalises from the cytoplasm to the nucleus until the onset of rapid fungal proliferation, suggesting during this initial infection period *U. maydis* encounters oxidative stress, which induces a Yap1-mediated response (Molina & Kahmann, 2007). *C. heterostrophus* GFP-CHAP1 also localises to the nucleus very early during the infection process. Nuclear localisation of CHAP1 is observed in germ tubes on the leaf surface even before they penetrate the leaf cuticle. During further progression of plant infection, CHAP1 remains in the nuclei of hyphae which are growing within the plant, whereas in hyphae proliferating on the leaf surface CHAP1 redistributes to the cytoplasm, suggesting that two very different environments with respect to oxidative stress are encountered by the fungus within and on the surface of the leaf. The activation and localisation of an AP-1 protein in a symbiotic fungus such as *E. festucae* during the colonisation is of great interest and would provide intriguing insight into the redox environment encountered by the fungus during the symbiosis.

1.3.6 Role of AP-1-like transcription factors in metabolite production

Yap1 and Yap1-like proteins have also been implicated in the production of, and response to, a variety of metabolites. In *S. cerevisiae* Yap1 is reversibly activated by methylglyoxal (MG), a natural glycolysis-derived metabolite. MG activation of Yap1 is achieved independently of Gpx3 and only c-CRD cysteines of Yap1 are necessary for MG activation, suggesting the mechanism is similar to that of thiol-reactive chemicals rather than the peroxide-induced disulfide bond activation mechanism (Maeta *et al.*, 2004).

In other fungi, Yap-like proteins regulate the production of primary and secondary metabolites. The Yap1 homologue in *Ashbya gossypii*, AgYap1, is required for riboflavin synthesis, a compound it overproduces in response to environmental stresses. Deletion of AgYap1 attenuates the oxidative stress-induced expression of the riboflavin biosynthetic gene, RIB4, with the concomitant reduction in riboflavin production. A further point of interest to the AgYap1 protein is the complete lack of CRDs, which are present in the Yap1 of the closely related *Eremothecium cymbalariae*. AgYap1 contains only two Cys residues with one of those located within the conserved bZIP domain. Regulation of AgYap1 is thus achieved through an oxidative stress-induced increase in *AgYAP1* gene expression, representing a novel mechanism of oxidative regulation of a Yap1 homologue (Walther & Wendland, 2012).

In *A. nidulans* a Yap-like protein regulates the production of sterigmatocystin, an anti-insect secondary metabolite (SM) that plays a key role in protecting *A. nidulans* colonies from fungivorous insects. RsmA (restorer of secondary metabolism), which is most closely related to *S. cerevisiae* Yap3, influences sterigmatocystin levels by inducing expression of genes encoding AflR and AflJ, a C6 transcription factor and an early regulatory factor, both required for sterigmatocystin biosynthesis (Yin *et al.*, 2012).

1.4 Redox sensors

As outlined above, the oxidation of AP-1 proteins Yap1 and Pap1 is not direct. Rather, the redox signal (H_2O_2) is primarily sensed by thiol peroxidases and transduced to the Yap1 or Pap1 via a cysteine thiol-disulfide exchange mechanism (D'Autreaux & Toledano, 2007). In the Yap1-Gpx3 redox relay, H_2O_2 reacts with the Cys-36 of Gpx3, oxidizing it to a sulfenic acid. The Cys-36-SOH then reacts with a cysteine (Cys-598) located in the C-terminal cysteine-rich domain (C-CRD) of Yap1, forming an intermolecular disulfide which, by thiol disulfide exchange, is rearranged

to an intermolecular disulfide between Cys-598 and Cys-303 in the N-terminal CRD of Yap1 (Wood *et al*., 2003a) (Figure 1.6). Using tandem mass spectrometry (MS/MS) Delaunay *et al*. (2002) confirmed disulfide linkages between Gpx3 and the c-CRD of Yap1. Specifically, prior to the formation of the first Yap1 intramolecular disulfide, Gpx3 Cys 36 bridges Yap1 Cys 598 by a disulfide (Delaunay *et al*., 2002). The second disulfide bridge between Cys-310 and Cys629 of Yap1 is presumably formed by a second oxidation cycle with Gpx3. The two disulfide bridges are located near each other on the surface of Yap1 and their formation disrupts the interaction of Crm1 with the nuclear export sequence (NES) of Yap1 (Figure 1.5B) (Wood *et al*., 2004, Yan *et al*., 1998). Once the NES is no longer accessible, the nuclear localisation signal (NLS) directs nuclear accumulation of Yap1, resulting in increased expression of Yap1 target genes. Activation of Pap1 by Tpx1 in *S. pombe* is thought to occur via the same basic catalytic mechanism involving the active-site Cys48 of Tpx1 and conserved Cys residues within Pap1 (Vivancos *et al*., 2005). Using non-reducing SDS PAGE coupled with western analysis Vivancos *et al*. (2005) detected an interaction between Tpx1 Cys48 and, most likely, Pap1 Cys501 or Cys532, both of which are located within the c-CRD. In a mechanism analogous to that of *S. cerevisiae* Yap1, the H_2O_2-induced Tpx1-Pap1 mixed disulfide is rearranged to form an intramolecular disulfide within the Pap1 target.

Gpx3 and Tpx1 also function as antioxidants, an activity due to their thiol-dependent peroxidase activity and independent of their aforementioned roles as redox sensors. The sulfenic acid intermediate can also react with a second resolving cysteine (Gpx3-Cys82 and Tpx1Cys169) within the proteins, forming an intramolecular disulfide bond accompanied by the detoxification of H_2O_2 to water and oxygen. Oxidised Gpx3 and Tpx1 are then recycled by the action of thioredoxin.

1.4.1 Thiol peroxidases

Thiol-dependent peroxidases are ubiquitous non-heme enzymes that function as antioxidants by catalyzing the reduction of various peroxides. Originally identified on the basis of their antioxidant capabilities, they are now emerging as important regulators of redox signalling (Inoue *et al*., 1999, Rhee *et al*., 1994, Rhee *et al*., 2012). Their catalytic activities are dependent on thiol groups of critical cysteine residues, hence their 'thiol-dependence'. Historically, thiol peroxidases have been divided into two major groups: peroxiredoxins (Prxs) and glutathione peroxidases (GPxs), based on the species involved in the regeneration of the reduced enzyme. Until recently it was thought that recycling of GPxs was strictly dependent on glutathione and Prxs on thioredoxin, however, as discussed below, exceptions to this general rule exist.

S. pombe possesses three Prx genes (TPX1, BCP and PMP20) and one GPx gene (GPX1). In comparison, five Prx genes (TSA1, TSA2, PRX1, DOT5 and AHP1) and 3 GPx genes (GPX1, GPX2 and GPX3) have been identified in *S. cerevisiae* (Kim *et al.*, 2010). GPX1 and GPX3 are paralogues retained after the whole genome duplication (WGD), whereas the duplicated copy of GPX2 appears to have been lost from the genome based on Yeast Gene Order Browser (YGOB) output (http://wolfe.gen.tcd.ie/ygob) or has arisen as a result of subsequent local duplication after the WGD event.

The GPx family is further divided into seleno-GPxs (S-GPxs) and nonseleno-GPxs (NS-GPxs), based on whether a cysteine or selenocysteine amino acid is involved in catalysis. The Prx family can be further subdivided into three classes, 1-Cys, typical 2-Cys and atypical 2-Cys, based on the presence and position of cysteine residues involved in catalysis (Table 1.3). As is often seen in rapidly emerging fields, reclassification leads to confusion regarding Prx nomenclature. For example the widely accepted PREX: PeroxiRedoxin classification index, a database of Prx subfamily assignments, groups mammalian Prx1-4 within the Prx1 subfamily (http://csb.wfu.edu/prex/index.php). Also, one of the six subfamilies is designated 'Tpx'. This is ambiguous because thiol peroxidase (Tpx) refers to Prxs not only within the Tpx subfamily but also the entire Prx family. Additionally, all three types of Prxs, 1-Cys, typical 2-Cys and atypical 2-Cys, can be found in more than one subfamily, further adding to the confusion.

Table 1.3 Thiol peroxidase subfamilies

Thiol Peroxidases	
Peroxiredoxins	Glutathione Peroxidases
1-Cys Prx	S-GPx
Typical 2-Cys Prx	NS-GPx
Atypical 2-Cys Prx	

Prx and GPx enzymes belong to the thioredoxin-fold (Trx-fold) class of proteins; a large grouping which also includes Trxs, glutaredoxins (Grxs), disulfide bond (Dsb) proteins and glutathione-S-transferases (GSTs). Whilst the protein families belonging to the Trx-fold class are numerous and diverse, they share a similar structural motif consisting of four β-strands clustered as a central β-sheet sandwiched by three α-

helices and a common active site motif (CXXC) and are thought to have evolved from a common thioredoxin-like ancestor (Atkinson & Babbitt, 2009).

Mechanism

Glutathione peroxidases and peroxiredoxins catalyze the reduction of hydrogen peroxide and alkyl hydroperoxides to water and alcohol, respectively, and rely on a conserved cysteine residue to carry out catalysis. The catalytic cysteine is oxidised to a sulfenic acid intermediate, which is resolved by a second cysteine forming an intramolecular disulfide. The disulfide bond is reduced by a second donor thiol, i.e. GSH or Trx, recycling the enzyme and completing the catalytic cycle.

Until recently it was commonly thought that reducing equivalents were supplied to GPxs by glutathione (GSH) and to Prxs by thioredoxin (Trx). However, many studies have now shown that not all Prxs use Trx as a reducing substrate and, in fact, some GPxs use reduced Trx for their regeneration (Tanaka *et al.*, 2005b, Rouhier *et al.*, 2005, Rouhier *et al.*, 2002). Based on sequence and structural homology, the three NS-GPxs of *S. cerevisiae* (Gpx1, Gpx2 and Gpx3) are phylogenetically similar to the mammalian phospholipid hydroperoxide glutathione peroxidase (PHGPx), a seleno-GPx. However, unlike mammalian GPxs, which are reduced by GSH, Trx is strictly required for the recycling of yeast Gpx3 and, to a lesser extent, Gpx2, which can also be reduced by GSH albeit at a lower efficiency than that achieved by Trx (Delaunay *et al.*, 2002, Tanaka *et al.*, 2005b). Although distinct yeast GPx and Tpx gene families emerged early during molecular evolution (Tanaka *et al.*, 2005b), given the preference for Trx as an electron donor, functionally yeast GPxs more closely resemble atypical 2-Cys Prxs (Inoue *et al.*, 1999).

Peroxiredoxin mechanisms

1-Cys, typical 2-Cys and atypical 2-Cys Prxs all share the same basic catalytic mechanism, in which the redox-active or peroxidatic cysteine (C_p) attacks the peroxide substrate, resulting in the formation of a sulfenic acid derivative of the enzyme (Wood *et al.*, 2003b). The presence and location of the resolving cysteine (C_R) and hence the recycling of the oxidised cysteine sulfinic acid is what differentiates the three types of enzyme. Typical 2-Cys Prxs are homodimeric. H_2O_2 oxidises the C_p of one subunit to a sulfenic acid (SOH) and the C_R, located in the second subunit, then reacts with the sulfenic acid to form a disulfide bridge. The intersubunit disulfide is reduced by Trx, regenerating the catalytically active thiol form of Prx. The resulting disulfide in the active site of Trx is then reduced by thioredoxin reductase (TR), using NADPH as an

electron donor. The catalytic cycle for atypical 2-Cys Prxs, such as *S. cerevisiae* Gpx1, Gpx2 and Gpx3, is similar except that the C_p and the C_R are contained within a single Prx subunit and thus the disulfide reduced by Trx is intramolecular (Tanaka *et al.*, 2005b, Wood *et al.*, 2003b). 1-Cys Prxs contain a conserved C_p but lack a C_R and the mechanism of reducing and recycling 1-Cys Prxs has been a point of uncertainty and great interest. Several small molecules, including glutathione, ascorbate, lipoic acid and cyclophilin A, are able to reduce various 1-Cys Prxs, however, the bona fide physiological electron donor for 1-Cys peroxiredoxins remains unclear (Greetham & Grant, 2009, Lee *et al.*, 2001, Peshenko & Shichi, 2001), (Figure 1.7).

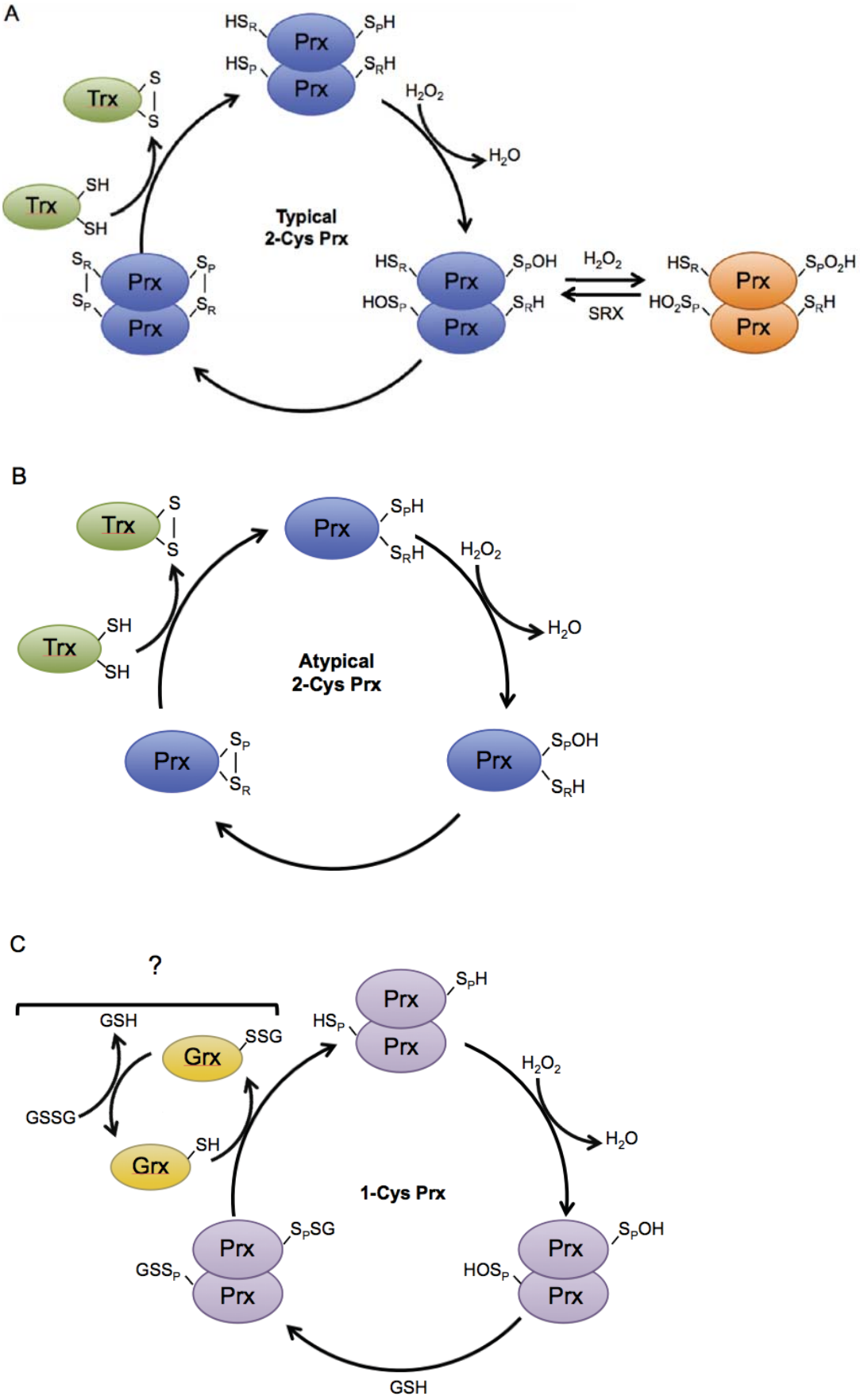
A
Trx
Trx
Prx
Prx
Typical
2-Cys Prx
H_2O_2
H_2O
SRX
B
Trx
Trx
Prx
Prx
Atypical
2-Cys Prx
H_2O_2
H_2O
C
?
GSH
GSSG
Grx
Grx
SSG
SH
Prx
Prx
1-Cys Prx
H_2O_2
H_2O
GSH

Figure 1.7 Peroxiredoxin mechanisms. The first step of peroxide reduction involves nucleophilic attack by the peroxidatic cysteine (S_PH) and formation of the cysteine sulfenic acid intermediate (S_POH) and is common to all Prxs. (A) Typical 2-Cys Prxs are homodimers that reduce H_2O_2 with a peroxidatic Cys-S_PH that oxidises to a Cys-SOH. The Cys-SOH then condenses with the resolving Cys-S_RH of the other subunit to form a disulfide, reduced by thioredoxin (TRX). (B) Atypical 2-Cys Prxs are monomers and the peroxidatic Cys-SOH condenses with the resolving Cys-S_RH on the same subunit to form an intramolecular disulfide, reduced by thioredoxin (TRX). (C) 1-Cys Prx are homodimers and contain only the peroxidatic Cys-S_PH but not the resolving Cys-S_RH. The exact regeneration mechanism remains unclear but may involve the glutaredoxin-glutathione system or other low molecular weight thiols. Figure adapted from (D'Autreaux & Toledano, 2007, Noguera-Mazon *et al.*, 2006, Wood *et al.*, 2003b).

Overoxidation

During the catalytic cycle, before it is able to form a disulfide, the sulfenic acid (Cys-SOH) of Prxs can be further oxidised by H_2O_2 to a sulfinic acid (SO_2H), a form which cannot be recycled by Trx1. This results in inactivation of the enzyme but is reversible by sulfiredoxin (SRX), an enzyme with sulfinic acid reductase activity, in an ATP-dependent manner (Biteau *et al.*, 2003). Reversible inactivation of *S. pombe* Tpx1 is observed when cells are exposed to elevated concentrations of H_2O_2, blocking both its role as a Pap1-redox sensor and an antioxidant. It has recently been proposed that hyperoxidation of Tpx1 to the Trx1-resistant sulfinic (SO_2H) form and temporary inactivation of the Tpx1-Pap1 redox relay is a crucial survival strategy to divert Trx1 towards other oxidised proteins, allowing their repair in times of acute oxidative stress (Day *et al.*, 2012). At high levels of H_2O_2 the Spc1/Sty1 MAPK pathway prevails. Spc1/Sty1, activated by Tpx1 in a thioredoxin peroxidase-independent manner, which is required for reactivation of the Tpx1-Pap1 redox relay as expression of the sulfiredoxin Srx1, depends on a Spc1/Sty1 transcriptional response (Vivancos *et al.*, 2005). This interplay of the signalling pathways represents an elegant system employed by *S. pombe* to fine tune the response to low and high levels of H_2O_2 (Veal *et al.*, 2004). This adaptation is thought to be specific to eukaryotic 2-Cys Prxs as prokaryotic Prxs are relatively resistant to overoxidation and furthermore lack a sulfiredoxin enzyme. Eukaryotic 1-Cys Prxs are also relatively resistant to overoxidation. Still, overoxidation of 1-Cys Prxs has been reported (Peshenko & Shichi, 2001), but the overoxidised sulfinic acid is not recycled by SRX. To date, only the 2-Cys Prx enzymes have been shown to cycle between thiol and sulfinic acid states, for 1-Cys Prxs and prokaryotic Prxs sulfinic acid formation may be an irreversible process associated with protein damage (Woo *et al.*, 2005). Interestingly, despite the functional resemblance of these yeast GPxs to 2-Cys Prxs, overoxidation has not been widely, if at all, reported for these enzymes.

Regulation of gene expression

In addition to a major antioxidant role Prxs and GPxs have been implicated as major regulators of gene expression, exemplified above by the Gpx3- and Tpx1-dependent activation of Yap1 and Pap1, respectively. The catalytic cysteine residues allow them to function as second messengers in thiol-based redox signalling systems as oxidative signals can be transferred, via these thiol groups, from peroxides to target proteins, thus activating transcriptional programs. Given the key role of thiol peroxidases in scavenging peroxides, in an *S. cerevisiae* strain lacking all five Prxs (Tsa1, Tsa2, Ahp1, nPrx, and mPrx) and all three GPxs (Gpx1, Gpx2, Gpx3), a rise in cellular

peroxide levels and a concomitant stimulation of gene expression in response to H_2O_2 may be expected. However, the converse was observed; H_2O_2-dependent changes in gene expression were disrupted in the thiol peroxidase null cells (Fomenko *et al.*, 2011). The disruption of peroxide-induced transcriptional response suggests the disruption of signalling pathways from H_2O_2 to transcription factors. Thus thiol peroxidases perform two roles in the cell: oxidation of target proteins and antioxidant defence (Fomenko *et al.*, 2011).

Peroxiredoxins and signalling

Although peroxiredoxins are now well-established regulators of redox-sensitive signalling, how they mediate these effects has not been fully resolved. Several plausible models to explain how they participate in peroxide-mediated cell signalling exist, including primarily the Redox Relay and Floodgate models.

The redox relays of yeast Gpx3-Yap1 and Tpx1-Pap1 are two well-characterised mechanisms for transmitting peroxide-based signals, however, it has remained unclear whether the protein oxidase functions of Gpx3 and Tpx1 are yeast-specific adaptations or whether they represent a more general principle of redox signalling. Recent work by Jarvis *et al*. (2012) in mammalian systems has shown that, under oxidative conditions, peroxiredoxin Prdx1 catalyses the oxidation of the Apoptosis signal-regulating kinase 1 (ASK1), a MAPKKK that activates JNK and p38 kinases, through transient formation of a Prdx1-ASK1 disulfide-linked complex. 'Mediated oxidation' by peroxiredoxins may be a widespread signalling mechanism.

The predisposition of eukaryotic Prxs to overoxidation has led to the development of the 'floodgate' hypothesis, by which the potent antioxidant capacity of Prxs keep basal H_2O_2 levels low, while permitting higher levels during signal transduction. During a signalling event, elevated H_2O_2 levels inactivate Prxs and permit the oxidation of less reactive redox signalling proteins (D'Autreaux & Toledano, 2007, Wood *et al*., 2003b). The reversibility of overoxidation of 2-Cys Prxs by sulfiredoxin provides an attractive model for signalling (Biteau *et al*., 2003). Much less is known about the overoxidation of 1-Cys Prxs, thus a possible floodgate function for 1-Cys Prxs in redox signalling has received less attention (Peshenko & Shichi, 2001, Wood *et al*., 2003b).

1.5 Aims

Given the involvement of ROS, highly reactive and potentially toxic molecules, in regulating the *E. festucae-L. perenne* symbiosis, the aim of this research was to investigate the cellular mechanisms employed by *E. festucae* to sense and respond to elevated levels of ROS. Specifically, the involvement of the AP-1-like transcription factor pathway in the oxidative stress response of *E. festucae* in axenic culture and in its ryegrass host, *L. perenne,* was investigated. Additionally, candidate upstream components responsible for sensing and transmitting the initial oxidant signal to the *E. festucae* AP-1 protein were explored based on the well-characterised pathways of *S. cerevisiae* and *S. pombe.*

The first aim of this research was to characterise the AP-1 transcription factor of *E. festucae* and was achieved by addressing the following objectives:

1. Determine if *E. festucae* YapA is a functional homologue of the *S. cerevisiae* AP-1 transcription factor, Yap1.

To this end the *yapA* gene was expressed in *S. cerevisiae* Δ*yap1* cells to test whether it could functionally complement the oxidative stress sensitivity defect of the Δ*yap1* strain.

2. Determine if YapA is required for protecting *E. festucae* from various forms of ROS and ensuing oxidative stress in axenic culture.

This required deletion of the *yapA* gene by homologous recombination and observation of the cellular effects when Δ*yapA* mutant spores and mycelia were subjected to a range of ROS and ROS-inducing compounds.

3. Determine if YapA is involved in the oxidative stress response of *E. festucae* in its host, *L. perenne*.

Two approaches were taken to address this objective. Firstly, ryegrass seedlings were inoculated with the Δ*yapA* strain and the symbiotic phenotype was analysed. Secondly, the activation of YapA at the inoculation site of ryegrass seedlings, inferred by its subcellular location, was analysed using an EGFP-tagged version of YapA.

The second aim of this research was to characterise the *E. festucae* homologues of *S. cerevisiae* Gpx3 and *S. pombe* Tpx1 and to test whether they serve as redox sensors for the activation of YapA in *E. festucae*. This was achieved by addressing the following objectives.

1. Determine if *E. festucae* GpxC and TpxA are homologues of *S. cerevisiae* Gpx3 and *S. pombe* Tpx1, respectively.

Two approaches were taken to address this objective. Firstly, the *gpxC* gene was expressed in *S. cerevisiae* Δ*gpx3* cells to test whether it could functionally complement the oxidative stress sensitivity defect of the Δ*gpx3* strain. Secondly, homology of GpxC and TpxA was assessed using a phylogenetic approach.

2. Determine if *E. festucae* GpxC and TpxA are involved in sensing and responding to ROS in axenic culture.

This required single Δ*gpxC* and Δ*tpxA* and double Δ*gpxC*Δ*tpxA* mutants to be created through homologous recombination, then observing the cellular effects when the mutant strains were subjected to a range of ROS and ROS-inducing compounds.

3. Determine if *E. festucae* GpxC and TpxA are responsible for activation of YapA under conditions of oxidative stress.

Activation of YapA, inferred by nuclear localization, in the Δ*gpxC,* Δ*tpxA* and Δ*gpxC*Δ*tpxA* mutant backgrounds was analysed using a GFP-tagged version of YapA. This experiment was performed in culture with exogenously supplied ROS (H_2O_2) and *in planta* at the inoculation site of ryegrass seedlings.

2 *Materials and Methods*

2.1 Strains and plasmids

Organisms and plasmids used in this study are listed in Table 2.1.

Table 2.1. Organisms and plasmids used in this study

Strain	Relevant characteristic(s)	Source or reference
S. cerevisiae		
PN2735	BY4741; MAT**a**; his3Δ1; leu2Δ0; met15Δ0; ura3Δ0 (wild type)	Euroscarf, Frankfurt
PN2736	BY4741; MAT**a**; his3Δ1; leu2Δ0; met15Δ0; ura3Δ0; YML007w::kanMX4 (Δ*yap1*)	Euroscarf, Frankfurt
PN2737	BY4741; MAT**a**; his3Δ1; leu2Δ0; met15Δ0; ura3Δ0; YIR037w::kanMX4 (Δ*gpx3*)	Euroscarf, Frankfurt
PN2845	BY4741; MAT**a**; his3 Δ 1; leu2 Δ 0; met15 Δ 0; ura3Δ0; YML007w::kanMX4 pGC8 (Δ*yap1*/*ScYAP1*)	This study
PN2846	BY4741; MAT**a**; his3Δ1; leu2Δ0; met15Δ0; ura3Δ0; YML007w::kanMX4 pGC6 (Δ*yap1*/*EfYapA*)	This study
PN2847	BY4741; MAT**a**; his3Δ1; leu2Δ0; met15Δ0; ura3Δ0; YML007w::kanMX4 pYES2 (Δ*yap1*/pYES2)	This study
PN2848	BY4741; MAT**a**; his3Δ1; leu2Δ0; met15Δ0; ura3Δ0; YIR037w::kanMX4 pGC7 (Δ*gpx3*/*ScGPX3*)	This study
PN2849	BY4741; MAT**a**; his3Δ1; leu2Δ0; met15Δ0; ura3Δ0; YIR037w::kanMX4 pGC5 (Δ*gpx3*/*EfGpxC*)	This study
PN2850	BY4741; MAT**a**; his3Δ1; leu2Δ0; met15Δ0; ura3Δ0; YIR037w::kanMX4 pYES2 (Δ*gpx3*/pYES2)	This study
PN2871	BY4741; MAT**a**; his3Δ1; leu2Δ0; met15Δ0; ura3Δ0 (WT / pGC18)	This study
PN2872	BY4741; MAT**a**; his3Δ1; leu2Δ0; met15Δ0; ura3Δ0; YML007w::kanMX4 (Δ*yap1* / pGC18)	This study
PN2873	BY4741; MAT**a**; his3Δ1; leu2Δ0; met15Δ0; ura3Δ0; YIR037w::kanMX4 (Δ*GPX3*/pGC18)	This study
E. festucae		
PN2278	Wild type (Fl1)	(Young *et al.*, 2005)
PN2739	Fl1 / Δ*yapA*::P*trpC-hph*; Hyg^R (Δ*yapA*#243)	This study
PN2740	Fl1 / Δ*yapA*::P*trpC-hph*; Hyg^R (Δ*yapA*#145)	This study
PN2787	Δ*yapA*/*yapA;* PN2739 / pGC11; Hyg^R; Gen^R (Δ*yapA*#243 / *yapA*)	This study
PN2788	Δ*yapA*/*yapA;* PN2740 / pGC11; Hyg^R; Gen^R (Δ*yapA*#145 / *yapA*)	This study
PN2741	Fl1 / Δ*gpxC*::P*trpC-npt*II-T*trpC*; Gen^R (Δ*gpxC*#10)	This study
PN2742	Fl1 / Δ*gpxC*::P*trpC-npt*II-T*trpC*; Gen^R (Δ*gpxC*#34)	This study
PN2821	Fl1 / Δ*tpxA*::P*trpC-hph*; Hyg^R (Δ*tpxA*#105)	This study
PN2822	Fl1 / Δ*tpxA*::P*trpC-hph*; Hyg^R (Δ*tpxA*#157)	This study
PN2828	PN2821 / Δ*gpxC*::P*trpC-npt*II-T*trpC*; Hyg^R; Gen^R (Δ*gpxC*Δ*tpxA*#128)	This study
PN2829	PN2821 / Δ*gpxC*::P*trpC-npt*II-T*trpC*; Hyg^R; Gen^R (Δ*gpxC*Δ*tpxA*#133)	This study
PN2830	PN2821 / Δ*gpxC*::P*trpC-npt*II-T*trpC*; Hyg^R; Gen^R (Δ*gpxC*Δ*tpxA*#168)	This study
PN2831	PN2821 / Δ*gpxC*::P*trpC-npt*II-T*trpC*; Hyg^R; Gen^R (Δ*gpxC*Δ*tpxA*#22)	This study

PN2789	PN2741/ pGC9/pJW19/pAN8-1; Hyg^R, Gen^R, Zeo^R (Δ*gpxC:: GFP-yapA, DsRed-stuA(NLS)*)	This study
PN2790	PN2278/pGC9, pJH19; Hyg^R (Fl1::*GFP-yapA, DsRed-stuA(NLS)*)	This study
PN2823	PN2821/pGC10/ pJW19/pSF17.8; Hyg^R; Gen^R (Δ*tpxA:: GFP-yapA, DsRed-stuA(NLS)*)	This study
PN2824	PN2278/pGC13; Gen^R (Fl1::*PcatA-EGFP*)	This study
PN2836	PN2739/pGC14; Hyg^R, Gen^R (Δ*yapA#*243*::PcatA-EGFP-CL1#*1)	This study
PN2837	PN2739/pGC14; Hyg^R, Gen^R (Δ*yapA#*243*::PcatA-EGFP-CL1#*4)	This study
PN2838	PN2278/pGC14; Gen^R (Fl1::*PcatA-EGFP-Cl1#*8)	This study
PN2839	PN2278/pGC14; Gen^R (Fl1::*PcatA-EGFP-Cl1#*9)	This study
PN2840	PN2278/pGC14; Gen^R (Fl1::*PcatA-EGFP-Cl1#*10)	This study
PN2841	PN2278/pGC14; Gen^R (Fl1::*PcatA-EGFP-Cl1#*11)	This study
PN2842	PN2740 Δ*yapA#*145/pGC14; Hyg^R, Gen^R (Δ*yapA#*145*::PcatA-EGFP-CL1#*1)	This study
PN2843	PN2740/pGC14; Hyg^R, Gen^R (Δ*yapA#*145*::PcatA-EGFP-CL1#*9)	This study
PN2844	PN2739 Δ*yapA#*243/pGC14; Hyg^R, Gen^R (Δ*yapA#*243*::PcatA-EGFP-CL1#*10)	This study
PN2851	PN2830/pGC9/pJW19/pAN8-1; Hyg^R, Gen^R, Zeo^R (Δ*gpxC*Δ*tpxA:: GFP-yapA, DsRed-stuA(NLS)*)	This study
PN2874	PN2278/pGC19/pJW19; Hyg^R (Fl1::*YAP1-EGFP, DsRed-stuA(NLS)*)	This study
PN2879	PN2739/pGC11/pGC14; Hyg^R, Gen^R (Δ*yapA#*243/*yapA::PcatA-EGFP-CL1#*1)	This study
E. coli		
PN4101	One Shot® TOP10/pGC4; Amp^R	This study
PN4103	One Shot® TOP10/pGC2; Amp^R	This study
PN4107	One Shot® TOP10/pGC6; Amp^R	This study
PN4108	One Shot® TOP10/pGC5; Amp^R	This study
PN4109	One Shot® TOP10/pGC7; Amp^R	This study
PN4110	One Shot® TOP10/pGC8; Amp^R	This study
PN4112	One Shot® TOP10/pGC10; Amp^R	This study
PN4113	One Shot® TOP10/pGC9; Amp^R	This study
PN4133	One Shot® TOP10/pGC11; Amp^R	This study
PN4135	One Shot® TOP10/pGC12; Amp^R	This study
PN4151	One Shot® TOP10/pGC13; Amp^R	This study
PN4174	One Shot® TOP10/pGC14; Amp^R	This study
PN4188	One Shot® TOP10/pGC16; Amp^R	This study
PN4193	One Shot® TOP10/pGC18; Amp^R	This study
PN4194	One Shot® TOP10/pGC19; Amp^R	This study

PN1390	One Shot® TOP10/pAN8-1; Amp^R	(Mattern *et al.*, 1988)
PN1862	One Shot® TOP10/pSF15.15; Amp^R	S. Foster
PN1866	One Shot® TOP10/pSF17.8; Amp^R	S. Foster
PN1687	One Shot® TOP10/pII99; Amp^R	(Namiki *et al.*, 2001)
PN4111	One Shot® TOP10/pPN94; Amp^R	(Takemoto *et al.*, 2006)
PN4134	One Shot® TOP10/pJW19; Amp^R	(Toews *et al.*, 2004)
PN4201	One Shot® TOP10/pYES2; Amp^R	Invitrogen
Plasmids		
pGC2	1.1-kb *Bgl*II/*Kpn*I fragment 5′ of *yapA* amplified with yap1/yap2 and 1.2-kb *Hind*III/*Xho*I fragment 3′ of *yapA* amplified with yap3/yap4 in pSF15.15	This study
pGC4	1.1-kb *Bgl*II/*Kpn*I 5′ of *gpxC* amplified with gpx1/gpx2 and 1.4-kb *Sal*I/*Sal*I fragment 3′ of *gpxC* amplified with gpx3/gpx4 in pSF17.8	This study
pGC5	0.5-kb *Eco*RI/*Xba*I *gpx*C cDNA fragment amplified with gpx5/gpx6 in pYES2	This study
pGC6	1.7-kb *Eco*RI/*Xba*I *yapA* cDNA fragment amplified with yap5/yap6 in pYES2	This study
pGC7	0.5-kb *Hind*III/*Xba*I *gpx3* gDNA fragment amplified with gpx7/gpx8 in pYES2	This study
pGC8	1.9-kb *Hind*III/*Xba*I *yap1* gDNA fragment amplified with yap7/yap8 in pYES2	This study
pGC9	1.7-kb y *Eco*RI/*Cla*I *yapA* cDNA fragment amplified with yap27/yap28 and 0.8-kb *Cla*I/*NotI* EGFP fragment amplified with GCGFP1/GCGFP2 in *Eco*RI/*Not*I site of pPN94 (*yapA-EGFP*)	This study
pGC10	0.8-kb *Eco*RI/*Cla*I *EGFP* fragment amplified with EGFP1/EGFP2 and 1.7-kb *Cla*I/*Not*I *yapA* cDNA fragment amplified with yap29/yap30 in *Eco*RI/*Not*I site of pPN94 (*EGFP-yapA*)	This study
pGC11	3.7-kb *Eco*RV/*Eco*RI fragment from cosmid 28E7 in pSF17.8	This study
pGC12	2.3-kb *Bgl*II/*Kpn*I fragment 5′ of *tpxA* amplified with tpx1/tpx2 and 2.5-kb *Bam*HI/*Xba*I fragment 3′ of *tpxA* amplified with tpx3/tpx4 in pSF15.15	This study
pGC13	1-kb *Xba*I/*Eco*RI P*catA* fragment amplified with pcatA3/pcatA4, cloned into *Xba*I/*Eco*RI site of pGC10, 1.8-kb *Xba*I/*Xho*I P*catA-EGFP* fragment cloned into *Xba*I/*Xho*I fragment in pSF17.8 (P*catA-EGFP*)	This study
pGC14	1.2-kb *Sac*II/*Nde*I fragment containing a 48 bp insert 3′ of P*catA-EGFP* amplified in two steps with pCatAF1/CL1R1 and pCatAF1/CL1R2 and replacing the *Sac*II/*Nde*I fragment in pGC13 (P*catA-EGFP-CL1*)	This study
pGC16	1-kb P*tpxA* fragment amplified with tpx37/tpx41 and 0.7-kb EGFP-CL1 fragment amplified with tpx39/tpx40, recombined in yeast and *Xba*I/*Nde*I P*tpxA-EGFP-CL1* fragment cloned into *Xba*I/*Nde*I site of pSF17.8 (P*tpxA-EGFP-CL1*)	This study
pGC18	2.7-kb *Eco*RI/*Not*I *yap1-EGFP* fragment from pGC19 cloned into *Eco*RI/*Not*I site of pYES2 (P*GAL1-Yap1-EGFP*)	This study

pGC19	2.0-kb *Eco*RI/*Not*I *yap1* fragment amplified with ScYap6/ScYap8 and 0.7-kb *EGFP* fragment amplified with GCGFP3/GCGFP4, recombined in yeast and *Eco*RI/*Not*I *YAP1-EGFP* fragment cloned into *Eco*RI/*Not*I site of pPN94 (P*TEF-YAP1-EGFP*)	This study
pSF15.15	pSP72 containing 1.4-kb HindIII P*trpC-hph* from pCB1004 cloned into *Sma*I site Amp^R; Hyg^R	S. Foster
pSF17.8	Amp^R; Gen^R	S. Foster
pII99	P*trpC-npt*II-T*trpC*; Amp^R/Gen^R	(Namiki *et al.*, 2001)
pPN94	pSF14.14 containing 0.8-kb *Sal*I/*Xba*I *tef* promoter in *Xho*I/*Xba*I site and 0.6-kb *Eco*RI/*Bgl*II T*trpC* in *Eco*RI/*Bgl*II site	(Vanden Wymelenberg *et al.*, 1997)
pAN8-1	P*gpd-sh ble*-T*trpC*; Amp^R/Zeo^R	(Mattern *et al.*, 1988)
pJW19	P*gpd-DsRed-stuA*(NLS), argB+ in pBluescript KS-; Amp^R	(Toews *et al.*, 2004)
pYES2	Amp^R; URA3	Invitrogen
pCR4-TOPO®	Amp^R; LacZα-*ccdB*	Invitrogen
Cosmids		
28E7	pMO-cosX clone Fl1 genomic DNA cosmid library containing the *yapA* gene and 5′UTR.	This study

Alternative names are indicated in parentheses

2.2 Medium and growth conditions

Unless specified otherwise, all media were prepared with Nanopure water supplied by a Barnstead NANOpure ultrapure water purification system from Thermo Scientific and sterilised by autoclaving at 121°C for 20 min.

2.2.1 Escherichia coli

Escherichia coli cultures containing plasmids (Table 2.1) were grown overnight at 37°C in LB (Luria-Bertani) broth, with shaking (200 rpm) or on LB agar containing 100 μg/ml ampicillin as previously described (Miller 1972). For short-term storage of *E. coli* strains, cultures were streaked onto LB plates and stored at 4°C. For long term storage cultures were stored in 50% (v/v) glycerol at -80°C.

2.2.1.1 Luria-Bertani (LB) medium

LB liquid medium (Miller, 1972) contained 5 g/L tryptone, 10 g/L yeast extract and 5 g/L NaCl, pH 7.0-7.5. For solid media, agar was added at 15 g/L.

2.2.1.2 SOC medium

SOC medium (Dower *et al.*, 1988) contained 20 mM glucose, 10 mM $MgCl_2$, 10 mM $MgSO_4.7H_2O$, 10 mM NaCl, 2.5 mM KCl, 20 g/L tryptone and 5 g/L yeast extract.

2.2.2 Saccharomyces cerevisiae

S. cerevisiae cultures (Table 2.1) were grown on synthetic complete (SC) medium (2.2.2.1) or Yeast-extract Peptone Dextrose (YPD) medium (2.2.2.2) at 30°C for three days. Expression from the GAL1 promoter in the pYES2 vector was induced with the addition of 2% (w/v) galactose and 2% (w/v) raffinose or repressed with the addition of 2% (w/v) glucose to the medium. For short-term storage of *S. cerevisiae* strains, cultures were streaked onto SC plates and stored at 4°C. For long term storage cultures were stored in 20% (v/v) glycerol at -80°C.

2.2.2.1 Synthetic Complete (SC) medium

SC medium (Kaiser *et al.*, 1994) contained 0.67% (w/v) yeast nitrogen base without amino acids, 0.2% (w/v) drop-out mix (–His/–Leu/–Met/–Trp or –Ura), amino acids as required: 0.01% (w/v) leucine, tryptophan and uracil, 0.005% (w/v) histidine and methionine and 2% (w/v) agar. For solid media Noble agar (Difco) was added at 15

g/L. 2% (w/v) carbon source (glucose or galactose and raffinose) was added after autoclaving.

2.2.2.2 Yeast Peptone Dextrose (YPD) medium

YPD medium (Bergman, 2001) contained 2% (w/v) peptone (Difco) and 1% (w/v) yeast extract. For solid media Noble agar (Difco) was added at 15 g/L. 2% (w/v) glucose was added after autoclaving. Adenine-supplemented YPD (YPDA) contained 0.003% (w/v) adenine hemisulfate in addition to the trace amount of adenine that is naturally present in YPD.

2.2.2.3 Hydrogen peroxide sensitivity assays

Hydrogen peroxide (0.8 to 1.25 mM) was incorporated into SC agar cooled to 50°C. *S. cerevisiae* cells were grown to A_{600} of 1.0 and serial 10-fold dilutions of cultures (10 μl) were spotted onto plates. Growth was assessed after three days incubation at 30°C. Plates containing hydrogen peroxide were stored and incubated in the dark to prevent breakdown of the hydrogen peroxide.

2.2.3 Epichloë festucae

E. festucae strains were grown at 22°C on PD agar for 5-10 days or in liquid PD medium, shaking at 150 rpm for 5 days. Protoplasts were regenerated in soft RG agar containing antibiotic overlaid on 1.5% (w/v) RG agar (2.2.3.2). Where selection was required the cultures were overlaid with an additional layer of soft agar containing antibiotic. For short term storage of *E. festucae* strains, cultures were inoculated onto PD agar plates (2.2.3.1) and stored at 4°C. For long term storage, cultures were stored in 15% (v/v) glycerol at -80°C.

2.2.3.1 Potato dextrose (PD) medium

PD broth contained 24 g/L potato dextrose (Difco), pH 6.5. For solid media agar was added at 15 g/L. For antibiotic selection hygromycin or geneticin was added to final concentrations of 150 μg/mL and 200 μg/mL, respectively.

2.2.3.2 Regeneration (RG) medium

RG medium contained 24 g/L potato dextrose (Difco), 0.8 M sucrose, pH adjusted to 6.5. Agar was added to a final concentration of 8 g/L for soft agar overlays and 15 g/L for base agar layers.

2.2.3.3 Oxidative stress sensitivity assays

To assess the sensitivity of fungal strains to oxidative stress-inducing conditions, mycelial plugs 5 mm in diameter were inoculated onto PD agar supplemented with stress-inducing agents. Oxidative stress was induced by addition of 0.5 - 2 mM H_2O_2 (spores), 4-8 mM H_2O_2 (mycelia), 40 μM menadione, 1 mM diamide, 7 mM KO_2 and 0.25 mM *tert*-butyl hydroperoxide (*t*-BOOH). H_2O_2 stress was also induced by subculturing strains adjacent to autoclaved Whatman 3MM chromatography paper discs soaked in 0.3 – 30% (v/v) H_2O_2 or placing soaked discs next to 3 day old cultures to assess growth sensitivity of new and established colonies, respectively. Growth was assessed after ten to fourteen days incubation at 22°C. Plates containing hydrogen peroxide were stored and incubated in the dark to prevent breakdown of the hydrogen peroxide.

2.2.3.4 Microaerophilic growth conditions

To assess growth of *E. festucae* under microaerophilic conditions, cultures were grown under oxygen-limiting conditions. Strains were grown on PD or RG plates in aerobic conditions for 3 days then transferred to double zip locked bags (GLAD®) containing an AnaeroPack® sachet (Mitsubishi Gas Chemical Company, Inc., Japan) and a dry anaerobic indicator strip (BD GasPak™).

2.2.4 Lolium perenne

2.2.4.1 Water agar

Water agar medium contained 25 g/L agar.

2.2.4.2 Seedling growth conditions

Surface-sterile ryegrass seeds were transferred to water agar plates where the seeds were allowed to germinate for 7 days at 22°C in continuous darkness prior to inoculation. Inoculated seedlings were returned to the dark for a further 7 days to continue etiolation, then transferred to continuous light for a final 7 days before planting the seedlings in root trainers containing commercial potting mix.

2.2.4.3 Plant growth conditions

Ryegrass plants were incubated in a temperature (19°C) and light-controlled (16 h/8 h light/dark cycle) growth room. Plants were provided with water as necessary.

2.3 DNA isolation

2.3.1 Plasmid and cosmid DNA

For plasmid and cosmid isolation from *E. coli*, the bacteria were grown overnight to a density of 1.5 – 5.0 A_{600} units per mL. The cells were collected by centrifugation (17,000 x ***g***, 1 min) and isolation of plasmid or cosmid DNA was performed by alkaline lysis and extraction using the High Pure plasmid isolation kit (Roche) according to the manufacturer's instructions.

2.3.2 Fungal genomic DNA

2.3.2.1 DNA purification

2.3.2.1.1 Byrd method

Pure, high molecular weight fungal genomic DNA was extracted from freeze-dried mycelium by the method of Byrd *et al*. (1990). Thirty mg of freeze-dried mycelium was ground to a fine powder in liquid nitrogen and resuspended in 800 µL of lysis buffer (150 mM EDTA, 50 mM Tris-HCl, 1% (w/v) SLS, pH8) containing 2 mg/mL Proteinase K. Samples were incubated at 70°C for 30 min then centrifuged at 17,000 x ***g*** for 20 min. The supernatant was immediately transferred to a fresh tube and the DNA purified by three phenol:chloroform (1:1) extractions, followed by one chloroform extraction. The DNA in the aqueous supernatant was precipitated with 1 volume of cold isopropanol at RT for 10 min or -20°C overnight. The precipitated DNA was washed in 70% (v/v) ethanol, air dried and resuspended in sterile Milli-Q water. Genomic DNA samples were stored at 4°C.

2.3.2.1.2 Rapid genomic DNA extraction

For small scale, rapid extraction of genomic DNA, mycelia were grown in PD broth for 1-3 days, transferred to lysis buffer (150 mM EDTA, 50 mM Tris-HCl, 1% (w/v) SLS) and incubated at 70°C for 30 min. The lysate was neutralised by the addition of 1 volume of potassium acetate (5 M). Samples were incubated on ice for 10 minutes and centrifuged at 17,000 x ***g*** for 20 min. DNA was isolated from the aqueous phase by precipitations with 0.7 volumes of 4°C isopropanol by centrifugation at 17,000 x ***g*** for 20 min and the pellet washed with 70% (v/v) ethanol, air dried and resuspended in 20 µL H_2O. Samples were stored at 4°C.

2.3.2.2 DNA concentration

Where necessary, genomic DNA was concentrated by adding 1/10th volume of 3 M sodium acetate and 1 volume of 95% ethanol to the samples and incubated at -20°C overnight. The DNA was recovered by centrifugation and the resulting pellet rinsed with 70% (v/v) ethanol to remove residual salts. Residual ethanol was allowed to evaporate off and the DNA resuspended in the desired volume of sterile Milli-Q water.

2.3.2.3 DNA hybridisations

E. festucae genomic digests were transferred to positively charged nylon/nitrocellulose membranes (Roche) using the method described by Southern (1975). DNA was fixed by UV light cross-linking in a Cex-800 UV light cross-linker (Ultra-Lum) at 254 nm for 2 min. The DNA probes were synthesised by random priming using Klenow DNA polymerase and [α-^{32}P]dATP (3000 Ci/mmol; Amersham Biosciences), using a High Prime DNA labeling kit (Roche) or by the incorporation of Digoxigenin-11-dUTP (DIG-11-dUTP) into DNA by the polymerase chain reaction using a PCR DIG probe synthesis kit (Roche). Hybridisations were performed according to the manufacturer's instructions and visualised either by autoradiography (^{32}P-labelled probes) or NBT/BCIP colour detection (DIG-labelled probes).

Cosmid clone 28E7 (*yapA*) was isolated from an Fl1 cosmid library (Tanaka 2005) by colony hybridisation as previously described (Takemoto 2006) using a 1.7 kb fragment of *yapA,* amplified using the Expand High Fidelity^{TM} PCR system and the yap5/yap6 primer pair, as a probe. The probe was labeled with [α-^{32}P]dATP as described above.

2.4 PCR amplification

All PCR assays were performed in 50 µl PCR vials and stored at 4°C until analyzed. Sequences of PCR primers are provided in Table 2.2

Table 2.2. Primers used in this study

Name	Sequence (5′ – 3′)	Used for
yap1	AGATCTCACGAGATGAAAAACGTTT	5′ *yapA* replacement construct
yap2	GGTACCGTGTTCTGTTGTTTGTTG	5′ *yapA* replacement construct
yap3	AAGCTTGACGGCGTTAAAGAACT	3′ *yapA* replacement construct
yap4	CTCGAGATGTGTACTCTGACGTTGT	3′ *yapA* replacement construct
gpx1	AGATCTAGCCTTTTAAGAAGCACAACG	5′ *gpxC* replacement construct
gpx2	GGTACCGAGTTTCACATGTGATCAGTA	5′ *gpxC* replacement construct
gpx3	GTCGACGGGATTTCATATGCTATG	3′ *gpxC* replacement construct
gpx4	GTCGACCTATGCATGTTAGCAACC	3′ *gpxC* replacement construct
tpx1	AGATCTAATAAGCTAAGGGTTCTC	5′ *tpxA* replacement construct
tpx2	GGTACCGAGTATATGTATGTATGATGC	5′ *tpxA* replacement construct
tpx3	GGATCCAATCAGGGAAGGCGAC	3′ *tpxA* replacement construct
tpx4	TCTAGACGTCCGTTATTGCTGCAA	3′ *tpxA* replacement construct
yap6	TCTAGACTAAGGCATGGTAGCGCCGT	screening *yapA* for replacement
yap9	ACGCACGAATGAATACAATAAACT	screening *yapA* for replacement
yap10	GATTTGTGTACGCCAGACAGTCC	screening *yapA* for replacement
yap11	CTGAACTCACCGCGACGTCTGT	screening *yapA* for replacement
yap15	GCGGGCAATCCACGTCATCA	screening *yapA* for replacement
yap21	CCGACTTCACTCACAACATCAGC	screening *yapA* for replacement
gpx9	ATGATGCCGCCACCTACGAAAT	screening *gpxC* for replacement
gpx10	AGAACTCGTCAAGAAGGCGATAGA	screening *gpxC* for replacement
gpx15	TCTTCCATACTGATCACATG	screening *gpxC* for replacement
gpx16	ATCGATCTGTGAACACAGAC	screening *gpxC* for replacement
gpx17	GGACACACATTCATCGTAGGTAT	screening *gpxC* for replacement
gpx18	GTACATACGGAGTAGTCCATAAACAT	screening *gpxC* for replacement
tpx13	CACACCAAGGCGTGAAACCCC	screening *tpxA* for replacement
tpx14	CAGTCCATTCCCACGTCTTGGTC	screening *tpxA* for replacement
tpx15	ACCCTCCTCCTTATTAGTAA	screening *tpxA* for

		replacement
tpx16	TGCTCCTTCAATATCAGTTC	screening *tpxA* for replacement
tpx17	AGCACTCGTCCGAGGGCAAA	screening *tpxA* for replacement
tpx18	ACGCATCCATCTTTGCCGAAC	screening *tpxA* for replacement
tpx37	GTAACGCCAGGGTTTTCCCAGTCACGACTC TAGATAATTACTTTAAGCTATTAA	P*tpxA-EGFP*-CL1 fusion construct
tpx39	ATGGTGAGCAAGGGCGAGGA	P*tpxA-EGFP*-CL1 fusion construct
tpx40	GCGGATAACAATTTCACACAGGAAACAGC CATATGCTACAGGTGGATGACGAAGT	P*tpxA-EGFP*-CL1 fusion construct
tpx41	GTGAACAGCTCCTCGCCCTTGCTCACCATG TTTTGAATGCGGGGA	P*tpxA-EGFP*-CL1 fusion construct
tpx42	ATGGCAGGCCCTCTCCG	cDNA/gDNA sequencing
tpx43	TTAGATCTGGGGAAGAGCAGT	cDNA/gDNA sequencing
yap5	GAATTCATGTCATCAAGTGGCAGCGG	*S. cerevisiae* complementation
yap6	TCTAGACTAAGGCATGGTAGCGCCGT	*S. cerevisiae* complementation
yap7	AAGCTTATGAGTGTGTCTACCGCCAAG	*S. cerevisiae* complementation
yap8	TCTAGATTAGTTCATATGCTTATTCAAAGC	*S. cerevisiae* complementation
gpx5	GAATTCATGGCCTCCGCCACGAGCTTCT	*S. cerevisiae* complementation
gpx6	TCTAGATTAAGCCTTCTTCGCCAATTCGT	*S. cerevisiae* complementation
gpx7	AAGCTTATGTCAGAATTCTATAAGCTAGCA CC	*S. cerevisiae* complementation
gpx8	TCTAGACTATTCCACCTCTTTCAAAAGTTC	*S. cerevisiae* complementation
yap27	GAATTCATGTCATCAAGTGGC	*yapA-EGFP* fusion construct
yap28	ATCGATAGGCATGGTAGCG	*yapA-EGFP* fusion construct
GCGFP1	ATCGATGGTGCTGGTGCTGG	*yapA-EGFP* fusion construct
GCGFP2	GCGGCCGCTTTACTTGTACAG	*yapA-EGFP* fusion construct
yap29	ATCGATTCATCAAGTGGCAGCGGAG	*EGFP-yapA* fusion construct
yap30	GCGGCCGCCTAAGGCATGGTAG	*EGFP-yapA* fusion construct
EGFP1	GAATTCATGGTGAGCAAGGG	*EGFP-yapA* fusion construct
EGFP2	ATCGATAACTCGAGACTTGTACAG	*EGFP-yapA* fusion construct
pcatA3	TCTAGACGTTTTCATTGAGCAACA	P*catA-EGFP* fusion construct
pcatA4	GAATTCTCTCGCGGTATTGGGG	P*catA-EGFP* fusion construct
pCatAF1	CCGCGGATGCAGGTCAAAACACGCACTTT	P*catA-EGFP*-CL1

	GCGAGTTTG	fusion construct
CL1 R1	CAGGGAGGAGAACCAGTTCTTGCAGGCTA GAACTCGAGACTTGTACAGCTCGTC	P*catA-EGFP*-CL1 fusion construct
CL1 R2	CATATGCAGGTGGATGACGAAGTGGGACA GGGAGGAGAACCAGTTCTTGCAG	P*catA-EGFP*-CL1 fusion construct
ScYap6	GTAACGCCAGGGTTTTCCCAGTCACGACG AATTCATGAGTGTGTCTACC	P*TEF-YAP1-EGFP* fusion construct
ScYap8	CCCTTGCTCACAGCACCAGCACCAGCACC ATCGATGTTCATATGCTTATT	P*TEF-YAP1-EGFP* fusion construct
GCGFP3	GCGGATAACAATTTCACACAGGAAACAGC GCGGCCGCTTTACTTGTACAG	P*TEF-YAP1-EGFP* fusion construct
GCGFP4	GGTGCTGGTGCTGGTGCT	P*TEF-YAP1-EGFP* fusion construct

2.4.1 Standard PCR

Standard PCR amplification was performed with *Taq* DNA polymerase (Roche). The reaction mixture contained 5 µl of 10x Taq Reaction buffer, 1 µl (0.2 µM final concentration) of each primer, 2.5 µl dNTPs (200 µM final concentration), 1 ng template DNA and 1 U of *Taq* polymerase. The following conditions were used: one cycle at 94°C for 2 min; 35 cycles at 94°C for 30 s, 45–68°C for 30 s and 72°C for 1 min per kb. Final extension consisted of one cycle at 72°C for 10 min.

2.4.2 High fidelity PCR

Where proofreading activity was required the Expand High Fidelity™ PCR system (Roche) or Phusion® High-Fidelity DNA Polymerase (Finnzymes) was used.

For amplification using the Expand High Fidelity™ PCR system the reaction mixture contained 5 µl of 10x Expand High Fidelity Buffer, 1 µl (0.2 µM final concentration) of each primer, 2.5 µl dNTPs (200 µM final concentration), 1 ng template DNA and 1.75 U of Expand High Fidelity Enzyme mix (Roche). The following conditions were used: one cycle at 94°C for 2 min; 35 cycles at 94°C for 30 s, 45–68°C for 30 s and 72°C for 1 min per kb. Final extension consisted of one cycle at 72°C for 10 min, and then tubes were stored at 4°C until analyzed.

For amplification using Phusion® High-Fidelity DNA Polymerase the reaction mixture contained 10 µl of 5x Phusion® HF Reaction buffer, 2.5 µl (0.5 µM final concentration) of each primer, 2.5 µl dNTPs (200 µM final concentration), 1 ng template DNA and 1 U of Phusion® polymerase. The following conditions were used: one cycle at 98°C for 30 s; 10 cycles at 98°C for 10 s, 55°C for 30 s and 72°C for 15 s per kb; 20

cycles at 98°C for 10 s and 72°C for 15 s per kb. Final extension consisted of one cycle at 72°C for 10 min, and then tubes were stored at 4°C until analyzed.

2.5 DNA manipulation

2.5.1 DNA quantification

Plasmid and cosmid DNA was quantified using a NanoPhotometer (Implen) as per the manufacturer's instructions.

Genomic DNA concentrations were estimated by comparing the fluorescent intensity of 1 µL samples of uncut genomic DNA with a series of Lambda (λ) DNA (Fermentas) mass standards (10-200 ng) in ethidium bromide-stained agarose gels (1% w/v) using a Molecular Imager® Gel Doc™ XR+ System with Image Lab™ Software #170- 8195 (Bio-Rad).

2.5.1.1 Plasmid/Cosmid DNA

2.5.2 Yeast recombinational cloning

Yeast recombinational cloning was carried out using the method outlined by Colot *et al*. (2006). A single FY834 colony from a fresh plate was inoculated into 5 ml of YPD and grown overnight at 30°C, shaking at 200 rpm. 1 ml of the overnight FY834 culture was inoculated into 50 ml YPD and grown, shaking at 200 rpm, for a further 4-5 h. The cells were pelleted (5 min; 2500 x ***g***) and washed with sterile H_2O, repelleted then resuspended in 1 ml of 100 mM LiAc. The cells were pelleted (15 s; 17,000 x ***g***) and resuspended in 400 µl of 100 mM LiAc. 50 µl aliquots of cells were pelleted (15 s; 17,000 x ***g***) and, to the cell pellet, 240 µl 50% PEG 4000, 36 µl 1M LiAc, 10 ml of 2 mg/ml single-stranded carrier DNA and 300 ng of each DNA fragment to undergo recombination was added. The suspension was vortexed then incubated at 30°C for 30 min then mixed by inverting and transferred to 42°C for 30 min. The cells were pelleted (15 s; 17,000 x ***g***) twice and resuspended in 1 ml H_2O then finally pelleted and resuspended in 50 ml H_2O. SD plates lacking uracil were spread with 30 µl aliquots of the transformed yeast cells and incubated at 30°C for 3-4 days.

2.5.2.1 Yeast 'smash and grab'

Transformed FY834 colonies were washed from plates with H_2O. The cells were pelleted (15 s; 17,000 x ***g***) and, to the cell pellet, 100 µl lysis buffer, 100 µl chloroform, 100 µl phenol and 100 µL of glass beads was added. The suspension was vortexed for 2 min and centrifuged (10 min; 17,000 x ***g***). The supernatant was transferred to a fresh

tube and then 10 µl of 3 M KOAc and 250 µl of isopropanol was added. The suspension was incubated at room temperature for 10 min, the cells pelleted (5 min; 13,000) and the pellet washed with 1 ml of 70% ethanol, air-dried and resuspended in 50 µL H_2O. Electrocompetent *E. coli* cells were transformed with 1 µl of DNA.

2.5.3 Restriction endonuclease digestion

Plasmid and cosmid DNA was digested at 37°C for 1-4 h. Digests containing ≤100 ng DNA were performed in 10 µL final volumes, with 2 U of restriction enzyme and digests containing ≥100 ng DNA were performed in a final volume of 50 µL, with 20 U of enzyme/µg, using the optimal reaction buffer for each enzyme. For Southern blot analysis 2 µg of *E. festucae* genomic DNA was digested overnight at 37°C in a final volume of 100 µL containing 10 µL 10x optimal buffer and 30 U of restriction enzyme. Reactions were stopped by addition of SDS loading dye.

2.5.4 Sub-cloning

Generally, TOPO® TA cloning was performed whereby PCR-amplified DNA fragments with 3′-A overhangs were subcloned into the pCR4-TOPO® vector (Invitrogen) containing single 3´-thymidine (T) overhangs.

2.5.4.1 A-tailing

Prior to ligation PCR products generated by proofreading DNA polymerases were first A-tailed by Taq DNA polymerase to facilitate cloning into the pCR4-TOPO® vector. PCR products were purified using the Wizard® SV Gel and PCR Clean-Up System (Promega) and then incubated at 72°C for 10 min with 5 U of Taq DNA polymerase, 1 µL Taq Reaction buffer and 200 nM dATP in a final volume of 10 µL.

2.5.4.2 TOPO ligation

PCR products with 3′-A overhangs were ligated into the pCR4-TOPO® vector by incubating purified PCR products with 10 ng pCR4-TOPO® vector and 1 µL salt solution (1.2 M NaCl, 0.06 M $MgCl_2$) in a total volume of 10 µL at room temperature for 30 min.

2.5.4.3 Alkaline phosphatase treatment of vectors

To prevent recircularisation of the vector, vector DNA was dephosphorylated with calf intestinal alkaline phosphatase (CIAP; Roche). Generally, 1 μg of digested vector was incubated with 1 U CIAP/pmol ends in 1x CIAP reaction buffer in a total volume of 70 μL for one h at 37°C.

2.5.4.4 Agarose gel purification

To extract and purifiy specific PCR amplification products or restriction digest fragments from agarose gels, ethidium bromide-stained gels were visualised with a Dark Reader™ Non-UV Transilluminator DR-88M (400-500 nm) and desired bands excised from the gel using a sterile scalpel blade. The gel slice was transferred to a microcentrifuge tube and the DNA fragment purified using the Wizard® SV Gel and PCR Clean-Up System (Promega).

2.5.4.5 PCR product purification

To remove excess nucleotides and primers, PCR products were purified using the Wizard® SV Gel and PCR Clean-Up System (Promega) according to the manufacturer's instructions.

2.5.4.6 Ligation

To ligate inserts into CIAP-treated vectors, 50 ng of vector was combined with insert in a 3:1 molar ratio of insert to vector and an equal volume of Ligation Mighty Mix, a mixture of T4 DNA ligase and ligation buffer (TaKaRa), was added. Ligations were performed at 16°C for 2 h.

2.5.4.7 E. coli transformation

Plasmids were transformed into chemically competent TOP10 *E. coli* cells by the heat-shock method. 6 μL of ligation (containing 10-100 ng vector DNA) was added to 50 μL of cells and incubated on ice for 20 min. Cells were heat-shocked at 42°C for 30 s then immediately transferred back to ice. 250 μL of 37°C SOC medium was added and then cells were incubated at 37°C with shaking (225 rpm) for 1 h. The cells were spread onto LB agar plates containing selective antibiotic as required and, once dry, the plates were incubated overnight at 37°C.

Plasmids were transformed into electrocompetent DH5α by the electroporation method. 1 µL of yeast plasmid DNA prepared by the 'smash and grab' method (2.5.2.1) was added to 50 µL of cells and the cell-DNA mixture transferred to cold 1 mm-electroporation cuvettes. The cuvettes were placed in the electroporator and pulsed at 2.0 kV, 200 Ω and 25 µF. 250 µl of 37°C SOC medium was added, the suspension incubated at 37°C with shaking (225 rpm) for 1 h. The cells were spread onto LB agar plates containing selective antibiotic as required and incubated overnight at 37°C.

2.5.4.7.1 CloneChecker™ System

Transformed *E. coli* clones were screened for recombinant plasmid using the CloneChecker™ System (Invitrogen). Colonies were resuspended in 8 µL lysis solution (Green Solution; proprietary components). Samples were heated at 99°C for 30 s in a thermal cycler, cooled to room temperature then 1 µL of 10x restriction enzyme buffer and 10 U of restriction enzyme added. After 15-30 min incubation at 37°C, restriction endonuclease digestion was stopped with the addition of 2 µL SDS loading dye and plasmid DNA digestion analyzed by agarose gel electrophoresis.

2.6 RNA manipulation

2.6.1 RNA isolation

Total RNA was isolated from *E. festucae* mycelium following the TRIzol® reagent protocol (Invitrogen). Mycelium grown in liquid culture was freeze-dried then ground in liquid nitrogen and the powder resuspended in 4 mL TRIzol and centrifuged at 11,000 x *g* for 10 min at 4°C. The aqueous phase was incubated at room temperature. After 5 min 0.2 volumes of chloroform was added, the samples mixed for 15 s and incubated for a further 3 min at room temperature. The samples were centrifuged at 11,000 x *g* for 15 min at 4°C. The aqueous phase was transferred to fresh 1.5 mL eppendorfs and isopropanol added to precipitate the RNA. The samples were centrifuged at 11,000 x *g* for 10 min at 4°C and the RNA pellets washed with 75% (v/v) ethanol, air-dried and resuspended in DEPC-treated water.

2.6.2 RT-PCR

One µg of *E. festucae* RNA was heat denatured and reverse transcribed using SuperScript™ II reverse transcriptase (Invitrogen) according to the manufacturer's instructions. Specific amplification of *yapA*, *gpxC* and *tpxA* cDNAs were performed using the primer pairs yap5/yap6, gpx5/gpx6 and tpx42/tpx43, respectively, using the Expand™ High Fidelity PCR System.

2.7 Preparation of complementation, deletion and expression constructs

2.7.1 S. cerevisiae complementation constructs

The *S. cerevisiae YAP1* (pGC8, Figure 8.5) and *GPX3* (pGC7, Figure 8.4) genomic complementation constructs were prepared by PCR amplification, using the Expand High Fidelity PCR system, of the 1.95 kb *YAP1* gene and the 0.5 kb *GPX3* gene using primers yap7/yap8 and gpx7/gpx8, respectively. The *E. festucae yapA* (pGC6, Figure 8.3) and *gpxC* cDNA (pGC5, Figure 8.2) complementation constructs were prepared by PCR amplification of the 1.7 kb *yapA* cDNA and 0.5 kb *gpx*C cDNA from *E. festucae* total mRNA, using the primer pairs yap5/yap6 and gpx5/gpx6, respectively. These fragments were then ligated into pCR4-TOPO, sequenced, and sub-cloned into the pYES2 vector (Invitrogen).

2.7.2 E. festucae gene deletion constructs

The *yapA* replacement construct, plasmid pGC2, was prepared by sequentially ligating into pSF15.15 (a pII99-based vector containing the *hph* cassette) a 1.1 kb *Bgl*II/*Kpn*I fragment 5′ of *yapA,* generated by PCR amplification using primer pair yap1/yap2, and a 1.2 kb *Hin*dIII/*Xho*I fragment 3′ of *yapA* generated by PCR amplification using primer pair yap3/yap4, as shown in Figure 8.7, Appendix 8.1.

The *gpxC* replacement construct, plasmid pGC4, was prepared by sequentially ligating into pSF17.8 (a pII99-based vector containing the *npt*II cassette) a 1.1-kb *Bgl*II/*Kpn*I fragment 5′ of *gpxC,* generated by PCR amplification using primer pair gpx1/gpx2, and a 1.4 kb *Sal*I/*Sal*I fragment 3′ of *gpxC*, generated by PCR amplification using primer pair gpx3/gpx4, as shown in Figure 8.9, Appendix 8.1.

The *tpxA* replacement construct, plasmid pGC12, was prepared by sequentially ligating into pSF15.15 a 2.3 kb *Bgl*II/*Kpn*I fragment 5′ of *tpxA,* generated by PCR amplification using primer pair tpx1/tpx2, and a 2.45 kb fragment 3′ of *tpxA,* generated by PCR amplification using primer pair tpx3/tpx4, as shown in Figure 8.10. The 3.8, 4.3 and 6.2 kb linear products of pGC2 (*yapA*), pGC4 (*gpxC*) and pGC12 (*tpxA*) used for transformation were amplified with primer pairs yap1/yap4, gpx1/gpx4, and tpx1/tpx4 using the Expand High Fidelity PCR system (Roche) according to the manufacturer's instructions. A 3.7 kb *Eco*RV/*Eco*RI fragment extending 740 bp upstream from the transcription start site of *yapA* and 639 bp downstream from the transcription termination site was digested from cosmid 28E7 and sub-cloned into pSF17.8 to generate the pGC11 *yapA* complementation vector.

2.7.3 Expression constructs

The YapA-EGFP fusion construct, pGC9, was prepared by cloning a *Eco*RI/*Cla*I fragment generated with the primer pair yap27/yap28 into the pPN94 vector. The translational stop codon of *yapA* was removed, and replaced by the EGFP coding region with its stop codon, creating a C-terminal in-frame fusion with the *yapA* gene. The P*catA-EGFP* reporter construct, pGC13, was prepared by sequentially ligating into pSF17.8 an *Xba*I/*Eco*RI fragment containing the 1 kb region upstream of the *catA* start codon and a 0.7 kb *Xba*I/*Eco*RI fragment containing the EGFP coding sequence. The P*catA* fragment was generated by PCR using the primer pair pcatA3/pcatA4, ligated into pGC10 and the P*catA-EGFP Xba*I/*Xho*I fragment subcloned into pSF17.8. The destabilised version of the P*catA-EGFP* reporter construct, P*catA-EGFP*u (pGC14), was generated by adding a 16-amino acid degron sequence (CL1=ACKNWFSSLSHFVIHL), to the C-terminus of EGFP. Two-step PCR, using the primer pairs pCatA/CL1 R1 and pCatA/CL1 R2, was used to generate the 1.2 kb *Sac*II/*Nde*I fragment which then replaced the corresponding region in the original P*catA-EGFP* vector (Bence *et al.*, 2001).

2.8 Fungal transformation

2.8.1 Transformation of S. cerevisiae

S. cerevisiae transformation was carried out using the lithium acetate/single stranded carrier DNA/polyethylene glycol method (Gietz & Woods, 2002). A loop full of yeast cells were scraped off colonies grown overnight at 30°C on YPD plates and resuspended in YPD broth to an A_{600} = 1. The cell suspension was centrifuged at 2500 x *g* for 5 min, the cells resuspended in 3 mL of sterile water and recentrifuged at 2500 x g for 5 min. The cell pellet was then resuspended in 1 mL of 100 mM LiAc and incubated for 10 min at 30°C. 100 µL aliquots of cells were pelleted, resuspended in the transformation mix (240 µL PEG 3,350 [50% w/v], 36 µL 1 M LiAc, 15 µL SS-DNA [10 mg/mL], 5 µL plasmid or linear DNA, 64 µL sterile H_2O) and incubated firstly at 30°C for 30 min then at 42°C for 20 min. The cells were then pelleted, resuspended in 100 µL sterile H_2O and the suspension plated onto SC minimal media lacking the appropriate amino acid to select for the presence of the plasmid.

2.8.2 Transformation of E. festucae

2.8.2.1 E. festucae protoplast preparation

E. festucae protoplasts were prepared using the method described by Young *et al*., (Young *et al*., 2005, Young *et al*., 1998). Mycelia was harvested from liquid cultures grown 5 days at 22°C shaking at 150 rpm, rinsed 3x with sterile water then rinsed with osmotic medium (OM) buffer (1.2 M $MgSO_4.7H_2O$, 10 mM Na_2HPO_4, pH adjusted to 5.8 with 100 mM $NaH_2PO_4.2H_2O$). The collected mycelia (5 g wet weight) were suspended in a (50 mL) solution of Lysing Enzymes from *Trichoderma harzianum* (Sigma) (10 mg/mL in OM buffer; filter sterilised, 45 μm filter) and incubated overnight at 16°C, shaking at 180 rpm. Protoplasts were filtered through Miracloth and harvested by adding 2 mL of ST (0.6 M sorbitol, 100 mM Tris-HCl, pH8) overlay buffer to 5 mL of protoplast suspension and centrifuging at 4, 4300 x g for 10 min at 4°C. Protoplasts were harvested from the lysing enzyme solution-ST interface and subsequently washed three times and resuspended in STC buffer (1 M sorbitol, 50 mM Tris-HCl, 50 mM $CaCl_2$ pH 8) to a final concentration of 1.25 x 10^8 protoplasts/mL. For long-term storage 80 μL protoplast aliquots were mixed with 20 μL PEG solution (40% PEG 4000, 50 mM $CaCl_2$, 1 M sorbitol, 50 mM Tris-HCl, pH 8).

2.8.2.2 Transformation of E. festucae protoplasts

Protoplasts were transformed with DNA using the method previously described by Itoh *et al*. (1994). Approximately 1.25 x 10^7 protoplasts in 100 μL aliquots (80 μL protoplast + 20 μL PEG solution) were mixed with 1 – 5 μg of linear or circular DNA, 2 μL of spermidine (50 mM) and 5 μL heparin (5 mg/mL) then incubated on ice for 30 min. 900 μL PEG solution was added, contents mixed well and incubated on ice for an additional 15-20 min. The protoplast suspension was mixed with 3.5 mL of soft overlay RG agar (0.8%) maintained at 50°C. The soft overlay agar containing the protoplasts was immediately poured over a layer of presolidified RG agar (1.6%) and incubated at 22°C overnight. The regenerating protoplasts were then overlaid with an additional 5 mL soft agar containing the relevant antibiotic. After solidification of the top agar, the plates were incubated at 22°C for 10-14 days until transformants grew through the antibiotic-containing overlay. Antibiotic resistant transformants were transferred to hygromycin- or geneticin-containing PD media and nuclear-purified by three rounds of subculturing onto antibiotic-containing media (Young *et al*., 2005).

2.8.2.3 Screening of E. festucae transformants

Putative *yapA* replacement mutants were screened by PCR using primers that flank

the *hph* cassette (yap22 and yap23; 1 kb wild type, 1.6 kb replacement) and the 5′ (yap9 and yap10; 2.6 kb) and 3′ (yap11 and yap21; 2.4 kb) flanking regions of the replacement. Putative *gpxC* replacement mutants were screened by PCR using primers that flank the *npt*II cassette (gpx15 and gpx16; 1 kb wild type, 1.9 kb replacement) and the 5′ (gpx9 and gpx10; 2.3 kb) and 3′ (gpx11 and gpx12; 2.9 kb) flanking regions of the replacement. Putative *tpxA* replacement mutants were screened by PCR using primers that flank the *hph* cassette (tpx13 and tpx14; 1-kb wild type, 1.6 kb replacement) and the 5′ (tpx15 and tpx16; 2.5 kb) and 3′ (tpx17 and tpx18; 2.5 kb) flanking regions of the replacement. For complementation of Δ*yapA* mutants, Δ*yapA* protoplasts were transformed with pGC11 and transformants selected in media containing 200 μg/ml geneticin. Reintroduction of the *yapA* gene was confirmed by PCR using the primer pair yap5/yap6.

Transformants expressing EGFP or DsRed fusion proteins were selected using an Olympus BX51 Stereomicroscope using Olympus filters U-MWIBA2 and U-MWIG2 to detect EGFP and DsRed (Discosoma red fluorescent protein), respectively.

2.9 Protein extraction

Total protein was isolated from *E. festucae* mycelia by the method of Pasquali *et al.* (2010). Mycelia were harvested from liquid cultures grown 5 days at 22°C shaking at 150 rpm, resuspended in 25 mL PD broth or PD broth containing 16 mM H_2O_2 and incubated for a further 45 min. Trichloroacetic acid (TCA) was added to a final concentration of 20% (v/v) and the samples were incubated for a further 30 min. Mycelia were collected by filtering through Miracloth, pressed between paper towels to remove excess liquid and 300 mg of semi-dried mycelia ground to a fine powder in liquid nitrogen and lysis buffer (50 mM Tris-HCl pH8, 2% (w/v) SDS, 0.1 mM EDTA, 0.2 mM PMSF). Samples were adjusted to 3 mL with further addition of lysis buffer and incubated for 1 h rotating at 4°C. The samples were then centrifuged at 12,000 x ***g*** for 15 min at 4°C, the supernatant transferred to a fresh tube and the remaining pellet resuspended in 3 mL lysis buffer. The samples were recentrifuged at 16,000 x ***g*** for 30 min at 4°C and the supernatants pooled. Proteins were precipitated with 20% (v/v) TCA in acetone at -20°C overnight. To monitor the YapA redox state the method provided by Delaunay *et al.* (2000) was followed. The TCA-precipitated protein was washed in acetone, air-dried and dissolved in buffer containing 100 mM Tris-HCl pH8, 75 mM iodoacetamide (IAA), 1 mM EDTA and 1% (w/v) SDS and incubated overnight at 4°C. Where indicated, Yap1 was dephosphorylated with 20 U calf intestinal phosphatase (Roche) for 45 min at 37°C. Protein samples were stored at -20°C.

2.10 SDS-PAGE

Protein extracts were separated by SDS–PAGE, according to the method of Laemmli (Laemmli 1970) after boiling in SDS sample buffer (62.5 mM Tris-HCl pH6.8, 2% (w/v) SDS, 10% (v/v) glycerol, 0.01% (w/v) bromophenol blue and 5% (v/v) β-mercaptoethanol. For non-reducing SDS-PAGE, β-mercaptoethanol was omitted from the sample buffer. All gels for detection of EGFP-tagged YapA were 8% and run at 150 V. Gels were stained with SimplyBlue™ SafeStain (Invitrogen) following the microwave protocol as per manufacturer's instructions and visualised using the Molecular Imager® Gel Doc™ XR+ System (Bio-Rad).

2.11 Western blotting

The separated proteins were transferred to a PVDF membrane for 30 min using a Trans-Blot SD Semi-Dry Electrophoretic Transfer Cell (Bio-Rad) according to the manufacturer's instructions. Membranes were blocked with 5% non-fat milk in TBS-Tween (TBS-T; 20 mM Tris-HCl, pH7.5, 150 mM NaCl, 0.1% Tween-20) for 1 h at room temperature and subsequently incubated in primary antibody (anti-GFP rabbit polyclonal antibody (Abcam) diluted 1/5000 for 1 h. Membranes were then washed in TBS-T (2 x 2 min, 1 x 10 min) and incubated with the horse radish peroxidase-conjugated secondary antibody diluted 1/20,000 for 1 h. After washing with TBT-T (2 x 2 min, 1 x 10 min), EGFP-tagged YapA was detected with the ECL Western Blotting System (GE Healthcare). Addition of luminol and peroxidase resulted in a chemiluminescent signal that was detected with a CCD camera.

2.12 Spore isolation and analysis

2.12.1 Spore isolation

For collection of spores, *E. festucae* cultures were grown on PD agar for 7-10 days at 22°C. The spores were vigorously washed from the surface of the colony with PD broth and a bent glass Pasteur pipette and the spore suspension was filtered through sterile glass wool.

2.12.2 H_2O_2 sensitivity assays

100 µL aliquots of spore suspensions were spread onto PD agar plates containing H_2O_2 ranging in concentration from 0.5-2 mM H_2O_2. The spread plates were allowed to dry and then incubated for 12 days at 22°C in the dark.

2.13 Microscopy

Cultures to be analysed by microscopy were inoculated onto a thin layer of PD agarose (2% w/v) layered on top of the base layer of PD agar (1.5% w/v) and grown for 5 days. For examination of *E. festucae* spores, spore suspensions were spread onto the PD agarose and examined after 16 h. Square blocks were cut from the agarose grown and placed in an imaging chamber (CoverWell, 20 mm diameter, 0.5 mm deep) (Molecular Probes) filled with 500 µl of PD broth and sealed with a 22 x 60 mm glass coverslip.

2.13.1 Light microscopy

E. festucae hyphae and germinating spores were analysed using a compound light microscope (Zeiss Axiophot, 40x objective) fitted with a DFC320 camera (Leica Microsystems).

2.13.2 Confocal microscopy

Expression of EGFP and DsRed in fungal cells was analysed by confocal laser scanning microscopy using a Leica SP5 DM6000B Confocal microscope (488 nm argon laser, 40x oil immersion objective, NA = 1.3). Images are displayed as a maximum projected stack of 5-10 confocal images, step size 1 µm. For activation of YapA-EGFP and Yap1-EGFP fusion proteins by H_2O_2, samples were incubated and imaged in PD broth containing 16 mM H_2O_2 after the specified time. YapA-EGFP was also activated by addition of 250 µM menadione to the PD broth. Differential interference contrast (DIC) imaging was used in conjunction with confocal microscopy and the DIC image overlaid on the confocal fluorescent images where indicated.

2.13.2.1 Image analysis

The total cellular fluorescence of each spore was quantified using ImageJ software. For each spore the level of fluorescence in each spore was calculated using the following formula: Corrected Total Cellular Fluorescence (CTCF) = Integrated Density - (Area of selected cell x Mean fluorescence of background readings) and values expressed as arbitrary units. Integrated Density = whole cell signal i.e. sum of pixel intensity, background readings = signal per pixel for a region selected beside cell (Gavet & Pines, 2010).

2.13.2.2 *Alexafluor (WGA-AF488) and aniline blue staining*

Pseudostem tissue from endophyte infected-plants was stained with aniline blue and Alexafluor® (WGA-AF488) to visualise hyphal growth and position of septa, respectively. Small (approx 3 x 7 mm) sections of leaf sheath from the lower-pseudostem section were soaked in 95% EtOH at 4°C overnight or for several weeks prior to analyzing. Samples were transferred to 10% (w/v) KOH and incubated for 3 h. Samples were then washed with PBS (pH7.4) then incubated in the staining solution (aniline blue 0.2 mg/mL, WGA-AF488 1 mg/mL, Tween 20 0.02%) for 30 min followed by a 10 min vacuum infiltration. Samples were observed by confocal microscopy. WGA-AF488 emission was detected at 498-558 nm (excitation, 488 nm). Aniline blue was detected at 449-555 nm (excitation 405 nm).

2.13.3 *Transmission electron microscopy (TEM)*

To examine hyphal ultrastructure and surrounding plant tissue, small discs (0.5 mm thick) of pseudostem tissue from 8-10 week old endophyte-infected plants were fixed in 3% glutaraldehyde and 2% formaldehyde in 0.1 M phosphate buffer, pH7.2 for 1 h and then transverse sections prepared for light microscopy and TEM as described by Spiers & Hopcroft (1993). Sections for light microscopy were stained with toluidine blue as described by Christensen *et al*. (2002). A Philips CM10 transmission electron microscope was used to examine the fixed samples and the images were acquired using a SIS Morada digital camera.

2.14 *Plant inoculation and growth*

2.14.1 *Seed sterilisation*

Endophyte-free seeds of *L. perenne* were surface sterilised by soaking in 50% sulfuric acid for 20 min, rinsing in sterile water, soaking in 2.5% sodium hypochlorite (50% (v/v) commercial bleach) for 20 min, rinsing in sterile water and transferring to sterile Whatman 3MM filter paper to dry.

2.14.2 *Seedling inoculation*

Sterile ryegrass seedlings were artificially infected using the seedling inoculation technique performed by Latch & Christensen (1985) whereby fungal mycelia are introduced into the seedling via a small incision across the shoot apical meristem.

2.14.3 Detection of endophyte infection by immunoblotting

Inoculated plants were tested for immunoblot detection using polyclonal rabbit antibodies, raised to homogenised mycelia of *N. lolii* Lp5 (Gwinn *et al.*, 1991). Tillers were cut transversely at the base of the plant and printed onto a nitrocellulose membrane (BDH) for several seconds. Membranes were incubated in blocking solution (20 mM Tris, 10 mM HCl, 50 mM NaCl, 0.5% non-fat milk powder [pH7.5]) at room temperature for 2 h then in blocking solution containing anti-*N. lolii* antibody diluted 1/1000 overnight at 4°C. Membranes were rinsed in blocking solution and then incubated with blocking solution containing anti-rabbit alkaline phosphatase-conjugated secondary antibody (Sigma) diluted 1/2000 for 2 h at room temperature. The alkaline phosphatase reaction was developed with Fast Red chromogen (Sigma) for 15 min.

2.14.4 Aniline blue staining

Hyphal growth in endophyte-infected plants was examined by staining of epidermal peels from outer leaf sheaths with aniline blue (0.05% (w/v) in lactic acid/glycerol/H_2O 1:2:1). Epidermal strips were placed onto a drop of aniline blue stain, the coverslip applied and boiled briefly over a small flame. A Zeiss Axiophot Compound Light Microscope was used to examine the stained samples.

2.15 DNA sequencing

DNA fragments were sequenced using the Sanger method: dideoxynucleotide chain termination method with the Big-Dye™ Terminator Version 3.1 Ready Reaction Cycle Sequencing Kit (Applied Biosystems) and separated using an ABI3730 genetic analyser (Applied Biosystems). Reactions were performed in a total volume of 20 µL, containing 300 ng plasmid and 3.2 pmol of M13 forward, M13 reverse or gene specific oligonucleotide primers, 0.875x ABI dilution buffer (Applied Biosystems) and 1.5 µL Big-Dye (Applied Biosystems). Sequence data were assembled and analysed using the MacVector sequence assembly software, version 12.0.5.

2.16 Bioinformatics

2.16.1 Acquisition of sequence data

E. festucae genes were identified by tBLASTn analysis of the *E. festucae* Fl1 (894) genome (http://csbio-l.csr.uky.edu/ef894-2011) with *S. cerevisiae* or *S. pombe* protein sequences. *S. cerevisiae* protein sequences were obtained from the SGC

(http://www.yeastgenome.org/). *S. pombe* protein sequences were obtained from GeneDB (http://old.genedb.org/genedb/pombe/). *C. albicans* and *Y. lipolytica* protein sequences were obtained from the Candida (http://www.candidagenome.org/) and Genolevures (http://www.genolevures.org/yali.html) Genome Databases. Other fungal sequences used in the phylogenetic analysis were retrieved from the NCBI GenBank database (http://www.ncbi.nlm.nih.gov/) or the Broad Institute (http://www.broad.mit.edu). Where homologues were identified by BLASTp analysis an E-value threshold of $1x10^{-6}$ was applied.

Gene annotation and naming are given in accordance with the Broad *Aspergillus* Comparative Database. The *E. festucae* genome sequence data, as curated by C.L. Schardl at the University of Kentucky are available at http://www.endophyte.uky.edu.

The *yapA, gpxC* and *tpxA* gene sequences of *E. festucae* strain Fl1 (894) have been deposited in the DDBJ/EMBL/GenBank databases under accession numbers *yapA,* KC121577*; gpxC,* KC121578*; tpxA,* KC244374 using Bankit.

2.16.2 Identity and similarity scores

Identity and similarity scores were calculated after ClustalW pairwise alignments of sequences using MacVector version 12.0.5.

2.16.3 Multiple sequence alignments

Amino acid sequence alignments were generated using ClustalW implemented in MEGA 5.05 with the default settings. Aligned sequences were trimmed as necessary and exported as a MEGA file for phylogenetic analysis.

2.16.4 Construction of phylogenetic trees

All phylogenetic trees were constructed in MEGA5.05 using the Maximum Likelihood method with a minimum of 2000 bootstrap replicates.

2.16.5 Promoter motif analysis

To identify canonical and variant Yap1 response element (YRE) motifs in the promoters of *E. festucae* genes the DNA Pattern Find analysis tool in the Sequence Manipulation Suite available at

http://www.bioinformatics.org/sms2/dna_pattern.html was used. Statistical analysis was performed using chi-square analysis with Yates correction.

2.16.6 Gene duplication analysis

The Yeast Genome Order Browser available at http://wolfe.gen.tcd.ie/ygob was used to check whether genes present in multiple copies in the *S. cerevisiae* genome arose from the whole genome duplication (WGD).

2.16.6.1 Protein predictions

Protein domains and molecular weights of the YapA, GpxC and TpxA proteins were predicted using the ExPASy Proteomics Server (http://ca.expasy.org/prosite/). The PSORT II Protein Prediction Server (http://psort.hgc.jp/form2.html) was used to predict the NLS and subcellular location of YapA. Where computational prediction of specific functional residues was not possible, predictions were based on sequence conservation with other fungal homologues.

3 Results

3.1 Identification and characterisation of an AP-1-like transcription factor

At the time of analysis the genome of the commonly used wild-type *E. festucae* laboratory strain 894 (Fl1, PN2278) had not been sequenced, thus initial analyses were performed using the genome sequence of the closely related *E. festucae* 2368 strain available at The Epichloë Genome Project (http://csbio-l.csr.uky.edu/ef2011). Also at this stage Yap1 homologues from fungi closely related to *E. festucae*, including *M. oryzae, F. oxysporum* and *N. crassa* were not characterised and the GenBank entries were annotated as hypothetical proteins and AP-1-like proteins. Therefore an initial tBLASTn analysis of the *E. festucae* 2368 genome was performed using the protein sequence of the well-characterised *S. cerevisiae* Yap1. A second tBLASTn analysis using the protein sequence of the putative *N. crassa* AP-1-like transcription factor was used to verify that the correct *E. festucae* protein was selected as the Yap1 homologue. Yap1 proteins from *M. oryzae* and *N. crassa* have since been characterised and GenBank entries updated accordingly (Guo *et al*., 2011, Tian *et al*., 2011). Following the availability of the *E. festucae* 894 (Fl1) genome at The Epichloë Genome Project (http://csbio-l.csr.uky.edu/ef894-2011) the tBLASTn analyses were repeated and the nucleotide sequences of the *yapA* genes in the *E. festucae* 2368 and 894 (Fl1) genomes were found to be identical.

The tBLASTn analysis of the *E. festucae* 894 (Fl1) genome with the *S. cerevisiae* Yap1 protein sequence identified a putative AP-1-like transcription factor (EfM2.092760; *E*-value $3x10^{-4}$) and a second bZIP transcription factor (EfM2.060870; *E*-value 0.25) encoded in the *E. festucae* genome. A reciprocal BLASTp analysis at NCBI with each predicted protein sequence indicated the first hit was related to numerous AP-1-like proteins from filamentous fungi whereas the lower-scoring hit was related to the fungal HapX transcription factor involved in iron regulation (Schrettl *et al*., 2010). For verification a second tBLASTn analysis of the *E. festucae* 894 (Fl1) genome, using the NCBI BLASTp hit from *N. crassa* (XP_957544.1) was performed. The first hit was again EfM2.092760 (*E*-value $9x10^{-96}$). In accordance with *E. festucae* gene nomenclature (Schardl 2010) the gene was designated *yapA* (gene model EfM2.018640; GenBank Accession number KC121577). It encodes a bZIP transcription factor that shares 12.4% amino acid identity and 29.4% similarity to the Yap1 transcription factor from *S. cerevisiae*. The *yapA* open reading frame is predicted to produce a polypeptide of 580 amino acids. The *E. festucae* YapA protein shares several conserved features with *S. cerevisiae* Yap1 including a nuclear localisation signal (NLS), nuclear export sequence (NES), basic leucine zipper (bZIP) domain, and two cysteine-rich domains (CRD) at the

N- and C- termini (Figure 3.1). Consistent with the presence of an NLS and an NES, the PSORT II program predicts both nuclear (74%) and cytoplasmic (9%) locations for YapA, in good agreement with the mechanism of other characterised Yap1-like proteins.

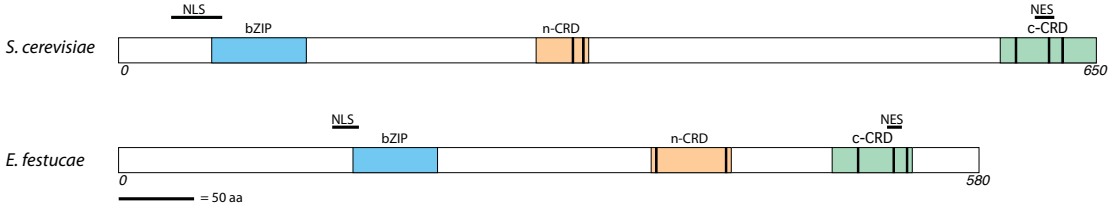

Figure 3.1 Schematic of *S. cerevisiae* Yap1 and *E. festucae* YapA. Characteristic motifs of *S. cerevisiae* Yap1 and *E. festucae* YapA proteins: the basic leucine zipper DNA binding domain (bZIP), the N- and C-terminal cysteine-rich domains (n-CRD and c-CRD) and the Nuclear Localisation Signal (NLS) and Nuclear Export Sequence (NES). Cysteine residues are represented by vertical black lines. Length of each protein in amino acids (aa) is indicated.

Both the bZIP and the c-CRD motifs are highly conserved among all of the fungal AP-1 transcription factors analysed (Figures 3.2A & B). Outside of these conserved motifs amino acid conservation is greatly reduced; *E. festucae* YapA shares 57% identity overall with the closest homologue FgAP1 from *F. graminearum* and between 12-16% identity with AP-1 proteins from the more distantly related basidiomycete fungus *Ustilago maydis* and yeast species, *S. cerevisiae, K. lactis, S. pombe* and *C. albicans*. This is partly due to the poor sequence conservation within the n-CRD of AP-1 proteins. A sequence alignment of the n-CRD from AP-1 homologues of various yeast and filamentous fungi identified a major difference in the amino acid sequence between yeast and filamentous fungal species in the domain, thus yeast n-CRD sequences were aligned separately to filamentous fungal n-CRD sequences (Figure 3.2C).

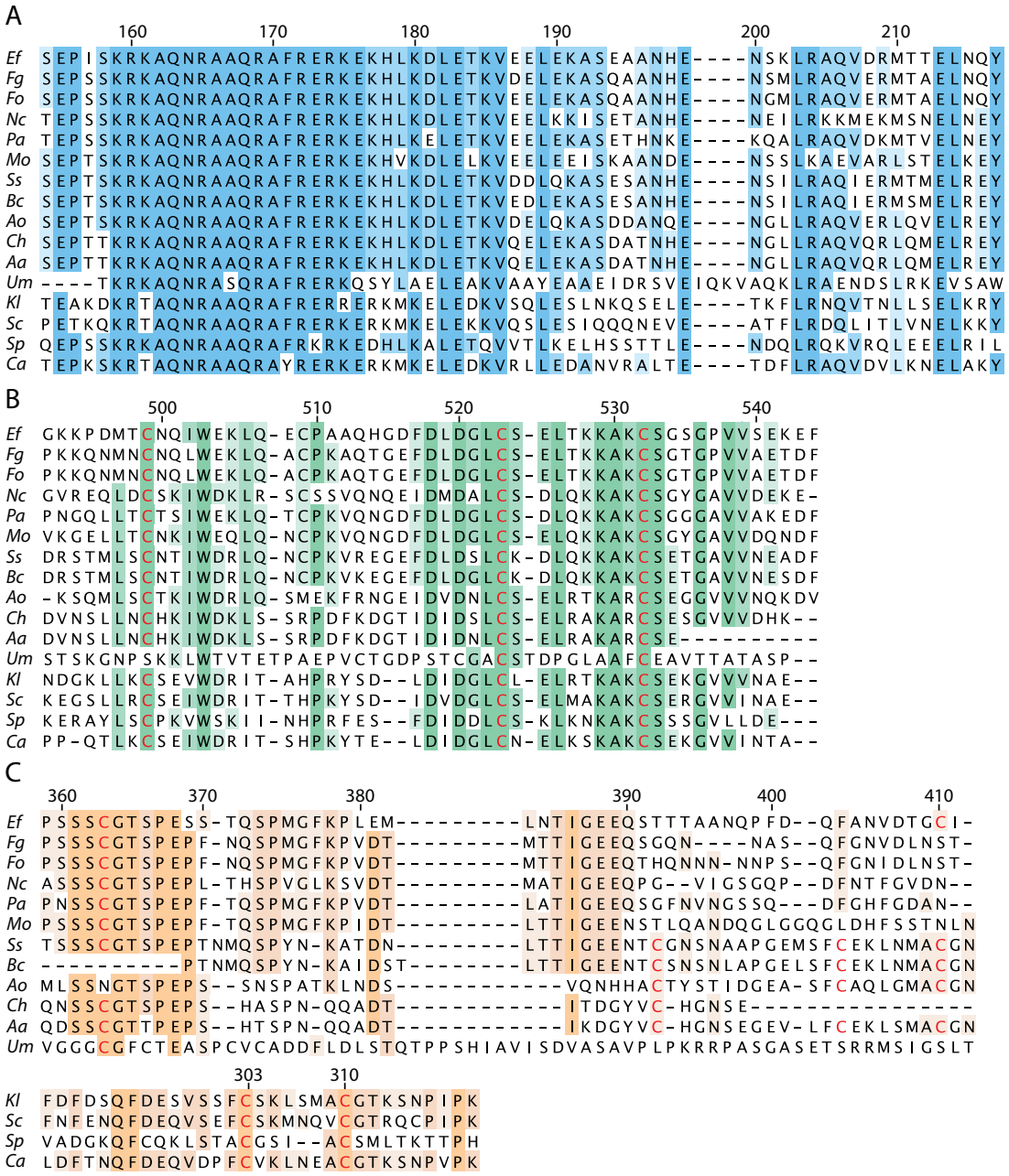

Figure 3.2 Multiple sequence alignments of bZIP domain, n-CRD and c-CRD. Conserved cysteine residues of fungal AP-1 proteins are highlighted in red. Numbering indicates amino acid residue position with respect to the *E. festucae* protein (bZIP (A), c-CRD (B) and upper n-CRD (C) sequences) or the *S. cerevisiae* protein (lower n-CRD (C) sequences).

In particular, the number, spacing and conservation of the cysteine residues within the n-CRD differs between yeast and filamentous fungi. In *E. festucae* YapA the spacing between potentially important cysteine residues is greatly increased in comparison to that of the yeast Yap1 homologues (Figure 3.2C). In the homologues from closely related fungi, *F. graminearum, F. oxysporum, N. crassa, P. anserina* and *M. oryzae* the second cysteine has been entirely lost from this domain. Figure 3.3 depicts the phylogenetic relationships between fungal AP-1 proteins and reveals that AP-1 proteins from filamentous fungi and yeast have diverged to form two separate clades.

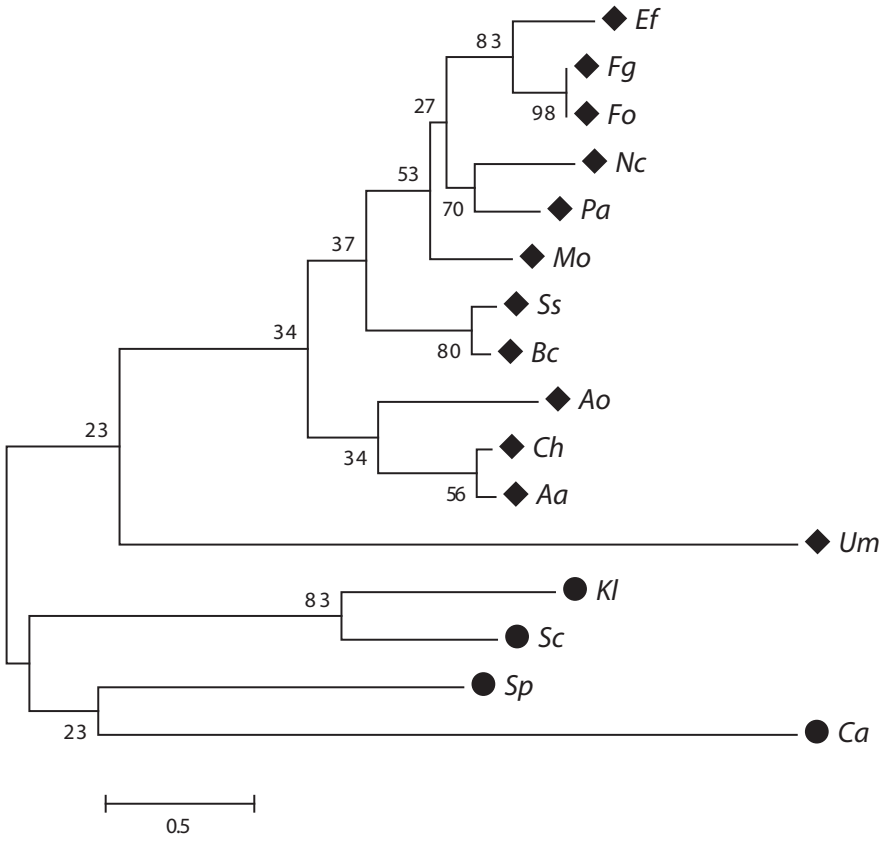

Figure 3.3 Maximum-likelihood dendrogram of fungal AP-1 proteins. Values above branches indicate bootstrap values based on 2000 replicates. Gene IDs with associated GenBank accession numbers in parentheses are as follows: Ef, *E. festucae* YapA EfM2.092760 (KC121577); Fg, *F. graminearum* FGSG_08800.3 (XP_388976.1); Fo, *F. oxysporum* FoAP1 (EGU84635.1); Nc, *N. crassa* NcAp-1, NCU03905.5 (XP_957544.2); Pa, *P. anserina* PaAP1 (XP_001905945.1); Mo, *M. oryzae* MoAP1 MGG_12814.7 (XP_001408783.1); Ss, *S. sclerotiorum* SSAP1 SS1G_09561.3 (XP_001589839.1); Bc, *B. cinerea* Bap1 BC1G_14094.1 (XP_001547321.1); Ao, *A. oryzae* AorAP1 AO090001000627 (XP_001819128.1); Ch, *C. heterostrophus* CHAP1 (AAS64313); Aa, *A. alternata* AaAP1 (ACM50933.1); Um, *U. maydis* Yap1 UM02191.1 (XP_758338.1); Kl, *K. lactis* KlYap1 (XP_451077.1); Sc, *S. cerevisiae* Yap1 YML007W (CAA41536.1); Sp, *S. pombe* Pap1 SPAC1783.07c (NP_593662.1); Ca, *C. albicans* Cap1 CaO19.1623 (XP_721702.1). ◆ = filamentous fungal species, ● = yeast species.

3.1.1 Redox western

To examine if H_2O_2 induces intramolecular disulfide bond formation in *E. festucae* YapA, the redox state of enhanced GFP (EGFP) tagged YapA in the wild-type strain was examined in the presence and absence of H_2O_2. The cellular oxidation state was preserved by treating cells with trichloroacetic acid (TCA), which protonates free thiol groups (Jara *et al*., 2007) and precipitates cellular proteins preventing further enzymatic activity and degradation (Sivaraman *et al*., 1997). Total protein extracts were prepared by acid lysis, then treated with iodoacetamide (IAA), to block free thiol groups (present on reduced cysteines), and YapA was detected by western blotting after non-reducing SDS-PAGE. This method allows the detection of intramolecular disulfide bonds as an increase in mobility (due to decreased reactivity with IAA) (Delaunay *et al*., 2000, Jara *et al*., 2007). Alkylation of free thiol groups of cysteine residues decreases the electrophoretic mobility of YapA due to the bulky nature of the compound (Figure 3.4A). The difference in reactivities of disulfide bond and free thiol states of cysteines towards IAA was used to confirm oxidation by H_2O_2 induces disulfide bond formation in YapA (Figure 3.4A). A higher mobility form of YapA was detected in samples from H_2O_2-treated cells compared to samples from cells not exposed to H_2O_2, prior to protein isolation (Figure 3.4B, lanes 1 & 2). This shift was not observed when samples were reduced with β-mercaptoethanol (βME) prior to electrophoresis (Figure 3.4B, lanes 3 & 4). These data demonstrate that H_2O_2 induces disulfide bond formation within YapA. Presumably this disulfide is formed between the conserved Cys363 in the n-CRD and one of the three conserved Cys residues in the c-CRD (Figure 3.1), however, further experimentation would be required to pinpoint the specific residues involved.

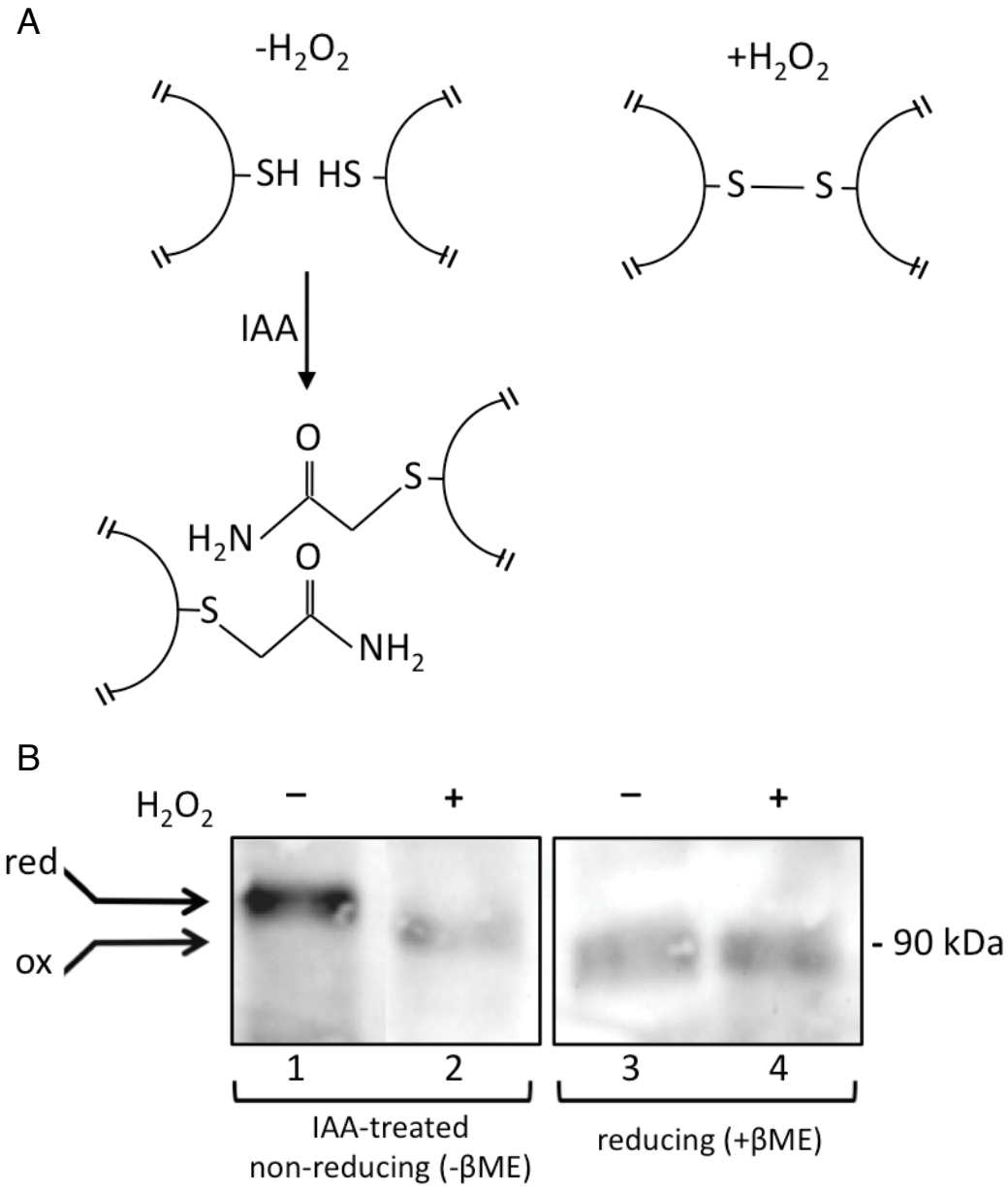

Figure 3.4 H_2O_2 oxidation of YapA. (A) Schematic showing free cysteine thiol groups of YapA in un-treated samples (-H_2O_2) and disulfide bond between cysteine thiol groups in H_2O_2-treated samples (+H_2O_2). Iodoacetamide (IAA) can alkylate free thiol groups but not disulfide-linked groups (B) Protein was extracted from WT cultures expressing EGFP-tagged YapA (PN2747) incubated with (+) and without (-) 16 mM H_2O_2 for 1 h. Protein extracts were treated with IAA and separated by SDS-PAGE without βME (non-reducing ((–βME)) (lanes 1 and 2), or with βME only (reducing ((+βME)) (lanes 3 and 4). YapA-EGFP was detected by chemiluminescence using an anti-GFP rabbit polyclonal antibody (Abcam) and a HRP-conjugated secondary antibody. Expected size of reduced YapA-EGFP fusion protein is 90 kDa.

3.2 *Identification and characterisation of the H_2O_2 sensor homologues*

The redox western blot analysis suggested oxidation of *E. festucae* YapA results in the formation of an intramolecular disulfide. This is likely to require an upstream H_2O_2 sensor that catalyses the disulfide bond formation in YapA. Two alternative modes of activation of the AP-1 transcription factor have been identified in yeast with a glutathione peroxidase (Gpx3) in *S. cerevisiae* and a thiol peroxidase (Tpx1) in *S. pombe* functioning as the H_2O_2 sensor for Yap1 and Pap1, respectively. It is unclear whether the activation of AP-1 transcription factors in filamentous fungi more closely resemble the redox relays of *S. cerevisiae* or *S. pombe*. A putative homologue of *S. cerevisiae GPX3* (also commonly referred to as *HYR1* (hydrogen peroxide resistance protein 1) and *ORP1* (oxidant receptor peroxidase 1)) was identified in the *E. festucae* 2368 genome, and subsequently in the 894 (Fl1) genome following its availability, using tBLASTn analysis with the *S. cerevisiae* Gpx3 amino acid sequence as a query. The homologues identified in both the *E. festucae* 2368 and 894 genomes (*E*-value 2 x 10^{-47}) were 99% identical in sequence and showed 67% similarity to the *S. cerevisiae* Gpx3. In accordance with *E. festucae* nomenclature (Schardl & Scott, 2010) the Fl1 gene was designated *gpxC* (gene model EfM2.018640) and the sequence has been deposited in GenBank (Accession number KC121578).

E. festucae gpxC is predicted to encode a 169 amino acid, 19 kDa protein (GpxC). GpxC contains a catalytic cysteine (Cys39) within the GPx active-site spanning amino acids 27-42, a resolving cysteine (Cys88) and the GPx signature motif spanning amino acids 66-73 (Figure 3.5). These motifs are conserved in other filamentous fungi and yeast GPx proteins (Figure 3.6).

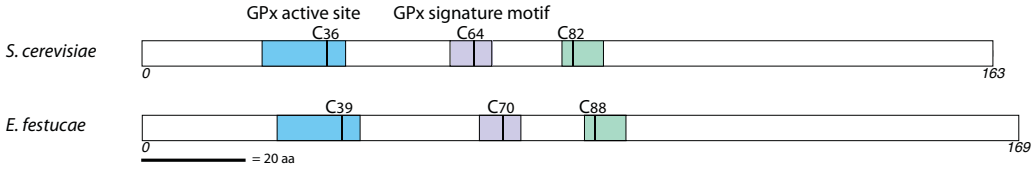

Figure 3.5 Schematic of *S. cerevisiae* Gpx3 and *E. festucae* GpxC. Characteristic motifs of *S. cerevisiae* Gpx3 and *E. festucae* GpxC proteins: catalytic cysteine within the GPx active-site motif (blue) the cysteine contained within the GPx family signature motif (purple) and the resolving cysteine within the conserved region (green) are represented by vertical black lines. Length of each protein in amino acids (aa) is indicated

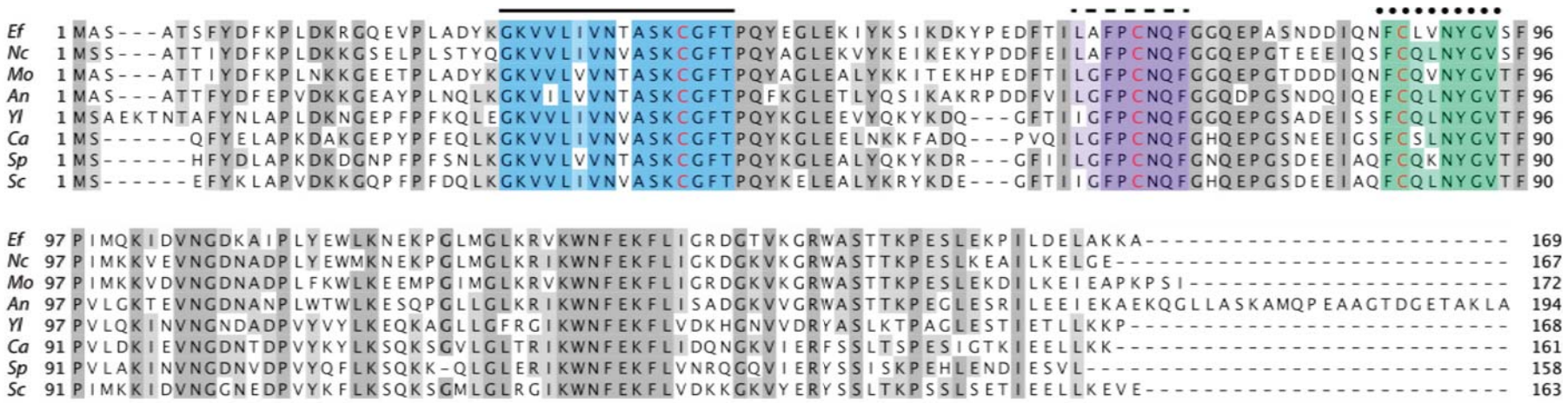

Figure 3.6 Multiple sequence alignment of fungal GPx proteins. Solid line indicates active-site motif, dashed line indicates GPx family signature motif and dotted line indicates region containing the resolving cysteine shown in Figure 3.5. Conserved cysteine residues are highlighted in red. In species where multiple Gpx3-like proteins were present (*C. albicans*) the protein sharing the highest identity and similarity (CaO19.86, XP_714295.1) to *S. cerevisiae* Gpx3 was aligned.

Furthermore, the overall similarity of these proteins is very high. BlastP searches were performed against fungal genomes at the Broad Institute (http://www.broad.mit.edu), and hits with high similarity scores were returned indicating the high degree of conservation of these proteins. While the *S. cerevisiae* genome has three *GPxs* (*GPX1*, *GPX2*, *GPX3*), just one is found in the genome of *E. festucae*, *S. pombe* and the other filamentous fungi analysed in this study (Figure 3.7). The *E. festucae* GpxC protein shares 67% similarity with *S. cerevisiae* Gpx3 and 66% and 58% similarity, at the amino acid level, with Gpx2 and Gpx1, respectively, indicating a high level of conservation within the GPx family.

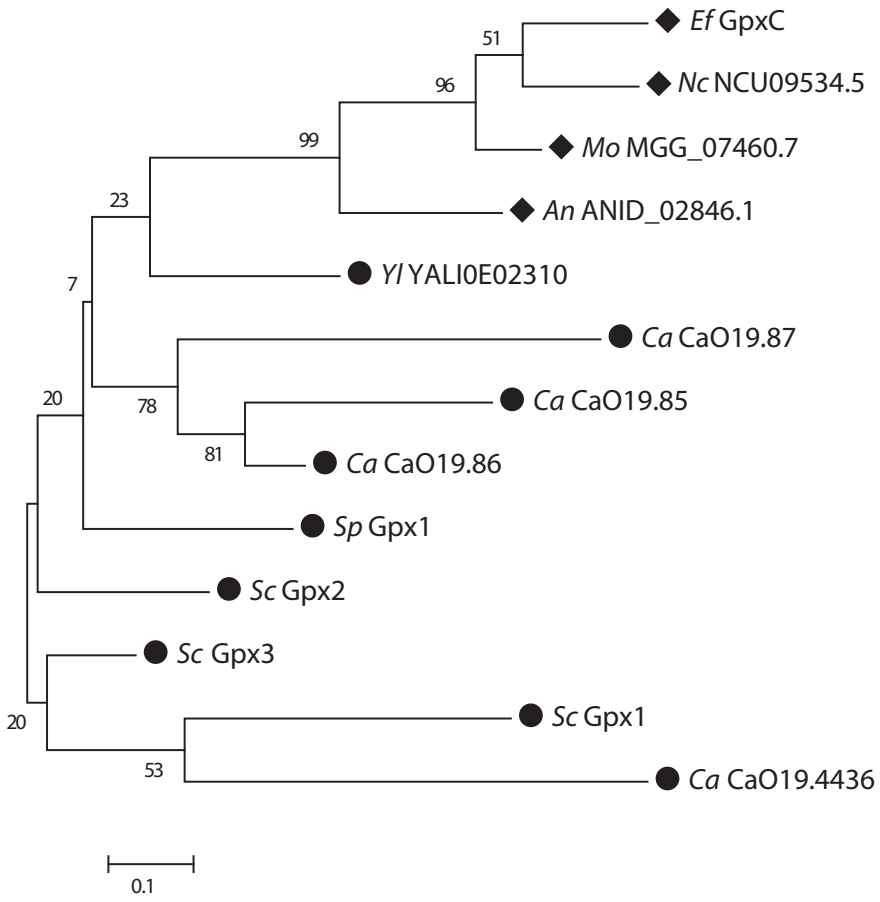

Figure 3.7 Maximum-likelihood dendrogram of fungal GPx proteins. Values above branches indicate bootstrap values based on 10,000 replicates. Gene IDs with associated GenBank accession numbers in parentheses are as follows: Ef, *E. festucae* GpxC EfM2.018640 (KC121578); Nc, *N. crassa* NCU09534.5 (XP_957919.1); Mo, *M. oryzae* MGG_07460.7 (XP_367549.2); An, *A. nidulans* ANID_02846.1 (XP_660450.1); Yl, *Y. lipolytica* YALI0E02310 (XP_503454.1); Ca, *C. albicans* CaO19.87 (XP_714296.1), CaO19.85 (XP_714294.1), CaO19.86 (XP_714295.1); Sp, *S. pombe* Gpx1 SPBC32F12.03c (NP_596146.1); Sc, *S. cerevisiae* Gpx2 YBR244W (NP_009803.1), Gpx3 YIR037W (NP_012303.1), Gpx1 YKL026C (NP_012899.1), Ca, *C. albicans* CaO19.4436 (XP_714081.1). ◆ = filamentous fungal species, ● = yeast species.

Three-dimensional (3D) modelling revealed that the similarity between *S. cerevisiae* Gpx3 and *E. festucae* GpxC at the sequence level is mirrored by similarity at the protein structure level. 3D structural models of *E. festucae* GpxC and *S. cerevisiae* Gpx3 were generated using I-TASSER protein structure prediction software based on a threading algorithm and analysed using Visual Molecular Dynamics (VMD) molecular graphics software (Figure 3.8). C-scores of 1.25 and 1.37 for GpxC and Gpx3, respectively, indicated high reliability of the models. As a reference and further indication of accuracy of the models these structures were compared to the solved crystal structure of Gpx3 (Zhang *et al.*, 2008). The overall structures of GpxC and Gpx3 adopt typical thioredoxin-like folds consisting of a four-stranded β-sheet sandwiched by three α-helices. The model of *E. festucae* GpxC predicts a β-hairpin in the characteristic N-terminal loop, which is not predicted in either the *S. cerevisiae* Gpx3 model or the crystal structure reference (Zhang *et al*., 2008). The side chains of Cys39 and Cys36 in the active sites of *E. festucae* GpxC and *S. cerevisiae* Gpx3, respectively, point towards the exterior of the protein and are solvent-exposed as are the resolving cysteine residues Cys88 and Cys82 (Figure 3.8A). Overall the 3D structures were well conserved providing further evidence that the GpxC and Gpx3 proteins are homologous. Using the ConSurf program (http://consurftest.tau.ac.il/) the amino acid sequences extracted from the 3D structures of GpxC were compared to homologous sequences using BLAST analysis then the multiple sequence alignment mapped onto the surface of the yeast Gpx3 structure. As expected, functional regions of *E. festucae* Gpx3 are highly conserved. (Figure 3.8B). For example regions surrounding the catalytic and resolving cysteine receive the highest conservation scores, whereas variability is seen in regions distal to the active site.

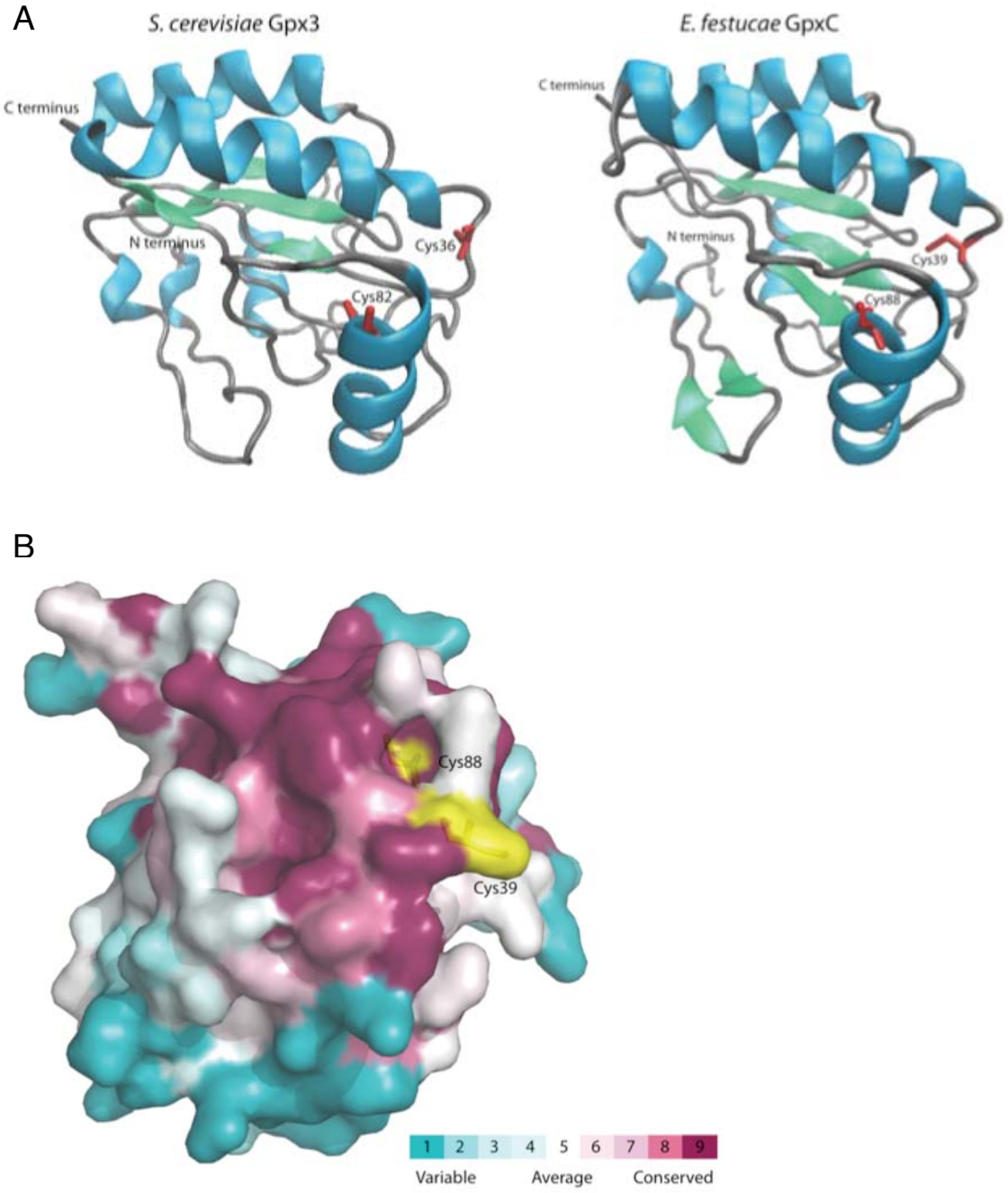

Figure 3.8 Structural representations of *S. cerevisiae* Gpx3 and *E. festucae* GpxC. (A) Overall 3D folds of *S. cerevisiae* Gpx3 and E. *festucae* GpxC proteins are shown. α-helices (blue) and β-strands (green). Side chains of conserved active site and resolving cysteines are represented as red sticks. (B) ConSurf model of *E. festucae* GpxC with the catalytic (Cys39) and resolving (Cys88) highlighted in yellow. The colour key indicates amino acid conservation from variable residues (blue) to highly conserved residues (purple).

A putative homologue of the *S. pombe* peroxiredoxin *TPX1* gene was identified in the *E. festucae* 2368 genome and, following its availability, the 894 (Fl1) genome using *S. pombe* Tpx1 amino acid sequence as a query for tBLASTn analysis. An *E*-value of 1 x 10^{-10} provided convincing evidence that the gene identified in the Fl1 genome was a homologue of *S. pombe* Tpx1. In accordance with *E. festucae* nomenclature (Schardl & Scott, 2010) the Fl1 gene was designated *tpxA* (gene model EfM2.113210) and the sequence has been deposited in GenBank (Accession number KC24437). Two additional putative peroxiredoxins were identified in the *E. festucae* 894 (Fl1) genome (gene models EfM2.064230 and EfM2.115510). Of the three *E. festucae* peroxiredoxins TpxA (EfM2.113210) was the most similar (26% identity) to *S. pombe* Tpx1 (Figure 3.9) and grouped in the same clade (clade A) of a fungal Prx phylogenetic tree (Figure 3.10). However, while Tpx1 from *S. pombe* contains both a peroxidatic cysteine (Cys48) and a resolving cysteine (Cys169) typical of 2-Cys Prxs, TpxA of *E. festucae* contains only a single cysteine residue (Cys47) and is therefore designated a 1-Cys peroxiredoxin (Figure 3.9).

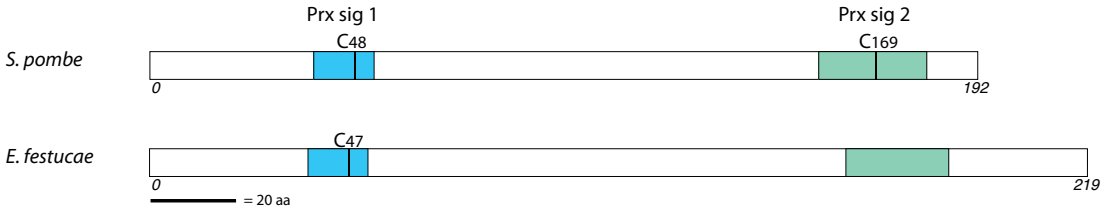

Figure 3.9 Schematic of *S. pombe* Tpx1 and *E. festucae* TpxA. Characteristic motifs of *S. pombe* Tpx1 and *E. festucae* TpxA proteins: Prx signature 1 (blue) and Prx signature 2 (and equivalent region in *E. festucae* TpxA) (green) containing peroxidatic (C48) and resolving (C169) cysteine residues of *S. pombe* Tpx1 and peroxidatic (C47) cysteine residue of *E. festucae* TpxA. Length of each protein in amino acids (aa) is indicated.

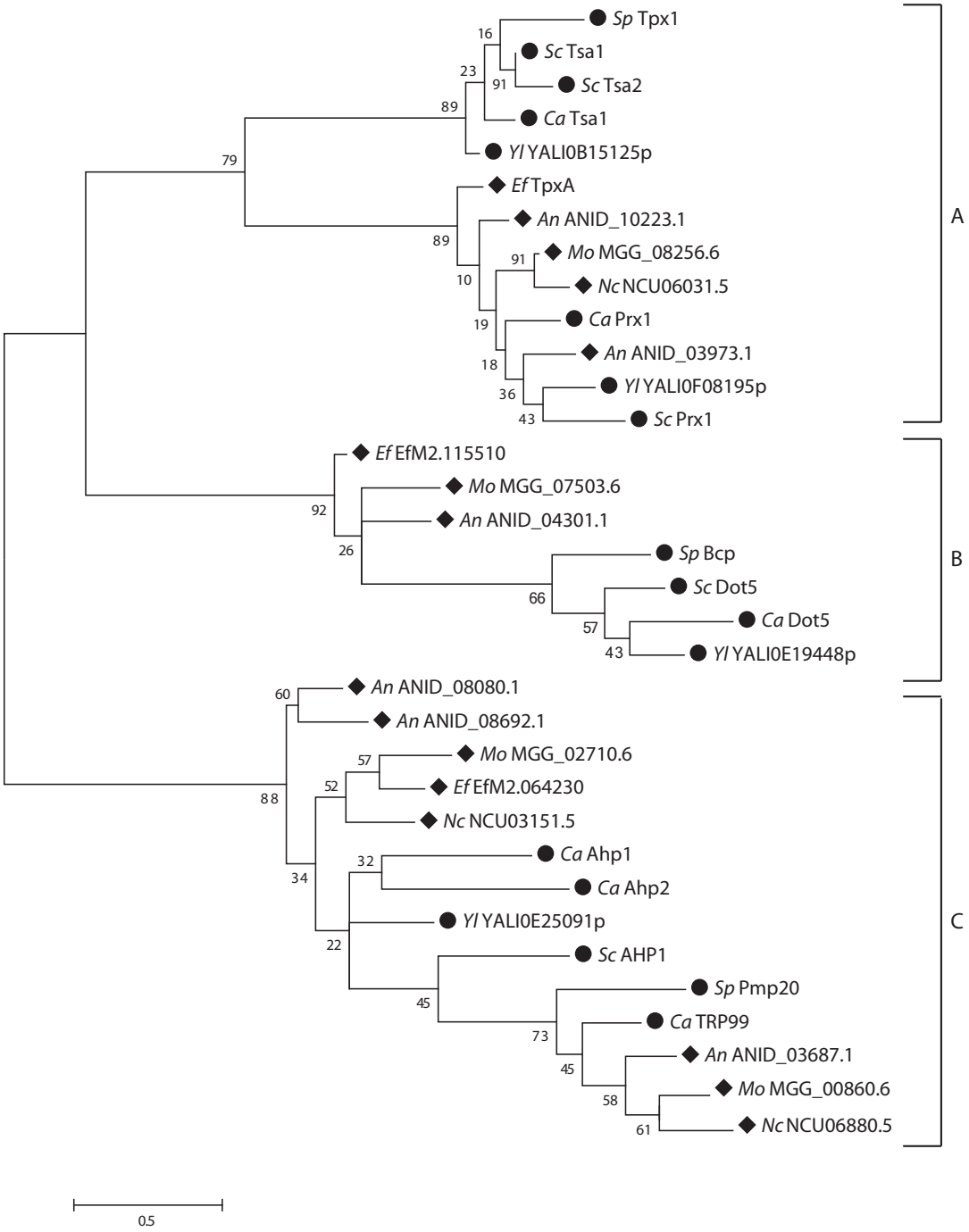

Figure 3.10 Maximum-likelihood dendrogram of fungal Prx proteins. Values above branches indicate bootstrap values based on 2000 replicates. Gene IDs with associated GenBank accession numbers in parentheses are as follows: Sp, *S. pombe* Tpx1 SPCC576.03c (NP_588430.1), Bcp SPBC1773.02c (NP_595117.1), Pmp20 SPCC330.06c (NP_587706.1); Sc, *S. cerevisiae* Tsa1 YML028W (NP_013684.1), Tsa2 YDR453C (NP_010741.1), Prx1 YBL064C (NP_009489.1), Dot5 YIL010W (NP_012255.1), Ahp1 YLR109W (NP_013210.1); Ca, *C. albicans* Tsa1 (XP_716082.1), Prx1 (XP_717002.1), Ahp1 (XP_720512.1), TRP99 (XP_715859.1), Ahp2 (XP_721312.1), Dot5 (XP_717789.1); Yl, *Y. lipolytica* YALI0B15125p (XP_500915.1), YALI0E25091p (XP_504381.1), YALI0F08195p (XP_505152.1) YALI0E19448p (XP_504146.1); Ef, *E. festucae* TpxA (EfM2.113210), Bcp-like (EfM2.115510), Pmp20-like (EfM2.064230); An, *A. nidulans* ANID_03973.1

(XP_661577.1), ANID_10223.1 (CBF85378.1), ANID_08080.1 (CBF73841.1), ANID_08692.1 (XP_681961.1), ANID_03687.1 (CBF75606.1), ANID_04301.1 (CBF77809.1); Mo, *M. oryzae* MGG_08256.6 (XP_362792.2), MGG_07503.6 (XP_367592.1), MGG_00860.6 (XP_368384.2), MGG_02710.6 (XP_366634.1); Nc, *N. crassa* NCU06031.5 (XP_959621.1), NCU06880.5 (XP_959227.1), NCU03151.5 (XP_964200.2). ◆ = filamentous fungal species, ● = yeast species.

The presence or absence of the second resolving cysteine correlates with the amino acid sequence surrounding the cysteine embedded within the first Prx signature motif (Figure 3.11); FTFVCPTEI in the 2-Cys Prx proteins and FTPVCTTEL in the 1-Cys Prx proteins (Rhee *et al.*, 2001). Prx proteins falling into the 1-Cys Prx category by this designation do not contain an additional resolving cysteine in the second Prx signature motif whereas those classified as 2-Cys Prx proteins do (Figure 3.11). Phylogenetic analysis suggests the two additional genes (EfM2.064230 and EfM2.115510) identified in *E. festucae* are homologues of *S. pombe* Pmp20 and Bcp, respectively (Figure 3.10).

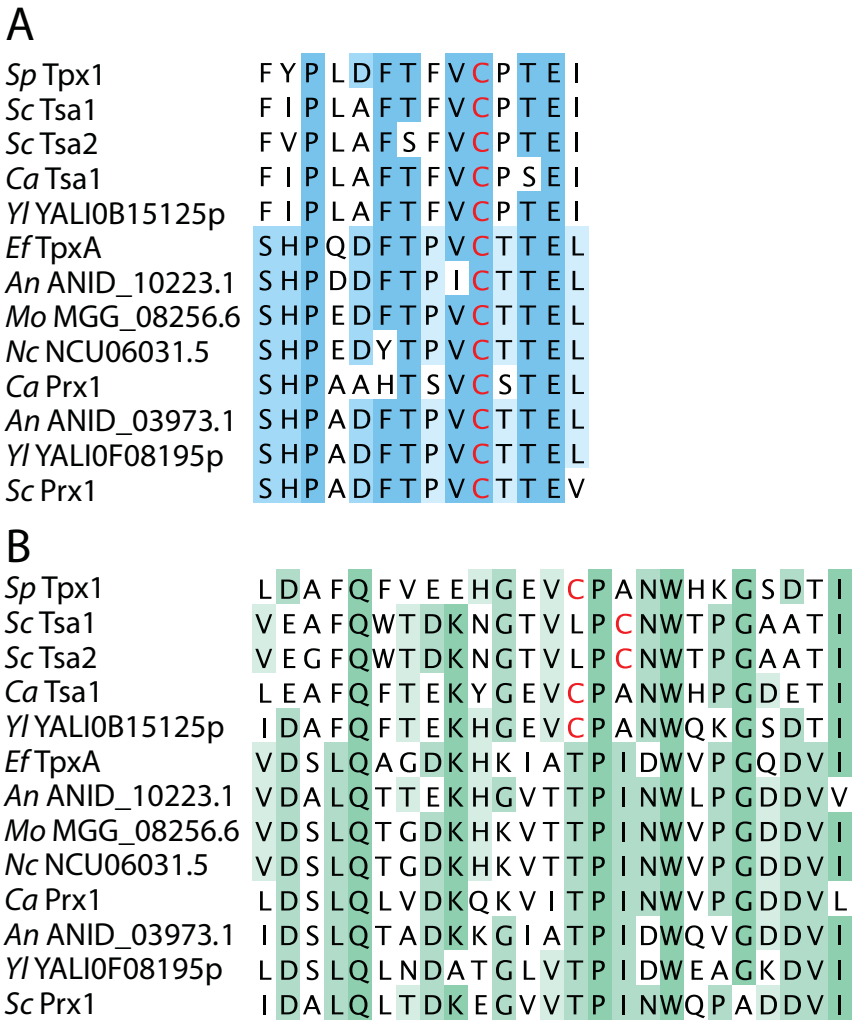

Figure 3.11 Multiple sequence alignment of Prx signature motifs. (A) The first Prx signature motif from peroxiredoxin proteins from clade A in Figure 3.10. Conserved peroxidatic cysteine residues are highlighted in red. (B) The second Prx signature motif from peroxiredoxin proteins from clade A in Figure 3.10. Conserved resolving cysteine residues, where present, are highlighted in red.

3.2.1 Other components

A further component essential for the regulation of Yap1 and Pap1 is the nuclear exportin Crm1 (Toone *et al.*, 1998) which facilitates export of Yap1 and Pap1 from the nucleus under basal conditions. A putative Crm1 homologue was identified in the *E. festucae* 894 (Fl1) genome (EfM2.033580, *E*-value 0.0). Reciprocal BLASTp analysis at NCBI hits other fungal homologues of the Crm1-superfamily. At the amino acid level the *E. festucae* Crm1 homologue shares 56% identity and 73% similarity with *S. pombe* Crm1 (SPAC1805.17) and 49% identity and 67% similarity with *S. cerevisiae* Crm1 (YGR218W). It is probable that the *E. festucae* homologue is a nuclear transport receptor and facilitates YapA export from the nucleus. In *S. cerevisiae* Ybp1 (Yap1-binding

protein 1) is required for Gpx3-induced activation of Yap1 in response to H_2O_2. A tBLASTn analysis failed to identify an equivalent protein in the *E. festucae* genome.

3.2.2 *Confirmation of yapA, gpxC and tpxA gene structure*

The complementary DNA (cDNA) sequences of *yapA*, *gpxC* and *tpxA* were specifically amplified from total *E. festucae* RNA and the genomic DNA (gDNA) sequences specifically amplified from *E. festucae* genomic DNA. The products were sub-cloned into the pCR4-TOPO® vector and sequenced using the Sanger method to confirm the complete coding region and intron-exon boundaries of the *yapA, gpxC* and *tpxA* genes as shown in Figure 3.12.

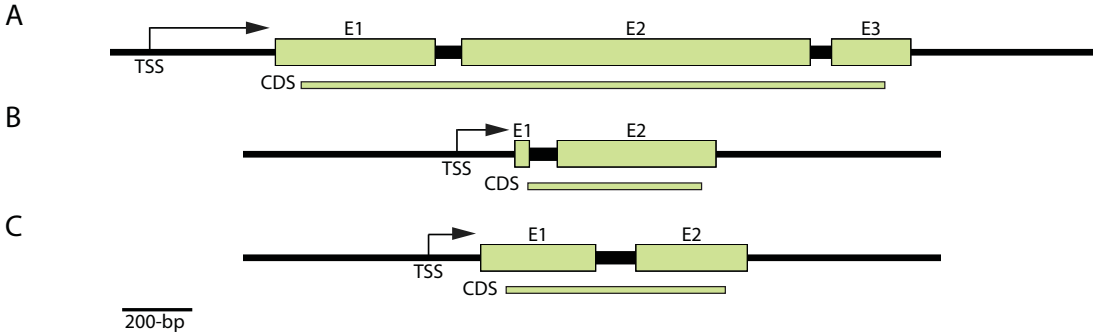

Figure 3.12 Structure of the *yapA, gpxC* and *tpxA* genes. Schematic of the *yapA* (A), *gpxC* (B) and *tpxA* (C) gene structures. Exons (E) are represented as numbered boxes and intervening introns as thicker black lines. Coding sequences (CDS) are shown as single green lines below the gene. TSS indicates the transcription start site and direction of transcription is indicated by arrow.

The *yapA* gene is predicted to consist of three exons (474, 1,034 and 235-bp) separated by 72 and 64-bp introns producing a coding sequence (CDS) 1,743 bp in length (Figure 3.12A). The coding sequence of the *yapA* gene, available at The Epichloë Genome Project web-based database, is based on FGeneSH gene predictions using *F. graminearum* parameters. Therefore the predicted intron/exon boundaries within the *yapA* gene were experimentally tested by sequencing the *yapA* locus using genomic DNA and cDNA templates and aligning the sequences using the MacVector nucleic acid sequence alignment feature. Sequences present in the genomic DNA but absent from the cDNA represent introns and indicate the positions of exon-intron boundaries. The sequence of the genomic DNA and predicted coding sequence at The Epichloë Genome Project website was found to be consistent with results obtained from sequencing the genomic DNA and cDNA and the *yapA* sequence subsequently deposited in GenBank (Accession number KC121577). Recently available data from high throughput transcriptome sequencing (RNA-seq) of *E. festucae* within its plant

host were used to verify the putative *yapA* transcription start site (TSS) (Eaton *et al.*, 2010). The RNA reads detected upstream of the *yapA* gene were consistent with the predicted TSS.

The *gpxC* gene consists of a 43-bp and 467-bp exon separated by a 79-bp intron producing a 510-bp CDS (Figure 3.12B). The intron/exon boundaries predicted for the *gpxC* gene, based on *F. graminearum*, were experimentally tested by sequencing the *gpxC* locus using genomic DNA and cDNA templates and aligning the sequences as outlined above. The predicted genomic and coding sequence at The Epichloë Genome Project website were consistent with results obtained from sequencing the genomic and DNA and cDNA of *gpxC*. However, the numeric values delimiting the exon/intron boundaries and hence exon length were incorrect. These values were adjusted accordingly and the updated *gpxC* sequence deposited in GenBank (Accession number KC121578). The RNA-seq data were used to verify the putative *gpxC* transcription start site (TSS) and mRNA reads extending 5′ from the annotated gene were consistent with the predicted TSS.

The *tpxA* gene consists of two similar sized exons (335 and 325-bp) interrupted by a 119-bp intron producing a 660-bp CDS (Figure 3.12C). The *F. graminearum*-based intron/exon boundaries predicted for the *tpxA* gene were experimentally tested by sequencing the *tpxA* locus using genomic DNA and cDNA templates. The predicted genomic and coding sequence at The Epichloë Genome Project website were consistent with results obtained from sequencing the genomic and DNA and cDNA of *tpxA* and the *tpxA* sequence deposited in GenBank (Accession number KC244374). The TSS was verified against the RNA-seq data.

While examining the RNA-seq data it was observed that the level of expression of *tpxA* was much greater than the levels of surrounding genes, placing *tpxA* in a transcriptional 'hot spot'. This likely reflects the high cellular abundance of Prx proteins, which in turn is an illustration of their physiological importance as protective antioxidants (Wood *et al.*, 2003a).

3.3 S. cerevisiae GPx gene family expansion

The presence of multiple GPx isoforms in *S. cerevisiae* and just a single GPx enzyme present in other yeast and fungal genomes analysed in this study raises the possibility that the extra copies in *S. cerevisiae* arose as a result of the ancient whole-genome duplication (WGD) event that occurred in the yeast lineage about 100 million years ago (Figure 3.13) (Wolfe & Shields, 1997).

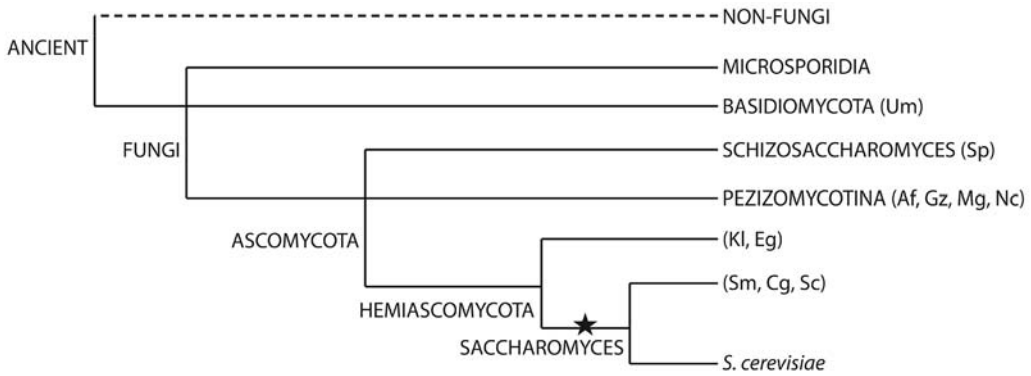

Figure 3.13 WGD in the yeast lineage. A phylogenetic tree adapted from Ekman & Elofsson (2010) to show the occurrence of the Whole Genome Duplication (WGD) in the yeast lineage. The WGD event that distinguishes *Saccharomyces* from the remainder of the Hemiascomycota is indicated with a star. Um, *Ustilago maydis;* Sp, *Schizosaccharomyces pombe*; Af, *Aspergillus fumigatus*; Gz, *Gibberella zeae*; Mg, *Magnaporthe grisea*; Nc, *Neurospora crassa*; Kl, *Kluyveromyces lactis*; Eg, *Eremothecium gossypii*; Sm, *Saccharomyces mikatae*; Cg, *Candida glabrata*; Sc, *Saccharomyces castellii*.

Analysis of gene copies present in pre- and post-genome duplication species, using the Yeast Gene Order Browser (http://wolfe.gen.tcd.ie/ygob), revealed that *GPX1* (YKL026C) and *GPX3* (HYR1/YIR037W) are paralogues arising from the WGD that have been retained in duplicate in the *S. cerevisiae* genome as well as *S. mikatae,* another post-WGD species. One copy was lost in the post-WGD species *K. africana*, *C. glabrata* and *N. castellii* (Figure 3.14A). Both *C. glabrata* and *N. castellii* possess a gene syntenic with *S. cerevisiae GPX1* whereas *K. africana* possesses a gene syntenic with *S. cerevisiae GPX3* indicating no preference for retention of either copy. No such partner exists for *GPX2* in *S. cerevisiae* (Figure 3.14B).

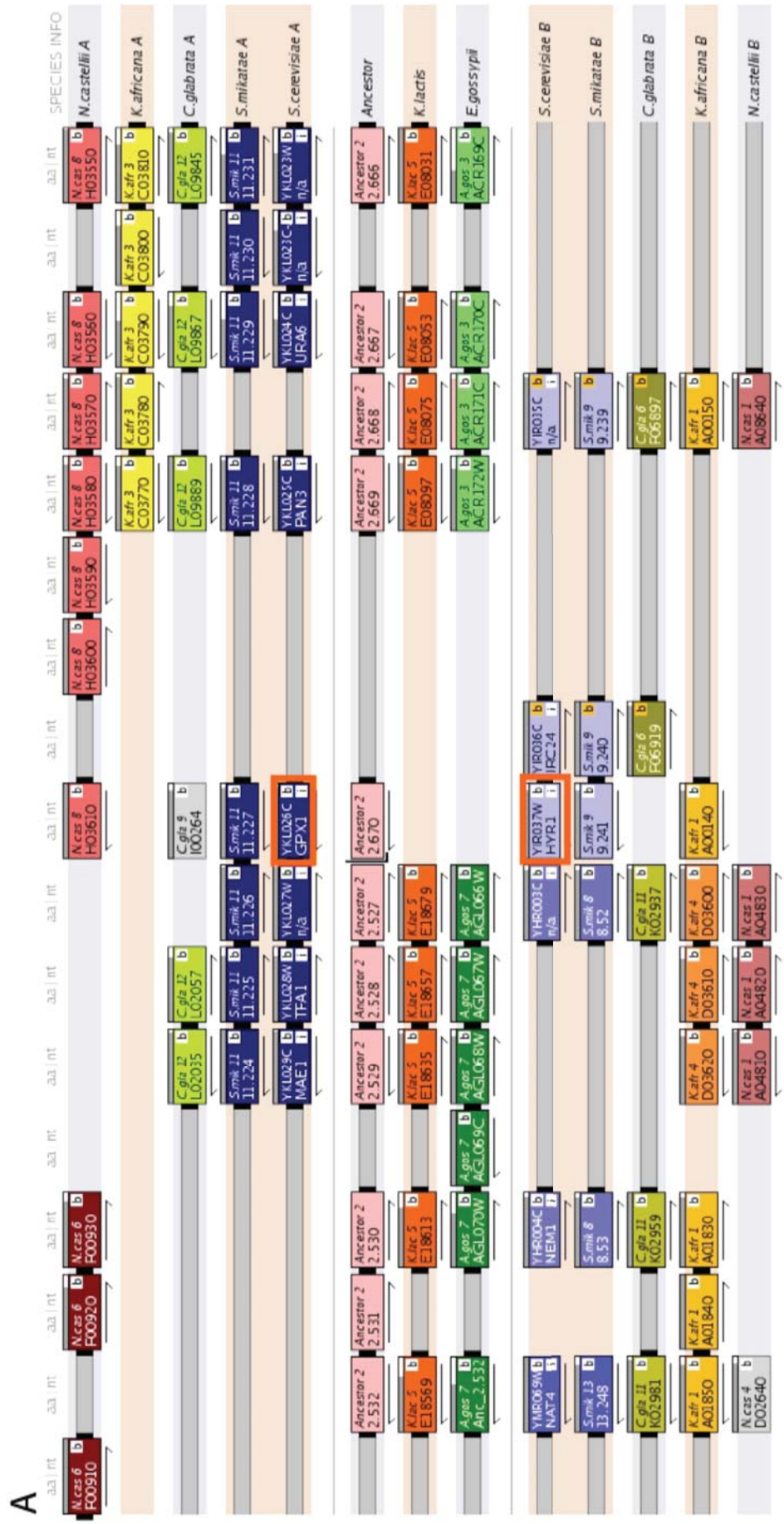
A
SPECIES INFO
N.castellii A
K.africana A
C.glabrata A
S.mikatae A
S.cerevisiae A
Ancestor
K.lactis
E.gossypii
S.cerevisiae B
S.mikatae B
C.glabrata B
K.africana B
N.castellii B

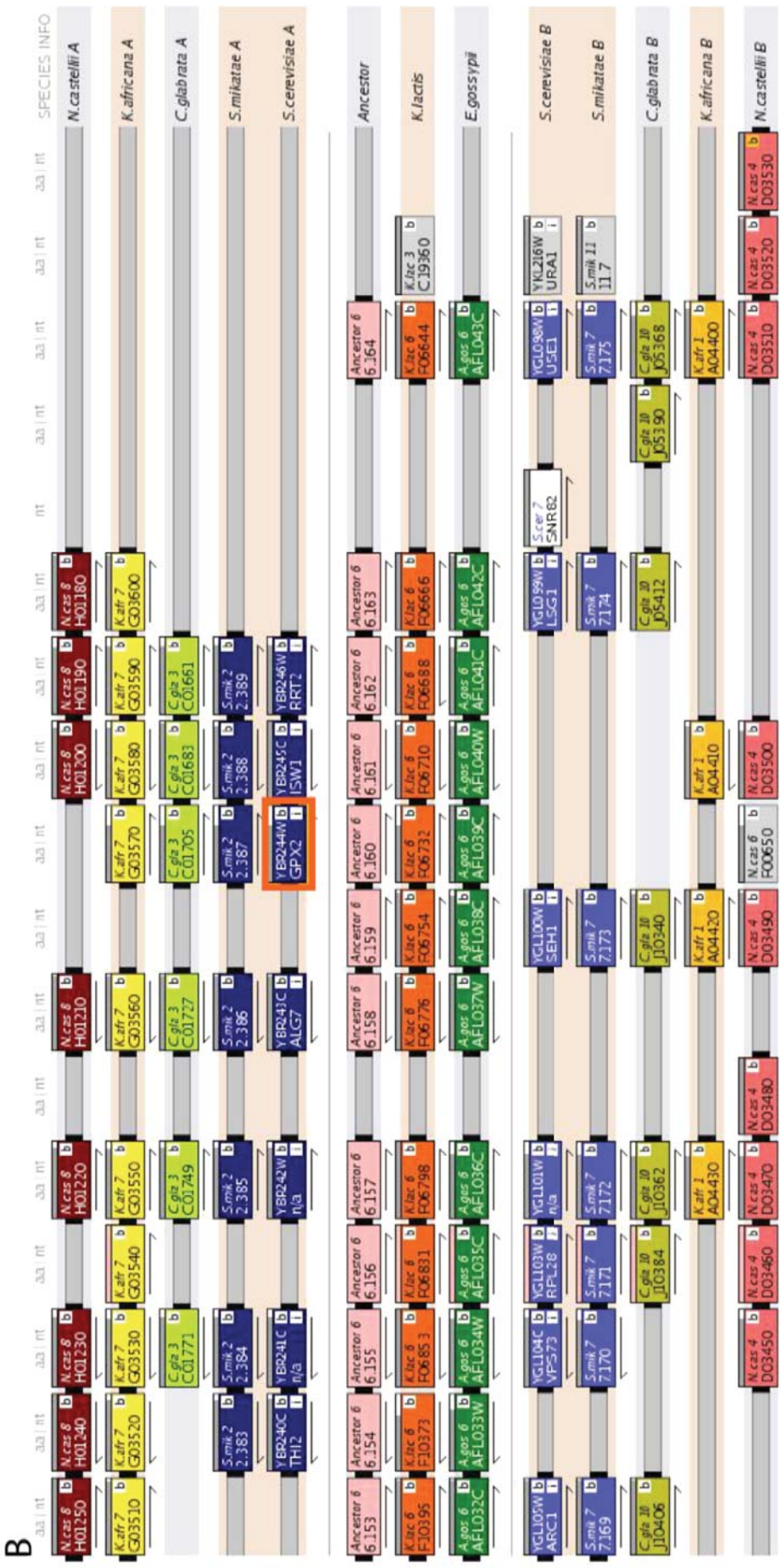

Figure 3.14 Contribution of WGD to the *S. cerevisiae* GPx gene family expansion. (A & B) Yeast Gene Order Browser (YGOB) screenshots. Each box represents a gene. The top five and bottom five tracks represent chromosomes from post-WGD species indicated on the right. The central three tracks represent the ancestral and pre-WGD species indicated on the right. (A) YGOB screenshot focused on the *S. cerevisiae GPX1* and *GPX3/HYR1* genes. *GPX1* and *GPX3/HYR1* are highlighted with an orange border. (B) Yeast Gene Order Browser (YGOB) screenshot focused on the *S. cerevisiae GPX2* gene. *GPX2* is highlighted with an orange border

To investigate why Gpx3, rather than Gpx1 and Gpx2, is involved in a redox relay with Yap1 in *S. cerevisiae* a 3D structural modeling approach was employed. Predicted structures of Gpx1, Gpx2 and Gpx3 were generated using I-TASSER. The highly conserved structures were aligned and visualised in VMD. In *S. cerevisiae* Gpx3 a hydrophobic pocket is formed by Val32, Tyr42, Pro63, and Phe127 near the active-site Cys36 and presumably plays an important role in substrate binding (Zhang *et al*., 2008). This warranted a closer analysis of these residues in the GPx homologues as changes in this region may influence the ability of Gpx3 to interact with Yap1. From the amino acid alignment the active-site Cys, as well as hydrophobic residues near the active-site, appear well-conserved (Figure 3.15A).

A

```
Sc Gpx1   1 ---MQEFYSFSPIDENGNPFPFNSLRNKVVLIVNVASHCAFTPQYKELEYLYEKYKSH---GLVIVAFPCGQFGNQEFEKDKEINK 80
Sc Gpx2   1 --MTTSFYDLECKDKKGESFKFDQLKGKVVLIVNVASKCGFTPQYKELEELYKKYQDK---GFVILGFPCNQFGKQEPGSDEQITE 81
Sc Gpx3   1 ---MSEFYKLAPVDKKGQPFPFDQLKGKVVLIVNVASKCGFTPQYKELEALYKRYKDE---GFTIIGFPCNQFGHQEPGSDEEIAQ 80
Sp Gpx1   1 ---MSHFYDLAPKDKDGNPFPFSNLKGKVVLVVNTASKCGFTPQYKGLEALYQKYKDR---GFIILGFPCNQFGNQEPGSDEEIAQ 80
Ef GpxC   1 MASATSFYDFKPLDKRGQEVPLADYKGKVVLIVNTASKCGFTPQYEGLEKIYKSIKDKYPEDFTILAFPCNQFGGQEPASNDDIQN 86

Sc Gpx1  81 FCQDKYGVTFPILHKIRCNGQKQDPVYKFLKNSVSGKSGIKMIKWNFEKFVVDRNGKVVKRFSCMTRPLELCPIIEELLNQPPEEQ 166
Sc Gpx2  82 FCQLNYGVTFPIMKKIDVNGSNADSVYNYLKSQKAGLLGFKGIKWNFEKFLVDSNGKVVQRFSSLTKPSSLDQEIQSLLSK----- 162
Sc Gpx3  81 FCQLNYGVTFPIMKKIDVNGGNEDPVYKFLKSQKSGMLGLRGIKWNFEKFLVDKKGKVYERYSSLTKPSSLSETIEELLKEVE--- 163
Sp Gpx1  81 FCQKNYGVTFPVLAKINVNGDNVDPVYQFLKSQKK-QLGLERIKWNFEKFLVNRQGQVIERYSSISKPEHLENDIESVL------- 158
Ef GpxC  87 FCLVNYGVSFPIMQKIDVNGDKAIPLYEWLKNEKPGLMGLKRVKWNFEKFLIGRDGTVKGRWASTTKPESLEKPILDELAKKA--- 169
```

B

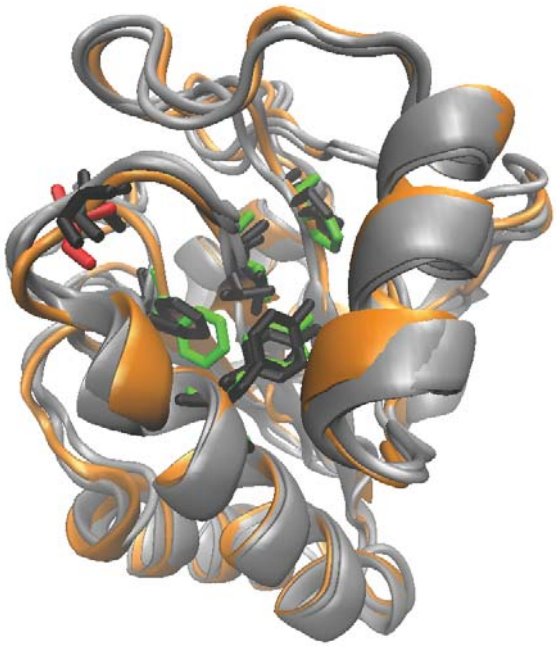

Figure 3.15 Comparison of *S. cerevisiae* GPxs. (A) Multiple sequence alignment of the *S. cerevisiae, S. pombe* and *E. festucae* GPx proteins. Conserved cysteine residues are highlighted in red. (B) Overlay of 3D structures of *S. cerevisiae* Gpx1 and Gpx2 (grey) on Gpx3 (orange). The active-site Cys36 of Gpx3 is highlighted in red and residues comprising the hydrophobic pocket (Val32, Tyr42, Pro63, and Phe127) of Gpx3 are highlighted in green. Equivalent residues of Gpx1 and Gpx2 are shown in black.

Mapping these conserved residues onto the 3D structures of Gpx1, Gpx2 and Gpx3 revealed that the predicted three-dimensional space they occupy is also very similar (Figure 15B). Thus the preference of Gpx3 as a redox sensor for Yap1 is unlikely to be influenced by the hydrophobic binding pocket or location of the active-site cysteine.

3.4 Complementation of yeast YAP1 and GPX3 mutants

To test whether YapA and GpxC are functional homologues of *S. cerevisiae* Yap1 and Gpx3, respectively, full-length cDNAs encoding *E. festucae* YapA and GpxC were cloned into the yeast expression vector pYES2 (Figure 8.2 & 8.3), in which the *GAL1* promoter allows galactose-induction and glucose-repression of genes at the transcriptional level. pGC5 and pGC6 were transformed into *S. cerevisiae* Δ*gpx3* and Δ*yap1* strains, respectively. *E. festucae yapA* and *gpxC* sequences were amplified from cDNA, so that only the exonic (coding) sequence was expressed in *S. cerevisiae*. Previous results of an *S. pombe STY1* complementation assay with the *E. festucae sakA* gene revealed that the *sakA* gene was mis-spliced in *S. pombe* and did not give rise to the correct coding sequence (Eaton *et al.*, 2008). In addition the Δ*yap1* and Δ*gpx3* strains were transformed with pYES2 vector (Figure 3.16 & 3.17) and pYES2 vector containing *S. cerevisiae YAP1* and *GPX3* (Figure 3.16 & 3.17). The Δ*gpx3* strain was intrinsically more resistant to H_2O_2 than the Δ*yap1* strain necessitating the use of a higher H_2O_2 concentration in this assay. Appropriate concentrations for each assay were determined by growing WT and mutant strains on a range of H_2O_2 concentrations and selecting the minimal concentration at which mutant growth was inhibited.

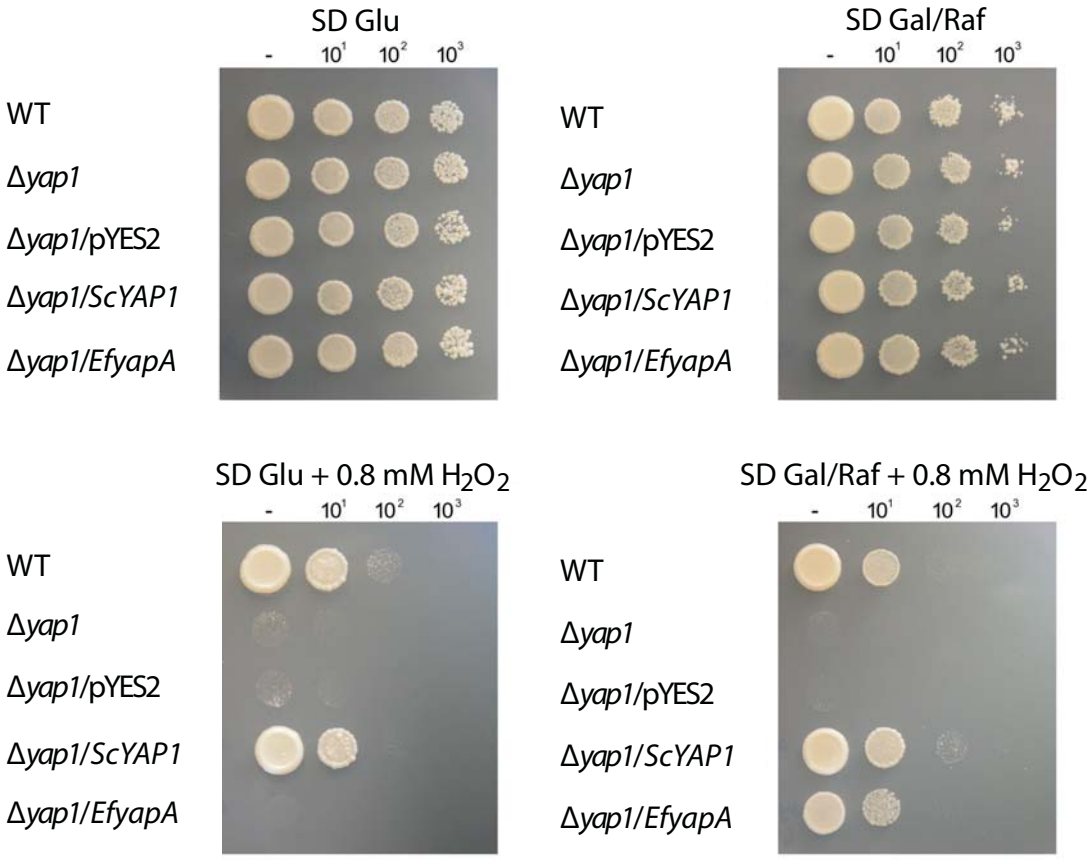

Figure 3.16 *S. cerevisiae* complementation by *E. festucae yapA*. The growth of *S. cerevisiae* WT BY4741 (PN2735), *S. cerevisiae* BY4741-ΔYML007W (Δ*yap1*; PN2736), and derivatives of this strain transformed with the empty vector pYES2 (PN2847), pYES2*ScYAP1* (PN2845) and pYES2*EfyapA* (PN2846) was tested on SD plates with glucose, SD plates with galactose and raffinose, SD plates with glucose supplemented with 0.8 mM H_2O_2, and SD plates with galactose and raffinose supplemented with 0.8 mM H_2O_2. Serial 10-fold dilutions of cultures indicated on the left were spotted.

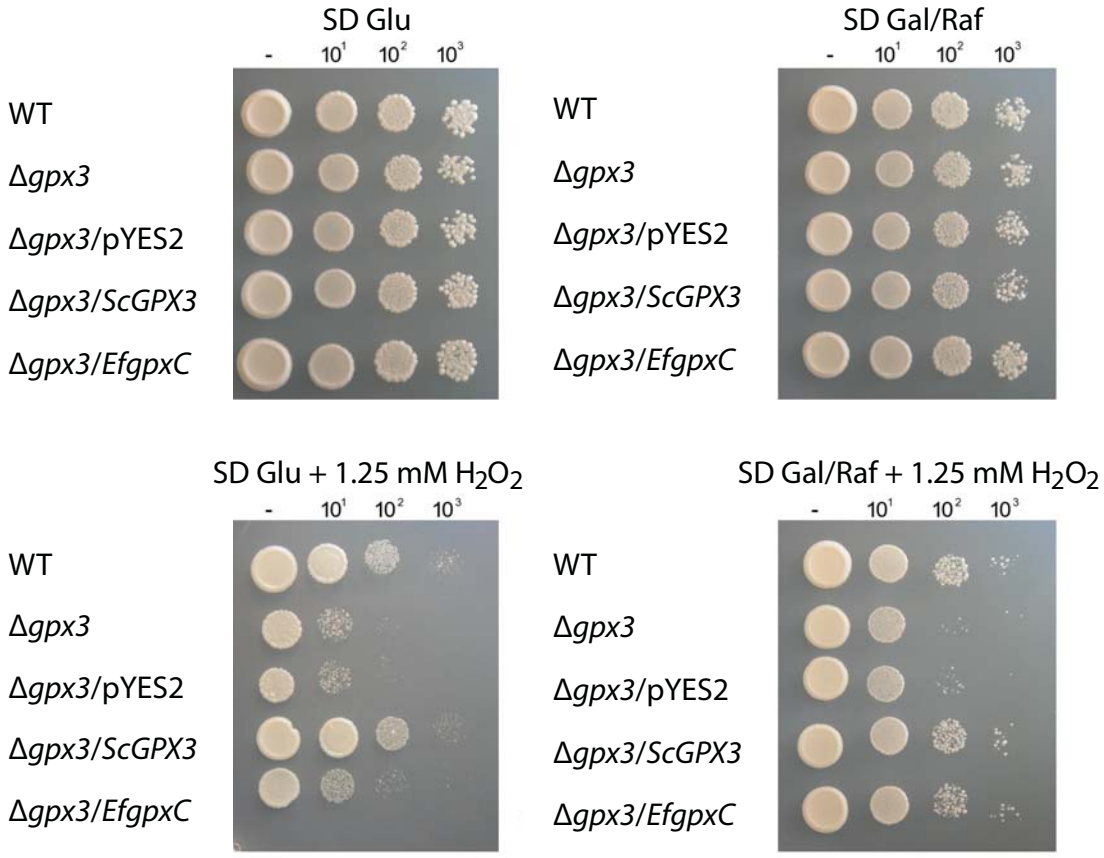

Figure 3.17 *S. cerevisiae* complementation by *E. festucae gpxC*. The growth of *S. cerevisiae* WT BY4741, *S. cerevisiae* BY4741-ΔYIR037W (Δ*gpx3*; PN2737), and derivatives of this strain transformed with the empty vector pYES2 (PN2850), pYES2*ScGPX3* (PN2848) and pYES2*EfgpxC* (PN2849) was tested on SD plates with glucose, SD plates with galactose and raffinose, SD plates with glucose supplemented with 1.25 mM H_2O_2, and SD plates with galactose and raffinose supplemented with 1.25 mM H_2O_2. Serial 10-fold dilutions of cultures indicated on the left were spotted.

On media containing 0.8 mM hydrogen peroxide and galactose, growth of the Δ*yap1* strain and the Δ*yap1*/pYES2 strain, a vector control, was significantly inhibited in comparison to the wild-type strain. Expression of *E. festucae* YapA (Δ*yap1*/Ef*yapA*) or *S. cerevisiae* Yap1 (Δ*yap1*/Sc*YAP1*) in Δ*yap1* was able to restore growth of the Δ*yap1* strain on H_2O_2 to levels comparable to wild-type (Figure 3.16). This indicates that *E. festucae yapA* is able to functionally complement the oxidative stress sensitivity defect of the *S. cerevisiae YAP1* mutant. However, it is evident from the number of colonies formed that complementation by *yapA* from *E. festucae* is less efficient than that achieved by *S. cerevisiae YAP1* (Figure 3.16). This may be due to reduced activity of the YapA protein or reduced expression of the YapA protein in *S. cerevisiae*. All strains grew equally well on media containing glucose. On glucose-containing medium to which 0.8 mM hydrogen peroxide was added both the wild-type strain and the

Δ*yap1*/Sc*YAP1* was able to grow. Growth of the Δ*yap1* strain complemented with the *S. cerevisiae YAP1* gene was presumably due to the inherent leakiness of the GAL1 promoter where low-level expression of *YAP1* under the GAL1 promoter is capable of rescuing the H_2O_2-sensitivity phenotype. The GAL1 promoter system is somewhat leaky on glucose-containing media and consequently essential gene deletants complemented with the cognate gene under GAL1 promoter regulation can, in some cases, grow on glucose-containing media (I. Dawes, personal communication, March 25, 2010).

S. cerevisiae Δ*gpx3* mutants are slightly more tolerant of hydrogen peroxide than Δ*yap1* mutants, potentially due to an alternative pathway for Yap1 activation in the absence of Gpx3 (Delaunay *et al*., 2002), thus complementation of the *S. cerevisiae Δgpx3* was tested on media containing 1.25 mM hydrogen peroxide and galactose. Although the effect of hydrogen peroxide on the *S. cerevisiae* Δ*gpx3* strain is less severe than that observed for the *S. cerevisiae* Δ*yap1* strain, growth of the *S. cerevisiae* Δ*gpx3* strain was reduced in comparison to the wild-type strain. Expression of *E. festucae* GpxC (Δ*gpx3*/Ef*gpxC*) or *S. cerevisiae* Gpx3 (Δ*gpx3*/Sc*GPX3*) in Δ*gpx3* was able to restore growth of the Δ*gpx3* strain on H_2O_2 to wild-type levels (Figure 3.17). Again, leakiness of the GAL1 promoter on glucose-containing media permitted the low-level expression of *S. cerevisiae GPX3* to restore growth to wild-type levels in the presence of H_2O_2. These findings indicate that both *E. festucae yapA* and *gpxC* are able to complement yeast Δ*yap1* and Δ*gpx3,* respectively, and confirm that functional homologues of both partners in the *S. cerevisiae* Yap1-Gpx3 redox relay are present in the *E. festucae* genome.

3.5 Targeted deletion of the yapA, gpxC and tpxA genes

To investigate the role of the *E. festucae* YapA protein and putative upstream regulatory proteins, GpxC and TpxA, in conferring resistance to various oxidative stress-inducing compounds, the corresponding genes were deleted by homologous recombination. The entire coding regions of *yapA* and *tpxA* were replaced with expression cassettes conferring resistance to hygromycin B and the coding region of *gpxC* was replaced with a geneticin resistance marker (Figures 3.18, 3.20, 3.22). Use of different selectable markers for *gpxC* and *tpxA* replacement allowed *gpxC* to be deleted in the Δ*tpxA* background to generate Δ*gpxC*Δ*tpxA* double mutants (Figure 3.24). Antibiotic-resistant transformants were screened by PCR to confirm the antibiotic resistance cassette had inserted correctly into the targeted gene locus. DNA was

isolated, using a rapid genomic DNA extraction procedure (Section 2.3.2.1.2), from potential replacement strains and amplified using primer pairs which bind within the flanking regions of the gene to be deleted (*yapA*: yap22/yap23; *gpxC*: gpx15/gpx16 and *tpxA*: tpx13/tpx14) and primer pairs which amplify over the 5′ and 3′ deletion cassette boundaries (*yapA*: yap11/yap21 and yap9/yap10; *gpxC*: gpx9/gpx10 and gpx17/gpx18; *tpxA*: tpx15/tpx16 and tpx17/tpx18) (Figures 3.18, 3.20, 3.22 & 3.24). PCR using primer pairs that flank the regions of the deleted gene will yield different sized products for the wild-type compared to deletion mutants as the wild-type gene is replaced by the deletion cassette. Transformants yielding both wild-type and mutant-sized bands contain an ectopic integration of the deletion cassette and were not selected for further analysis. PCR using primer pairs which amplify over the 5′ and 3′ deletion cassette boundaries will only yield a product if the gene deletion cassette has integrated at the correct locus to replace the wild-type copy of the gene. Transformants yielding the PCR products consistent with targeted gene deletion were further examined by Southern blot analysis (Figures 3.19, 3.21, 3.23 & 3.25).

Southern analysis of *Pst*I-digested Δ*yapA* genomic DNA revealed 6.7 and 4.7 kb bands consistent with integration of the pGC2 resistance cassette at the *yapA* locus. A single band corresponding to the size of the gene replacement cassette was also detected, which is indicative of the 3.8 kb pGC2 fragment inserting multiple times at the target locus. No additional bands were detected which would indicate ectopic insertion of the gene replacement cassette elsewhere in the genome. The additional insertions of the resistance cassette at the *yapA* locus is unlikely to have spurious effects, as the *yapA* gene is deleted whether single or multiple cassettes integrate at the target locus. However, to address the possibility of spurious effects where a phenotype was observed for the *yapA* mutant it was complemented by reintroduction of a single copy of the *yapA* locus (pGC11) (Figure 3.19). Integration of the complementation construct was confirmed by PCR, using primer pair yap5/yap6.

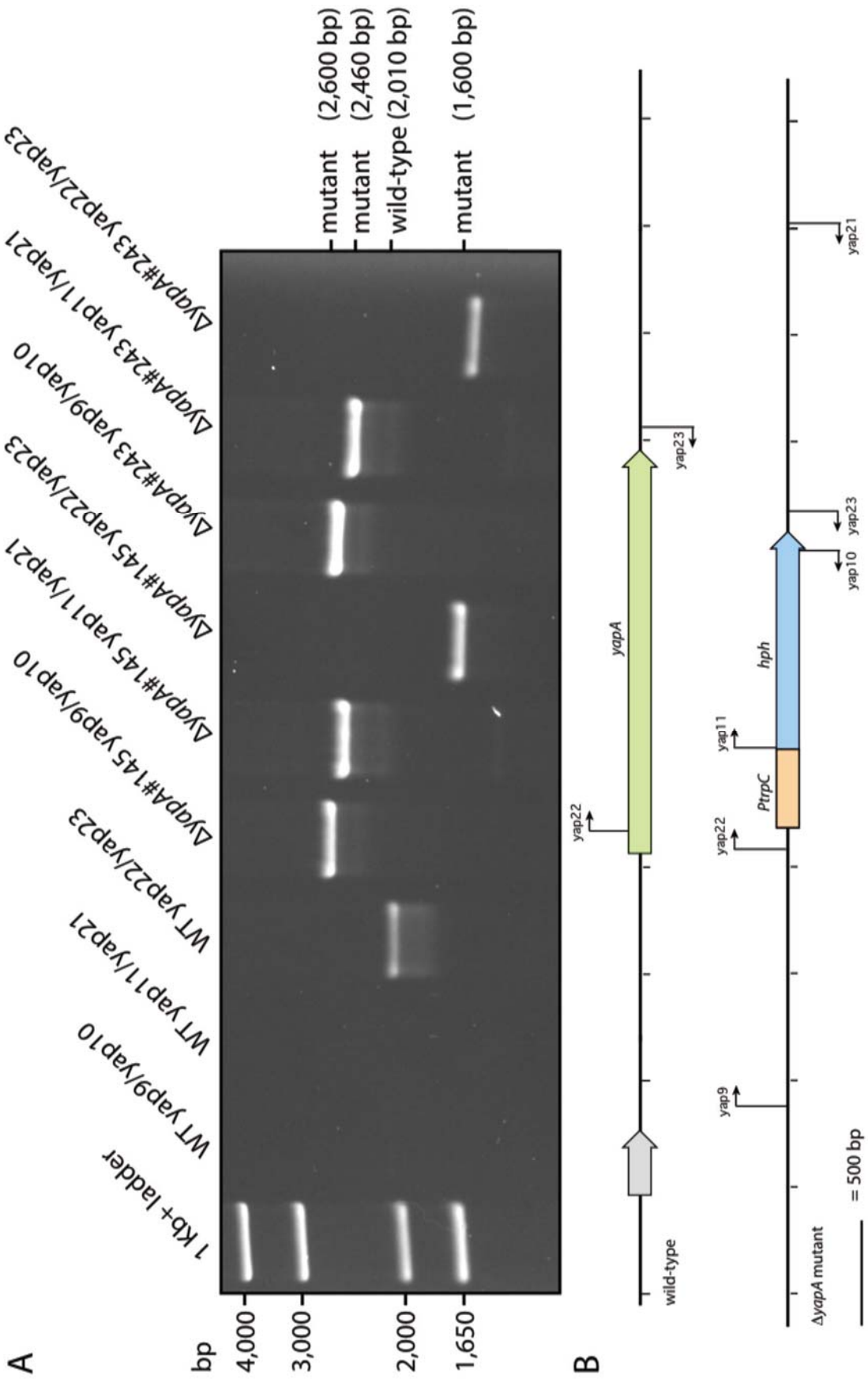
A
1 kb+ ladder
WT yap9/yap10
WT yap11/yap21
WT yap22/yap23
ΔyapA#145 yap9/yap10
ΔyapA#145 yap11/yap21
ΔyapA#145 yap22/yap23
ΔyapA#243 yap9/yap10
ΔyapA#243 yap11/yap21
ΔyapA#243 yap22/yap23
bp
4,000
3,000
2,000
1,650
mutant (2,600 bp)
mutant (2,460 bp)
wild-type (2,010 bp)
mutant (1,600 bp)
B
wild-type
yap22
yapA
yap23
ΔyapA mutant
yap9
yap22
PtrpC
yap11
hph
yap10
yap23
yap21
= 500 bp

Figure 3.18 PCR to confirm *E. festucae yapA* deletion. (A) PCR screening of *yapA* gene replacement strains. Primer pair yap22/yap23 flanks the *yapA* gene and yields a 2,010 bp product for wild-type and a 1,600 bp product for Δ*yapA* mutants. Primer pair yap9/yap10 amplifies over the 5′ deletion cassette boundary and yields a 2,600 bp product for Δ*yapA* mutants. Primer pair yap11/yap21 amplifies over the 3′ deletion cassette boundary and yields a 2,460 bp product for Δ*yapA* mutants. (B) Schematic of the wild-type *yapA* locus and replacement of the corresponding region with the *hph* resistance cassette in the Δ*yapA* mutant. Grey arrow indicates gene flanking *yapA*.

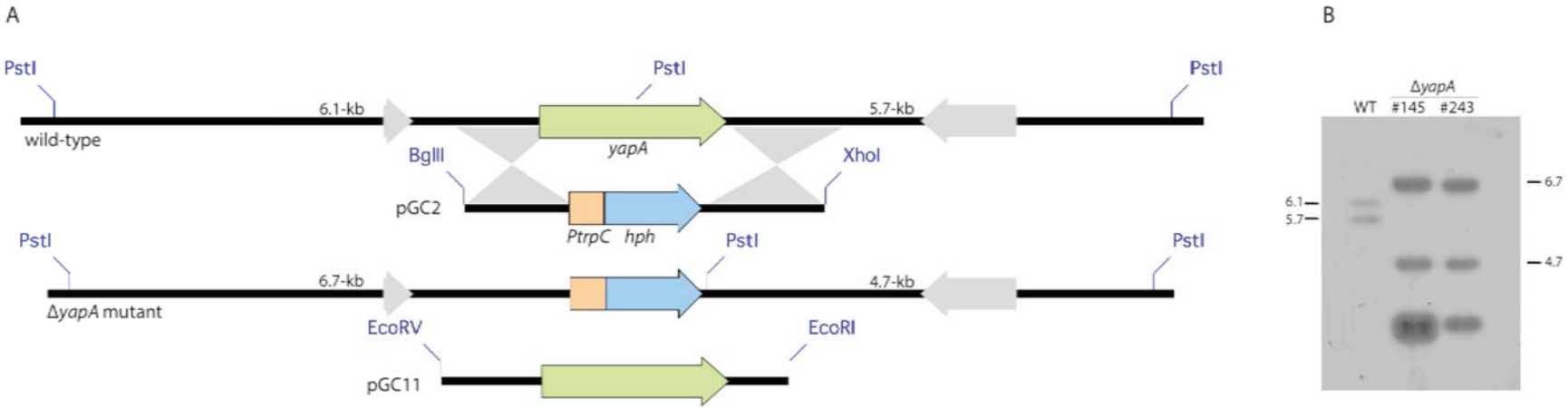

Figure 3.19 Southern blotting to confirm *E. festucae yapA* deletion. (A) Schematic of the wild-type *yapA* locus, linearised replacement construct (pGC2), Δ*yapA* mutant genomic locus and complementation construct (pGC11). The regions of recombination between homologous sequences flanking the *yapA* locus and *hph* resistance cassette are indicated by grey shading. Restriction enzyme sites used to generate linear replacement (*Bgl*II, *Xho*I) and complementation fragments (*Eco*RV, *Eco*RI) and for Southern analysis (*Pst*I) are indicated. Grey arrows indicate genes flanking *yapA*. (B) Autoradiograph of Southern blot of *Pst*I digests (1 μg) of *E. festucae* WT PN2278 (lane 1), Δ*yapA*#145 PN2740 (lane 2) and Δ*yapA*#243 PN2739 (lane 3) genomic DNA, probed with ^{32}P-labelled pGC2. The expected fragment sizes are 6.1- and 5.7-kb for wild-type and 6.7- and 4.7-kb for the Δ*yapA* mutants.

Southern analysis of Δ*gpxC,* Δ*tpxA* and Δ*gpxC*Δ*tpxA* double mutants showed a banding pattern consistent with integration of a single gene replacement cassette at the target locus (Figure 3.21, 3.23 and 3.25). As phenotype analysis did not uncover any observable effects resulting from deletion of the *gpxC* and *tpxA* genes, Δ*gpxC,* Δ*tpxA* and Δ*gpxC*Δ*tpxA* strains were not complemented in accordance with the standard practice of performing genetic complementation only when a mutant phenotype is observed.

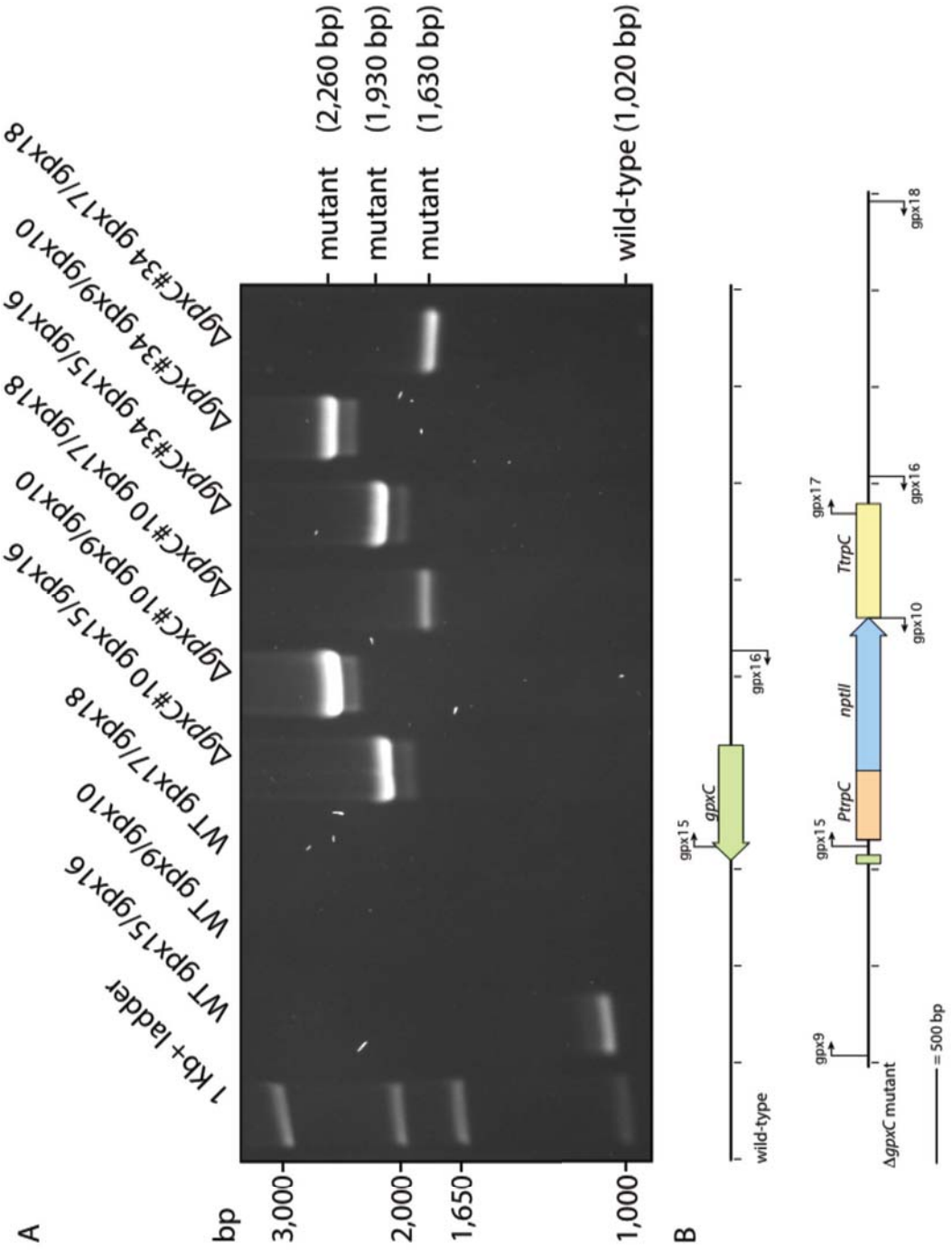
A
bp
3,000
2,000
1,650
1,000
1 kb+ ladder
WT gpx15/gpx16
WT gpx9/gpx10
WT gpx17/gpx18
ΔgpxC#10 gpx15/gpx16
ΔgpxC#10 gpx9/gpx10
ΔgpxC#10 gpx17/gpx18
ΔgpxC#34 gpx15/gpx16
ΔgpxC#34 gpx9/gpx10
ΔgpxC#34 gpx17/gpx18
mutant (2,260 bp)
mutant (1,930 bp)
mutant (1,630 bp)
wild-type (1,020 bp)
B
gpx15
gpxC
gpx16
wild-type
gpx17
TtrpC
gpx16
nptII
gpx15
PtrpC
gpx10
gpx9
ΔgpxC mutant
gpx18
= 500 bp

Figure 3.20 PCR to confirm *E. festucae gpxC* deletion. (A) PCR screening of *gpxC* gene replacement strains. Primer pair gpx15/gpx16 flanks the *gpxC* gene and yields a 1,020 bp product for wild-type and a 1,930 bp product for Δ*gpxC* mutants. Primer pair gpx9/gpx10 amplifies over the 5′ deletion cassette boundary and yields a 2,260 bp product for Δ*gpxC* mutants. Primer pair gpx17/gpx18 amplifies over the 3′ deletion cassette boundary and yields a 1,630 bp product for Δ*gpxC* mutants. (B) Schematic of the wild-type *gpxC* locus and replacement of the corresponding region with *npt*II resistance cassette in the Δ*gpxC* mutant.

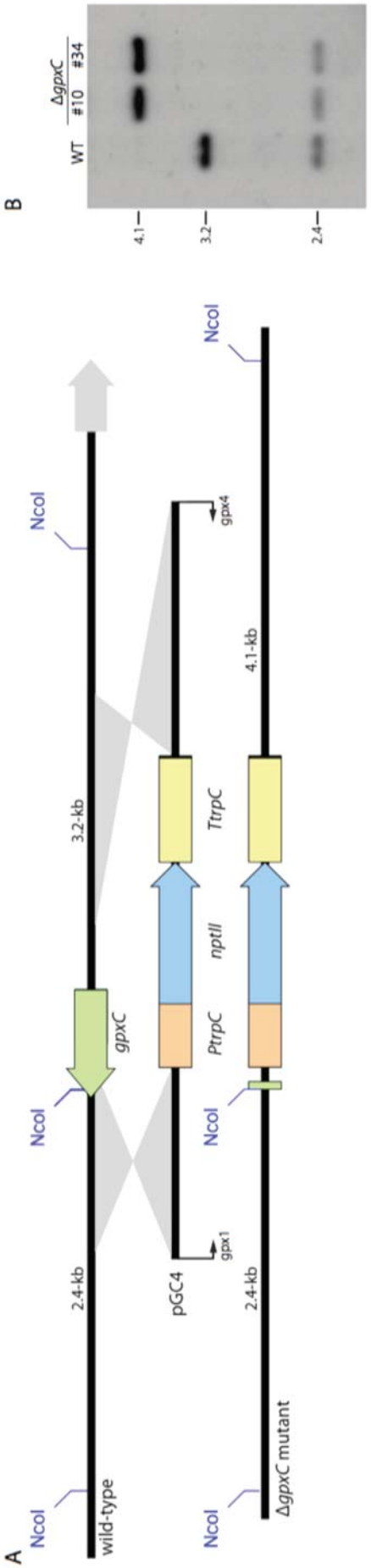

Figure 3.21 Southern blotting to confirm *E. festucae gpxC* deletion. (A) Schematic of the wild-type *gpxC* locus, linearised replacement construct (pGC4) and Δ*gpxC* mutant genomic locus. The regions of recombination between homologous sequences flanking the *gpxC* locus and *npt*II resistance cassette are indicated by grey shading. Primer pair gpx1/gpx4 used to generate linear replacement fragment and restriction enzyme sites used for Southern analysis (*Nco*I) are indicated. Grey arrow indicates gene flanking *gpxC* (B) Autoradiograph of Southern blot of *Nco*I digests (1 µg) of *E. festucae* WT (lane 1), Δ*gpxC*#10 PN2741 (lane 2) and Δ*gpxC*#34 PN2742 (lane 3) genomic DNA, probed with ^{32}P-labelled pGC4. The expected fragment sizes are 3.2- and 2.4-kb for wild-type and 4.1- and 2.4-kb for the Δ*gpxC* mutants.

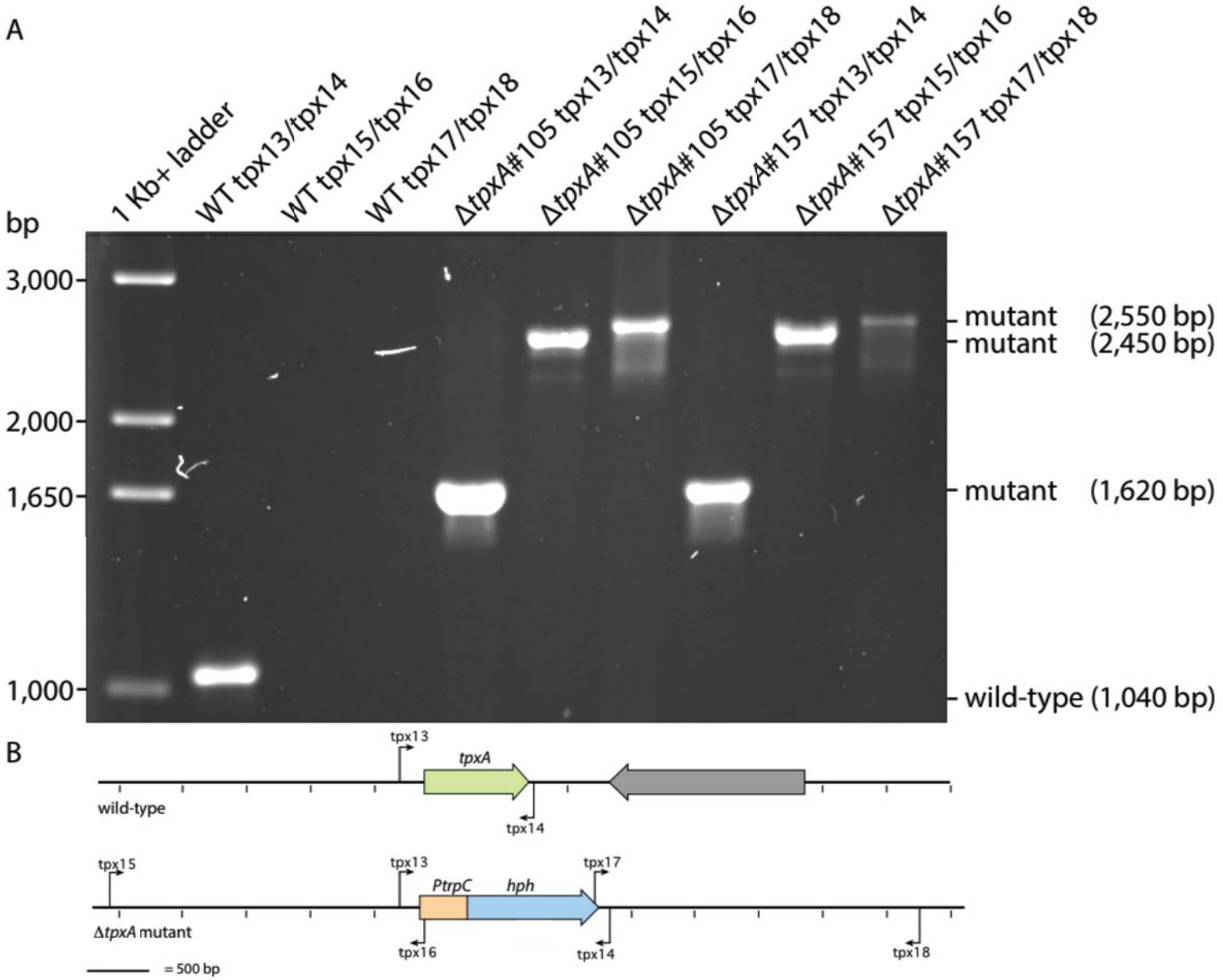
A
1 Kb+ ladder
WT tpx13/tpx14
WT tpx15/tpx16
WT tpx17/tpx18
ΔtpxA#105 tpx13/tpx14
ΔtpxA#105 tpx15/tpx16
ΔtpxA#105 tpx17/tpx18
ΔtpxA#157 tpx13/tpx14
ΔtpxA#157 tpx15/tpx16
ΔtpxA#157 tpx17/tpx18
bp
3,000
2,000
1,650
1,000
mutant (2,550 bp)
mutant (2,450 bp)
mutant (1,620 bp)
wild-type (1,040 bp)
B
tpx13
tpxA
wild-type
tpx14
tpx15
tpx13
tpx17
PtrpC
hph
ΔtpxA mutant
tpx16
tpx14
tpx18
= 500 bp

Figure 3.22 PCR to confirm *E. festucae tpxA* deletion. (A) PCR screening of *tpxA* gene replacement strains. Primer pair tpx13/tpx14 flanks the *tpxA* gene and yields a 1,040 bp product for wild-type and a 1,620 bp product for Δ*tpxA* mutants. Primer pair tpx15/tpx16 amplifies over the 5′ deletion cassette boundary and yields a 2,450 bp product for Δ*tpxA* mutants. Primer pair tpx17/tpx18 amplifies over the 3′ deletion cassette boundary and yields a 2,550 bp product for Δ*tpxA* mutants. (B) Schematic of the wild-type *tpxA* locus and replacement of the corresponding region with *hph* resistance cassette in the Δ*tpxA* mutant. Grey arrow indicates gene flanking *tpxA*

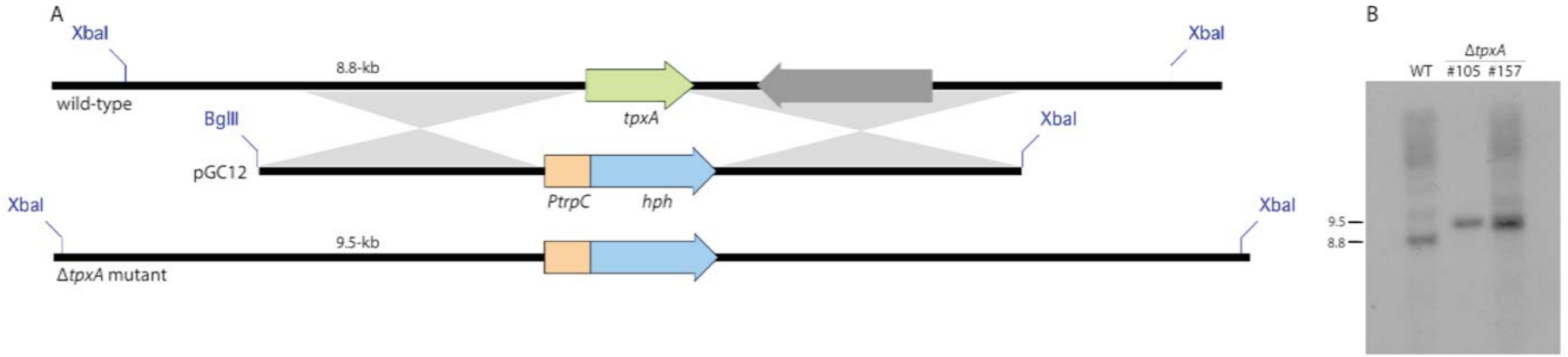

Figure 3.23 Southern blotting to confirm *E. festucae tpxA* deletion. (A) Schematic of the wild-type *tpxA* locus, linearised replacement construct (pGC12) and Δ*tpxA* mutant genomic locus. The regions of recombination between homologous sequences flanking the *tpxA* locus and *hph* resistance cassette are indicated by grey shading. Restriction enzyme sites used to generate the linear replacement fragment (*Bgl*II, *Xba*I) and for Southern analysis (*Xba*I) are indicated. Grey arrow indicates gene flanking *tpxA* (B) Autoradiograph of Southern blot of *Xba*I digests (1 μg) of *E. festucae* WT (lane 1), Δ*tpxA*#105 PN2821 (lane 2) and Δ*tpxA*#157 PN2822 (lane 3) genomic DNA, probed with ^{32}P-labelled pGC12. The expected fragment sizes are 8.8-kb for wild-type and 9.5-kb for the Δ*tpxA* mutants.

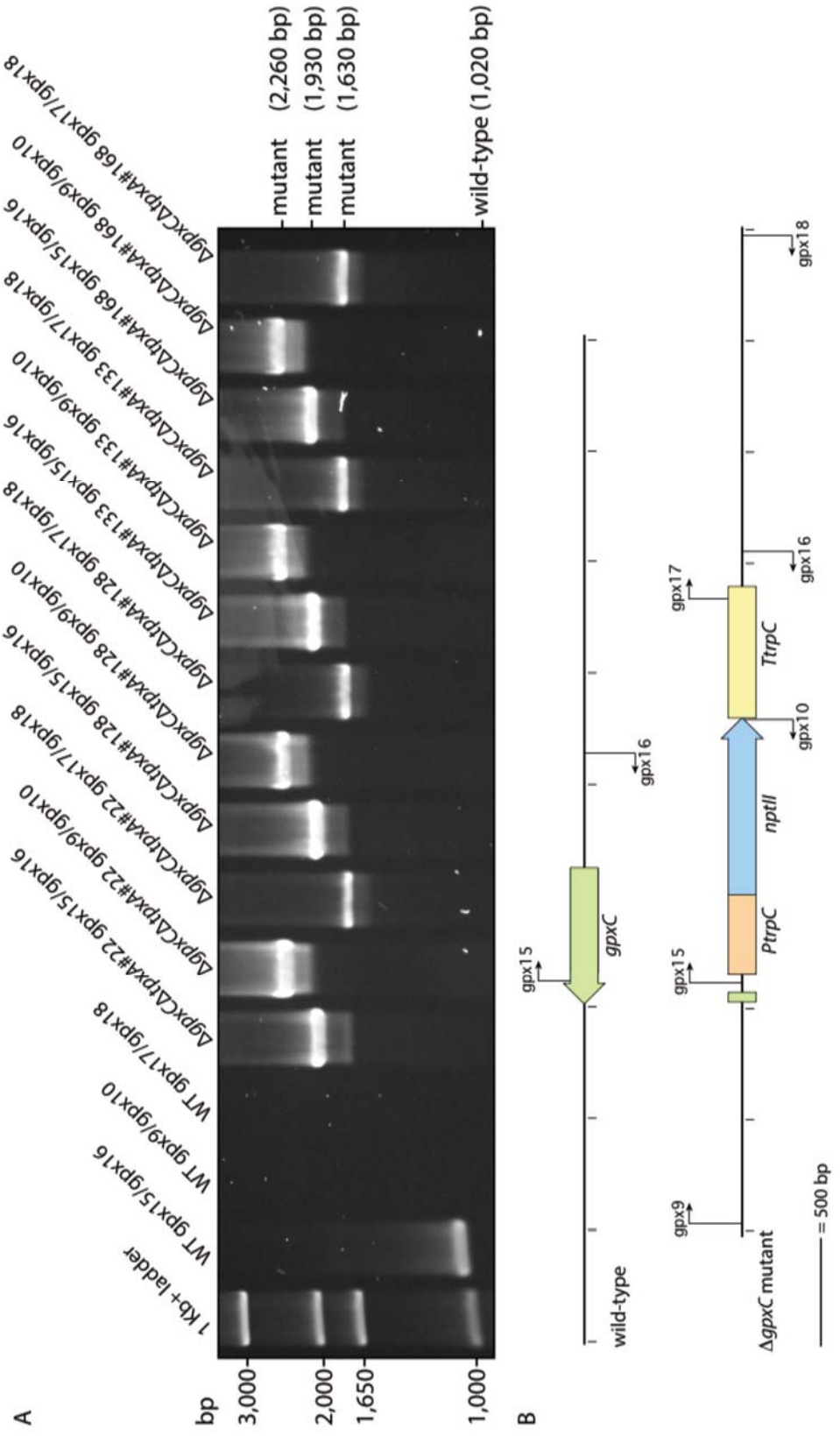
A
bp
3,000
2,000
1,650
1,000
1 Kb+ ladder
WT gpx15/gpx16
WT gpx9/gpx10
WT gpx17/gpx18
ΔgpxC(tpxA#22 gpx15/gpx16
ΔgpxC(tpxA#22 gpx9/gpx10
ΔgpxC(tpxA#22 gpx17/gpx18
ΔgpxC(tpxA#128 gpx15/gpx16
ΔgpxC(tpxA#128 gpx9/gpx10
ΔgpxC(tpxA#128 gpx17/gpx18
ΔgpxC(tpxA#133 gpx15/gpx16
ΔgpxC(tpxA#133 gpx9/gpx10
ΔgpxC(tpxA#133 gpx17/gpx18
ΔgpxC(tpxA#168 gpx15/gpx16
ΔgpxC(tpxA#168 gpx9/gpx10
ΔgpxC(tpxA#168 gpx17/gpx18
wild-type (1,020 bp)
mutant (1,630 bp)
mutant (1,930 bp)
mutant (2,260 bp)
B
wild-type
gpx15
gpxC
gpx16
ΔgpxC mutant
gpx9
gpx15
PtrpC
nptII
TtrpC
gpx17
gpx10
gpx16
gpx18
= 500 bp

Figure 3.24 PCR to confirm *E. festucae gpxC* deletion in Δ*tpxA*. (A) PCR screening of Δ*gpxC*Δ*tpxA* double deletion strains. Primer pair gpx15/gpx16 flanks the *gpxC* gene and yields a 1,020 bp product for wild-type and a 1,930 bp product for Δ*gpxC* mutants. Primer pair gpx9/gpx10 amplifies over the 5′ deletion cassette boundary and yields a 2,260 bp product for Δ*gpxC* mutants. Primer pair gpx17/gpx18 amplifies over the 3′ deletion cassette boundary and yields a 1,630 bp product for Δ*gpxC* mutants. (B) Schematic of the wild-type *gpxC* locus and replacement of the corresponding region with *npt*II resistance cassette in the Δ*gpxC*Δ*tpxA* mutant.

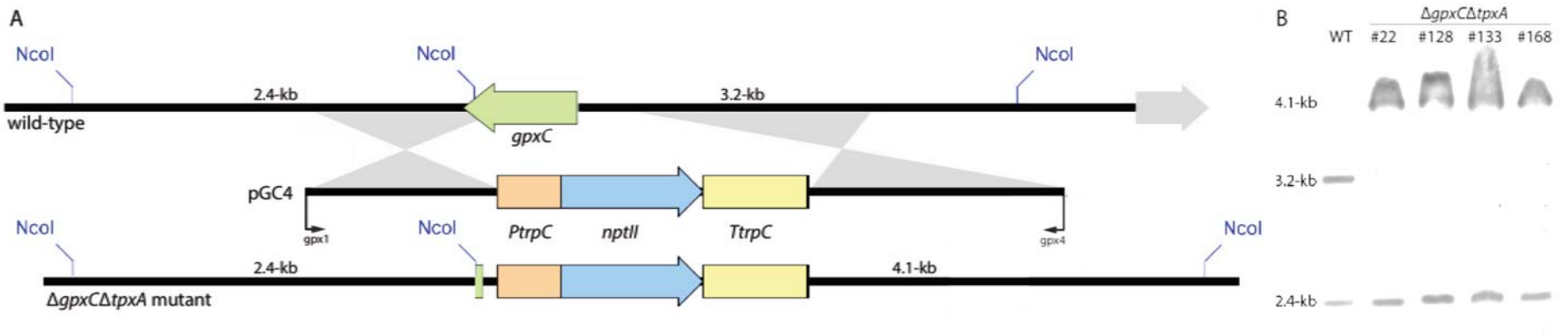

Figure 3.25 Southern blotting to confirm *E. festucae gpxC* deletion in Δ*tpxA*. (A) Schematic of the wild-type *gpxC* locus, linearised replacement construct (pGC4) and Δ*gpxC* mutant genomic region. The regions of recombination between homologous sequences flanking the *gpxC* locus and *npt*II resistance cassette are indicated by grey shading. Primer pair gpx1/gpx4 used to generate linear replacement fragment and restriction enzyme sites used for Southern analysis (*Nco*I) are indicated. Grey arrow indicates gene flanking *gpxC*. (B) Autoradiograph of Southern blot of *Nco*I digests (1 µg) of *E. festucae* WT (lane 1), Δ*gpxC*Δ*tpxA*#22 PN2831 (lane 2), Δ*gpxC*Δ*tpxA*#128 PN2828 (lane 3), Δ*gpxC*Δ*tpxA*#133 PN2829 (lane 4) and Δ*gpxC*Δ*tpxA*#168 PN2830 (lane 5) genomic DNA, probed with DIG-labeled gpx1/gpx4 PCR fragment from pGC4. The expected fragment sizes are 3.2- and 2.4-kb for wild-type and 4.1- and 2.4-kb for the Δ*gpxC*Δ*tpxA* mutants.

For each gene deletion experiment, two independent mutants showing a Southern blot hybridisation pattern consistent with homologous integration of the resistance cassette and loss of the wild-type gene were selected for further characterisation. Single and double gene replacement mutants are referred to, throughout the text, by the gene that has been deleted and the number of the transformant selected for further characterisation. i.e. Δ*yapA*#145, Δ*yapA*#243, Δ*gpxC*#10, Δ*gpxC*#34, Δ*tpxA*#105, Δ*tpxA*#157, Δ*gpxC*Δ*tpxA*#22 and Δ*gpxC*Δ*tpxA*#168. The two independently complemented transformants of Δ*yapA*#145 and Δ*yapA*#243 selected for further analysis are referred to by the deletion strain and the gene with which it has been complemented. i.e. Δ*yapA*#145/*yapA* (PN2788) and Δ*yapA*#243/*yapA* (PN2787).

3.6 In culture analyses

3.6.1 Mycelial oxidative stress sensitivity

To assess the sensitivity of Δ*yapA*, Δ*gpxC*, Δ*tpxA* and Δ*gpxC*Δ*tpxA* strains to oxidative stress-inducing conditions, mycelial plugs were inoculated onto PD agar supplemented with various stress-inducing compounds including the thiol-oxidising agents menadione and diamide as well as peroxides, H_2O_2 and *t*-butyl hydroperoxide (*t*-BOOH), and superoxide-generating KO_2 (Figure 3.26). Appropriate concentrations of the above compounds were selected by determining the concentration at which wild-type growth was inhibited and then using the maximum concentration at which no difference in wild type growth was observed. Vegetative mycelial growth of the Δ*yapA* mutants was severely reduced on 40 μM menadione and to a lesser extent on 1 mM diamide in comparison to wild-type. Expression of YapA in the complemented Δ*yapA*/*yapA* strains restored growth on menadione and diamide to wild-type levels indicating that the sensitivity observed in the Δ*yapA* mutants was due to the loss of protection against oxidative stress mediated by the YapA transcription factor. Mycelial growth of the Δ*yapA* strains was not altered in comparison to wild-type on media containing 4 mM H_2O_2, 0.25 mM *t*-BOOH or 7 mM KO_2 (Figure 3.26). Growth of the Δ*yapA* strains was also similar to wild-type on 6 and 8 mM H_2O_2 (Data not shown). The lack of sensitivity to H_2O_2 was surprising given that, to date, all published studies of fungal AP-1 mutants report sensitivity to hydrogen peroxide. Therefore, the H_2O_2-sensitivity test of *E. festucae* mutants was repeated using an alternative method to verify the initial findings. When Δ*yapA* mutants were inoculated adjacent to Whatman paper discs soaked in H_2O_2 (0.3 – 30 %) or H_2O_2-soaked discs transferred to plates with 3 day old colonies, again sensitivity was not elevated in comparison to wild-type, clearly demonstrating that YapA is not required for vegetative mycelial resistance to

hydrogen peroxide-induced oxidative stress. Mycelial plugs of the Δ*gpxC*, Δ*tpxA* and double Δ*gpxC*Δ*tpxA* mutants were also inoculated onto the media specified above (Figure 3.26). Growth of these strains was similar to wild-type on all tested media indicating GpxC and TpxA are dispensable for resistance to oxidative stress.

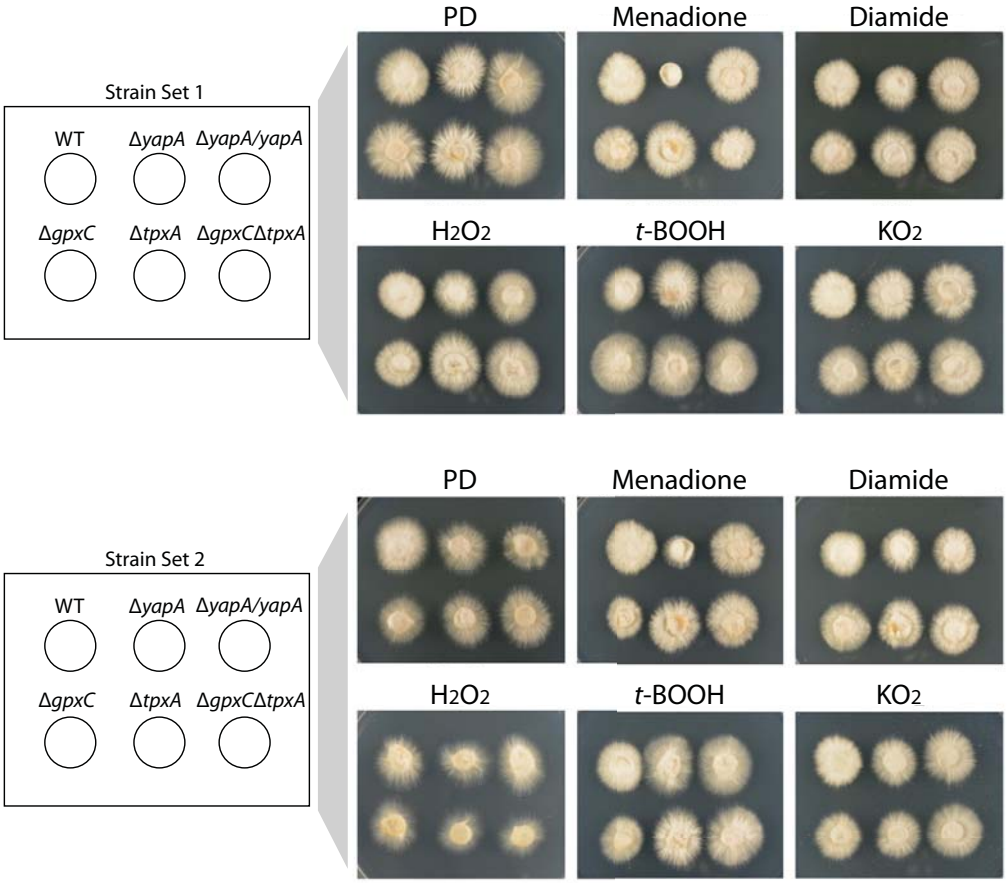

Figure 3.26 Oxidative stress sensitivity of *E. festucae* deletion strains. Agar plugs 5 mm in diameter of strains indicated were inoculated onto potato dextrose (PD) medium and PD medium containing 40 μM menadione, 1 mM diamide, 4 mM H_2O_2, 0.25 mM *t*-BOOH and 7 mM KO_2 and cultured at 22°C for 7 days. Strain set 1 (Top) includes WT, Δ*yapA*#145, Δ*yapA*#145/*yapA*, Δ*gpxC*#10, Δ*tpxA*#105 and Δ*gpxC*Δ*tpxA*#22 strains. Strain set 2 (Bottom) includes WT, Δ*yapA*#243, Δ*yapA*#243/*yapA*, Δ*gpxC*#34, Δ*tpxA*#157 and Δ*gpxC*Δ*tpxA*#168 strains.

3.6.2 Conidial hydrogen peroxide sensitivity

To investigate the possibility of a developmental stage-specific role for YapA in the resistance against peroxides, spores were harvested from *E. festucae* cultures and the spore suspensions spread onto PD medium containing H_2O_2 at concentrations ranging from 0.25-1 mM. Regardless of the strain, *E. festucae* spores are markedly more sensitive than vegetative mycelia to H_2O_2. While wild-type *E. festucae* vegetative mycelia was able to grow on concentrations of up to 8 mM H_2O_2, germination of wild-type spores was inhibited by 1 mM H_2O_2 (Figure 3.27A). Spores derived from the wild-type strain were able to germinate on PD media containing 0.5 mM H_2O_2 whereas spores of the Δ*yapA* strain showed markedly reduced germination on 0.5 mM H_2O_2. Reintroduction of the *yapA* gene restored H_2O_2 resistance of the spores back to wild-type levels (Figure 3.27A). Differential interference contrast (DIC) microscopy showed that the Δ*yapA* spores germinating on 0.25 mM H_2O_2 closely resembled germinating wild-type spores both in morphology and timing of germ tube initiation and elongation (Figure 3.27B). H_2O_2-sensitivity of spores derived from Δ*gpxC* or Δ*tpxA* strains resembled that of the wild-type strain indicating GpxC and TpxA are not required for conidial resistance to peroxide stress (Figure 3.28).

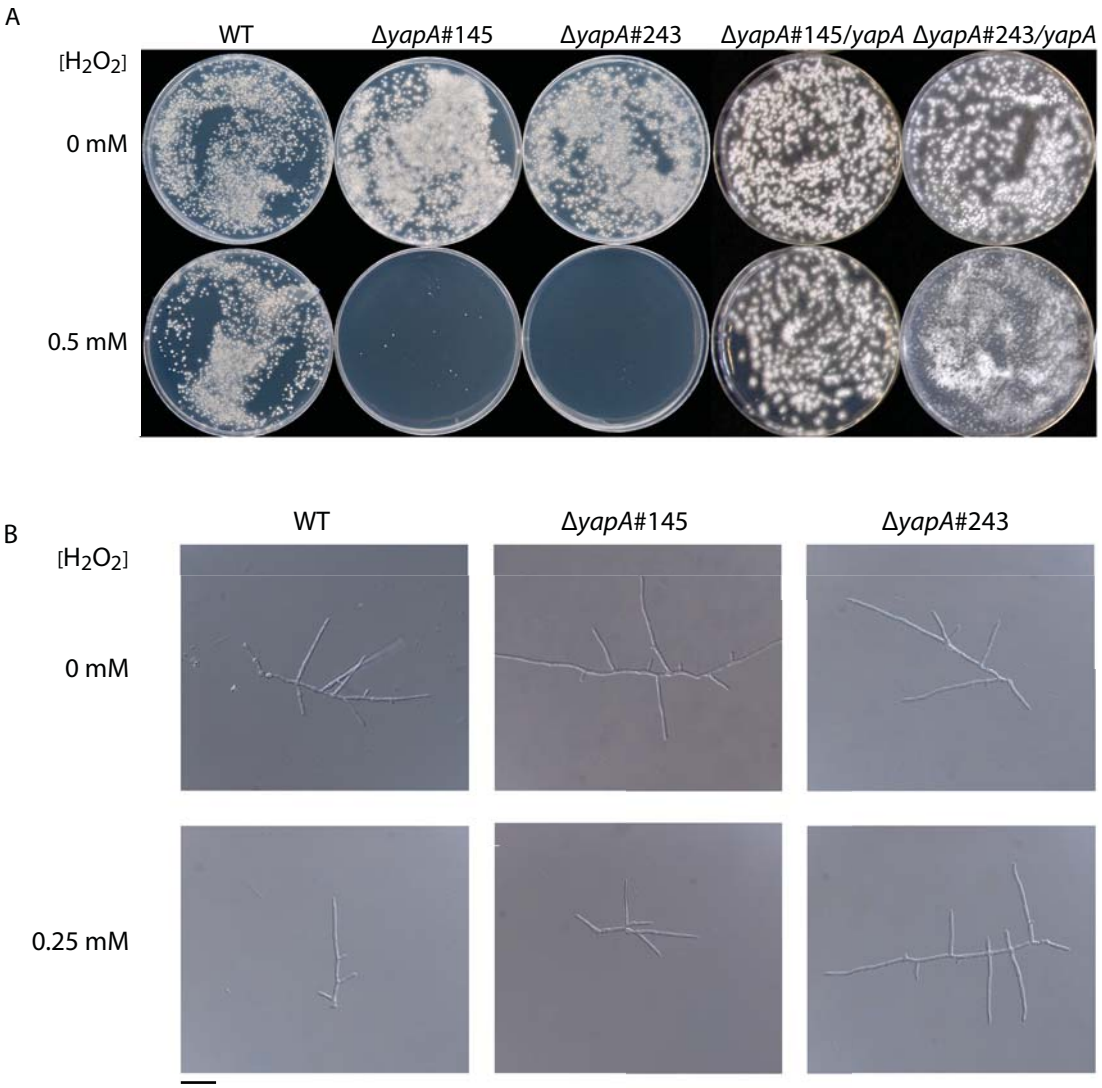

Figure 3.27 H_2O_2 sensitivity of *E. festucae* Δ*yapA* conidia. 250 µl of spore suspensions of indicated strains were spread over the surfaces of plates of PD medium and PD medium containing H_2O_2 and the spores allowed to germinate at 22 ºC for 12 days. (A) Germination of wild-type (Fl1), Δ*yapA*#145 and Δ*yapA*#243 and complemented Δ*yapA*#145/*yapA* and Δ*yapA*#243/*yapA* spores on PD (0 mM) and PD containing 0.5 mM H_2O_2. (B) DIC images of germinating wild-type (Fl1) and Δ*yapA*#145 and Δ*yapA*#243 spores 48 h post-harvest on PD agarose medium containing 0 and 0.25 mM H_2O_2. Bar = 10 µm.

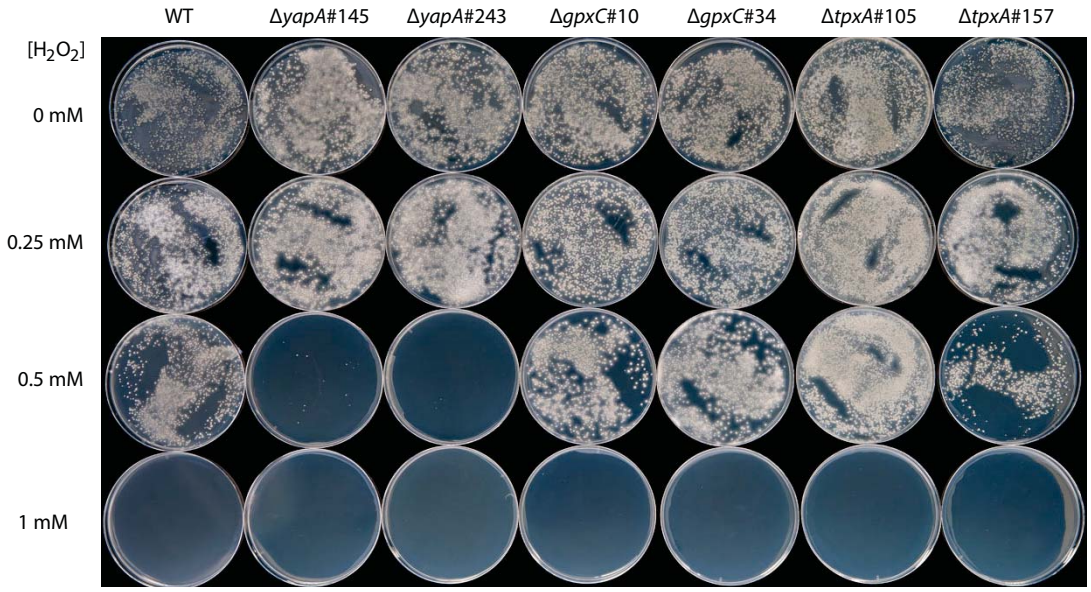

Figure 3.28 Conidial H_2O_2 sensitivity of *E. festucae* deletion strains. Germination of wild-type (Fl1), Δ*yapA*#145 and Δ*yapA*#243, Δ*gpxC*#10 and Δ*gpxC*#34 and Δ*tpxA*#105 and Δ*tpxA*#157 spores on PD medium containing H_2O_2 at concentrations 0-1 mM.

To explain the elevated sensitivity of Δ*yapA* spores to H_2O_2 we proposed that the YapA regulon includes a gene encoding a spore-specific catalase, an enzyme responsible for H_2O_2 detoxification exclusively in *E. festucae* conidia. A homologue of the *Aspergillus nidulans* spore-specific catalase, *catA* (Navarro *et al.*, 1996), was identified in *E. festucae* (EfM2.069120). The predicted protein shares 61.5% identity and 74.1% similarity with *A. nidulans* CatA. The promoter of the *E. festucae catA* gene was fused to EGFP to monitor its expression. Initially, an EGFP reporter driven by the *catA* promoter (P*catA-EGFP*) was used. When examined by fluorescence confocal microscopy, a proportion of wild-type spores showed very bright EGFP fluorescence, indicating high-level expression of the reporter gene. However, a moderate level of fluorescence was observed overall for the wild-type and Δ*yapA* strains. As spores form and develop over a number of hours it was reasoned that, during this time, low-level expression in the Δ*yapA* strains could build-up to levels comparable with the wild-type strain. To ensure rapid turnover of the EGFP, a degron sequence was fused to the C-terminus of the EGFP, and this construct (P*catA-EGFP*-CL1) was expressed in wild-type and Δ*yapA* strains (Figure 3.29A). EGFP fluorescence could be detected in wild-type spores but not vegetative mycelia, confirming its spore-specific expression (Figure 3.29B). Spores of the Δ*yapA* mutant strains showed a significant reduction ($p < 0.001$) in EGFP fluorescence, indicating reduced *catA* promoter activity, compared to that observed for wild-type spores (Figure 3.30). EGFP fluorescence was restored in the *yapA* complemented strain (PN2879) indicating the reduction in EGFP reporter gene

expression is due to lack of *yapA* expression. This result strongly suggests that YapA is required for *catA* promoter activity and subsequent *catA* expression and that the sensitivity of Δ*yapA* conidia to H_2O_2 is due to decreased expression of *catA*

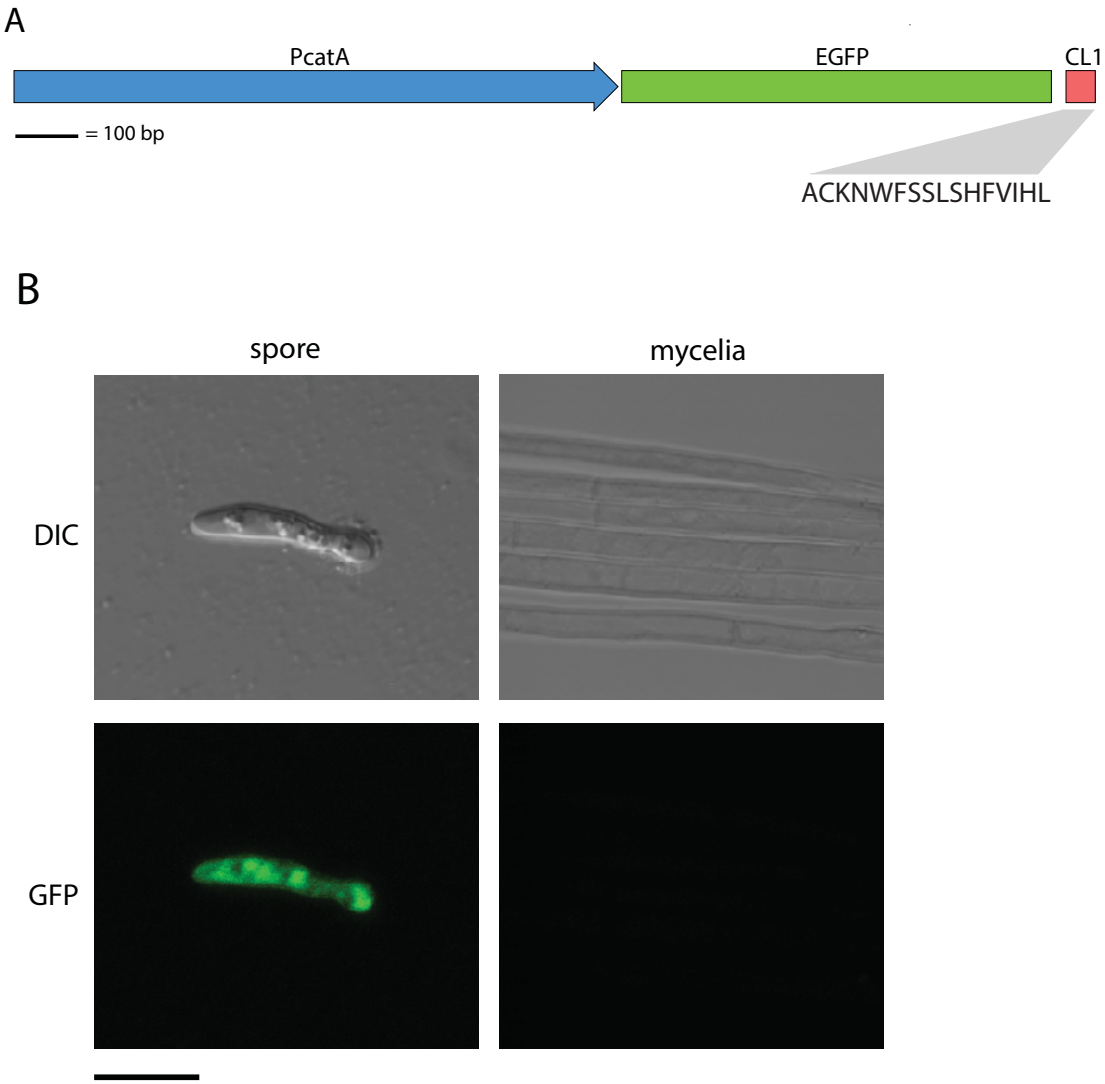

Figure 3.29 Spore-specific catalase reporter (A) Schematic of the EGFP reporter construct containing the *catA* promoter fused to degron-tagged EGFP (P*catA-EGFP-CL1;* pGC14). (B) Confocal and DIC microscopy images confirming the spore-specific expression of the P*catA-EGFP-CL1* reporter. Bar = 10 μm.

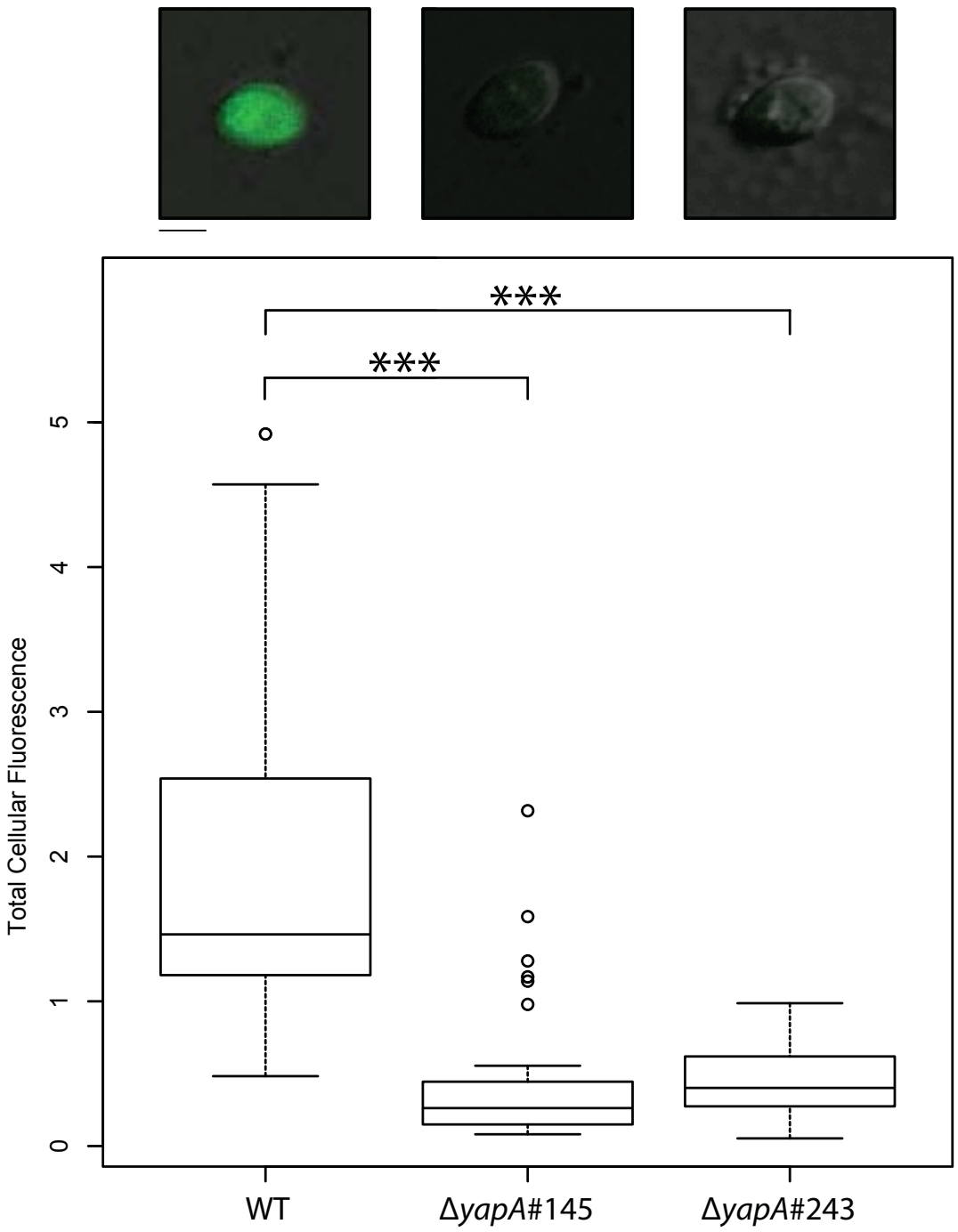

Figure 3.30 Expression of *catA* in the Δ*yapA* mutant. Box plot of total fluorescence per spore, indicating a significant decrease in GFP fluorescence in Δ*yapA* spores relative to the wild-type (WT) spores. Box plot was generated using R and evaluated using the Welch two sample t-test. Δ*yapA*#145 vs. WT p = 7.04 x 10^{-16} and Δ*yapA*#243 vs. WT p = 2.2 x 10^{-16}. WT n = 83, Δ*yapA*#145 n = 31, Δ*yapA*#243 n = 91. The total cellular fluorescence of each spore was quantified using ImageJ software. The image analysis was performed on maximum intensity projection images that were generated from 5 x 1 µm confocal Z-stacks. Representative merged DIC and confocal fluorescence images showing EGFP expression in wild-type (WT), Δ*yapA*#145

and Δ*yapA*#243 spores are shown above box plot. Bar = 2 μm. Multiple transformants including Fl1::*PcatA-EGFP-Cl1* (PN2838, PN3839, PN2840, PN2841), Δ*yapA*#243::*PcatA-EGFP-CL1*#1 (PN2836, PN2837, PN2844) and Δ*yapA*#145::*PcatA-EGFP-CL1* (PN2842, PN2843) were analysed.

3.7 Identification of Yap1-Responsive Elements (YRE) in putative YapA targets

In *S. cerevisiae* Yap1 is known to recognise and bind to the Yap1-Responsive Element (YRE) TTA(C/G)TAA in target genes. However only about half of the *S. cerevisiae* Yap1 target genes contain this canonical YRE while others contain variant YRE motifs such as TGACAAA, TGAGTAA, TTACAAA and possibly other, yet to be experimentally confirmed, YRE motifs (He & Fassler, 2005, Toone *et al*., 1998). Given that the EGFP reporter analysis indicated that YapA may regulate the expression of *catA,* it was hypothesised YapA binding motifs may be present in the 1 kb *catA* promoter region. While the TGAGAAA motif present in the *catA* promoter region is very similar to variant YREs identified by He and Fassler (2005), this specific sequence does not appear to be a functional YRE in *S. cerevisiae.*

In *N. crassa* Tian *et al*. (2011) identified an H_2O_2-responsive and NcAp1-regulated regulon of 45 genes, 14 of which contained a *N. crassa cis*-regulatory element TTA(T/C)(T/C)AAT, similar to the *S. cerevisiae* YRE. Using a tBLASTn analysis, 38 homologues of the 45 *N. crassa* genes were identified in the *E. festucae* genome (Tables 3.1 and 8.1). Among this gene set is *E. festucae catA,* the homologue of *N. crassa* catalase 2, *cat-2*, (NCU05770). The 1-kb region upstream of the start codon of each gene was analysed for the presence of a YRE motif resembling the canonical *S. cerevisiae* motif TTA(C/G)TAA. Figure 3.31 illustrates the 7- and 8-bp YRE motifs enriched in the putative YapA target gene set.

Figure 3.31 Identification of YRE motifs. WebLogo of 7- and 8-bp YRE motifs enriched in putative YapA target gene set.

These motifs were identified using a DNA Pattern Find analysis tool based on similarity to the other fungal YRE motifs consisting of two inverted TTA half-sites separated by 1 or 2 bases. The promoter regions were also analysed for variant motifs, either experimentally tested (V1) by He & Fassler (2005) (TGACAAA, TGAGTAA or TTACAAA) or untested (V2) consistent with the T(T/G)A(C/G)(C/G)(A/T)AA and T(T/G)A(C/G)(A/T)AA patterns. A set of 72 unrelated promoters from annotated *E. festucae* genes were included in the analysis as a negative control data set to test how frequently the motifs occur by chance (Table 3.1 and 8.2). While there is no evidence to suggest homologues of any of the genes in the negative control data set are regulated by AP-1 transcription factors in other organisms, it cannot be entirely ruled out that they are not *E. festucae* YapA targets until appropriate experimentation is carried out. A *cis*-regulatory element resembling the *S. cerevisiae* canonical motif was significantly enriched in the promoters of the YapA target gene set (P value <0.005). 13 of the 38 potential YapA targets (34%) contained a canonical YRE motif in their promoters compared to just 7 out of 72 (10%) in the negative control gene set (Table 3.1) The promoters of a further 5 potential YapA targets contained motifs similar to the variant YRE motifs examined by He & Fassler (2005). 47% of the potential YapA target promoters contained either a canonical or a V1 variant YRE motif, a significant enrichment (P value < 0.05). In addition, motifs resembling the variant YRE motifs that have not been experimentally confirmed as a YRE (V2, untested variant) are present in a further 10 promoters of the YapA target gene set, including *catA*, with 74% of

promoters in the potential YapA-regulated gene set containing a canonical, tested (V1) or untested variant (V2) YRE (P value < 0.01) (Table 3.1). Promoters were scored for the presence or absence of a YRE motif and thus this analysis did not distinguish between promoters containing single of multiple copies of canonical or variant motifs within one promoter.

Table 3.1 YRE motif enrichment analysis.

	Contains canonical YRE motif	Contains V1 or canonical YRE motif	Contains V1, V2 or canonical YRE motif
YapA target genes	13/38 (34 %)	18/38 (47 %)	28/38 (74 %)
Control genes	7/72 (10 %)	16/72 (22 %)	33/72 (46 %)
	$P = 0.0037$	$P = 0.0125$	$P = 0.0095$

Canonical (TTA(C/G)TAA, TTA(CG)(ATCG)TAA, Variant 1 (V1; TGACAAA, TGAGTAA, TTACAAA) and Variant 2 (V2; T(T/G)A(C/G)(A/T)AA, T(T/G)A(C/G)(C/G)(A/T)AA) YRE motifs in the promoters (1000 bp upstream of ATG start codon) of *E. festucae* genes were identified using the DNA Pattern Find analysis tool in the Sequence Manipulation Suite available at http://www.bioinformatics.org/sms2/dna_pattern.html and the enrichment of these predicted motifs in putative *E. festucae* YapA target gene set vs. the negative control gene set evaluated using chi-square analysis with Yates correction. YapA target genes, homologues of NcAp-1-dependent, H_2O_2-responsive genes in *N. crassa*. Control genes, unrelated genes not previously shown to be YapA dependent or H_2O_2-responsive; V1, Variant 1 YRE motif, experimentally confirmed by He & Fassler (2005);V2, Variant 2 YRE motif, not confirmed by He & Fassler (2005).

The promoters of other potential YapA-regulated targets including SODs, thioredoxins, glutathione peroxidase and thiol peroxidase were examined for the presence of a YRE. The promoters of TpxA (EfM2.113210) and an Fe-superoxide dismutase (EfM2.015090) were rich in motifs resembling the conserved YRE, suggesting YapA may be involved in regulation of their expression (Table 8.3). In light of this observation, the *tpxA* promoter was fused to the EGFP-CL1 reporter (pGC16) and the expression analysed in wild-type and Δ*yapA* backgrounds. However, no obvious difference in expression between wild-type and Δ*yapA* mutants was observed and the fluorescence was not evenly distributed. Given the general abundance of Prx proteins within cells it is probable that a difference in expression between wild-type and Δ*yapA* strains would be difficult to observe and overexpression may contribute to the apparent mislocalisation.

3.8 YapA activation

3.8.1 Activation of YapA by H_2O_2 in axenic culture

To determine whether YapA accumulates in the nucleus in response to peroxide a GFP fusion approach was employed. In response to H_2O_2, the YapA protein accumulated in the nucleus (Figure 3.32). Given *S. cerevisiae* glutathione peroxidase (Gpx3) and the *S. pombe* thiol peroxidase (Tpx1) are responsible for the initial sensing of the H_2O_2 signal and activation of their respective AP-1 transcription factors (Bozonet *et al*., 2005, Delaunay *et al*., 2002, Vivancos *et al*., 2005), we tested whether either of the *E. festucae* homologues, GpxC and TpxA, were responsible for activation of YapA under conditions of oxidative stress. To monitor cellular localisation, and hence activation, of YapA the full-length *yapA* cDNA was fused at the C-terminus to the EGFP coding region and placed under the control of a translation elongation factor (*TEF*) promoter (pGC9, Figure 8.12). An N-terminal EGFP-YapA fusion was also created (pGC10, Figure 8.13) and both YapA-EGFP and EGFP-YapA displayed the expected nuclear redistribution from the cytoplasm in H_2O_2-stressed hyphae. In wild-type hyphae, YapA-EGFP was cytoplasmically localised in the absence of oxidative stress (PD media only). Upon addition of 16 mM H_2O_2 YapA-EGFP rapidly redistributed to the nuclei, where it colocalised with a DsRed-StuA(NLS) nuclear marker. In the Δ*gpxC* and Δ*tpxA* mutant backgrounds YapA-EGFP still translocated from the cytoplasm to the nucleus in response to H_2O_2 with a similar redistribution time to that observed for the wild type strain suggesting that GpxC and TpxA are not essential for YapA activation (Figure 3.32). Similarly, in the Δ*gpxC*Δ*tpxA* double deletion mutant, YapA-EGFP localised to the nucleus in response to H_2O_2 ruling out the possibility that GpxC and TpxA have overlapping functions in YapA activation (Figure 3.32).

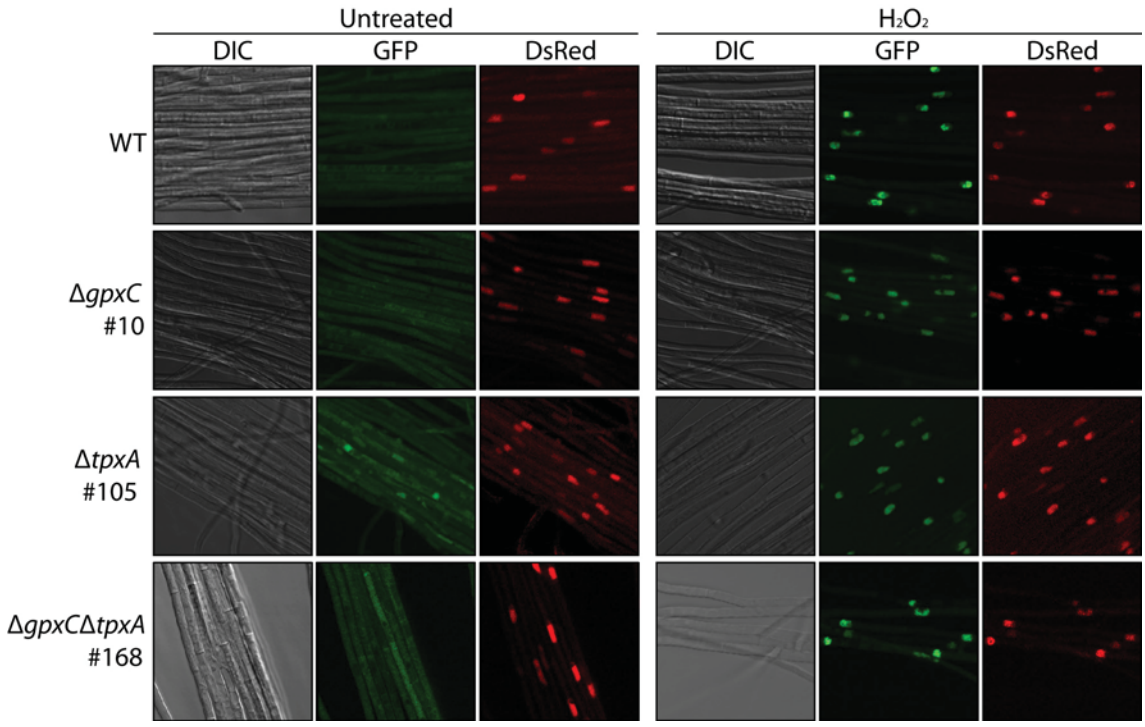

Figure 3.32 H_2O_2 activation of YapA-EGFP in axenic culture. WT (PN2790), Δ*gpxC*#10 (PN2789), Δ*tpxA*#105 (PN2823) and Δ*gpxC*/Δ*tpxA*#168 (PN2851) cultures expressing YapA-EGFP and the nuclear marker DsRed-StuA(NLS) were examined using confocal laser scanning and DIC microscopy before (untreated) and 30 min after treatment with 16 mM H_2O_2. Each box represents 50 x 50 μm.

To assess whether these proteins play a developmental stage specific role in the regulation of YapA, localisation of the YapA-EGFP fusion protein was also examined in germinating spores. YapA-EGFP localised to the cytoplasm indicating that spores are not in an inherent state of oxidative stress (Figure 3.33). Exogenous H_2O_2 application induced the relocalisation of YapA-EGFP to the nucleus in the wild-type, Δ*gpxC*, Δ*tpxA* and Δ*gpxC*Δ*tpxA* strains indicating that the developmental state of the fungus does not influence the regulation of YapA (Figure 3.33).

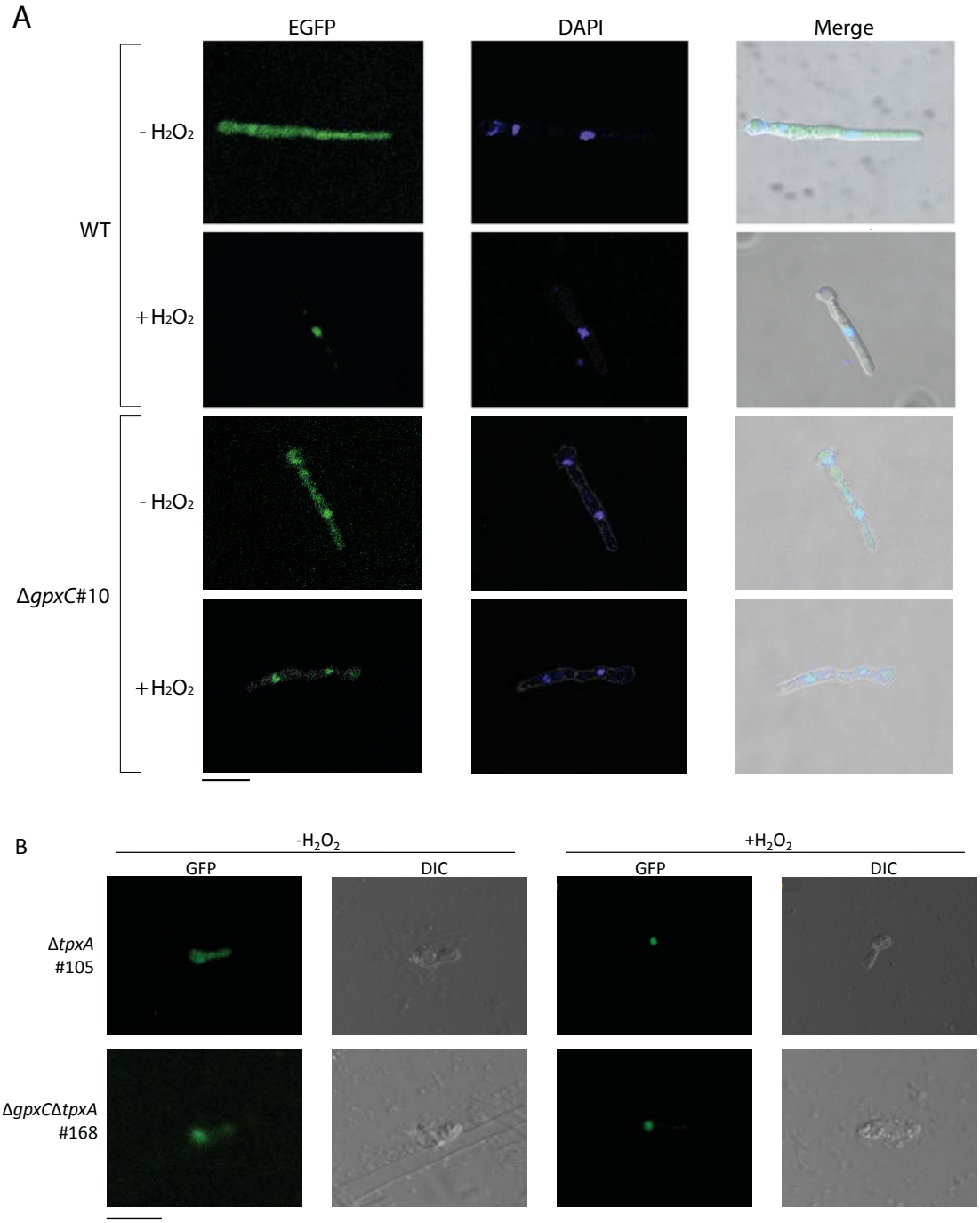

Figure 3.33 H_2O_2 activation of YapA-EGFP in asexual spores. (A) WT and Δ*gpxC*#10 spores expressing YapA-EGFP, stained with DAPI were examined using confocal laser scanning and DIC microscopy before (-H_2O_2) and 30 min after treatment with 4 mM H_2O_2 (+H_2O_2). (B) Δ*tpxA*#105 and Δ*gpxC*/Δ*tpxA*#168 spores expressing YapA-EGFP were examined using confocal laser scanning and DIC microscopy before (-H_2O_2) and 30 min after treatment with 4 mM H_2O_2 (+H_2O_2). Bar = 10 μm.

Additionally, menadione (250 μM) also induced redistribution of YapA from the cytoplasm to the nucleus (Figure 3.34). This response was more acute than that induced by H_2O_2 treatment. Nuclear relocalisation following treatment with H_2O_2 occured after approximately 30 min, whereas relocalisation following treatment with menadione occured within 5 min and the response was more pronounced with strong and complete nuclear fluorescence. The differences in the timing of the response induced by H_2O_2 and menadione may reflect the different modes of activation by these two oxidants. Menadione activates *S. cerevisiae* Yap1 directly through cysteine adduct formation, whereas H_2O_2 is indirectly sensed through an upstream redox sensor protein and it is plausible a similar situation may exist for *E. festucae* YapA.

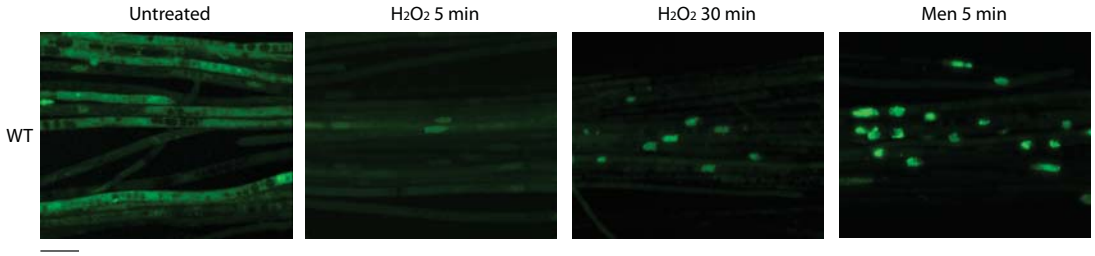

Figure 3.34 H_2O_2 and menadione activation of YapA-EGFP in axenic culture. WT expressing YapA-EGFP in PD only (untreated), 5 and 30 min after treatment with 16 mM H_2O_2 and 5 min after treatment with 250 μM menadione (Men). Bar = 10 μm.

3.8.2 Activation of S. cerevisiae Yap1 by H_2O_2 in E. festucae cells

To assess whether *E. festucae* possesses a redox sensor capable of activating *S. cerevisiae* Yap1, a Yap1-EGFP fusion construct (pGC19, Figure 8.15) was created and expressed in *E. festucae*. To confirm correct translation and fluorescence of the Yap1-EGFP fusion protein in the endogenous host, the *YAP1-EGFP* fragment was placed under the control of the GAL1 promoter in the pYES2 vector (pGC18, Figure 8.14) and expressed in *S. cerevisiae* WT, Δ*yap1* and Δ*gpx3* cells (Figure 3.35). As previously demonstrated by Delaunay *et al*. (2002) a GFP-tagged Yap1 protein localises to the nucleus following treatment with 0.4 mM H_2O_2 in WT and Δ*yap1 S. cerevisiae* cells. In Δ*gpx3* cells Yap1-GFP remains cytoplasmic following treatment with H_2O_2 confirming its requirement for activation and nuclear localisation of Yap1.

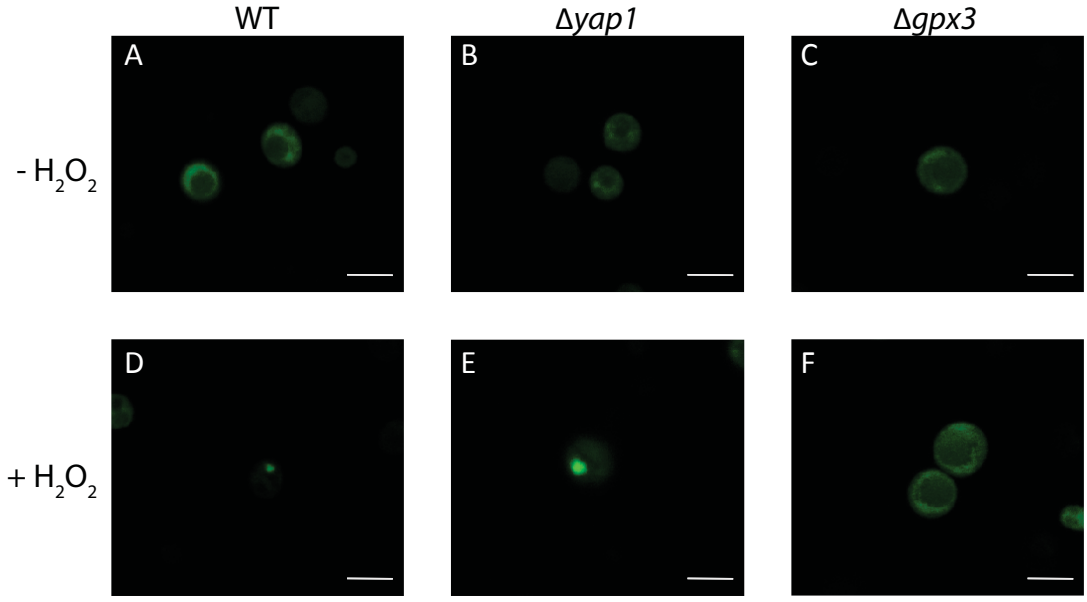

Figure 3.35 Subcellular localisation of Yap1 in *S. cerevisiae*. Confocal images of *S. cerevisiae* cells expressing Yap1-EGFP under the control of the GAL1 promoter (pGC18) in WT (PN2871), Δ*yap1* (PN2872) and Δ*gpx3* (PN2873) strains in the absence of H_2O_2 (- H_2O_2) and in cells treated with 0.4 mM H_2O_2 (+ H_2O_2) for 10 min. Bar = 5 μm.

To facilitate expression of the Yap1-EGFP fusion protein in *E. festucae,* the *YAP1-EGFP* fragment was placed under the control of the *TEF* promoter (pGC19; Figure 8.15) and expressed in *E. festucae* WT and Δ*gpxC* cells (Figure 3.36). Cytoplasmic EGFP fluorescence was observed in unstressed wild-type (WT) *E. festucae* cultures, however, redistribution from the cytoplasm to the nucleus was not observed following treatment with 16 mM H_2O_2. One possible reason for this result may be the lack of a Ybp1 homologue in *E. festucae.* Ybp1 is required for nuclear localisation of Yap1 in response to H_2O_2 stress but not the thiol-oxidising agent diamide (Veal *et al*., 2003). However, Yap1-EGFP also did not relocalise to the nucleus when cultures were treated with 250 μM of thiol-oxidising menadione suggesting accessory proteins, in addition to Ybp1, are required for Yap1 activation that are not present in *E. festucae*. Alternatively, the homologue of the *S. cerevisiae* Yap1 nuclear import protein, Pse1, in *E. festucae* (EfM2.011700) might not be capable of importing *S. cerevisiae* Yap1, despite sharing high amino acid sequence identity (38.4%) (Isoyama *et al*., 2001).

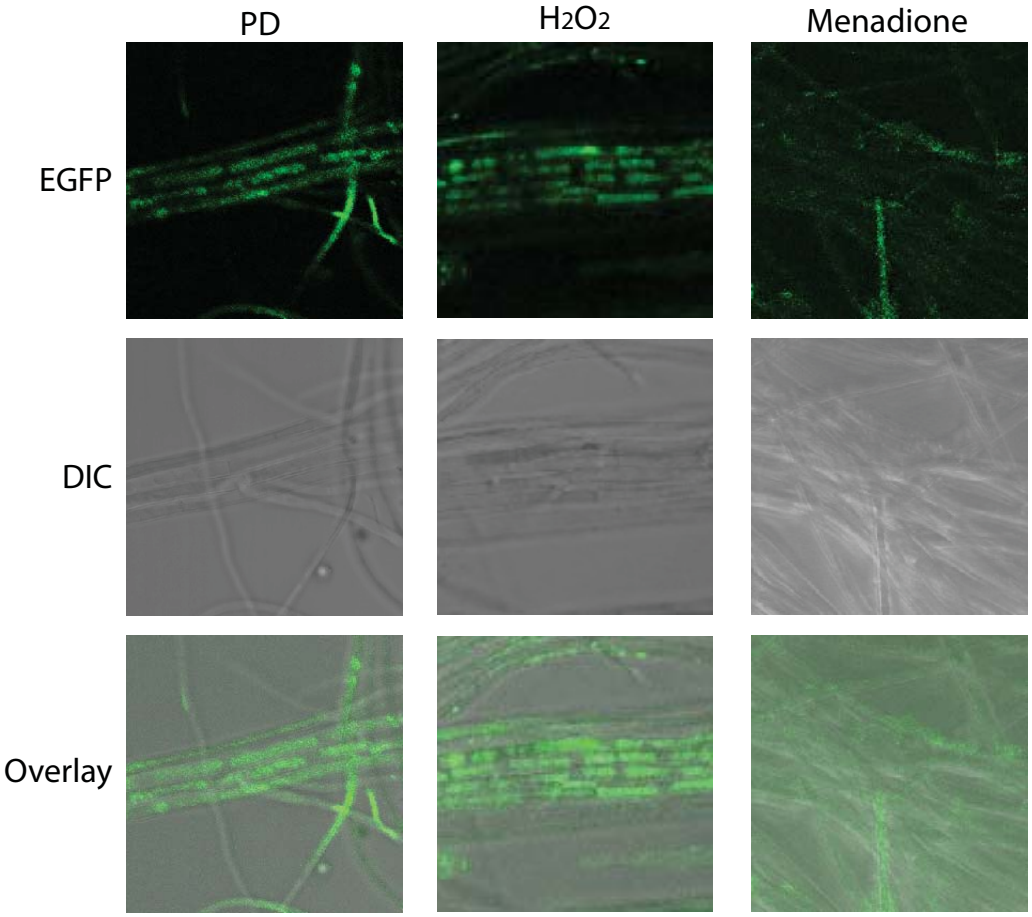

Figure 3.36 Subcellular localisation of Yap1 in *E. festucae*. Confocal and DIC images of *E. festucae* cultures expressing Yap1-EGFP under the control of the TEF promoter (pGC19) in WT (PN2874) in untreated hyphae (PD) and in hyphae treated with 16 mM H_2O_2 or 250 μM menadione. Bar = 10 μm.

In *S. cerevisiae Yap1-EGFP* was controlled by the galactose-inducible GAL1 promoter, whereas in *E. festucae Yap1-EGFP* was under the control of the *TEF* promoter, a strong promoter driving relatively high levels of expression. Overexpression may lead to artifacts such as misfolding, incorrect or incomplete processing, or mislocalisation of the foreign protein (Cereghino & Cregg, 2000). While Yap1-EGFP was largely cytoplasmic in *E. festucae* a degree of mislocalisation is also evident and may confound interpretation of these results.

3.9 In planta activation

3.9.1 Activation of YapA following wounding and inoculation of L. perenne

To infect perennial ryegrass seedlings with a particular *E. festucae* strain it is necessary make a 2-3 mm longitudinal slit, with a sterile scalpel, in the meristematic region of the grass seedling using the inoculation technique developed by Latch & Christensen (1985). Physically wounding plants in such a way has previously been shown to induce an increase in hydrogen peroxide levels inside plants (Le Deunff *et al.*, 2004, Orozco-Cardenas & Ryan, 1999). As this wounding response is likely to better represent physiological oxidative stress-inducing conditions encountered by *E. festucae* than tests in axenic culture, we monitored YapA activation in *E. festucae* growing within the wounded plant. Consistent with the rapid generation of H_2O_2 in response to wounding, within 30 minutes of inoculation YapA-EGFP localised to the nucleus of wild-type (WT) hyphae (Figure 3.37).

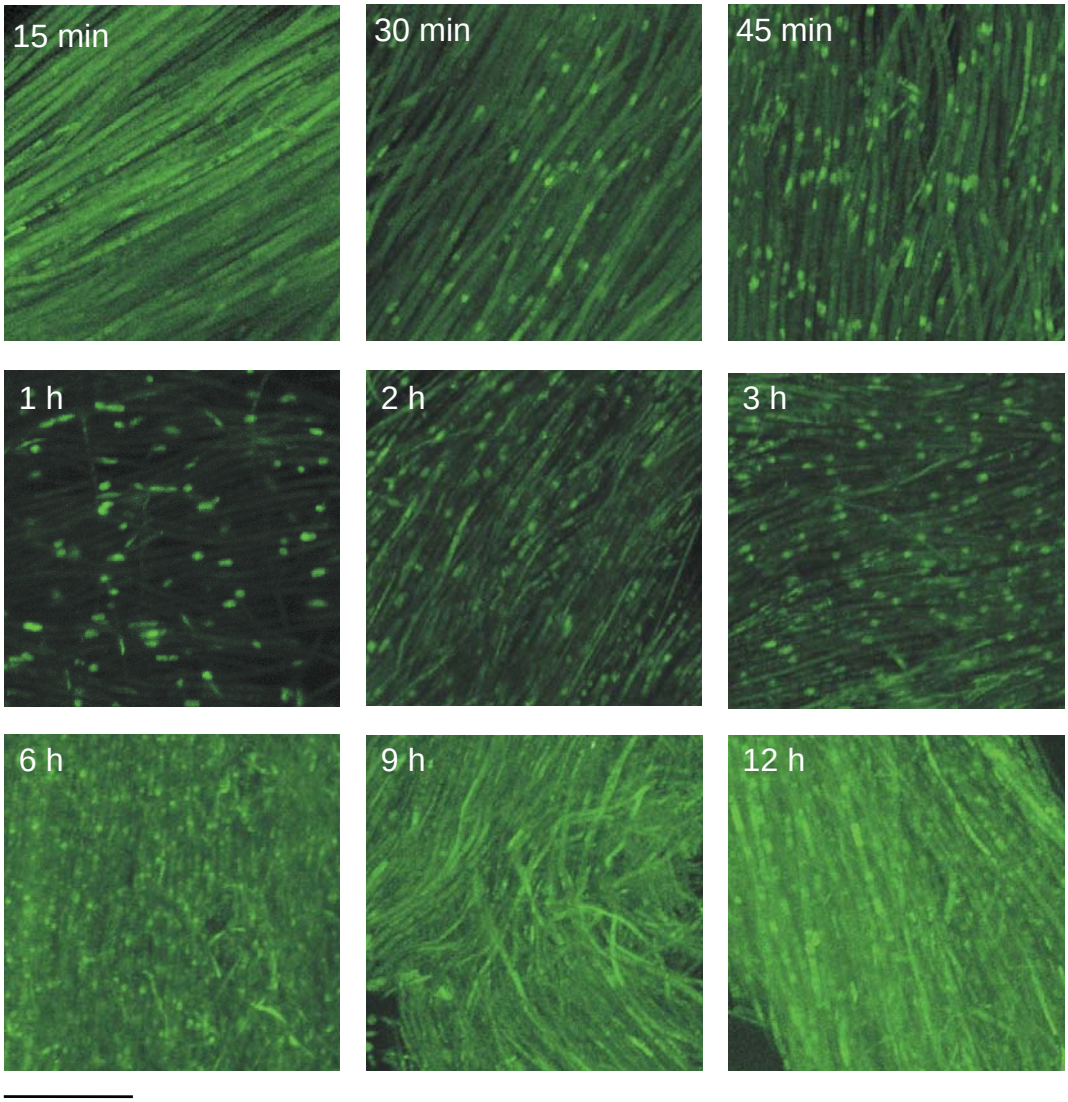

Figure 3.37 Time course of YapA-EGFP localisation. (A) WT (PN2790) expressing YapA-EGFP was inoculated into the meristematic region of grass seedlings and the subcellular localisation of YapA-EGFP examined using confocal laser scanning microscopy at the time points indicated. Bar = 10 μm.

Rapid migration of YapA-EGFP to nuclei was also observed in hyphae not in direct contact with the wounded plant cells indicating H_2O_2 may act as a diffusible signal to trigger the widespread response within the fungal hyphae. The localisation of YapA-EGFP in the nucleus was transient, peaking 1 h post inoculation followed by a gradual redistribution to the cytoplasm over 6-9 h. Despite the rapid localisation of YapA-EGFP to the nucleus, YapA was not essential for establishing infection of ryegrass seedlings. The infection of ryegrass seedlings was not compromised in *E. festucae* Δ*yapA* mutants, suggesting that *E. festucae* possesses redundant mechanisms to cope with this acute burst of H_2O_2 following inoculation.

To examine the involvement of TpxA and GpxC in the activation of YapA in a physiological environment, seedlings were inoculated with Δ*gpxC,* Δ*tpxA* and Δ*gpxC*Δ*tpxA* strains expressing YapA-EGFP. The cellular localisation of YapA-EGFP in these strains was imaged 1 h post inoculation. A strong and rapid activation of YapA was observed in the Δ*tpxA* mutant indicating that it is not required for YapA activation *in planta.* Hyphae of *gpxC* and Δ*gpxC*Δ*tpxA* strains in contact with the wounded plant surface displayed very poor EGFP expression with no sign of YapA-EGFP nuclear accumulation (Figure 3.38) suggesting GpxC may be required for viability and EGFP fluorescence of these cultures on inoculated seedlings.

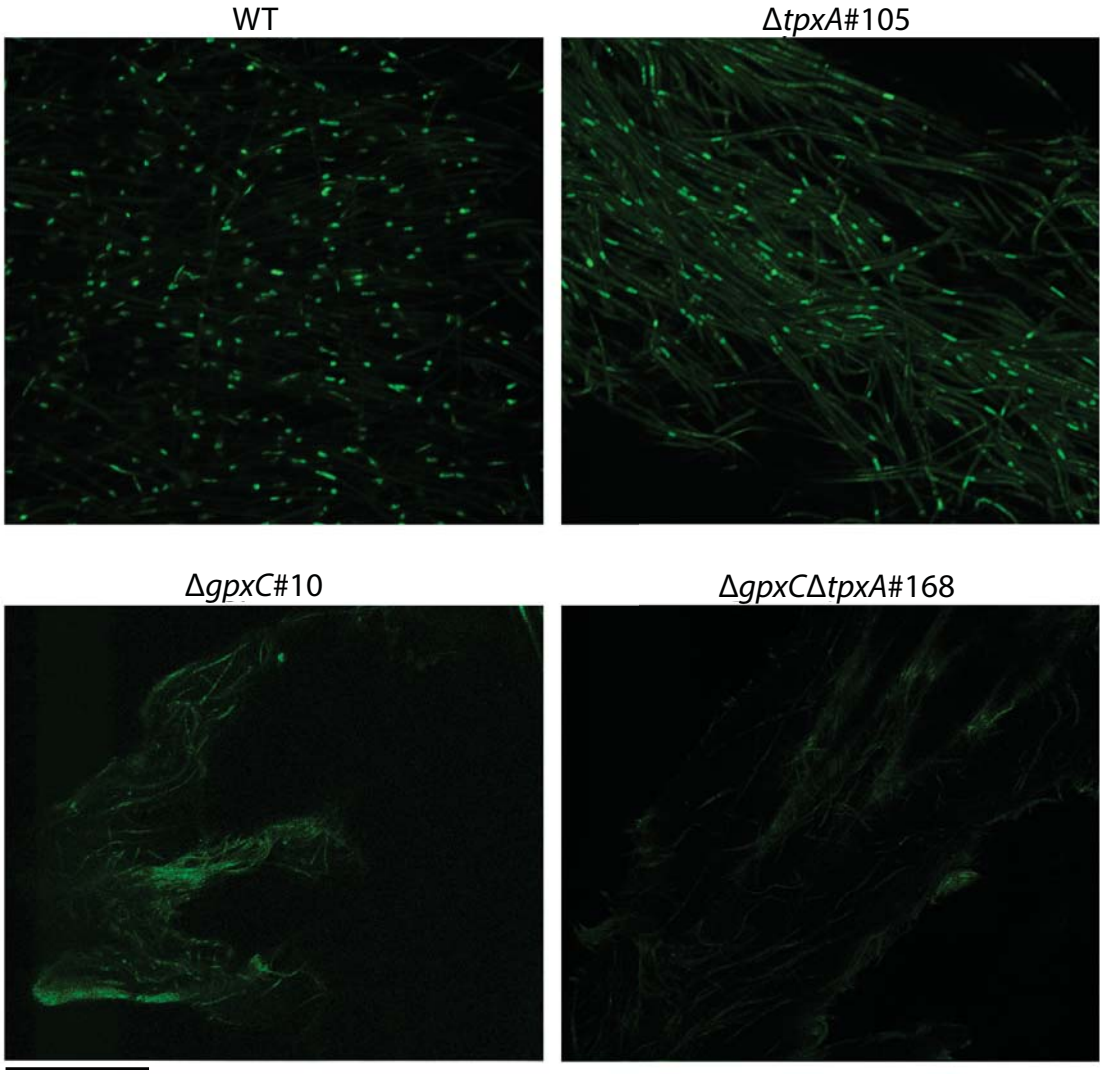

Figure 3.38 Localisation of YapA-EGFP in hyphae post-inoculation. WT (PN2790), Δ*tpxA*#105 (PN2823), Δ*gpxC*#10 (PN2789) and Δ*gpxC*Δ*tpxA*#168 (PN2851) expressing YapA-EGFP were inoculated into the meristematic region of the grass seedling and the subcellular localisation of YapA-EGFP examined using confocal laser scanning microscopy 1 h post-inoculation. Bar = 50 μm.

To further investigate the observed lack of fluorescence, YapA-EGFP expression in the Δ*gpxC*#10 strain was examined in various conditions. Figure 3.39A shows that hyphae towards the edges of the mycelial inoculum, and therefore not in direct contact with the seedling, displayed strong cytoplasmic YapA-EFGP expression. To examine if the loss of EGFP expression in these cultures was recoverable, YapA-EGFP expression in the Δ*gpxC* strain was also examined 16 h post inoculation (Figure 3.39B). A much stronger, cytoplasmic EGFP signal was observed in these cultures indicating that the culture is able to recover from the wound-induced burst of ROS encountered 1 h post inoculation. However, hyphae directly in contact with the inoculation slit still fluoresced very poorly. Further experimentation would be required to test whether these hyphae are viable. While the failure to express YapA-EGFP 16 h post inoculation suggests they are not, this is unlikely to significantly impede colonisation by these strains as recovered hyphae can still infect the plant. As a control, strains grown in axenic culture were treated with 16 mM H_2O_2 and, as expected and previously shown, nuclear localisation was observed after 1 h (Figure 3.39C). On the surface of unwounded seedlings cytoplasmic EGFP fluorescence was observed (Figure 3.39D). This indicates that on unwounded seedlings the Δ*gpxC*#10 culture is not under oxidative stress. Furthermore, it suggests the lack of EGFP fluorescence observed in this strain on wounded seedlings is due to the lack of GpxC-mediated detoxification of plant-produced ROS at the wound site.

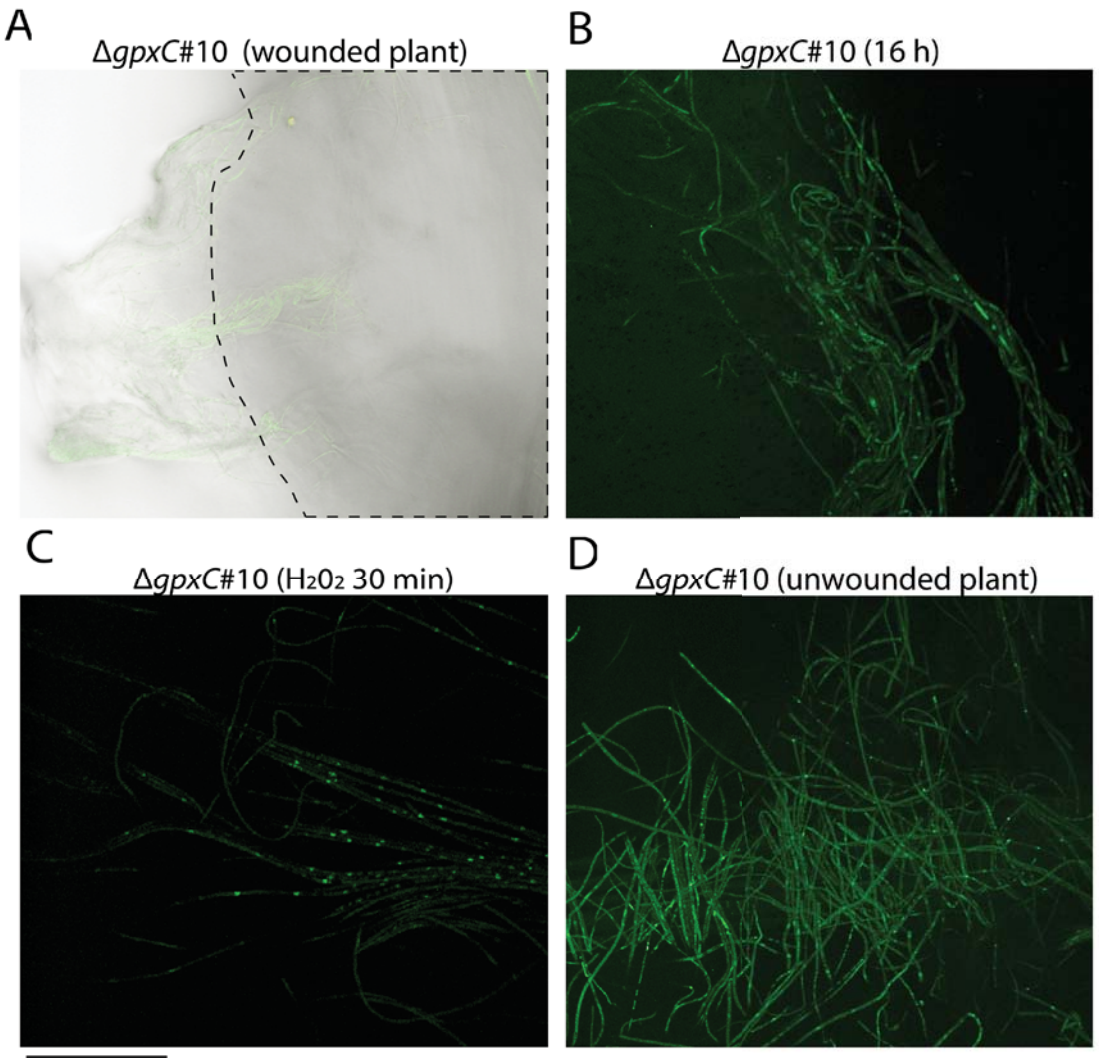

Figure 3.39 Localisation of YapA-EGFP in Δ*gpxC* hyphae post-inoculation. (A) Overlay of GFP and DIC images 1 h post-inoculation showing hyphae on and adjacent to plant surface. Region within dotted line indicates seedling. EGFP expression is reduced in hyphae on the plant surface. (B) EGFP recovery 16 h post-inoculation. (C) Axenically grown hyphae treated with 16 mM H_2O_2 for 30 min. (D) Hyphae on the surface of unwounded seedling. Bar = 50 μm.

3.9.2 Sporulation of E. festucae cultures on L. perenne seedlings

In the course of carrying out analysis of YapA-EGFP localisation following inoculation it was observed that 3-4 days post inoculation (dpi) wild-type *E. festucae* cultures profusely sporulate on the surface of inoculated seedlings (Figure 3.40A). In contrast, sporulation in axenic culture is observed at a much lower frequency. Spore-bearing conidiophores grew from hyphae on the surface on the seedling and also from endophytic hyphae within the seedling. The red arrow in Figure 3.40A indicates the region where the emerging conidiophore has penetrated through the plant cuticle. To determine whether initiation of sporulation required a

wounded seedling, mycelia were transferred to unwounded seedlings. Profuse sporulation was also observed, 3 dpi, in *E. festucae* cultures transferred to unwounded seedlings (data not shown) indicating that the ryegrass seedling alone was capable of inducing sporulation and that it was not due to a sporulation-inducing signal produced following plant inoculation. To eliminate the possibility of the nutrient-poor water agar medium alone inducing sporulation mycelia was also transferred to water agar. A very low-level of sporulation was observed after 3 days growth on this medium indicating that the seedling is responsible for inducing sporulation rather than the nutrient-poor agar medium that the seedling and fungal colony were grown on. Sporulation at the inoculation site was also examined in Δ*yapA*#145 and Δ*yapA*#243 mutants. No obvious differences in sporulation were observed for the Δ*yapA* strains in comparison to wild-type (Figure 3.40B). This indicates that while YapA is important for mediating a response to wound-induced ROS at the inoculation site (Figure 3.37), lack of YapA does not impair key processes such as sporulation.

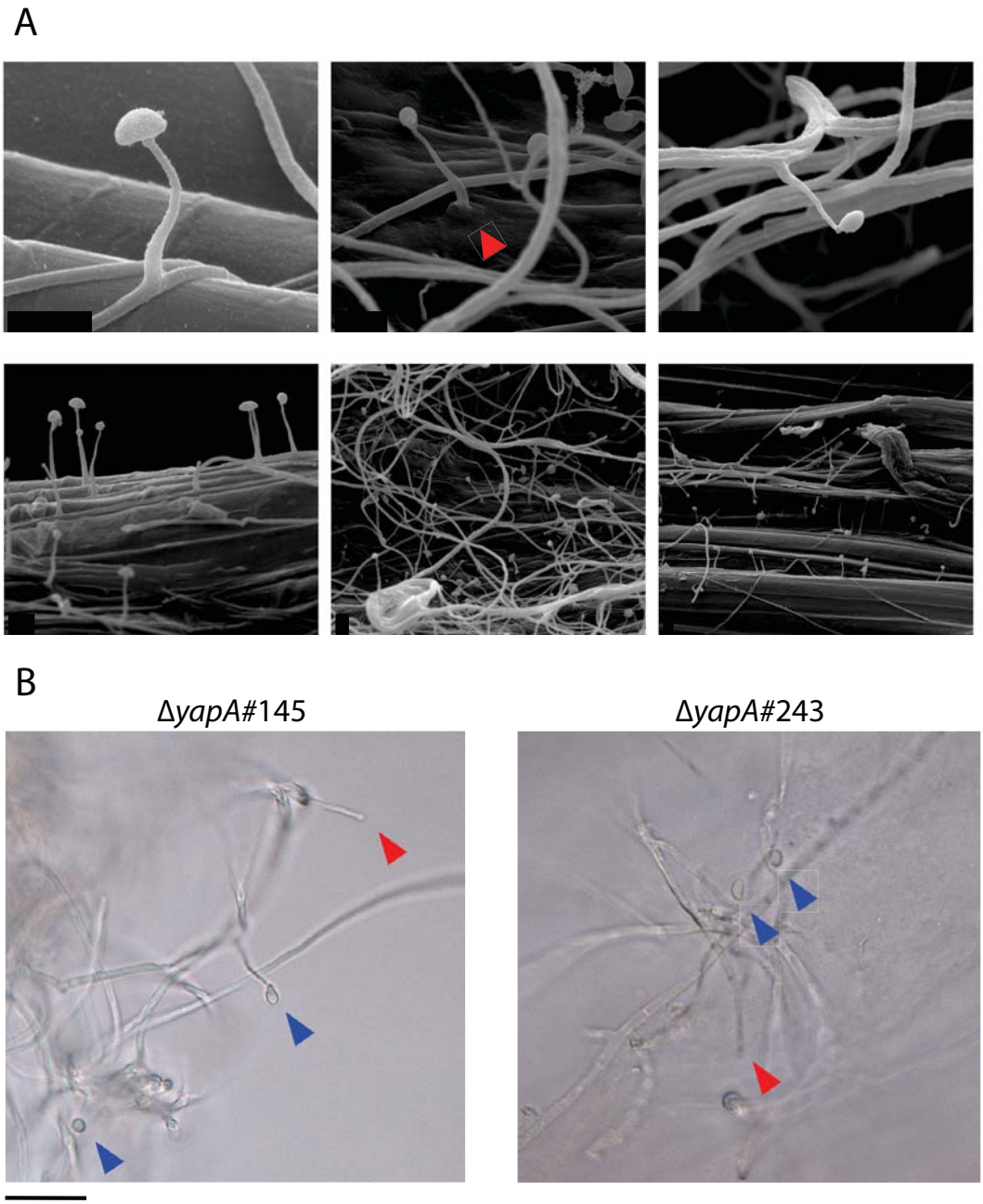

Figure 3.40 Sporulation of *E. festucae* cultures on *L. perenne* seedlings. (A) Series of SEM images of sporulating *E. festucae* wild-type (Fl1) cultures 4 days post inoculation (dpi) at the inoculation site. Red arrowhead indicates conidiophore emerging from plant. Bars = 10 μm. (B) Light microscopy (LM) images of sporulating *E. festucae* Δ*yapA*#145 and Δ*yapA*#243 cultures 4 days post-inoculation (dpi) at the inoculation site. Blue arrowheads indicate spores. Red arrowheads indicate conidiophores. Bars = 20 μm.

3.9.3 Symbiotic plant interaction of E. festucae mutants

As ROS, produced by NoxA, have been shown to regulate the growth of *E. festucae* in perennial ryegrass (Tanaka *et al*., 2006), we tested whether *yapA, gpxC* and *tpxA* were required for establishment and maintenance of a symbiotic interaction between *E. festucae* and perennial ryegrass. Plants inoculated with the Δ*yapA*, Δ*gpxC*, Δ*tpxA* and Δ*gpxC*Δ*tpxA* mutants had identical host colonisation and interaction phenotypes as observed for the wild-type strain. Figure 3.41 illustrates that the ability of Δ*yapA*, Δ*gpxC*, Δ*tpxA* and Δ*gpxC*Δ*tpxA* mutants to infect ryegrass seedlings was not compromised nor was the survival of seedlings inoculated with these strains compromised indicating that YapA, GpxC and TpxA are not required for infection of *L. perenne* by *E. festucae.* Analysis of infection rate and survival of inoculated *L. perenne* seedlings was carried out and results are summarised in Table 3.2.

Strain	Planted	Survived	Infected	% survival	% infection
Experiment 1					
WT	24	10	8	41.7	80
Δ*gpxC*#10	28	17	14	60.7	82.4
Δ*gpxC*#34	26	21	15	80.8	71.4
Δ*yapA*#145	26	17	15	65.4	88.2
Δ*yapA*#243	20	12	9	60	75
Experiment 2					
WT	28	21	11	75.0	52.4
Δ*gpxC*#10	32	15	10	46.9	66.7
Δ*gpxC*#34	32	18	14	56.3	77.8
Δ*yapA*#145	40	32	26	80.0	81.3
Δ*yapA*#243	40	26	17	65.0	65.4
Experiment 3					
WT	24	12	8	50.0	66.7
Δ*gpxC*#10	28	18	10	64.3	55.6
Δ*gpxC*#34	24	9	6	37.5	66.7
Δ*yapA*#145	32	13	10	40.6	76.9
Δ*yapA*#243	36	20	12	55.6	60.0
Experiment 4					
WT	68	44	39	64.7	88.6
Δ*gpxC*#10	77	60	41	77.9	68.3
Δ*gpxC*#34	48	24	17	50.0	70.8
Δ*yapA*#145	80	59	42	73.8	71.2
Δ*yapA*#243	84	72	43	85.7	59.7
Experiment 5					
WT	22	18	10	81.8	55.6
Δ*gpxC*#10	23	21	10	91.3	47.6
Δ*gpxC*#34	22	19	15	86.4	78.9
Δ*yapA*#145	22	20	12	90.9	60.0
Δ*yapA*#243	21	21	12	100.0	57.1
Δ*tpxA*#105	22	21	14	95.4	66.7
Δ*tpxA*#157	22	19	15	86.4	78.9
Δ*gpxC*Δ*tpxA*#22	22	22	18	100.0	81.8
Δ*gpxC*Δ*tpxA*#128	22	20	15	90.9	75.0
Δ*gpxC*Δ*tpxA*#133	22	19	12	86.4	63.2
Δ*gpxC*Δ*tpxA*#168	22	17	11	77.3	64.7

Table 3.2 Analysis of the *E. festucae-L. perenne* association. Number of surviving and infected perennial ryegrass seedlings inoculated with strains indicated in five independent experiments. Percent survival ((Survived/Planted) x 100%), Percent infection ((Infected/Survived) x 100%).

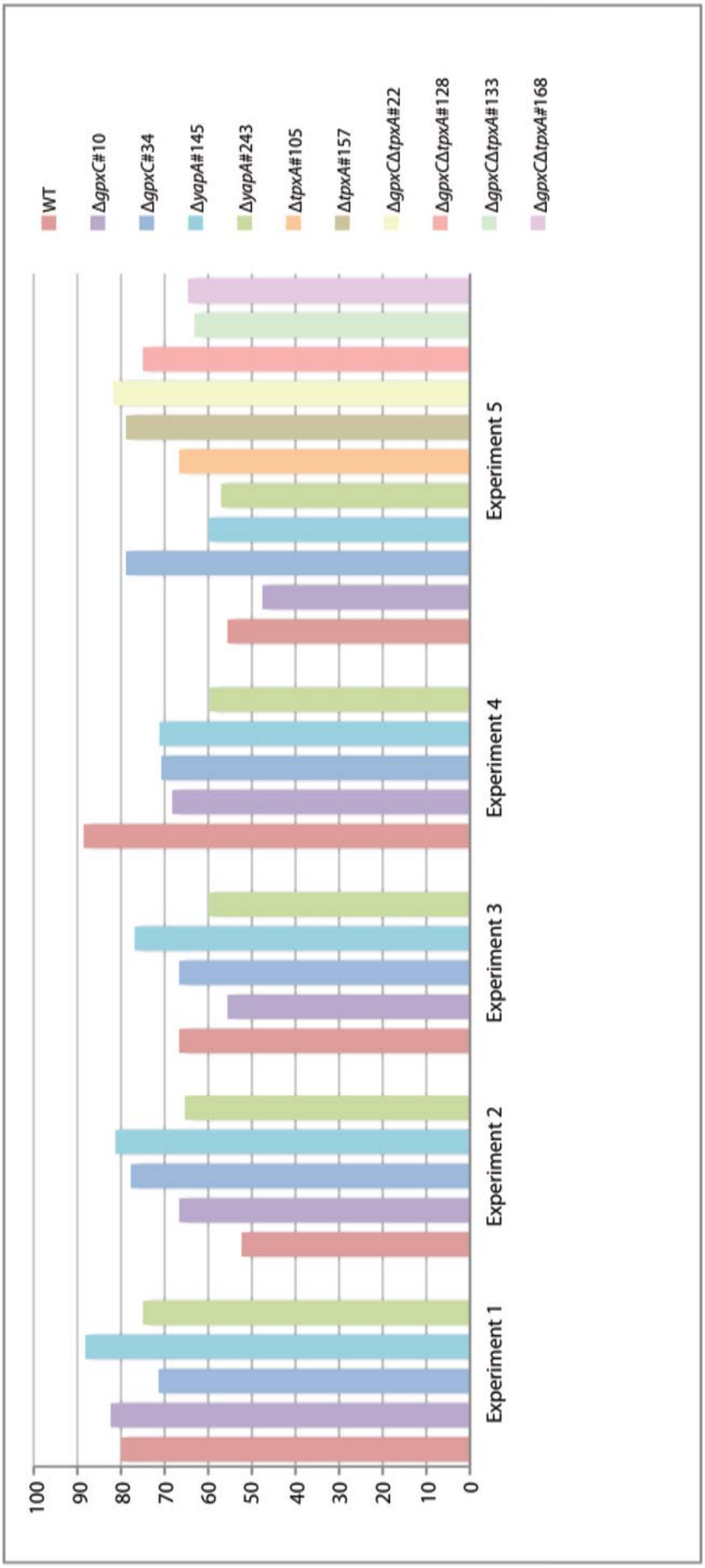

Figure 3.41 Plant infection rate analysis. Percent infection of surviving plants inoculated with strains indicated from five independent experiments (Experiment 1-5

The plant survival and infection rate study outlined above was a meta-analysis, with results combined from five independent studies. Overall, no trends in plant infection or survival were observed. There was a large variation in the number of inoculated seedlings between individual experiments, ranging from 20-84, and also a large variation in the number of surviving plants, ranging from 9-72. This variability in the data and, in some cases, low numbers makes statistical analyses difficult. Approaches such as logistic regression or general linear mixed models (GLMM) are necessary to deal with complex data such as this. If statistical analyses were carried out on survival rates of endophyte-inoculated plants, control plants that were not presented with any fungus would need to be included in the study. Survival rates in the control would give some indication of the contribution of random effects that contribute to plant survival and allow any effect specific to the mutant to be analysed. From the data presented (Figure 3.41) it is apparent that none of the mutants show a consistently reduced ability to infect the plant host, thus further statistical analyses were not carried out.

Symbiotic phenotypes of perennial ryegrass plants infected with Δ*yapA*, Δ*gpxC*, Δ*tpxA* and Δ*gpxC*Δ*tpxA* mutants resembled that observed for wild-type infection (Figure 3.42). The endophytic colonisation patterns of the mutants were visualised using the fluorescent dyes WGA-AlexaFluor488 and aniline blue, which stain chitin-rich septa and the fungal cytoplasm, respectively. Confocal analysis of the WGA-AlexaFluor488- and aniline blue-stained samples confirmed endophytic growth within the host plant is unaltered in the mutant associations (Figure 3.43). *In planta,* sparsely branched hyphae grow in the intercellular spaces parallel to the longitudinal axis of the leaf.

Figure 3.42 Analysis of the *E. festucae-L. perenne* association. Photographs taken 8 weeks after inoculation with the following strains as indicated: *E. festucae* wild-type (WT), Δ*yapA*#145, Δ*yapA*#243, Δ*gpxC*#10, Δ*gpxC*#34, Δ*tpxA*#105, Δ*tpxA*#157 and Δ*gpxC*Δ*tpxA*#22.

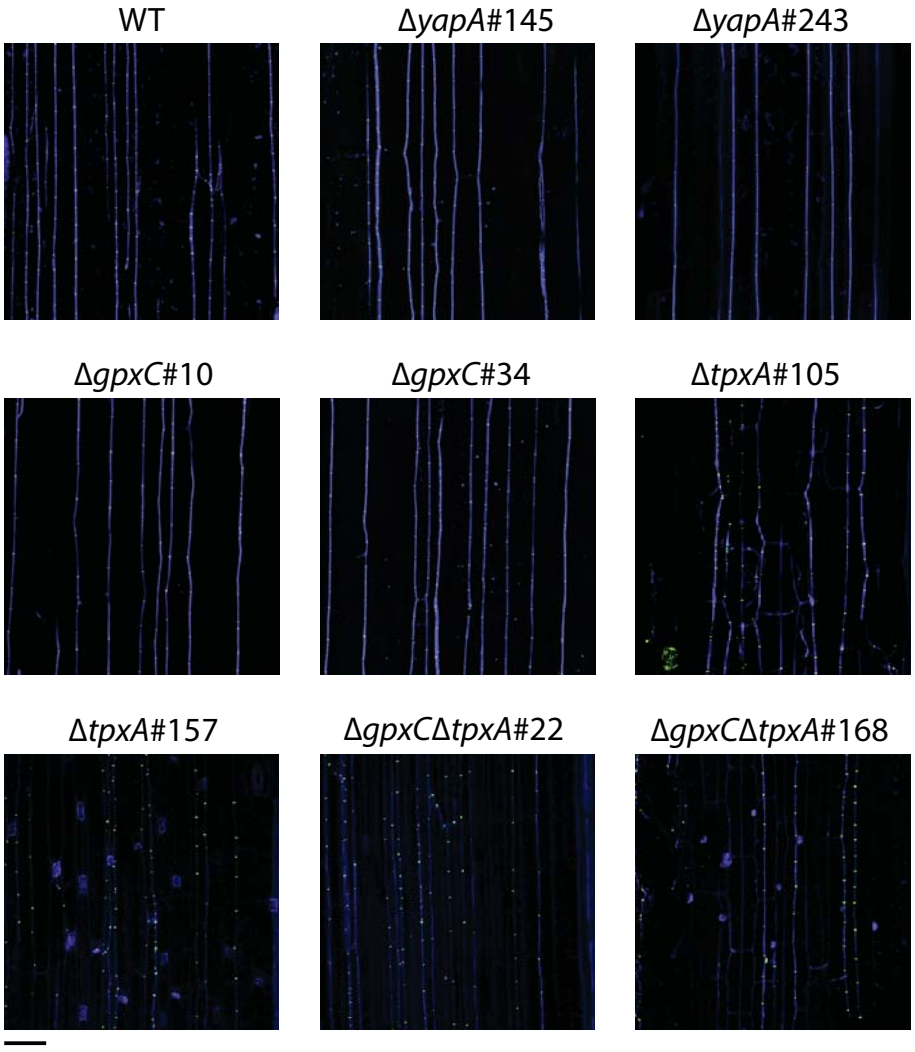

Figure 3.43 Confocal analysis of the *E. festucae-L. perenne* association. Confocal depth series images of longitudinal sections through *L. perenne* pseudostem tissue, infected with *E. festucae* strains as indicated: *E. festucae* wild-type (WT), Δ*yapA*#145, Δ*yapA*#243, Δ*gpxC*#10, Δ*gpxC*#34, Δ*tpxA*#105, Δ*tpxA*#157, Δ*gpxC*Δ*tpxA*#22 and Δ*gpxC*Δ*tpxA*#168, stained with Alexafluor (WGA-AF488) and aniline blue. Images were generated by maximum intensity projection of 10 x 1 μm confocal Z-stacks. Bar = 50 μm.

3.10 Formation of arthroconidia during transformation

In the course of examining fungal transformants, the formation of arthroconidia was observed; an intriguing physiological observation that was subsequently examined in greater detail. The standard procedure for transforming circular plasmid or linear DNA into *E. festucae* requires the formation of protoplasts by enzymatic digestion of the cell wall. The protoplasts are exposed to the DNA in the presence of

polyethylene glycol (PEG) and calcium chloride and regenerated in semi-solid agar overlaid with antibiotic, to select for successful transformations (Figure 3.44).

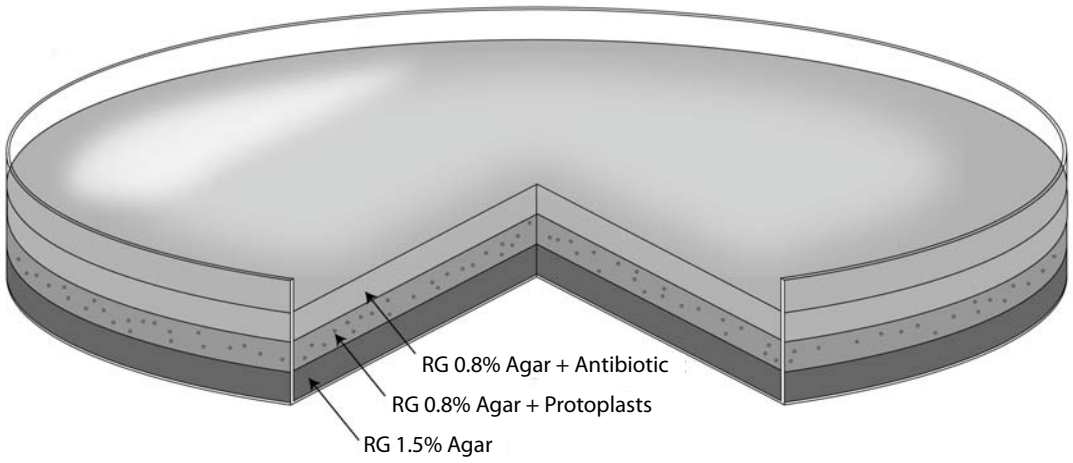

Figure 3.44 Media and culture components in *E. festucae* transformation. Diagrammatic representation of a Petri dish illustrating the media and culture components present in a standard *E. festucae* transformation procedure. The bottom layer contains 4 mm RG 1.5% agar. The middle layer contains protoplasts suspended in 1 mm RG 0.8% agar. The top layer contains 1.25 mm RG 0.8% with antibiotic selection.

Geneticin at a concentration of 200 μg/mL was used to select for transformed *E. festucae* protoplasts. Antibiotic resistant transformants, growing within and on the surface of the RG agar overlay were analysed by microscopy. To observe fungal morphology, cells were stained with aniline blue and analysed by light microscopy. Figure 3.45A shows the characteristic filamentous growth of aniline blue-stained *E. festucae* hyphae growing on the surface of RG agar. At the edge of the colony, hyphal growth was highly polarised, with more branching observed towards the centre of the colony. Towards the tips, hyphae were devoid of lateral branches with very few septa and no hyphal constrictions (Figure 3.45A). In contrast, examination of aniline blue-stained colonies growing just below the surface of the agar, revealed morphology consistent with the formation of arthroconidia, a type of spore arising from the segmentation of pre-existing fungal hyphae (Figure 3.45B). *E. festucae* hyphae were constricted at regular intervals, generating elongated compartments approximately 8-10 μm in length. Individual arthroconidia were not observed suggesting separation from the chain of arthroconidia and germination to form new hyphae and mycelium did not occur at the stage observed. This distinct morphology was observed throughout the entire colony. Further observations of the cellular morphology of colonies growing below the surface of the RG agar overlay were made using confocal microscopy

coupled with DIC, as well as TEM. Confocal imaging of DAPI-stained arthroconidia showed that each individual compartment contained a single nucleus (Figure 3.45C). TEM analysis of arthroconidia revealed that the arthroconidia were compartmentalised, by a septum of similar structure to the surrounding fungal cell wall (Figure 3.45D). The constrictions observed at the septa were not observed in hyphae growing on the surface of the agar (Figure 3.45E).

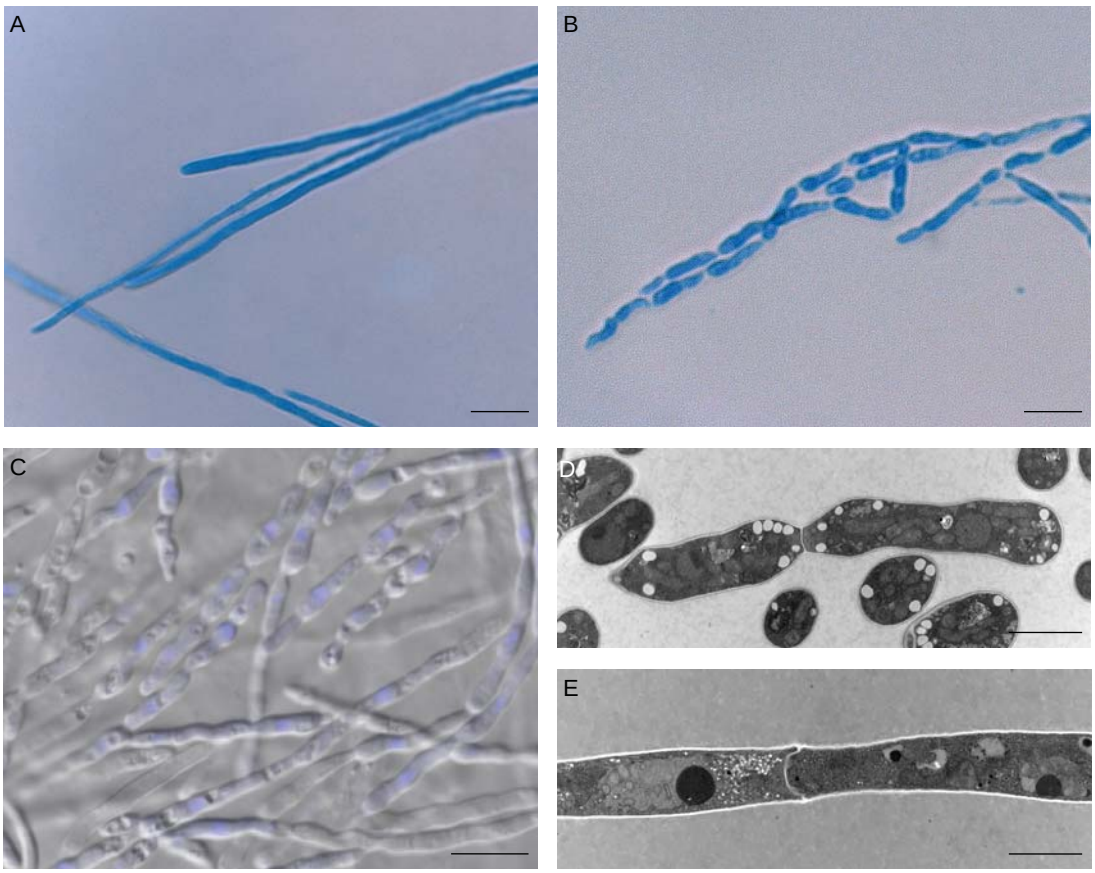

Figure 3.45 Formation of arthroconidia in regenerating *E. festucae* protoplasts. (A) Light microscopy image of aniline blue-stained *E. festucae* hyphae growing on the surface of a 1.5% RG agar plate. Bar = 10 μm. (B) Light microscopy image of aniline blue-stained *E. festucae* cells, regenerated from protoplasts, growing through antibiotic overlay layer. Bar = 10 μm. (C) Overlay of DIC and confocal microscopy image of DAPI-stained *E. festucae* cells, regenerated from protoplasts, growing through antibiotic overlay layer Bar = 10 μm. (D) TEM image of a longitudinal section through wild-type *E. festucae* cells growing through antibiotic overlay layer. Bar = 2 μm. (E) TEM image of a longitudinal section through wild-type *E. festucae* hyphae growing on the surface of RG agar. Bar = 2 μm.

3.10.1 Oxidative status of arthroconidia

To test whether the regenerating hyphae show changes in cellular redox status *E. festucae* protoplasts were transformed with the P*catA-EGFP* construct and transformants growing through the RG agar overlay were examined by confocal microscopy. Hyphae of the transformants had the same segmented appearance as previously observed and a strong EGFP signal was observed in these cells (Figure 3.46A). The activation of the P*catA* promoter indicates firstly, these cells are spore-like and secondly, that they are subject to oxidative stress. The P*catA* promoter normally drives the expression of the spore-specific catalase, *catA*. When coupled to EGFP

(P*catA-EGFP*; pGC13) it promoted strong fluorescence in the arthroconidia, similar to that observed in asexual spores harvested from *E. festucae* mycelia, suggesting that the arthroconidia structures observed were of a spore-like nature. The activation of the *catA* promoter also suggests ROS levels are elevated in the arthroconidia, requiring the activation of the catalase to detoxify hydrogen peroxide and prevent oxidative stress. The oxygen tension beneath the selective agar overlay is likely to be reduced, limiting O_2 availability to the protoplasts. Oxygen deprivation is associated with excessive ROS formation in many cell types (Blokhina & Fagerstedt, 2010), thus it is possible that regenerating protoplasts experience oxidative stress as a result of the anoxic environment encountered as they grow through the RG agar layer. To this end, *E. festucae* cultures were grown on the surface of PD agar plates in a microaerophilic environment for 5 days and examined by light microscopy. Hyphae of the microaerophilically grown cultures appeared segmented, reminiscent of the growth and morphology of transformants growing through the RG agar overlay (Figure 3.46B). Furthermore, in microaerophilically grown cultures the P*catA-EGFP* is strongly expressed similar to that observed in arthroconidia growing through the RG agar overlay (Figure 3.46C). However, the morphology of microaerophilically grown cultures did not entirely resemble that of the arthroconidia. Under microaerophilic growth conditions hyphae had more lateral branches and variable compartment sizes. This suggests that while depletion of oxygen may contribute to the formation of arthroconidia, other factors are also involved such as the geneticin present in the antibiotic overlay.

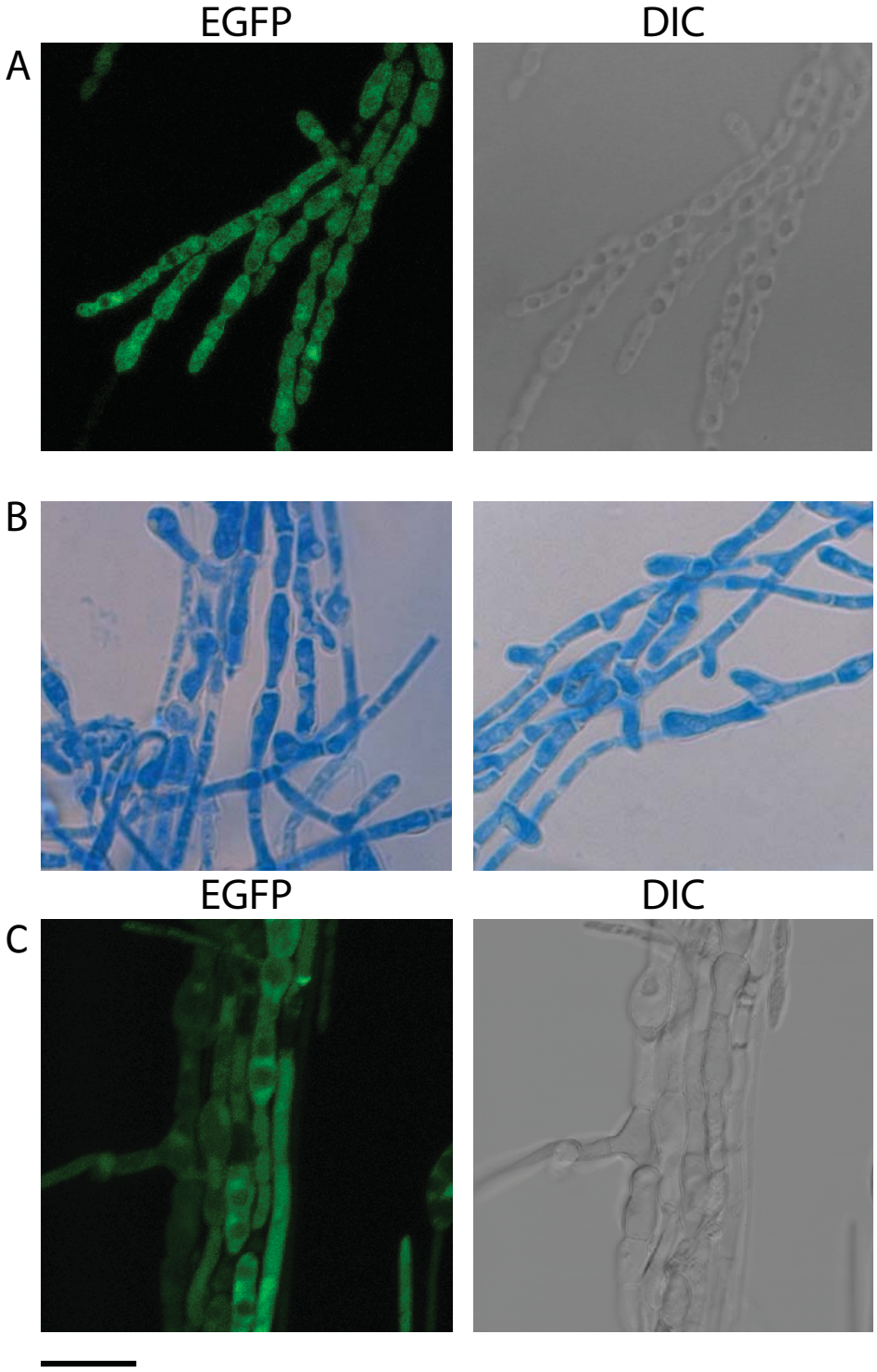

Figure 3.46 Oxidative status of arthroconidia. (A) Fluorescence confocal (EGFP) and DIC microscopy images of wild-type *E. festucae* cells growing through antibiotic overlay layer, expressing P*catA-EGFP* (PN2824). (B) Light microscopy images of aniline blue-stained, microaerophilically grown, wild-type *E. festucae* cells. (C) Fluorescence confocal (EGFP) and DIC microscopy images of microaerophilically grown wild-type *E. festucae* cells expressing P*catA-EGFP*. Bar = 10 μm.

To explore how widespread arthroconidia formation is among fungi, the morphology of *M. oryzae,* growing through the antibiotic overlay following transformation, was observed. Arthroconidia was observed in transformed *M. oryzae* cells indicating that formation of arthroconidia may be a general occurrence in transformed ascomycetes fungi (Figure 3.47, A. Tanaka, unpublished data, 2012).

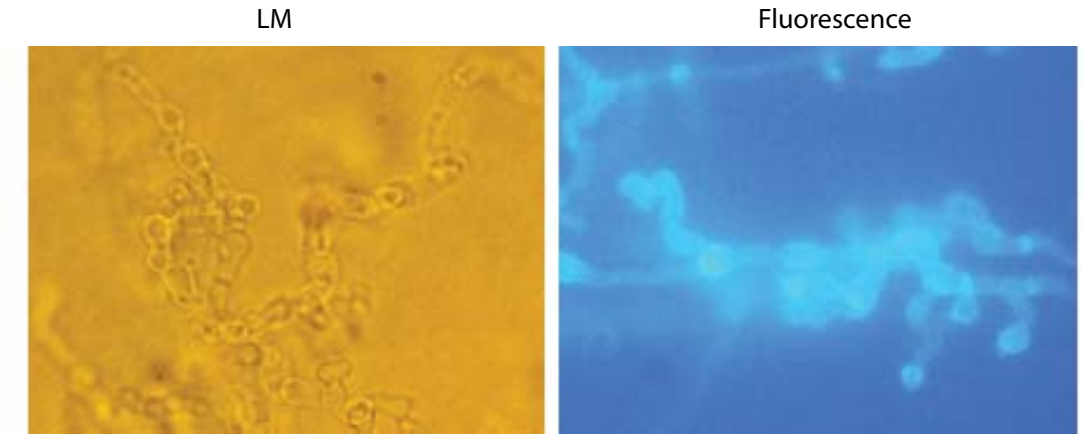

Figure 3.47 Formation of arthroconidia in *M. oryzae*. Light microscopy (LM) and fluorescence images of *M. oryzae* cells growing through antibiotic overlay layer.

4 Discussion

4.1 Characterisation of YapA, an AP-1-like transcription factor

The experimental results described in this thesis demonstrate *E. festucae* YapA is an AP-1-like bZIP transcription factor involved in the oxidative stress response. YapA contains NLS and NES motifs consistent with regulation by nuclear/cytoplasmic compartmentalisation. However, analysis of the functional domains in YapA revealed several important features of AP-1 homologues from filamentous fungi, which were different to yeast. From multiple sequence alignments it was evident that the n-CRD was not conserved in *E. festucae*, and more broadly, in other filamentous fungi. Within the n-CRD the two cysteine residues involved in disulfide bonds in the oxidised form of *S. cerevisiae* Yap1 are highly conserved in the homologues of *S. pombe*, *C. albicans* and *K. lactis* reflecting the crucial role they play in protein activity. By comparison, an alignment of n-CRD domains present in Yap1 homologues of filamentous fungi showed that equivalent cysteines are not conserved. In contrast, equivalent cysteines in the c-CRD are well conserved between yeast and filamentous fungi. The c-CRD region of *E. festucae* YapA is likely to be crucial for regulation, as in yeast modifications to the c-CRD prevent the interaction of the nuclear exportin, Crm1 with the NES within this region (Kuge *et al*., 1998, Ouyang *et al*., 2011). Indeed, the c-CRD region is required for responding to a variety of oxidative stress-inducing compounds including hydroperoxides such as H_2O_2 and *t*-BOOH, as well as chemicals with thiol reactivity such as menadione, diamide, NEM. The n-CRD region, however, is required specifically for responding to hydroperoxides. Hydroperoxide activation occurs through thiol peroxidase-directed disulfide bond formation between cysteines in the n-CRD and c-CRD (Wood *et al*., 2003a). In contrast, chemicals with thiol reactivity (menadione, diamide, NEM) activate Yap1 through covalent modification of cysteine thiols in the c-CRD.

In *S. cerevisiae* Yap1 two disulfide bridges (Cys303-Cys598 and Cys310-Cys629), connecting the n-CRD and c-CRD, are formed in response to peroxide stress (Wood *et al*., 2003a). In *E. festucae* and other filamentous fungi, just a single cysteine within the n-CRD consensus motif SSSCGTSPEP appears to be highly conserved. While fungal species *B. cinerea and A. oryzae* did not contain a conserved cysteine within this motif, the possibility of misannotation must be considered. The highly conserved consensus sequence is taken to be representative of the filamentous fungi in this study. *E. festucae* does contain a second cysteine widely separated from the first in the n-CRD consensus. However, other fungi including *N. crassa, F. graminearum, F. oxysporum, P. anserina* and *M. oryzae* do not possess a second cysteine in this region. This raised the question of whether H_2O_2-activation of *E. festucae* YapA was achieved through disulfide bond formation. While redox western analysis confirmed that H_2O_2 does activate *E. festucae*

YapA through a mechanism involving disulfide bonds, the number and spatial orientation of the disulfides are likely to differ compared to yeast Yap1 proteins. This may have implications for H_2O_2-activation of filamentous fungal Yap1 proteins, as both disulfides appear to be required for activation of yeast Yap1. In *S. cerevisiae* formation of the first disulfide between Cys303 of the n-CRD and Cys598 in the c-CRD is thought to disrupt the interaction of Yap1 with the nuclear exportin Crm1 but full Yap1 activation is not achieved until a second disulfide between Cys310 and Cys629 is formed (Delaunay *et al*., 2000). Activation of a $Yap1^{C310A}$ mutant is partial and delayed (Delaunay *et al*., 2000). The Cys310-Cys629 disulfide is thought to confer stability to the folded structure of Yap1 as in a $Yap1^{C629A}$ mutant the Cys303-Cys598 disulfide is less stable (Wood *et al*., 2003a).

Regardless of the sequence differences observed in the n-CRD, Yap1 homologues of filamentous fungi are responsive to H_2O_2 and localise to the nucleus (Lev *et al*., 2005, Lin *et al*., 2009, Molina & Kahmann, 2007, Tian *et al*., 2011). Here we have shown the *E. festucae* YapA-EGFP fusion protein localises to the nucleus of *E. festucae* cells in response to H_2O_2 and menadione indicating that YapA is capable of perceiving both stress signals and translocating to the nucleus, properties necessary and sufficient to activate genes required for the response to both forms of oxidative stress (Delaunay *et al*., 2000, Kuge *et al*., 1997). *E. festucae yapA* complemented *S. cerevisiae* Δ*yap1*, although not to the same degree as native *S. cerevisiae YAP1*. In agreement with this result *yap1* from *U. maydis* also partially complements *S. cerevisiae* Δ*yap1* suggesting fungal homologues are not as active or stable as Yap1 in *S. cerevisiae* or not expressed at a similar level to *S. cerevisiae* Yap1 (Molina & Kahmann, 2007).

The Yap1 homologue of *A. gossypii*, AgYap1, completely lacks both CRDs but still mediates a response to oxidative stress. Unlike other fungal Yap1 homologues, AgYap1 is constitutively nuclear and does not possess a nuclear export sequence. Expression of *AgYap1* is induced by H_2O_2 stress suggesting a novel, cysteine-independent mechanism of regulation operates in *A. gossypii* (Walther & Wendland, 2012). The complete lack of CRDs in AgYap1 is unique among characterised Yap1 homologues. To date, regulation of all other characterised Yap1 homologues is achieved via nuclear/cytoplasmic compartmentalisation. Phosphorylation of nuclear-localised Yap1 has also been observed in *S. cerevisiae*, and might play an important role in the activation of Yap1, however the exact mechanisms remain unclear (Delaunay *et al*., 2000). The novel AP-1 activation mechanism observed in *A. gossypii* highlights the possibility of other H_2O_2-dependent AP-1 activation mechanisms be it at the level of gene expression or otherwise.

4.1.1 *Mycelial resistance of ΔyapA mutants to oxidative stress*

GFP-localisation and yeast complementation experiments confirmed the involvement of YapA in transmitting H_2O_2-stress signals. However, phenotypic characterisation of *E. festucae* deletion mutants in culture revealed that Δ*yapA* mutants did not show elevated mycelial sensitivity to H_2O_2. Previous studies in a variety of other filamentous fungi and yeast have shown deletion of AP-1 transcription factor-encoding genes confer H_2O_2 sensitivity. For example AP-1 deletion mutants of *A. nidulans*, *A. alternata*, *B, cinerea, M. oryzae* and *N. crassa* all show elevated hyphal sensitivity to H_2O_2 compared to their corresponding wild-type strain (Asano *et al*., 2007, Guo *et al*., 2011, Lin *et al*., 2009, Temme & Tudzynski, 2009, Tian *et al*., 2011). *E. festucae* is an exception among filamentous fungi and yeast in that the AP-1 transcription factor is not essential for mycelial resistance to H_2O_2 and indicates a highly robust peroxide defence system.

Oxidative stress-sensitivity is often gauged by cellular responses to H_2O_2, however a wide variety of compounds can impose oxidative stress on cells and often the components required for detoxification of one stress agent are not required for detoxification of another (Fomenko *et al*., 2011). Thus, the mycelial sensitivity of *E. festucae* deletion mutants to oxidative stress elicited from agents other than H_2O_2, including menadione and diamide, was also investigated. Vegetative mycelia of Δ*yapA* mutants showed reduced growth on media containing menadione and, to a lesser extent, diamide. As discussed above, thiol-reactive chemicals such as menadione activate yeast Yap1 and Pap1 through a different mechanism to H_2O_2 (Azevedo *et al*., 2003, Castillo *et al*., 2002). Menadione activation is direct and involves only the c-CRD whereas H_2O_2 activation is indirect and involves both CRDs. These oxygen-derived oxidative stress-inducing species often fall under the all-encompassing term 'reactive oxygen species' (ROS). While this term is useful for broad descriptions of both oxygen radicals and certain oxidizing agents that are easily converted into radicals, a deeper understanding of how cells respond to these stresses requires the consideration of the properties of the individual ROS. Menadione is converted to semiquinone radicals by various flavoenzymes, including NADPH cytochrome P450 reductase, NADH cytochrome b_5 reductase, and NADH-ubiquinone reductase. In the presence of oxygen the semiquinone is oxidised back to menadione with the concomitant generation of ROS (Chung *et al*., 1999). Additionally, menadione induces oxidative stress non-enzymatically by oxidising thiol groups of proteins (Luikenhuis *et al*., 1998). In comparison, diamide also oxidises intracellular thiols, both low-molecular mass thiols and protein sulfhydryls, but is not directly responsible for the production of free radicals or other ROS (Dalle-Donne *et al*., 2005, Guo *et al*., 2010, Kosower & Kosower,

1995). The greatly elevated sensitivity of Δ*yapA* mutants to menadione compared to diamide may be an indication of more severe oxidative stress imposed on cells by menadione given the dual modes of oxidative stress generation.

The formation of *S*-glutathione conjugates represents an important mechanism for detoxification of electrophilic compounds such as menadione. Glutathione *S*-transferases catalyse the formation of menadione *S*-glutathione conjugates, which are then exported from the cell by a glutathione *S*-conjugate pump (Zadzinski *et al*., 1998). Alternatively, menadione-generated superoxide anions can be converted to H_2O_2 by superoxide dismutase enzymes (SODs) and the H_2O_2 subsequently detoxified by catalases (Gille & Sigler, 1995). In line with this Thorpe *et al.* (2004) found that the genome-wide transcriptional changes triggered by H_2O_2 and menadione in *S. cerevisiae* cells were only partially overlapping with distinct expression profiles (Thorpe *et al*., 2004). A similar transcriptional analysis in vegetative mycelia of *A. nidulans* revealed *gstA* (glutathione *S*-transferase) was upregulated in response to diamide and menadione whereas expression was not altered in response to H_2O_2 treatment and *sodA* (CuZn-superoxide dismutase) was upregulated specifically in response to menadione (Pocsi *et al*., 2005). The findings outlined above show that different gene products are implicated in cellular resistance to different forms of ROS and offer a possible explanation for the selective sensitivity of *E. festucae* Δ*yapA* mutants to specific oxidative stress-inducing agents. In vegetative mycelia of *E. festucae*, YapA may not be necessary for the activation of catalase-encoding genes, which are responsible for H_2O_2 detoxification, but essential for the expression of SOD- and GST-encoding genes required for detoxifying menadione-generated superoxide and overcoming thiol oxidation, respectively. In agreement with this hypothesis canonical Yap1 response elements (YREs) were identified in the promoter regions of the putative FeSOD-encoding gene (EfM2.015090) and also in the promoter region of two putative GST-encoding genes (EfM2.019890 and EfM2.013580) (Table 8.3). Additionally, variant YREs are also found in the promoter regions of the MnSOD- and CuZn-SOD-encoding genes (EfM2.013840 and EfM2.120580). However, further experimentation would be required to confirm the involvement of YapA in transcriptional activation of these genes.

4.1.2 Conidial sensitivity of ΔyapA mutants to oxidative stress

The sensitivity of Δ*yapA* mutants towards H_2O_2 was manifested only in asexual spores. ROS levels are elevated in germinating conidia and are thought to have an important role in development (Lledias *et al*., 1999, Scott & Eaton, 2008, Semighini & Harris, 2008). In *A. nidulans*, an accumulation of ROS, directed towards the emerging germ tube, regulates apical dominance (Semighini & Harris, 2008). It is possible that in

mycelia of Δ*yapA* mutants, ROS detoxification mechanisms are sufficient to cope with externally applied H_2O_2, whereas in Δ*yapA* conidia these mechanisms are insufficient to cope with exogenous H_2O_2 stress on top of the already high levels of ROS in spores.

Results in this thesis suggest that YapA controls the expression of a spore-specific catalase and offers an explanation as to why an H_2O_2-sensitivity defect was only observed in Δ*yapA* spores. CatA expression was examined in spores derived from the wild-type and Δ*yapA* strains using an EGFP-reporter system. Initial analysis, using the P*catA-EGFP* reporter, showed very bright EGFP fluorescence in a proportion of wild-type spores, however overall EGFP appeared to accumulate to similar levels in wild-type and Δ*yapA* strains. Addition of the CL1 degron at the C-terminus of P*catA-EGFP* (P*catA-EGFP*-CL1) allowed *de novo* expression to be monitored and minimised confounding effects of low-level expression in the Δ*yapA* strains. The CL1 degron sequence, specific for ubiquitination and degradation by the proteasome, is reported to confer a 20-30 min half-life on EGFP (Bence *et al.*, 2001). Using the P*catA*-EGFP-CL1 reporter EGFP fluorescence was significantly reduced in spores lacking *yapA*, consistent with the notion that expression of *catA* is dependent on the YapA transcription factor.

In *A. nidulans*, deletion of the *atfA* gene encoding a transcription factor regulated by the SakA MAPK results in conidial, but not mycelial, H_2O_2-sensitivity (Hagiwara *et al.*, 2008). Both expression and activity of the spore-specific catalase, CatA, is reduced in Δ*atfA* mutant conidia compared to wild-type, suggesting *catA* transcription is developmentally regulated in a spore-specific manner by the AtfA transcription factor (Lara-Rojas *et al.*, 2011, Navarro *et al.*, 1996). The expression and activity of catalase enzymes have also been investigated in closely related *Aspergillus* species. In *A. ochraceus,* the Yap1 homologue, AoYap1, was shown to regulate expression of the spore-specific catalase, Ao*catA* (Reverberi *et al.*, 2012). In the ΔAo*yap1* mutant, a reduction in Ao*catA* expression is accompanied by a reduction in total cellular catalase activity, indicating AoYap1 may regulate multiple catalases. Regulation of multiple catalases by a Yap1 homologue is observed in *A. fumigatus* where AfYap1 activates the expression of the mycelial catalases Cat2 and, to a lesser extent, Cat1 in H_2O_2-treated mycelia (Pocsi *et al.*, 2005). *A. fumigatus* also possesses a conidial catalase CatA and it would be interesting to investigate whether AfYap1 also regulates *catA* expression in an H_2O_2-treated spore suspension.

To substantiate the hypothesis that *catA* is a target for YapA, the putative promoter region of *catA* was examined for transcription factor binding sites. Fernandes *et al.* (1997) first identified the preferred *S. cerevisiae* Yap1 binding site as TTACTAA,

consisting of two, inverted TTA half-sites. As more Yap1 target genes were identified, the consensus YRE of TTA(G/C)T(A/C)A was reported by (Toone *et al*., 1998). Although no YRE motif was identified in the promoter of the *E. festucae catA* gene, this does not necessarily discount the role of YapA in its activation. Of the genes comprising the *S. cerevisiae* Yap1 regulon only about half of them contain an identifiable YRE in their promoters, yet Yap1 still binds to the promoter region of genes such as *TSA1* which lack a canonical YRE (Lee *et al*., 1999). This strongly points to the existence of a novel DNA element, in addition to the YRE, recognised by Yap1 transcription factors. Using a *lacZ* reporter assay He & Fassler (2005) found that mutation of the TGAGTAA consensus YRE to variants TTACAAA or TTAGAAA in the cytochrome c peroxidase *CCP1* promoter still permitted Yap1-dependent induction in response to H_2O_2. While the TGAGAAA sequence identified in the *E. festucae catA* promoter is very similar to variant motifs identified by He & Fassler (2005), their analyses showed that this motif cannot substitute for the consensus TGAGTAA motif in the *CCP1* promoter. This ability of the TTAGAAA but not the TGAGAAA motif to partially substitute for the consensus YRE is somewhat surprising as TGAGAAA contains a single T→A change at position 5, whereas TTAGAAA contains a G→T change at position 2 in addition to a T→A change at position 5 yet still retains partial function.

The identification of novel YREs by He & Fassler (2005), through modification of existing sequence elements highlights a degree of flexibility in the sequence recognised by Yap1. However, it also highlights the importance of the two TTA inverted half-sites in the optimal YRE, TTACTAA. While substitution of one half-site to TGA retains Yap1 inducibility, the simultaneous substitution of both YRE half-sites to TGA to generate TGAC/GTCA, alters the specificity of the target sequence for the AP-1 protein, Gcn4p (Ellenberger *et al*., 1992, Fernandes *et al*., 1997, He & Fassler, 2005). Preferential binding sites for Yap1 homologues have been identified in a number of fungi including *C. albicans* Cap1, *A. fumigatus* AfYap1, *S. pombe* Pap1 and *N. crassa* NcAP1 using classic experimental approaches such as DNaseI footprint analysis and bioinformatic approaches such as homology searching (Fujii *et al*., 2000, Lessing *et al*., 2007, Tian *et al*., 2011, Znaidi *et al*., 2009). YRE motifs are well-conserved among yeast and filamentous fungi, typically consisting of two TTA inverted half-sites separated by C and/or G; *C. albicans* Cap1 TTA(C/G)TAA, *A. fumigatus* Afyap1 TTA(G/C/T)TAA and *S. pombe* Pap1 TTACGTAA (Fujii *et al*., 2000, Lessing *et al*., 2007, Znaidi *et al*., 2009). Using the inverted TTA half-site as criteria we identified a YRE motif that was enriched in the promoters of a number of candidate YapA targets including the thiol peroxidase Tpx1 as well as glutathione-S-transferase, superoxide dismutase, flavin oxidoreductase and NADPH dehydrogenase-encoding genes (Table 8.1, 8.2 and 8.3). In comparison the

YRE motif, TTA(T/A)(T/A)AAT predicted for *N. crassa* Nc-Ap1 targets is quite different in that the inverted half site is lost, and the AT-rich sequences are no longer separated by G or C nucleotides (Qiao *et al*., 2008, Tian *et al*., 2011). S. *cerevisiae* Yap1 has been shown to bind DNA as a homodimer (Deppmann *et al*., 2006). The molecular symmetry of the homodimer is reflected in the inverted half-sites recognised by the DNA binding domain of each subunit. The TGAGAAA sequence identified in the promoter region of *catA* does not contain a TTA half-site, suggesting it may not be a functional YRE. However, analysis in *S. cerevisiae* has revealed a Yap1-dependent but YRE-independent component of the oxidative stress response. Disruption of both Yap1 targets in the *CCP1* promoter did not completely abolish Yap1-dependent expression and strongly suggests Yap1 regulates CCP1 through a mechanism other than that involving YREs (He & Fassler, 2005). Indirect regulation of the spore-specific catalase, CatA by the AtfA transcription factor has been observed in *A. fumigatus.* Disruption of the *DprA* gene, encoding a dehydrin-like protein regulated by AtfA, results in reduced CatA activity. Thus, it is plausible that, similar to CatA regulation by AtfA in *A. fumigatus*, *E. festucae* YapA may regulate CatA by indirect mechanisms, negating the requirement for YREs in the promoter of *catA* (Hoi *et al*., 2011).

4.2 Conidiation in E. festucae

4.2.1 Arthroconidiation

Activation of the P*catA-EGFP* reporter was also observed in *E. festucae* transformants growing through the agar overlay. Further analysis revealed a segmented appearance of the hyphae reminiscent of arthroconidia or arthrospores formed by a large variety of fungi in response to stress. Expression of the *catA* reporter revealed two important aspects of the arthroconidia morphology. Firstly, given the spore-specificity of *catA* expression in *E. festucae,* these experiments provided evidence that these structures are spore-like. Secondly, the strong reporter expression is indicative of oxidative stress and suggests H_2O_2-detoxification by catalase is a crucial function in these arthroconidia.

There is a great diversity in the fungal species that form arthroconidia and while morphologically diverse, arthroconidia are generally recognised as asexual spore-like structures resulting from the segmentation of pre-existing hyphae (Barrera, 1986). Arthroconidia are an important means of transmission for many mammalian pathogenic fungi and consequently the literature is dominated by reports of medically important fungi such as *Microsporum*, *Epidermophyton* and *Trichophyton* dermatophytes as well as coccidioidomycosis-causing *Coccidioides* species (Farnoodian *et al*., 2009, Stevens, 1995). It has been proposed that these infectious propagules (arthroconidia)

are important for the survival of the fungus in the hostile environment of the host and unsurprisingly certain environmental stresses induce arthroconidiation (Barrera, 1986). A variety of environmental factors including temperature, pH and O_2 availability stimulate arthroconidia production in a range of fungi and it is possible that one or more of these factors contributed to the observed arthroconidiation in *E. festucae* transformants (Yazdanparast & Barton, 2006).

Reduced oxygen tension beneath the agar overlay is thought to have a major contribution to formation of arthroconidia in *E. festucae* as reducing the O_2 availability to surface-grown cultures produced similar morphological effects. Furthermore, depletion of oxygen in these cultures also resulted in activation of the P*catA-EGFP* reporter. This strongly suggests that the limited oxygen availability encountered by the protoplasts beneath the agar overlay is one of the key contributing factors towards arthroconidiation. While the morphology of microaerophilically grown cultures was similar to the originally observed arthroconidial form, they were not identical suggesting that while reduced O_2 tension beneath the agar surface may contribute to the formation of arthroconidia, other factors are also involved.

The finding that regenerating hyphae of *M. oryzae* also formed very similar structures when growing through the agar overlay is of great interest as it implies that this may be a more general phenomenon in fungi (A. Tanaka, unpublished data, 2012). If conversion to an arthroconidial state is required for growing through the agar overlay, these observations may have potential implications for isolating certain gene deletion mutants in *E. festucae* and, more broadly, a range of fungal species. From the morphological appearance of *E. festucae* cultures growing through the agar overlay, it is apparent that dramatic changes to the cellular structure take place. Hence, disruption of genes that confer cell wall defects may not be identified if mutants are incapable of growing through the agar overlay. Given the resemblance of arthroconidia to asexual spores, it is also possible that deletion of genes involved in sporulation may prevent strains defective in sporulation from penetrating the agar overlay. Furthermore, the strong P*catA-EGFP* expression suggests oxidative stress is high in these cells, which may prevent oxidative stress-sensitive mutants growing through the overlay.

4.2.2 H_2O_2-sensitivity of spores

Wild-type *E. festucae* conidia (asexual spores) are markedly more sensitive than vegetative mycelia to H_2O_2. The elevated sensitivity of *E. festucae* spores to H_2O_2 appears to be a characteristic not widely shared with other fungi. Angelova *et al*. (2005)

examined the oxidative stress-sensitivity of 12 fungal species, including *Humicola*, *Fusarium*, *Alternaria*, *Cladosporium*, *Penicillium* and *Aspergillus* and found that spores of these strains could withstand much higher H_2O_2 concentrations than that tolerated by *E. festucae* in this study. The marked difference observed in the sensitivity of *E. festucae* spores may reflect the differences in lifestyles and ecological niches inhabited by these organisms. In many fungal-plant pathogen lifecycles, conidia play a central role in the disease cycle as the primary inoculum source for dissemination of the fungus. Conidia of *B. cinerea* are extremely resistant to stress such as H_2O_2 and often must survive extended periods exposed to the environment before encountering a suitable host. In contrast, *E. festucae* is predominantly a mutualistic symbiont and is largely transmitted vertically through the seed. Therefore, it is not so strongly dependent on asexual conidia for its perpetuation of infection and may not have faced the same evolutionary selection pressures to produce spores tolerant to environmental stresses external to the plant, such as UV-induced oxidative stress.

4.2.3 Sporulation in planta

Isolation of asexual conidia from *E. festucae* can be challenging as it sporulates poorly in axenic culture. However, enhanced sporulation was observed 2-3 days after transferring mycelia onto the meristematic region of one-week old perennial ryegrass seedlings. Sporulation was observed on both slit-wounded and unwounded seedlings, indicating that the plant itself, rather than secondary effects related to a wounding response, induces sporulation. Molecules on the plant surface such as oxylipins have previously been shown to regulate sporulation of fungal pathogens *Fusarium verticillioides* and *Colletotrichum graminicola* on maize plants and similar molecules produced by *L. perenne* may induce sporulation in *E. festucae* (Gao *et al.*, 2007).

The formation of epiphyllous hyphae and sporulation on the leaf surface has also been observed as part of the natural life cycle in later stages of the association (Moy *et al.*, 2000). While infection naturally occurs through host florets by germinating ascospores during the sexual stage of the *E. festucae* lifecycle, the asexual sporulation observed on the epiphyllous mycelium may facilitate transmission to new hosts in the asexual phase of the fungal life cycle (Moy *et al.*, 2000). Alternatively, environmental stresses such as nutrient starvation can induce asexual sporulation in fungi (Adams *et al.*, 1998). It is possible that the sporulation observed in *E. festucae* cultures transferred to *L. perenne* seedlings reflects the poor nutrient availability on the plant surface. However, water agar alone did not induce extensive sporulation in *E. festucae* cultures. Furthermore, nutrient-dependent asexual sporulation in other fungi tends to occur in submerged cultures rather than surface-grown colonies (Adams *et al.*, 1998). Thus, the

plant surface appears to serve as an environmental cue to induce asexual sporulation.

4.3 Role of YapA in planta

4.3.1 Symbiotic phenotype of ΔyapA mutants

YapA was not essential for endophyte infection of the perennial ryegrass host. Growth and morphology of *E. festucae* Δ*yapA* mutants within the host appeared normal and the outward appearance of infected perennial ryegrass plants resembled that of wild-type infected plants. This contrasts with the virulence role for many Yap1 homologues of phytopathogenic fungi. Infection of the host triggers a hypersensitive response (HR) by the plant, which includes generation of ROS from an oxidative burst. The localised cell death ensuing from the oxidative burst limits the spread of a biotrophic pathogen but facilitates colonisation by necrotrophs. Therefore, deletion of the gene encoding the ROS-detoxifying AP-1 transcription factor tends to result in reduced virulence in susceptible biotrophic fungi. Accordingly, AP-1 deletion mutants of biotrophic fungi, *U. maydis* and *M. oryzae,* display hypersensitivity to H_2O_2 and impaired virulence (Guo *et al*., 2011, Molina & Kahmann, 2007). In contrast, deletion of the AP-1 homologue in necrotrophic fungi, *C. heterostrophus* and *B. cinerea*, does not impair virulence (Lev *et al*., 2005, Temme & Tudzynski, 2009). However, this is an oversimplified generalisation as deletion of the *AaAP1* gene in the necrotrophic fungal species *A. alternata* also results in significantly reduced pathogenicity. With respect to AP-1 deletions, *A. alternata* is an exception and the authors suggest reduced virulence of the *AaAP1* mutant may be a consequence of their inability to detoxify ROS (Lin *et al*., 2009). In contrast to these pathogens, *E. festucae* is a mutualistic symbiont but may be considered a biotrophic fungus as growth of the endophyte is intimately linked to growth of the ryegrass host. In expanding leaves the fungal hyphae grow rapidly. Beyond the leaf expansion zone, growth of the endophyte also ceases, yet hyphae remain metabolically active for the life of the leaf (Christensen *et al*., 2002). Despite the biotrophic lifestyle of *E. festucae,* deletion of *yapA* did not impair colonisation. However, analysis of YapA activation in wounded seedlings suggested that *E. festucae* also encounters plant-generated ROS early during infection.

4.3.2 YapA activation in response to plant wounding

It has long been assumed that the artificial inoculation technique used to introduce *Epichloë* endophytes into seedlings elicits a host defence response but evidence confirming this has, until now, been lacking. Results presented here substantiate this assumption and identify YapA as an important mediator of ROS detoxification. Activation of YapA, inferred by nuclear redistribution, occurs over a time period

consistent with the increase in ROS observed in wounded *L. perenne* leaf blades (Le Deunff *et al*., 2004). The role of AP-1 transcription factors in overcoming plant defence responses is common among fungi. In penetrating germ tubes of *C. heterostrophus* and *U. maydis,* GFP-tagged AP-1 proteins localise to nuclei suggesting a key role in protection from a burst of ROS that occurs in response to pathogen-induced wounding (Lev *et al*., 2005, Molina & Kahmann, 2007). We propose a protective role for *E. festucae* YapA when the fungus encounters host-produced ROS such as during infection of wound sites. The potential involvement of *E. festucae* YapA in detoxification of a plant-produced oxidative burst is the first reported observation in a fungal symbiont. This finding has implications for the study of *E. festucae-L. perenne* associations in the lab and, on a wider scale, natural *Epichloë* endophyte associations. Experimentally, YapA could function as a 'biosensor' and provide insight into the time period over which this acute plant response occurs. YapA activation subsides after 12 h, indicating the fungus is no longer in a state of oxidative stress. It is possible that the inability of some *E. festucae* mutants to infect *L. perenne* may be due to an inability to tolerate this oxidative burst. Thus, delaying inoculation until this burst subsides may allow these previously described infection mutants to colonise the host. In natural plant-endophyte associations, grazing by mammalian herbivores may initiate a wounding response similar to that induced by the artificial inoculation technique. The transient increase in host-produced ROS would be potentially damaging to the endophyte and necessitate an efficient mechanism that enables the endophyte to cope with elevated ROS as well as providing cross-protection to host plant tissues. This study reveals that *E. festucae* YapA is part of a robust H_2O_2 detoxification system to cope with this plant defence response. It is likely that YapA fulfills this function by responding to the plant-produced H_2O_2. However, given the potential role for YapA in detoxification of *S*-glutathione conjugates in mycelia it is also possible that YapA could be responding to an electrophilic plant-derived metabolite that requires elimination from the cell in much the same way as menadione (Zadzinski *et al*., 1998).

4.4 Redox Relays

AP-1 transcription factors have been characterised in a range of filamentous fungi such as *A. fumigatus, A. alternata, B. cinerea, C. heterostrophus, M. oryzae* and *N. crassa,* however, the mechanism by which oxidative stress is sensed and transduced to the AP-1 protein is not known. In *S. cerevisiae* and *S. pombe*, thiol peroxidase-mediated peroxide signaling to Yap1 and Pap1, respectively, has been well characterised. The Yap1-Gpx3 and Pap1-Tpx1 redox relay systems now serve as models for thiol-based redox signaling and have contributed significantly to the understanding of cellular redox control in many other organisms (Gutscher *et al*., 2009, Jarvis *et al*., 2012). Strong

evidence, based on kinetic data, supports a more general role for thiol peroxidases as H_2O_2-signal transducers. The high efficiency and abundance of these proteins in cells suggests they play major roles not only in peroxide defence, but also in regulating peroxide-mediated cell signalling (Winterbourn & Hampton, 2008). A connection between thiol peroxidase-mediated H_2O_2 signal transduction and AP-1 transcription factor activation remains to be found in filamentous fungi. However, thiol peroxidase-mediated signalling has recently been shown to occur in mammalian systems, supporting the generality of this mechanism (Jarvis *et al.*, 2012). In mammalian cells, peroxiredoxin Prdx1 catalyses the oxidation of the Apoptosis Signal-regulating Kinase 1 (ASK1), a MAPKKK that activates JNK and p38 kinases, through the transient formation of a Prdx1-ASK1 disulfide-linked complex. Knockdown of Prdx1 inhibited the oxidation of ASK1 and activation of p38. Overexpression of Prdx2 also interfered with this process. Additionally, mixed disulfide intermediates were also observed for the mitochondrial Prx enzyme, Prdx3, suggesting it might function in mitochondrial redox signal transduction. Taken together, these results suggest a general involvement of peroxiredoxins in mammalian peroxide signaling (Jarvis *et al.*, 2012).

Until now, the assumption based on the *S. cerevisiae* and *S. pombe* redox relay models, has been that either a Gpx3- or Tpx1-like enzyme activates fungal Yap1 homologues through disulfide bond formation (Molina & Kahmann, 2007). Therefore, the two known redox-relay mechanisms of AP-1 activation were examined in *E. festucae.* Specifically, we tested whether the Gpx3 and Tpx1 homologues in *E. festucae* served as H_2O_2-sensors for YapA.

4.4.1 Characterizing GpxC

GPx proteins are highly conserved across the Ascomycota. The signature sequences are conserved in both yeast and filamentous fungi suggesting that these proteins serve as redox sensors in fungi other than *S. cerevisiae.* While in most fungi a single GPx enzyme is present, in *S. cerevisiae* three GPx isoforms (Gpx1, Gpx2 and Gpx3) exist. *GPX1* and *GPX3* are paralogues arising from the WGD where both have been retained. Gpx1, Gpx2 and Gpx3 all share a very high degree of sequence identity. When overexpressed in Δ*gpx3* cells, *GPX2* can partially rescue peroxide sensitivity suggesting the antioxidant function of the *S. cerevisiae* GPxs may be overlapping (Tanaka *et al.*, 2005b). Expression of Gpx3 homologues from *E. festucae* (*gpxC*) and *M. oryzae* (*HYR1*) functionally complements the peroxide sensitivity defect of *S. cerevisiae* Δ*gpx3,* despite being more closely related to *S. cerevisiae* Gpx2 (Huang *et al.*, 2011). While a degree of redundancy in the antioxidant function exists between Gpx1, Gpx2, Gpx3, there are no reports of Gpx2 and Gpx1 involvement in Yap1 activation

(Avery & Avery, 2001, Ohdate *et al.*, 2010, Tanaka *et al.*, 2005b).

Mutational analysis of the conserved cysteines (Cys36 and Cys82) in Gpx3 indicates back-up mechanisms exist for peroxidase activity but not Yap1 activation. A strain with a substitution of the peroxidatic cysteine Cys36 (Cys^{C36S}), required for both Yap1 activation and peroxidase activity, was as sensitive to H_2O_2 as the Δ*GPX3* strain whereas a strain in which the resolving cysteine, required only for the peroxidase function, had been substituted (Cys^{C82S}) showed wild-type H_2O_2-tolerance (Delaunay *et al.*, 2002). This suggests the primary function of Gpx3 may be to relay peroxide signals to Yap1, a specialised role not shared by Gpx1 or Gpx2 (Delaunay *et al.*, 2002). This raises the intriguing question: 'what sets Gpx3 apart from Gpx1 and Gpx2 in such a way that it is the physiological redox sensor for Yap1?'. Several hypotheses exist, including subcellular compartmentalisation of the GPxs. While Gpx3 localises to the cytoplasm (Huh *et al.*, 2003), other subcellular localisations, including the peroxisomal matrix and mitochondria, have been reported for Gpx1 and Gpx2, respectively (Ohdate & Inoue, 2012, Ukai *et al.*, 2011). It is therefore possible that only Gpx3 can promote oxidation of Yap1 in the cytoplasm. Alternatively, subtle structural changes in the GPx proteins may influence the specificity for the Gpx3-Yap1 interaction.

The efficient peroxidase function of Gpx3 will compete with Gpx3-mediated Yap1 activation. Thus, to facilitate efficient transfer of the peroxide signal to Yap1 a mechanism to prevent condensation of the Gpx3 Cys36-SOH with the resolving cysteine of Gpx3 is required (D'Autreaux & Toledano, 2007). The catalytic and resolving cysteines found in the *S. cerevisiae* Gpx3 protein are absolutely conserved in all fungal GPx proteins analysed indicating they are very important for protein function. In *S. cerevisiae*, Gpx3 mutations in either of these two cysteines leads to loss of peroxidase activity so it is likely that mutation of these residues in other fungal homologues would also lead to loss of function (Zhang *et al.*, 2008). Overall, the structures of these GPx proteins are very similar and the conserved cysteines occupy relatively similar positions in the proteins, as do residues in the catalytic triad (Gln70 Trp125 Cys36) (Ma *et al.*, 2007). In *S. cerevisiae* Gpx3 hydrophobic residues near Cys36 such as Val32, Tyr42, Pro63, and Phe127 are partially solvent-exposed and thought to form a hydrophobic pocket, indicative of a potential role in substrate binding (Zhang *et al.*, 2008). These residues are well conserved in the GPxs of *S. cerevisiae* as well as Gpx1 of *S. pombe* and GpxC of *E. festucae* and thus do not offer an explanation for the specific interaction of *S. cerevisiae* Gpx3-Cys36 with Yap1. Amino acid changes, specific to Gpx3, may be the most informative regarding the specific activity towards Yap1. However, few amino acid changes, exclusive to *S. cerevisiae* Gpx3, occur in these highly similar proteins and of the changes that are only found in Gpx3 it is difficult to predict

what effect they will have on function. Further in-depth analysis will be required to resolve how specificity is conferred on Gpx3 in the *S. cerevisiae* Gpx3-Yap1 redox relay.

4.4.2 Characterizing TpxA

Tpx1, along with Bcp and Pmp20 comprise the peroxiredoxin family of redox sensor proteins in *S. pombe* (Kim *et al.*, 2010). Phylogenetic analysis identified TpxA as the closest homologue of *S. pombe* Tpx1 in *E. festucae*. Based on the signature motif present in *E. festucae* TpxA it is a predicted peroxiredoxin like its homologue, *S. pombe* Tpx1. However, Tpx1 is a 2-Cys Prx, whereas *E. festucae* TpxA is a 1-Cys Prx. Inspection of the Prx signature motifs of Tpx1 homologues from other yeast and filamentous fungi revealed that this difference extends to all filamentous fungal Tpx1-like proteins analysed. The presence or absence of a second cysteine correlates with the distinct sequence motifs surrounding the first cysteine in Prx signature 1 and this was observed in the alignment of fungal Prx signature motifs. The consensus sequence of FTFVCPTEI in Prx signature 1, conserved in yeast 2-Cys Prxs, predicts a second cysteine in Prx signature 2 (Rhee *et al.*, 2001). In contrast, 1-Cys Prxs contain the FTPVCTTEL consensus motif in Prx signature 1. Sequences identical or close to this consensus were found in Tpx1 homologues from filamentous fungi, including *E. festucae* TpxA, as well as 1-Cys Prxs from yeast. Filamentous fungi do have 2-Cys Prxs but they appear to be more closely related to atypical 2-Cys Prxs in yeast such as *S. pombe* Bcp and Pmp20. As discussed by Morel *et al.* (2008), filamentous fungi do not appear to possess typical 2-Cys Prxs homologous to Tpx1 suggesting 2-Cys Tpx1-type peroxiredoxins are a yeast-specific adaptation. Furthermore, the absence of a 2-Cys Prx-type homologue in *E. festucae* and other filamentous fungi correlates with the absence of a sulfiredoxin (Srx) homologue, an enzyme that reverses the hyperoxidation of typical 2-Cys Prxs (Biteau *et al.*, 2003, Morel *et al.*, 2008).

Both the C_P (Cys48) and the C_R (Cys169) of *S. pombe* Tpx1 are required for its role in redox signal transduction to Pap1 (Bozonet *et al.*, 2005, Vivancos *et al.*, 2005). A Cys169 Tpx1 mutant is still able to form an intermolecular disulfide with Pap1 but this disulfide is not resolved to an intramolecular disulfide within Pap1 (Bozonet *et al.*, 2005). If TpxA participates in a redox relay similar to the *S. pombe* Tpx1-Pap1 system, an external electron donor might be required to fulfill the function of the resolving C_R (Cys169) in *S. pombe* Tpx1. There is no inherent reason for 1-Cys Prxs, such as *E. festucae* TpxA, to not have a role in redox signal transduction (C. Winterbourn, personal communication, November 11, 2010). Conceivably, signals could be relayed to thiol-containing target proteins by a 1-Cys Prx as rearrangement of the intermolecular disulfide to an intramolecular disulfide within the target protein that results in the

recycling of the 1-Cys Prx without requiring a resolving cysteine. This occurs in the *S. cerevisiae* Gpx3-Yap1 redox relay where, of the three cysteines present in Gpx3, only Cys36 is required for the oxidative activation of Yap1 (Delaunay *et al*., 2002). Formation of the intramolecular disulfide within Yap1 occurs with the concomitant release of resolved Gpx3 (Figure 1.6). Thus, it is plausible that a 1-Cys Prx such as TpxA could transduce a redox signal to a thiol-containing target protein. However, the *S. pombe* 2-Cys Prx is susceptible to reversible hyperoxidation, a property linked to its role in oxidative stress signalling. Tpx1 coordinates a response to low levels of peroxide stress through H_2O_2-induced oxidation and activation of Pap1. Recycling of oxidised Pap1 and Tpx1 depletes the pool of reduced thioredoxin (Trx1) and limits the reduction of other substrates by Trx1. However, under acute oxidative stress, Tpx1 is hyperoxidised to an inactive state. This allows Trx1 to reduce other substrates such as methionine sulfoxide reductase, Mxr1, allowing repair of oxidised damaged proteins crucial for cell survival under extreme stress (Day *et al*., 2012). 1-Cys and atypical 2-Cys Prxs such as *E. festucae* TpxA and *S. cerevisiae* Gpx3 are, by comparison, less sensitive to hyperoxidation suggesting this mechanism is unlikely to occur (Rhee *et al*., 2012). While 1-Cys Prxs remain relatively uncharacterised, data are accumulating to suggest a signalling function, independent of peroxidase activity, as shown for mammalian Prx6 (Choi 2011). Prx6 binds and inhibits the activity of cysteine-aspartic proteases essential for DED caspase-induced cell death (Choi *et al*., 2011). Prx6 is the only member of the 1-Cys Prx subfamily in mammals but future research in other organisms may reveal a more general involvement of 1-Cys Prxs in cell signalling.

4.4.3 Culture phenotypes of ΔgpxC and ΔtpxA mutants

Growth of the *E. festucae* Δ*gpxC*, Δ*tpxA* and Δ*gpxC*Δ*tpxA* strains was not impaired on H_2O_2. Thiol peroxidases remain relatively unstudied in fungi other than yeast. This study is the first to examine a Tpx1 homologue and, to date, *M. oryzae* HYR1 is the only characterised Gpx3 homologue from filamentous fungi. Mycelial growth of the *M. oryzae* Δ*hyr1* mutant is very sensitive to H_2O_2. The Δ*hyr1* mutant is also sensitive to ROS produced within the plant throughout infection and consequently, virulence is reduced (Huang *et al*., 2011). This further supports the notion that *E. festucae* possesses multiple overlapping mechanisms to defend against peroxide stress and highlights the importance for *E. festucae* to maintain highly robust peroxide defences. A degree of overlap also exists between the thiol peroxidases of *S. cerevisiae*. In addition to Gpx1-3, *S. cerevisiae* possesses multiple other thiol peroxidases including Tsa1, Tsa2 and Prx1, Pmp20 and Bcp. Deletion of individual thiol peroxidases has a variable effect on oxidative stress-sensitivity of *S. cerevisiae* depending on the gene deleted and nature of

the oxidant used to impose stress. Deletion of individual thiol peroxidases in *S. cerevisiae* tended to have a relatively minor effect whereas combinatorial deletion of multiple thiol peroxidases had a much more profound impact on oxidative stress sensitivity (Fomenko *et al.*, 2011). Furthermore, the contribution of thiol peroxidases to oxidative stress resistance appeared to be additive with the *S. cerevisiae* mutant lacking all eight thiol peroxidases showing the most severe oxidative stress-sensitivity phenotype. Interestingly, *S. cerevisiae* cells lacking all, or almost all thiol peroxidases except Gpx2 or Gpx3 were still viable, however, the gene expression changes in response to H_2O_2 were no longer observed. This suggests that thiol peroxidases in *S. cerevisiae* comprise a peroxide-dependent signalling network (Fomenko *et al.*, 2011). The thiol peroxidase family of *E. festucae* as well as *S. pombe* and other filamentous fungi is, by comparison, reduced. As discussed previously *S. pombe* possesses a single Gpx homologue (Gpx1) and three peroxiredoxin homologues (Tpx1, Bcp and Pmp20). Similarly, *E. festucae* also possesses a single Gpx1 homogloue and Tpx1, Bcp and Pmp20 homologues. *E. festucae* thiol peroxidases may too constitute cellular signaling networks, however, this remains to be tested.

4.4.4 Thiol peroxidase-mediated YapA activation

While Gpx3 and Tpx1 are essential for the peroxide-induced nuclear accumulation of Yap1 and Pap1, respectively (Bozonet *et al.*, 2005, Delaunay *et al.*, 2002), deletion of neither the Gpx3 or the Tpx1 homologue in *E. festucae* (GpxC and TpxA) prevented an EGFP-tagged YapA protein from accumulating in the nucleus of *E. festucae* cells in response to H_2O_2. Localisation of EGFP-tagged YapA was examined in the Δ*gpxC*Δ*tpxA* background to address the possibility of redundancy between GpxC and TpxA. YapA-EGFP still localised to the nucleus in an H_2O_2-dependent manner in the Δ*gpxC*Δ*tpxA* strain suggesting there may be even further redundancy among thiol peroxidases in the H_2O_2-induced activation of *E. festucae* YapA or that activation of YapA by H_2O_2 is achieved by an as yet unknown mechanism.

In the field spermatia or ascospores of *Epichloë* endophytes mediate colonization of new host ryegrass plants through the stigmas of florets (Chung & Schardl, 1997). In the lab new associations are established artificially by introducing *E. festucae* mycelium into a 2-3 mm longitudinal incision in the meristematic region of the grass seedling, made using a sterile scalpel (Latch & Christensen, 1985). A burst of ROS occurs in response to the physical wounding of the seedling during this artificial inoculation procedure (Le Deunff *et al.*, 2004). This oxidative burst the fungus is then exposed to may represent more physiological conditions of oxidative stress as opposed to flooding *E. festucae* cultures with solutions of H_2O_2 as described above. Thus, we examined

whether YapA-EGFP still localised to the nucleus in strains lacking GpxC and TpxA. In doing so, we uncovered a potential antioxidant role for GpxC in early stages of plant infection. The loss of YapA-EGFP expression observed in Δ*gpxC* and Δ*gpxC*Δ*tpxA* hyphae indicates these mutants may be compromised by a wound-induced response from the plant. YapA-EGFP localises to the nucleus in a Δ*tpxA* strain during infection suggesting the observed loss of fluorescence is a result of the *gpxC* deletion. Cytoplasmic fluorescence was restored in cultures 16 h post-inoculation suggesting that the fungus is not permanently compromised and no longer in a state of oxidative stress. Why EGFP expression was temporarily lost is unclear at this stage but is presumably due to sensitivity towards host-produced ROS resulting from the loss of GpxC. Several explanations are possible including oxidation and/or degradation of YapA-EGFP, quenching of EGFP fluorescence or downregulation of the TEF promoter. Given the rapid rate at which fluorescence was lost, oxidative degradation of EGFP is plausible. Alternatively, EGFP fluorescence may be quenched by another compound under conditions of oxidative stress. Quenching of GFP fluorescence has been observed in response to pH and temperature changes (Elsliger *et al.*, 1999, Leiderman *et al.*, 2006). It is possible that in cells lacking GpxC the physiological environment for EGFP is altered, through changes in the redox or pH conditions, thus quenching EGFP fluorescence. Alternatively, if growth of the fungus is arrested during this oxidative burst, encountered by the fungus during colonisation, then down regulation of the TEF (translation elongation factor) promoter is also a possibility as processes such as translation would no longer drive the *TEF* promoter.

Despite these observations, GpxC is not essential for the establishment and maintenance of the symbiotic interaction between *E. festucae* and perennial ryegrass. If host colonisation is initially impaired in *E. festucae* strains lacking GpxC, the recovery 16 h post-inoculation would allow delayed colonisation without an observed reduction in infection. Moreover, deletion of *gpxC* and *tpxA* did not alter growth and morphology of the fungus within the host nor was growth of the host plant affected. To date, a *GPX3* homologue has been deleted in just one other filamentous fungus, *M. oryzae.* While *M. oryzae* **Δ***hyr1* mutants do not appear susceptible to an initial oxidative burst by the plant they do appear to be sensitive to plant-produced ROS encountered in later stages of infection and consequently virulence is reduced (Huang *et al.*, 2011).

To investigate whether *E. festucae* possessed all necessary components for regulation and activation of the *S. cerevisiae* Yap1 transcription factor EGFP-tagged Yap1 was expressed in *E. festucae*. The Yap1-EGFP fusion protein localised to the cytoplasm in unstressed hyphae and remained cytoplasmic when hyphae were treated

with H_2O_2 or menadione at concentrations previously shown to induce rapid relocalisation of the *E. festucae* YapA-EGFP fusion to the nucleus. The activation of Yap1 by H_2O_2 is dependent on both Gpx3 and Ybp1 whereas thiol-reactive compounds directly target Yap1 through cysteine adduct formation, independently of Gpx3 or Ybp1 (Veal *et al.*, 2003). This differential activation provided an opportunity to test whether the lack of peroxide-induced Yap1 activation in *E. festucae* was due to lack of either an equivalent Gpx3 H_2O_2-signal transducer or Ybp1 accessory protein.

In *S. cerevisiae,* Ybp1 is required for the Yap1-Gpx3 complex to form. The function of Ybp1 in the *S. cerevisiae* Gpx3-Yap1 redox relay is still largely unknown but it has been proposed to serve as a scaffold to facilitate the Gpx3-Yap1 redox interaction (Veal *et al.*, 2003). The Ybp1 protein is likely to be an *S. cerevisiae* specific adaptation, as no Ybp1 homologue exists in the genome of *E. festucae* and other filamentous fungi. It is possible that another scaffold protein is present in *E. festucae* and capable of stabilizing an interaction between Yap1 and GpxC. As treatment with menadione also failed to induce nuclear localisation of Yap1 in *E. festucae* hyphae this suggests factors other than Gpx3 and Ybp1 are required for Yap1 activation in *S. cerevisiae,* which are not present in foreign hosts such as *E. festucae.* While Ybp1 is necessary for peroxide-induced activation of Yap1 but not activation by thiol reactive agents, it is plausible that other, yet to be identified, accessory proteins exist in *S. cerevisiae* which facilitate activation by thiol-modifying agents.

4.4.5 Alternative hypotheses

The experiments in axenic culture and *in planta* indicate YapA is not regulated by the thiol peroxidases GpxC or TpxA. A number of alternative hypotheses for H_2O_2-mediated activation of YapA and filamentous fungal Yap1 homologues need to be proposed. The possibilities of redundancy among thiol peroxidases and importance of thiol-peroxidase mediated disulfide bond formation are discussed below.

4.4.6 Redundancy

There may be redundancy among thiol peroxidases for YapA activation that extends beyond GpxC and TpxA tested here. Results by Delaunay *et al.* (2002) indicate a degree of overlap in H_2O_2-sensing exists among thiol peroxidases. In an *S. cerevisiae* strain expressing a truncated Ybp1 protein, the *S. pombe* Tpx1 homologue, Tsa1, interacts with and activates Yap1 (Tachibana *et al.*, 2009). This back-up activation mechanism might account for the higher H_2O_2 tolerance of the Δ*GPX3* strain compared to the Δ*YAP1* strain. In addition to *gpxC* and *tpxA* just two other thiol peroxidases

(EfM2.115510 and EfM2.064230) related to *S. pombe* Bcp and Pmp20 peroxiredoxins were identified in *E. festucae.* Peroxiredoxins in general are ideal candidates for H_2O_2 signal transduction, given their high reactivity with H_2O_2 and high abundance in cells (Winterbourn & Hampton, 2008). However, neither Bcp- or Pmp20-related proteins have previously been shown to function in redox signal transduction (Kim *et al.*, 2010). At this stage, no further candidates for the upstream H_2O_2-sensor for YapA are apparent.

4.4.7 Disulfide bond activation

This study is the first to report H_2O_2-induced disulfide-bond formation in a Yap1 homologue from a filamentous fungus. The lack of H_2O_2 reactivity and oxidation-induced change of conformation of *S. cerevisiae* $Yap1^{C303A}$ and $Yap1^{C598A}$ demonstrates the requirement for two disulfide bonds in yeast. However, a multiple sequence alignment of Yap1 homologues suggests there is potential to form just a single disulfide between the n- and c-CRD in some other filamentous fungi. It is possible that a second disulfide is formed in *E. festucae* between Cys410 in the n-CRD and a Cys residue within the c-CRD. Alternatively, formation of one disulfide in *E. festucae* YapA may be sufficient to disrupt the interaction with a nuclear exportin and achieve full activation. Presumably, disulfide bond formation would be mediated by a thiol peroxidase yet to be identified. The yeast redox relay systems of *S. cerevisiae* and *S. pombe* rely on the direct interaction of Gpx3 and Tpx1 with the AP-1 transcription factor target, thus the cysteine residues in the c-CRD, interacting with Gpx3 or Tpx1 are likely to be solvent exposed and accessible. In accordance with this hypothesis, the high resolution nuclear magnetic resonance (NMR) structure of oxidised Yap1 determined by Wood *et al.* (2004) shows the Cys303–Cys598 and Cys310–Cys629 disulfide bonds to be largely solvent exposed. Cysteine residues in the c-CRD are well conserved in filamentous fungi indicating potential for interactions with upstream redox-sensing proteins.

Based on what is known in yeast, reversible disulfide bond formation mediated by a thiol peroxidase is the most likely mechanism of activation in *E. festucae*. However, the involvement of thiol peroxidases and exact mechanisms of disulfide formation in the activation of YapA remain unclear. The possibility of direct oxidation and oxidation by secondary oxidation products is explored below.

4.4.8 Direct oxidation

Direct oxidation of the *E. coli* OxyR transcription factor has been well documented (Storz *et al*., 1990). OxyR is activated by H_2O_2 through the formation of an intramolecular disulfide bond, which induces a conformational change and allows OxyR to activate the transcription of antioxidant genes. Activated OxyR is subsequently deactivated by enzymatic reduction of the disulfide bond (Storz *et al*., 1990). Experiments by Okazaki *et al.* (2007) using a reconstituted *in vitro* redox system have shown that Yap1 can be oxidised by Gpx3 in the absence of Ybp1 and also directly oxidised by H_2O_2 (Okazaki *et al*., 2007). The abundance of Prx and GPx proteins in cells and the efficiency with which they react with H_2O_2 makes it unlikely that other, less reactive, proteins such as AP-1 transcription factors would be able to directly react with H_2O_2 *in vivo* (Jarvis *et al*., 2012, Winterbourn & Hampton, 2008). Indeed, oxidation of Yap1 was accelerated in the presence of Gpx3 and the Trx/Trr/NADPH reduction system suggesting Gpx3-mediated oxidation of Yap1 by H_2O_2 and Trx-mediated reduction of Yap1 are catalytically favorable and likely to represent the physiological situation *in vivo* (Okazaki *et al*., 2007). The ability of Gpx3 to oxidise Yap1 in the absence of Ybp1 *in vitro* is reasonable given the predicted scaffold function for Ybp1. The number of targets and possibility of non-specific activation in this reconstituted system is low, whereas in cells Ybp1 may be necessary to bring Gpx3 and Yap1 together to facilitate oxidation. Moreover, *in vivo* Gpx3 functions as both an antioxidant and a peroxide sensor for Yap1. The antioxidant mechanism whereby the catalytic Cys condenses with the resolving Cys to form a disulfide within Gpx3 is catalytically more favourable than that required to promote Yap1 oxidation because of the higher effective molarity of the vicinal resolving cysteine (D'Autreaux & Toledano, 2007). Thus, *in vivo* the Ybp1 scaffold is essential to promote the reaction between Gpx3 and Yap1.

4.4.9 Secondary oxidation products

Although H_2O_2 is likely to be intercepted by peroxiredoxins and glutathione peroxidases before reaching other target proteins, by-products generated in the detoxification of H_2O_2 may activate these targets. Delaunay *et al.* (2002) suggest that the higher H_2O_2 tolerance of the *S. cerevisiae* Δ*GPX3* strain may be due to Gpx3-independent activation of Yap1 by such oxidation by-products. Given that the Gpx3 homologue, GpxC, does not appear to activate *E. festucae* YapA potential Yap1 H_2O_2-activation mechanisms which do not involve the Gpx3 are of great interest, and could provide significant insight into the mechanisms of H_2O_2-induced activation of Yap1 homologues in filamentous fungi. While the conversion of H_2O_2 to water and oxygen by catalase enzymes is thought to be the major route of H_2O_2 detoxification in cells, decomposition can also generate a number of by-products. As indicated in Figure 1.2,

H_2O_2 can be converted to hydroxyl radicals and hydroxide ions in the presence of Fe^{2+}. It is unlikely that the hydroxyl radicals generated in this reaction could directly activate Yap1. While hydroxyl radicals react well with thiol groups, they are too indiscriminate to show selectivity towards any target (Winterbourn & Hampton, 2008). Peroxidases are a large family of enzymes that catalyse the conversion of H_2O_2 to H_2O according to the following reaction: e^- donor + H_2O_2 = oxidised e^- donor + $2H_2O$ (Welinder *et al.*, 1992). A wide variety of electron donor substrates are utilised and it is plausible that Yap1 may also be activated by one or more of these oxidised species generated in the breakdown of H_2O_2.

4.5 Functional redundancy in oxidative stress sensing pathways

While a link between *E. festucae* YapA, GpxC and/or TpxA has not been established in this study it has revealed that various antioxidant defences, shown to be important for infection in other phytopathogenic fungi, are non-essential for the symbiotic interaction of *E. festucae* with its grass host. This suggests ROS protection systems in *E. festucae* are very robust.

4.5.1 SakA MAPK pathway

Functionally overlapping pathways might operate in *E. festucae* to protect against H_2O_2-induced oxidative stress. The stress-activated MAPK signalling pathway contains three MAP kinases (MAPKKK, MAPKK, MAPK) in series whose sequential phosphorylation and activation culminates in the phosphorylation and activation of a bZIP transcription factor (Wilkinson *et al.*, 1996). This pathway is critical for resistance to H_2O_2 stress in other fungi and yeast, including *A. nidulans, S. pombe* and *C. albicans* (Alonso-Monge *et al.*, 2003, Degols *et al.*, 1996, Kawasaki *et al.*, 2002). The *S. cerevisiae* Hog1 stress-activated MAPK was originally characterised based on its role in the osmotic stress response, however, recent studies have shown an involvement of both the Hog1 MAPK kinase pathway and the upstream Sln1-Ssk1 two-component system in oxidative stress response (Haghnazari & Heyer, 2004, Singh, 2000). In comparison, the *E. festucae* Hog1 MAPK homologue, SakA, is not essential for resistance to H_2O_2 stress, yet SakA localises to the nucleus in response to H_2O_2 and functionally complements H_2O_2-sensitivity of an *S. pombe STY1* mutant (Eaton *et al.*, 2008).

4.5.2 Skn7

Other pathways that culminate in the induction of antioxidant proteins have also been identified in filamentous fungi and yeast, including those involving the Skn7 and

Msn2/Msn4 transcription factors (Fassler & West, 2011). These additional oxidative stress-responsive transcription regulators have been extensively studied in *S. cerevisiae*, and substantial overlap between the Yap1 and Skn7 and, to a lesser extent, Msn2/Msn4 H_2O_2-inducible regulons has been demonstrated (Krems *et al.*, 1996, Lee *et al.*, 1999, Martinez-Pastor *et al.*, 1996). Skn7 and Msn2/Msn4 homologues exist in *E. festucae* (Skn7, EfM2.015190 and Msn2/4, EfM2.033120) and, while their role in the oxidative stress response remains to be studied, it is plausible that the vegetative mycelial form of *E. festucae* is protected against H_2O_2-stress by multiple, back-up, mechanisms. The lack of mycelial H_2O_2 sensitivity in both the Δ*sakA* and Δ*yapA* mutants suggests the stress-activated MAPK and the AP-1 pathways may be functionally redundant in mediating resistance against H_2O_2 stress. This would indicate that defence against peroxide stress is so vital for *E. festucae* that the cell has multiple back-up mechanisms conferring robustness to peroxide stress. Indeed, a fungal Cu/Zn superoxide dismutase (Cu/Zn-SOD), SodA, is one of the most abundantly expressed proteins in the *N. lolii-L. perenne* symbiosis (Zhang *et al.*, 2011). Analysis of transcriptome data generated from an *E. festucae–L. perenne* association showed that the *sodA* homologue is also one of the most highly expressed genes in this interaction (Eaton *et al.*, 2010). This strongly suggests that ROS detoxification by the Cu/Zn-SOD is crucial for the symbiosis and highlights the importance of defence systems to protect the fungus from ROS *in planta*. Interestingly, the *E. festucae sodA* deletion mutant did not show a symbiotic defect, again, highlighting the existence of redundant mechanisms for ROS resistance in *E. festucae* (Zhang *et al.*, 2011).

Overall several key themes have emerged from this research. Firstly, the redundancy in oxidative stress sensing systems employed by *E. festucae* is becoming increasingly apparent, in line with what previous researchers have shown (Eaton *et al.*, 2008, Zhang *et al.*, 2011). *E. festucae* appears to possess a robust oxidative stress defence network whereby back-up mechanisms provide protection when the function of other components is compromised. This suggests that perturbations to redox homeostasis and ensuing oxidative stress may be commonly encountered by *E. festucae*, necessitating efficient coping mechanisms.

Secondly, differences in the requirement for an AP-1 detoxification system as well as thiol peroxidase-mediated defence compared to other filamentous fungi reflects the unique lifestyle of this organism.

Finally, this study highlights that despite the relatively close phylogenetic relationship between yeast and filamentous fungi, the regulatory mechanisms of signalling processes may not be evolutionarily conserved between these species. Here

we have shown that the regulation of the YapA transcription factor in *E. festucae* does not resemble that of either Yap1 in *S. cerevisiae* or Pap1 in *S. pombe.* The presence of homologous components is often assumed to indicate conservation of a particular pathway or mechanism. The data presented here shows that while components involved in AP-1 regulation in yeast can also be found in *E. festucae*, they do not appear to be involved in a conserved mechanism of YapA activation, a finding that more broadly applies to the characterisation of other signalling pathways in filamentous fungi based on the model yeast species, *S. cerevisiae* and *S. pombe*.

5 Summary and Conclusions

This PhD thesis focused predominantly on characterizing the role of the *E. festucae* AP-1 transcription factor, YapA, in oxidative stress responses. Investigating the potential role of thiol peroxidases, GpxC and TpxA, as upstream redox sensors involved in YapA activation was also a primary focus of the research. The major findings and implications of this research are summarised below.

Deletion of the AP-1 transcription factor-encoding gene, *yapA,* did not confer mycelial sensitivity to hydrogen peroxide, a compound commonly used to induce oxidative stress in cells. This result is in distinct contrast to the H_2O_2-sensitivity that results when genes encoding *yap1*-like transcription factors are disrupted in all other fungi characterised to date.

The YapA transcription factor is not essential for the regulation of gene expression in response to hydrogen peroxide in the mycelial form of E. festucae.

Deletion of either or both *gpxC* and *tpxA* genes did not result in increased H_2O_2-sensitivity suggesting GpxC and TpxA are not essential for H_2O_2-resistance but are part of a robust antioxidant system in *E. festucae.* Homologues of *gpxC* and *tpxA* remain largely uncharacterised in fungi other than yeast, however, based on the predicted antioxidant function of GpxC and TpxA the wild-type H_2O_2-tolerance of Δ*gpxC* and Δ*tpxA* mutants is somewhat surprising. This result highlights the redundancy in *E. festucae* ROS detoxification systems that extend beyond the thiol peroxidases GpxC and TpxA evident from the wild-type tolerance of the Δ*gpxC*Δ*tpxA* double deletion strain.

E. festucae possesses an extensive ROS detoxification network capable of robust protection against oxidative stress.

Mycelial growth of the Δ*yapA* strain was impaired on media containing menadione and, to a lesser extent, diamide. The sensitivity of the Δ*yapA* mutant to specific types of ROS may be a reflection of the molecular diversity of these species and the different modes of YapA activation. Activation of Yap1 by these thiol-reactive electrophiles is achieved through direct adduction to one or more cysteine residues within the C-terminal cysteine-rich domain (c-CRD) of Yap1, which inhibits its association with the Crm1 nuclear exportin (Ouyang *et al.*, 2011). In contrast, activation of Yap1 by H_2O_2 involves initial signal reception by GPX3 and formation of the Yap1-Gpx3 intermolecular disulfide intermediate which is later converted to an intramolecular disulfide bond between cysteine residues in the c-CRD and n-CRD (Gulshan *et al.*, 2011).

The cellular responses to oxidative stress in E. festucae vary depending on the nature of the oxidant. E. festucae YapA is required for resistance against the thiol-

reactive oxidative stress-generating species, menadione and diamide.

While deletion of *yapA* did not affect mycelial sensitivity to H_2O_2, it did, however, result in a spore-specific sensitivity to H_2O_2. *E. festucae* spores are inherently more sensitive to H_2O_2 than is the vegetative mycelial form, and much more sensitive than spores produced by many other fungal species considered in this study. Spores of the Δ*yapA* mutants were significantly more sensitive to H_2O_2 than wild-type spores.

In E. festucae spore germination was more sensitive to H_2O_2 than was mycelial growth. E. festucae YapA is developmentally required for H_2O_2-resistance and plays an important role in the resistance of germinating spores to H_2O_2.

The H_2O_2-sensitivity of Δ*yapA* mutants observed specifically in spores of *E. festucae* indicated YapA may be involved in the regulation of a spore-specific catalase. A GFP-reporter approach, using a high-turnover EGFP variant, confirmed that expression of the spore-specific catalase-encoding gene, *catA,* was dependent on YapA for expression. While a canonical YRE motif was not identifiable in the *catA* promoter this does not discount the possibility that it is a YapA target gene as YREs are not found in all *S. cerevisiae* Yap1 target genes.

Expression of the spore-specific specific catalase, catA, is dependent on YapA and accounts for the spore-specific H_2O_2-sensitivity observed in the ΔyapA mutant.

H_2O_2-tolerance of spores was not affected by deletion of *gpxC* or *tpxA,* both singularly and in combination, suggesting the antioxidant function of these enzymes is not essential for H_2O_2-resistance of spores. Furthermore, this indicates that these thiol peroxidases do not play essential or overlapping roles in transmitting peroxide signals to YapA

H_2O_2-resistance of spores is not compromised in the absence of gpxC and tpxA indicating the H_2O_2-protective antioxidant activity of thiol peroxidases in E. festucae is overlapping and robust.

YapA relocalises to the nucleus in an oxidative stress-dependent manner. Treatment with both the commonly used oxidant H_2O_2 and the thiol-oxidising agent menadione induced nuclear localisation of the YapA-EGFP fusion. Nuclear localisation was not impaired in the Δ*gpxC,* Δ*tpxA* or Δ*gpxC*Δ*tpxA* deletion backgrounds suggesting homologues of *S. cerevisiae* and *S. pombe* redox relay sensors, Gpx3 and TpxA are not required for YapA activation in *E. festucae*.

YapA is a bona fide AP-1 transcription factor regulated through nuclear-cytoplasmic partitioning. Nuclear localisation is not dependent on putative redox sensors GpxC or TpxA suggesting the mechanism of YapA activation in E. festucae is

unlike the Gpx3-Yap1 and Tpx1-Pap1 redox relay mechanisms which occur in the model yeast species, S. cerevisiae and S. pombe, respectively.

Deletion of *yapA, gpxC* or *tpxA* did not affect the symbiotic interaction of *E. festucae* with its ryegrass host, *L. perenne*. Plants infected with Δ*yapA,* Δ*gpxC,* Δ*tpxA* or Δ*gpxC*Δ*tpxA* strains resembled wild-type-infected plants. Growth and morphology of the endophytic hyphae also resembled that of wild-type.

YapA, GpxC and TpxA are not essential for the successful establishment and maintenance of the symbiotic interaction of E. festucae with its perennial ryegrass host.

While host colonisation of Δ*yapA* mutants was not impaired, the transient nuclear localisation of YapA in hyphae at the wound-inoculation site indicates that YapA may be involved, but not essential, for protecting the fungus against host-derived ROS. The time period over which nuclear localisation and cytoplasmic redistribution was observed was consistent with a role for YapA in detoxification of a wound-induced oxidative burst. The dispensability of YapA in host infection is particularly intriguing given the apparent plant oxidative burst it encounters following inoculation. Other fungal AP-1 mutants, specifically biotrophic fungi, are impaired in colonisation due to the role of the AP-1 transcription factor in an oxidative stress response system to overcome this host oxidative burst.

E. festucae YapA is activated in fungal hyphae exposed to wounded plant tissues that occurs as a result of the fungal inoculation procedure.

Regenerating protoplasts transformed using PEG-mediated DNA delivery transition through an arthroconidial state. These cells are spore-like and potentially in a state of oxidative stress given the high levels of expression of the *catA* GFP-reporter. It is likely that the low oxygen tension encountered by regenerating protoplasts beneath the surface of the antibiotic overlay contributes to formation of arthroconidia as incubation of cultures in microaerophilic conditions induced the formation of similar, but not identical, structures.

The transformation procedure, used to introduce DNA into E. festucae protoplasts induces the formation of arthroconidia.

6 Future Work

This study has produced a number of novel findings with implications for the function and activation of the YapA transcription factor in *E. festucae*. The objectives detailed at the outset of this study have been addressed, however, several intriguing questions have been raised and a number of exciting new research avenues uncovered. This chapter outlines the future research directions that need to be pursued in order to build a deeper understanding of the role and regulation of the AP-1 transcription factor, YapA, in the fungal symbiont, *E. festucae*. Increasing evidence suggests certain thiol peroxidases act as oxidant receptors to pass on redox signals to targets proteins through specific protein-protein interactions. Further research into this area is also required to better understand the role of thiol peroxidase-based redox signal transduction in filamentous fungi.

6.1 Towards an understanding of YapA redox regulation

To elucidate the regulatory mechanisms underlying the YapA oxidative stress response, it is essential to identify downstream targets of YapA, and, in turn, how YapA is regulated. Promoter motif analyses and GFP reporter approaches used in this study provided an indication of several potential YapA targets. Homologues in other fungi control large oxidative stress regulons of up to 45 genes (Lee *et al*., 1999, Tian *et al*., 2011). Thus a larger scale approach such as transcriptome analysis is necessary to identify targets of YapA in *E. festucae*. Knowledge of YapA targets would provide a valuable insight into the biological role of this transcription factor in *E. festucae* and allow cross-species comparisons of other AP-1 regulons. This information would also allow further characterisation of YRE motifs and variant YapA recognition motifs in the promoters of YapA target genes.

The redox western analysis indicated that in response to H_2O_2 stress, a disulfide bond is formed in YapA. However, the precise mechanism remains unclear. Further experimentation is necessary to determine the number of disulfides formed and the residues involved. Much of the uncertainty lies in the n-CRD domain on YapA. Thus, mutation of the N-terminal cysteines (Cys363 and Cys410) to alanines singularly and in combination would reveal the importance of these residues in the oxidative activation of this protein. Subcellular localisation of EGFP-tagged YapA variants, $YapA^{C363A}$ and $YapA^{C410A}$, will reveal whether they participate in oxidative activation of this protein. Redox western analysis using these mutated YapA proteins would allow us to pinpoint which of the N-terminal residues are involved in disulfide bond formation. An absence of an H_2O_2-induced shift, indicative of YapA oxidation, would indicate the involvement of the particular substituted cysteine. While the C-terminal cysteines (Cys499, Cys523 and Cys532) are conserved among fungal Yap1 homologues, similar

analysis with YapA^{C499A}, YapA^{C523A} and YapA^{C532A} mutants would provide insight into which residues participate in interdomain disulfide formation with the n-CRD. The outcome of these experiments will be of great importance for understanding not only the activation mechanism of *E. festucae* YapA but also other filamentous fungal Yap1 homologues.

This study has explored the role of the YapA transcription factor in sensing oxidative stress in *E. festucae*. The involvement of the *E. festucae* stress-activated MAPK pathway in oxidative stress sensing has also previously been explored (Eaton *et al*., 2010). Section 4.5 discussed the possibility of redundancy among oxidative stress sensing pathways. Given the intimate involvement of the Skn7 transcription factor/response regulator with Yap1 in *S. cerevisiae* it is of great interest to investigate the role of the Skn7 homologue in *E. festucae*. Creation of Δ*skn7* and Δ*yapA*Δ*skn7* strains would provide an opportunity to explore the cooperation and overlapping roles of Skn7 and YapA in oxidative stress protection in *E. festucae.*

6.2 Towards an understanding of thiol peroxidases in signal transduction

The existence and nature of an H_2O_2-sensor for YapA sensor is a 'burning question'. At this stage of the study we have exhausted all likely thiol peroxidase candidates. As outlined above, a more detailed understanding of YapA activation is required before we pursue the elusive H_2O_2 sensor. In other words, we may be fishing in a lake with no fish.

Given the high likelihood of a signalling role for Prx proteins, based on kinetic data, it will be of great interest to identify TpxA and GpxC targets other than YapA. The interaction of Prx proteins with target proteins is likely to be transient and induced under certain conditions thus classic approaches such as coimmunoprecipitation and yeast-two-hybrid may not detect such protein-protein interactions. Detection of an interaction with an unknown target is also particularly challenging as *in vivo* approaches such as Bimolecular fluorescence complementation (also known as BiFC) cannot be used. Crosslinking protein interaction analysis might allow transient interactions of a thiol peroxidase with an unknown component in a signalling cascade to be stabilised and thus allow characterisation of interaction complexes.

The sensitivity of cultures lacking GpxC at the wound site of inoculated perennial ryegrass seedlings also requires further analyses to understand the role of GpxC as an antioxidant. This result is intriguing, as H_2O_2-sensitivity was not observed for strains

lacking GpxC in culture. Future work will involve determining what causes YapA-EGFP expression to be lost and the specific cellular effects of the wound-induced ROS towards strains lacking GpxC.

Overall, these additional experiments represent a new phase of the research. The experiments proposed for YapA would contribute to a better understanding of its role in sensing and responding to changes in the redox state of the cell. The further investigation into TpxA and GpxC would contribute significant insights into the emerging field of peroxiredoxin-mediated cell signaling. At present, much of what is known about peroxiredoxin-mediated signalling is based on a limited number of examples, particularly in budding and fission yeasts. Further studies may uncover more examples and variations from the paradigmatic regulation of peroxidase-signalling in *S. cerevisiae* and *S. pombe,* adding to the growing knowledge of redox-baed signalling.

7 References

Adams, T. H., J. K. Wieser & J. H. Yu, (1998) Asexual sporulation in *Aspergillus nidulans*. *Microbiology and Molecular Biology Reviews* **62**: 35-54.

Aguilera, J., S. Rodriguez-Vargas & J. A. Prieto, (2005) The HOG MAP kinase pathway is required for the induction of methylglyoxal-responsive genes and determines methylglyoxal resistance in *Saccharomyces cerevisiae*. *Molecular Microbiology* **56**: 228-239.

Aguirre, J., W. Hansberg & R. Navarro, (2006) Fungal responses to reactive oxygen species. *Medical Mycology* **44**: S101-S107.

Alarco, A. M. & M. Raymond, (1999) The bZip transcription factor Cap1p is involved in multidrug resistance and oxidative stress response in *Candida albicans*. *Journal of Bacteriology* **181**: 700-708.

Alonso-Monge, R., F. Navarro-Garcia, E. Roman, A. I. Negredo, B. Eisman, C. Nombela & J. Pla, (2003) The Hog1 mitogen-activated protein kinase is essential in the oxidative stress response and chlamydospore formation in *Candida albicans*. *Eukaryotic Cell* **2**: 351-361.

Angel, P. & M. Karin, (1991) The Role of Jun, Fos and the Ap-1 complex in cell-proliferation and transformation. *Biochimica Et Biophysica Acta* **1072**: 129-157.

Angelova, M. B., S. B. Pashova, B. K. Spasova, S. V. Vassilev & L. S. Slokoska, (2005) Oxidative stress response of filamentous fungi induced by hydrogen peroxide and paraquat. *Mycological Research* **109**: 150-158.

Apel, K. & H. Hirt, (2004) Reactive oxygen species: Metabolism, oxidative stress, and signal transduction. *Annual Review of Plant Biology* **55**: 373-399.

Asano, Y., D. Hagiwara, T. Yamashino & T. Mizuno, (2007) Characterization of the bZip-type transcription factor NapA with reference a to oxidative stress response in *Aspergillus nidulans*. *Bioscience Biotechnology and Biochemistry* **71**: 1800-1803.

Atkinson, H. J. & P. C. Babbitt, (2009) An atlas of the thioredoxin fold class reveals the complexity of function-enabling adaptations. *PLoS Computational Biology* **5**: e1000541.

Avery, A. M. & S. V. Avery, (2001) *Saccharomyces cerevisiae* expresses three phospholipid hydroperoxide glutathione peroxidases. *Journal of Biological Chemistry* **276**: 33730-33735.

Avery, S. V., (2011) Molecular targets of oxidative stress. *Biochemical Journal* **434**: 201-210.

Azevedo, D., F. Tacnet, A. Delaunay, C. Rodrigues-Pousada & M. B. Toledano, (2003) Two redox centers within Yap1 for H_2O_2 and thiol-reactive chemicals signaling. *Free Radical Biology and Medicine* **35**: 889-900.

Banno, S., R. Noguchi, K. Yamashita, F. Fukumori, M. Kimura, I. Yamaguchi & M. Fujimura, (2007) Roles of putative His-to-Asp signaling modules HPT-1 and RRG-2, on viability and sensitivity to osmotic and oxidative stresses in *Neurospora crassa*. *Current Genetics* **51**: 197-208.

Barrera, C. R., (1986) Formation and germination of fungal arthroconidia. *Critical Reviews in Microbiology* **12**: 271-292.

Belozerskaia, T. A. & N. N. Gessler, (2007) Reactive oxygen species and the strategy of the antioxidant defense in fungi: a review. *Applied Biochemistry and Microbiology* **43**: 565-575.

Bence, N. F., R. M. Sampat & R. R. Kopito, (2001) Impairment of the ubiquitin-proteasome system by protein aggregation. *Science* 292: 1552-1555.

Bergman, L. W., (2001) Growth and Maintenance of Yeast. *Methods in Molecular Biology* **177**: 9-14.

Berna, A. & F. Bernier, (1999) Regulation by biotic and abiotic stress of a wheat germin gene encoding oxalate oxidase, a H_2O_2-producing enzyme. *Plant Molecular Biology* **39**: 539-549.

Biteau, B., J. Labarre & M. B. Toledano, (2003) ATP-dependent reduction of cysteine-sulphinic acid by *S. cerevisiae* sulphiredoxin. *Nature* **425**: 980-984.

Blokhina, O. & K. V. Fagerstedt, (2010) Oxidative metabolism, ROS and NO under oxygen deprivation. *Plant Physiology and Biochemistry* **48**: 359-373.

Bozonet, S. M., V. J. Findlay, A. M. Day, J. Cameron, E. A. Veal & B. A. Morgan, (2005) Oxidation of a eukaryotic 2-Cys peroxiredoxin is a molecular switch controlling the transcriptional response to increasing levels of hydrogen peroxide. *Journal of Biological Chemistry* **280**: 23319-23327.

Bradley, D. J., P. Kjellbom & C. J. Lamb, (1992) Elicitor-induced and wound-induced oxidative cross-linking of a proline-rich plant-cell wall protein - a novel, rapid defense response. *Cell* **70**: 21-30.

Brewster, J. L., T. Devaloir, N. D. Dwyer, E. Winter & M. C. Gustin, (1993) An osmosensing signal transduction pathway in yeast. *Science* **259**: 1760-1763.

Buck, V., J. Quinn, T. Soto Pino, H. Martin, J. Saldanha, K. Makino, B. A. Morgan & J. B. Millar, (2001) Peroxide sensors for the fission yeast stress-activated mitogen-activated protein kinase pathway. *Molecular Biology of the Cell* **12**: 407-419.

Byrd, A. D., C. L. Schardl, P. J. Songlin, K. L. Mogen & M. R. Siegel, (1990) The beta-tubulin gene of *Epichloë typhina* from perennial ryegrass (*Lolium perenne*). *Current Genetics* **18**: 347-354.

Cabiscol, E., E. Piulats, P. Echave, E. Herrero & J. Ros, (2000) Oxidative stress promotes specific protein damage in *Saccharomyces cerevisiae*. *Journal of Biological Chemistry* **275**: 27393-27398.

Cadenas, E., (1989) Biochemistry of oxygen toxicity. *Annual Review of Biochemistry* **58**: 79-110.

Calvo, I. A., P. Garcia, J. Ayte & E. Hidalgo, (2012) The transcription factors Pap1 and Prr1 collaborate to activate antioxidant, but not drug tolerance, genes in response to H_2O_2. *Nucleic Acids Research* **40**: 4816-4824.

Castillo, E. A., J. Ayte, C. Chiva, A. Moldon, M. Carrascal, J. Abian, N. Jones & E. Hidalgo, (2002) Diethylmaleate activates the transcription factor Pap1 by covalent modification of critical cysteine residues. *Molecular Microbiology* **45**: 243-254.

Cereghino, J. L. & J. M. Cregg, (2000) Heterologous protein expression in the methylotrophic yeast *Pichia pastoris*. *FEMS Microbiology Reviews*. **24**: 45-66.

Chen, R. E. & J. Thorner, (2007) Function and regulation in MAPK signaling pathways: lessons learned from the yeast *Saccharomyces cerevisiae*. *Biochimica et Biophysica Acta* **1773**: 1311-1340.

Choi, H., J. W. Chang & Y. K. Jung, (2011) Peroxiredoxin 6 interferes with TRAIL-induced death-inducing signaling complex formation by binding to death effector domain caspase. *Cell Death and Differentiation* **18**: 405-414.

Christensen, M. J., R. J. Bennett & J. Schmid, (2002) Growth of *Epichloë*/*Neotyphodium* and p-endophytes in leaves of *Lolium* and *Festuca* grasses. *Mycological Research* **106**: 93-106.

Chung, K. R. & C. L. Schardl, (1997) Sexual cycle and horizontal transmission of the grass symbiont, *Epichloë typhina*. *Mycological Research* **101**: 295-301.

Chung, S. H., S. M. Chung, J. Y. Lee, S. R. Kim, K. S. Park & J. H. Chung, (1999) The biological significance of non-enzymatic reaction of menadione with plasma thiols: enhancement of menadione-induced cytotoxicity to platelets by the presence of blood plasma. *FEBS letters* **449**: 235-240.

Clay, K. & C. Schardl, (2002) Evolutionary origins and ecological consequences of endophyte symbiosis with grasses. *American Naturalist* **160**: S99-S127.

Colot, H. V., G. Park, G. E. Turner, C. Ringelberg, C. M Crew, L. Litvinkova, R. L. Weiss, K. A. Borkovich & J. C. Dunlap, (2006) A high-throughput gene knockout procedure for *Neurospora* reveals functions for multiple transcription factors. *Proceedings of the National Academy of Sciences of the United States of America* **103**: 10352-10357.

D'Autreaux, B. & M. B. Toledano, (2007) ROS as signalling molecules: mechanisms that generate specificity in ROS homeostasis. *Nature Reviews Molecular Cell Biology* **8**: 813-824.

Dalle-Donne, I., D. Giustarini, R. Colombo, A. Milzani & R. Rossi, (2005) S-glutathionylation in human platelets by a thiol-disulfide exchange-independent mechanism. *Free Radical Biology and Medicine* **38**: 1501-1510.

Das, K. C. & C. K. Das, (2000) Thioredoxin, a singlet oxygen quencher and hydroxyl radical scavenger: Redox independent functions. *Biochemical and Biophysical Research Communications* **277**: 443-447.

Day, A. M., J. D. Brown, S. R. Taylor, J. D. Rand, B. A. Morgan & E. A. Veal, (2012) Inactivation of a peroxiredoxin by hydrogen peroxide is critical for thioredoxin-mediated repair of oxidized proteins and cell survival. *Molecular Cell* **45**: 398-408.

Degols, G., K. Shiozaki & P. Russell, (1996) Activation and regulation of the Spc1 stress-activated protein kinase in *Schizosaccharomyces pombe*. *Molecular Cell Biology* **16**: 2870-2877.

Delaunay, A., A. D. Isnard & M. B. Toledano, (2000) H_2O_2 sensing through oxidation of the Yap1 transcription factor. *EMBO Journal* **19**: 5157-5166.

Delaunay, A., D. Pflieger, M. B. Barrault, J. Vinh & M. B. Toledano, (2002) A thiol peroxidase is an H_2O_2 receptor and redox-transducer in gene activation. *Cell* **111**: 471-481.

del Rio, L. A., F. J. Corpas, L. M. Sandalio, J. M. Palma, M. Gómez & J. B. Barroso, (2002) Reactive oxygen species, antioxidant systems and nitric oxide in peroxisomes. *Journal of Experimental Botany* **53**: 1255-1272.

Deppmann, C. D., R. S. Alvania & E. J. Taparowsky, (2006) Cross-species annotation of basic leucine zipper factor interactions: Insight into the evolution of closed interaction networks. *Molecular Biology and Evolution* **23**: 1480-1492.

Doke, N., (1983) Involvement of superoxide anion generation in the hypersensitive response of potato tuber tissues to infection with an incompatible race of *Phytophthora infestans* and to the hyphal wall components. *Physiological Plant Pathology* **23**: 345-357.

Draculic, T., I. W. Dawes & C. M. Grant, (2000) A single glutaredoxin or thioredoxin gene is essential for viability in the yeast *Saccharomyces cerevisiae*. *Molecular Microbiology* **36**: 1167-1174.

Eaton, C. J., M. P. Cox, B. Ambrose, M. Becker, U. Hesse, C. L. Schardl & B. Scott, (2010) Disruption of signaling in a fungal-grass symbiosis leads to pathogenesis. *Plant Physiology* **153**: 1780-1794.

Eaton, C. J., I. Jourdain, S. J. Foster, J. S. Hyams & B. Scott, (2008) Functional analysis of a fungal endophyte stress-activated MAP kinase. *Current Genetics* **53**: 163-174.

Egan, M. J., Z. Y. Wang, M. A. Jones, N. Smirnoff & N. J. Talbot, (2007) Generation of reactive oxygen species by fungal NADPH oxidases is required for rice blast disease. *Proceedings of the National Academy of Sciences of the United States of America* **104**: 11772-11777.

Ekman, D. & A. Elofsson, (2010) Identifying and quantifying orphan protein sequences in fungi. *Journal of Molecular Biology* **396**: 396-405.

Ellenberger, T. E., C. J. Brandl, K. Struhl & S. C. Harrison, (1992) The GCN4 basic region leucine zipper binds DNA as a dimer of uninterrupted alpha helices: crystal structure of the protein-DNA complex. *Cell* **71**: 1223-1237.

Elsliger, M. A., R. M. Wachter, G. T. Hanson, K. Kallio & S. J. Remington, (1999) Structural and spectral response of green fluorescent protein variants to changes in pH. *Biochemistry* **38**: 5296-5301.

Farnoodian, M., S. A. Yazdanparast & M. F. Sadri, (2009) Effects of environmental factors and selected antifungal agents on arthroconidia production in common species of *Trichophyton* genus and *Epidermophyton floccosum*. *Journal of Biological Sciences* **9**: 561-566.

Fassler, J. S. & A. H. West, (2011) Fungal Skn7 stress responses and their relationship to virulence. *Eukaryotic Cell* **10**: 156-167.

Fernandes, L., C. Rodrigues-Pousada & K. Struhl, (1997) Yap, a novel family of eight bZIP proteins in *Saccharomyces cerevisiae* with distinct biological functions. *Molecular and Cellular Biology* **17**: 6982-6993.

Finkel, T., (2011) Signal transduction by reactive oxygen species. *Journal of Cell Biology* **194**: 7-15.

Flattery-O'Brien, J., L. P. Collinson & I. W. Dawes, (1993) *Saccharomyces cerevisiae* has an inducible response to menadione which differs from that to hydrogen peroxide. *Journal of General Microbiology* **139**: 501-507.

Folmer, V., N. Pedroso, A. C. Matias, S. C. Lopes, F. Antunes, L. Cyrne & H. S. Marinho, (2008) H_2O_2 induces rapid biophysical and permeability changes in the plasma membrane of *Saccharomyces cerevisiae*. *Biochimica Et Biophysica Acta* **1778**: 1141-1147.

Fomenko, D. E., A. Koc, N. Agisheva, M. Jacobsen, A. Kaya, M. Malinouski, J. C. Rutherford, K. L. Siu, D. Y. Jin, D. R. Winge & V. N. Gladyshev, (2011) Thiol peroxidases mediate specific genome-wide regulation of gene expression in response to hydrogen peroxide. *Proceedings of the National Academy of Sciences of the United States of America* **108**: 2729-2734.

Foreman, J., V. Demidchik, J. H. Bothwell, P. Mylona, H. Miedema, M. A. Torres, P. Linstead, S. Costa, C. Brownlee, J. D. Jones, J. M. Davies & L. Dolan, (2003) Reactive oxygen species produced by NADPH oxidase regulate plant cell growth. *Nature* **422**: 442-446.

Foyer, C. H. & G. Noctor, (2005) Redox homeostasis and antioxidant signaling: A metabolic interface between stress perception and physiological responses. *Plant Cell* **17**: 1866-1875.

Fujii, Y., T. Shimizu, T. Toda, M. Yanagida & T. Hakoshima, (2000) Structural basis for the diversity of DNA recognition by bZIP transcription factors. *Nature Structural Biology* **7**: 889-893.

Furukawa, K., Y. Hoshi, T. Maeda, T. Nakajima & K. Abe, (2005) *Aspergillus nidulans* HOG pathway is activated only by two-component signalling pathway in response to osmotic stress. *Molecular Microbiology* **56**: 1246-1261.

Gao, X., W. B. Shim, C. Gobel, S. Kunze, I. Feussner, R. Meeley, P. Balint-Kurti & M. Kolomiets, (2007) Disruption of a maize 9-lipoxygenase results in increased resistance to fungal pathogens and reduced levels of contamination with mycotoxin fumonisin. *Molecular Plant-Microbe Interactions* **20**: 922-933.

Gavet, O. & J. Pines, (2010) Progressive activation of CyclinB1-Cdk1 coordinates entry to mitosis. *Developmental Cell* **18**: 533-543.

Giesbert, S., T. Schurg, S. Scheele & P. Tudzynski, (2008) The NADPH oxidase Cpnox1 is required for full pathogenicity of the ergot fungus *Claviceps purpurea*. *Molecular Plant Pathology* **9**: 317-327.

Gietz, R. D. & R. A. Woods, (2002) Transformation of yeast by lithium acetate/single-stranded carrier DNA/polyethylene glycol method. *Methods in Enzymology* **350**: 87-96.

Gille, G. & K. Sigler, (1995) Oxidative stress and living cells. *Folia Microbiologica* **40**: 131-152.

Govrin, E. M. & A. Levine, (2000) The hypersensitive response facilitates plant infection by the necrotrophic pathogen *Botrytis cinerea*. *Current Biology* **10**: 751-757.

Greetham, D. & C. M. Grant, (2009) Antioxidant activity of the yeast mitochondrial one-Cys peroxiredoxin is dependent on thioredoxin reductase and glutathione in vivo. *Molecular Cell Biology* **29**: 3229-3240.

Gulshan, K., S. S. Lee & W. S. Moye-Rowley, (2011) Differential oxidant tolerance determined by the key transcription factor Yap1 is controlled by levels of the Yap1-binding protein, Ybp1. *The Journal of Biological Chemistry* **286**: 34071-34081.

Guo, M., Y. Chen, Y. Du, Y. H. Dong, W. Guo, S. Zhai, H. F. Zhang, S. M. Dong, Z. G. Zhang, Y. C. Wang, P. Wang & X. B. Zheng, (2011) The bZIP Transcription Factor MoAP1 Mediates the Oxidative Stress Response and Is Critical for Pathogenicity of the Rice Blast Fungus *Magnaporthe oryzae*. *Plos Pathogens* **7**.

Guo, M. Y., K. Satoh, B. Qi, T. Narita, O. Katsumata-Kato, M. Matsuki-Fukushima, J. Fujita-Yoshigaki & H. Sugiya, (2010) Thiol-oxidation reduces the release of amylase induced by beta-adrenergic receptor activation in rat parotid acinar cells. *Biomedical Research* **31**: 293-299.

Gutscher, M., M. C. Sobotta, G. H. Wabnitz, S. Ballikaya, A. J. Meyer, Y. Samstag & T. P. Dick, (2009) Proximity-based protein thiol oxidation by H_2O_2-scavenging peroxidases. *Journal of Biological Chemistry* **284**: 31532-31540.

Guzik, T. J., R. Korbut & T. Adamek-Guzik, (2003) Nitric oxide and superoxide in inflammation and immune regulation. *Journal of Physiology and Pharmacology* **54**: 469-487.

Gwinn, K. D., M. H. Collins-Shepard & B. B. Reddick, (1991) Tissue print-immunoblot, an accurate method for the detection of *Acremonium coenophialum* in tall fescue. *Phytopathology* **81**: 747-748.

Haghnazari, E. & W. D. Heyer, (2004) The Hog1 MAP kinase pathway and the Mec1 DNA damage checkpoint pathway independently control the cellular responses to hydrogen peroxide. *DNA Repair (Amst)* **3**: 769-776.

Hagiwara, D., Y. Asano, J. Marui, K. Furukawa, K. Kanamaru, M. Kato, K. Abe, T. Kobayashi, T. Yamashino & T. Mizuno, (2007) The SskA and SrrA response regulators are implicated in oxidative stress responses of hyphae and asexual spores in the phosphorelay signaling network of *Aspergillus nidulans*. *Bioscience Biotechnology and Biochemistry* **71**: 1003-1014.

Hagiwara, D., Y. Asano, T. Yamashino & T. Mizuno, (2008) Characterization of bZip-Type Transcription Factor AtfA with Reference to Stress Responses of Conidia of *Aspergillus nidulans*. *Bioscience Biotechnology and Biochemistry* **72**: 2756-2760.

Hahn, H., M. T. McManus, K. Warnstorff, B. J. Monahan, C. A. Young, E. Davies, B. A. Tapper & B. Scott, (2008) *Neotyphodium* fungal endophytes confer physiological protection to perennial ryegrass *Lolium perenne* subjected to a water deficit. *Environmental and Experimental Botany* **63**: 183-199.

Halliwell, B., (2006) Reactive species and antioxidants. Redox biology is a fundamental theme of aerobic life. *Plant Physiology* **141**: 312-322.

Halliwell, B. & J. M. Gutteridge, (1992) Biologically relevant metal ion-dependent hydroxyl radical generation. *FEBS Letters* **307**: 108-112.

Hawkins, B. J., M. Madesh, C. J. Kirkpatrick & A. B. Fisher, (2007) Superoxide flux in endothelial cells via the chloride channel-3 mediates intracellular signaling. *Molecular Biology of the Cell* **18**: 2002-2012.

He, X. J. & J. S. Fassler, (2005) Identification of novel Yap1p and Skn7p binding sites involved in the oxidative stress response of *Saccharomyces cerevisiae*. *Molecular Microbiology* **58**: 1454-1467.

He, X. J., K. E. Mulford & J. S. Fassler, (2009) Oxidative stress function of the *Saccharomyces cerevisiae* Skn7 Receiver Domain. *Eukaryotic Cell* **8**: 768-778.

Hidalgo, E. & B. Demple, (1994) An iron-sulfur center essential for transcriptional activation by the redox-sensing SoxR protein. *EMBO Journal* **13**: 138-146.

Hidalgo, E., H. Ding & B. Demple, (1997) Redox signal transduction via iron-sulfur clusters in the SoxR transcription activator. *Trends in Biochemical Sciences* **22**: 207-210.

Hoi, J. W. S., C. Lamarre, R. m. Beau, I. Meneau, A. Berepiki, A. Barre, E. Mellado, N. D. Read & J. P. Latgé, (2011) A novel family of dehydrin-like proteins is involved in stress response in the human fungal pathogen *Aspergillus fumigatus*. *Molecular Biology of the Cell* **22**: 1896-1906.

Huang, K., K. J. Czymmek, J. L. Caplan, J. A. Sweigard & N. M. Donofrio, (2011) HYR1-mediated detoxification of reactive oxygen species is required for full virulence in the rice blast fungus. *PLoS Pathogens* **7**: e1001335.

Huh, W. K., J. V. Falvo, L. C. Gerke, A. S. Carroll, R. W. Howson, J. S. Weissman & E. K. O'Shea, (2003) Global analysis of protein localization in budding yeast. *Nature* **425**: 686-691.

Ikner, A. & K. Shiozaki, (2005) Yeast signaling pathways in the oxidative stress response. *Mutation Research-Fundamental and Molecular Mechanisms of Mutagenesis* **569**: 13-27.

Inoue, Y., T. Matsuda, K. Sugiyama, S. Izawa & A. Kimura, (1999) Genetic analysis of glutathione peroxidase in oxidative stress response of *Saccharomyces cerevisiae*. *Journal of Biological Chemistry* **274**: 27002-27009.

Isoyama, T., A. Murayama, A. Nomoto & S. Kuge, (2001) Nuclear import of the yeast AP-1-like transcription factor Yap1p is mediated by transport receptor Pse1p, and this import step is not affected by oxidative stress. *Journal of Biological Chemistry* **276**: 21863-21869.

Itoh, Y., R. Johnson & B. Scott, (1994) Integrative transformation of the mycotoxin-producing fungus, *Penicillium paxilli*. *Current Genetics* **25**: 508-513.

James, T. Y., F. Kauff, C. L. Schoch, P. B. Matheny, V. Hofstetter, C. J. Cox, G. Celio, C. Gueidan, E. Fraker, J. Miadlikowska, H. T. Lumbsch, A. Rauhut, V. Reeb, A. E. Arnold, A. Amtoft, J. E. Stajich, K. Hosaka, G. H. Sung, D. Johnson, B. O'Rourke, M. Crockett, M. Binder, J. M. Curtis, J. C. Slot, Z. Wang, A. W. Wilson, A. Schussler, J. E. Longcore, K. O'Donnell, S. Mozley-Standridge, D. Porter, P. M. Letcher, M. J. Powell, J. W. Taylor, M. M. White, G. W. Griffith, D. R. Davies, R. A. Humber, J. B. Morton, J. Sugiyama, A. Y. Rossman, J. D. Rogers, D. H. Pfister, D. Hewitt, K. Hansen, S. Hambleton, R. A. Shoemaker, J. Kohlmeyer, B. Volkmann-Kohlmeyer, R. A. Spotts, M. Serdani, P. W. Crous, K. W. Hughes, K. Matsuura, E. Langer, G. Langer, W. A. Untereiner, R. Lucking, B. Budel, D. M. Geiser, A. Aptroot, P. Diederich, I. Schmitt, M. Schultz, R. Yahr, D. S. Hibbett, F. Lutzoni, D. J. McLaughlin, J. W. Spatafora & R. Vilgalys, (2006) Reconstructing the early evolution of Fungi using a six-gene phylogeny. *Nature* **443**: 818-822.

Jara, M., A. P. Vivancos, I. A. Calvo, A. Moldon, M. Sanso & E. Hidalgo, (2007) The peroxiredoxin Tpx1 is essential as a H_2O_2 scavenger during aerobic growth in fission yeast. *Molecular Biology of the Cell* **18**: 2288-2295.

Jarvis, R. M., S. M. Hughes & E. C. Ledgerwood, (2012) Peroxiredoxin 1 functions as a signal peroxidase to receive, transduce, and transmit peroxide signals in mammalian cells. *Free Radical Biology and Medicine* **53**: 1522-1530.

Kawasaki, L., O. Sanchez, K. Shiozaki & J. Aguirre, (2002) SakA MAP kinase is involved in stress signal transduction, sexual development and spore viability in *Aspergillus nidulans*. *Molecular Microbiology* **45**: 1153-1163.

Kellis, M., B. W. Birren & E. S. Lander, (2004) Proof and evolutionary analysis of ancient genome duplication in the yeast *Saccharomyces cerevisiae*. *Nature* **425**: 617-624.

Kim, J. S., M. A. Bang, S. Lee, H. Z. Chae & K. Kim, (2010) Distinct functional roles of peroxiredoxin isozymes and glutathione peroxidase from fission yeast, *Schizosaccharomyces pombe*. *Biochemistry and Molecular Biology Reports* **43**: 170-175.

Kim, W. H., J. H. Chung, J. H. Back, J. Y. Choi, J. H. Cha, H. Y. Koh & Y. S. Han, (2003) Molecular cloning and characterization of an NADPH quinone oxidoreductase from *Kluyveromyces marxianus*. *Journal of Biochemistry and Molecular Biology* **36**: 442-449.

Kosower, N. S. & E. M. Kosower, (1995) Diamide: an oxidant probe for thiols. *Methods in Enzymology* **251**: 123-133.

Krems, B., C. Charizanis & K. D. Entian, (1996) The response regulator-like protein Pos9/Skn7 of *Saccharomyces cerevisiae* is involved in oxidative stress resistance. *Current Genetics* **29**: 327-334.

Kuge, S., M. Arita, A. Murayama, K. Maeta, S. Izawa, Y. Inoue & A. Nomoto, (2001) Regulation of the yeast Yap1p nuclear export signal is mediated by redox signal-induced reversible disulfide bond formation. *Molecular Cell Biology* **21**: 6139-6150.

Kuge, S. & N. Jones, (1994) YAP1 dependent activation of TRX2 is essential for the response of *Saccharomyces cerevisiae* to oxidative stress by hydroperoxides. *Embo Journal* **13**: 655-664.

Kuge, S., N. Jones & A. Nomoto, (1997) Regulation of yAP-1 nuclear localization in response to oxidative stress. *Embo Journal* **16**: 1710-1720.

Kuge, S., T. Toda, N. Iizuka & A. Nomoto, (1998) Crm1 (Xpol) dependent nuclear export of the budding yeast transcription factor yAP-1 is sensitive to oxidative stress. *Genes to Cells* **3**: 521-532.

Kuldau, G. A., J. S. Liu, J. F. White, M. R. Siegel & C. L. Schardl, (1997) Molecular systematics of *Clavicipitaceae* supporting monophyly of genus *Epichloë* and form genus *Ephelis*. *Mycologia* **89**: 431-441.

Lam, Y. T., R. Stocker & I. W. Dawes, (2010) The lipophilic antioxidants alpha-tocopherol and coenzyme Q10 reduce the replicative lifespan of Saccharomyces cerevisiae. *Free Radical Biology and Medicine* **49**: 237-244.

Lamarre, C., O. Ibrahim-Granet, C. Du, R. Calderone & J. P. Latge, (2007) Characterization of the SKN7 ortholog of *Aspergillus fumigatus*. *Fungal Genetics and Biology* **44**: 682-690.

Lamb, C. & R. A. Dixon, (1997) The oxidative burst in plant disease resistance. *Annual Review of Plant Physiology and Plant Molecular Biology* **48**: 251-275.

Lara-Ortiz, T., H. Riveros-Rosas & J. Aguirre, (2003) Reactive oxygen species generated by microbial NADPH oxidase NoxA regulate sexual development in *Aspergillus nidulans*. *Molecular Microbiology* **50**: 1241-1255.

Lara-Rojas, F., O. Sanchez, L. Kawasaki & J. Aguirre, (2011) *Aspergillus nidulans* transcription factor AtfA interacts with the MAPK SakA to regulate general stress responses, development and spore functions. *Molecular Microbiology* **80**: 436-454.

Latch, G. C. M. & M. J. Christensen, (1985) Artificial infection of grasses with endophytes. *Annals of Applied Biology* **107**: 17–24.

Lawrence, C. L., C. H. Botting, R. Antrobus & P. J. Coote, (2004) Evidence of a new role for the high-osmolarity glycerol mitogen-activated protein kinase pathway in yeast: Regulating adaptation to citric acid stress. *Molecular and Cellular Biology* **24**: 3307-3323.

Le Deunff, E., C. Davoine, C. Le Dantec, J. P. Billard & C. Huault, (2004) Oxidative burst and expression of germin/oxo genes during wounding of ryegrass leaf blades: comparison with senescence of leaf sheaths. *Plant Journal* **38**: 421-431.

Lee, J., C. Godon, G. Lagniel, D. Spector, J. Garin, J. Labarre & M. B. Toledano, (1999) Yap1 and Skn7 control two specialized oxidative stress response regulons in yeast. *Journal of Biological Chemistry* **274**: 16040-16046.

Lee, S. P., Y. S. Hwang, Y. J. Kim, K. S. Kwon, H. J. Kim, K. Kim & H. Z. Chae, (2001) Cyclophilin a binds to peroxiredoxins and activates its peroxidase activity. *Journal of Biological Chemistry* **276**: 29826-29832.

Leiderman, P., D. Huppert & N. Agmon, (2006) Transition in the temperature-dependence of GFP fluorescence: from proton wires to proton exit. *Biophysical Journal* **90**: 1009-1018.

Lessing, F., O. Kniemeyer, I. Wozniok, J. Loeffler, O. Kurzai, A. Haertl & A. A. Brakhage, (2007) The *Aspergillus fumigatus* transcriptional regulator AfYap1 represents the major regulator for defense against reactive oxygen intermediates but is dispensable for pathogenicity in an intranasal mouse infection model. *Eukaryotic Cell* **6**: 2290-2302.

Leuchtmann, A., C. L. Schardl & M. R. Siegel, (1994) Sexual compatibility and taxonomy of a new species of *Epichloë* symbiotic with fine fescue grasses. *Mycologia* **86**: 802-812.

Lev, S., R. Hadar, P. Amedeo, S. E. Baker, O. C. Yoder & B. A. Horwitz, (2005) Activation of an AP1-like transcription factor of the maize pathogen *Cochliobolus heterostrophus* in response to oxidative stress and plant signals. *Eukaryotic Cell* **4**: 443-454.

Levine, A., R. Tenhaken, R. Dixon & C. Lamb, (1994) H_2O_2 from the oxidative burst orchestrates the plant hypersensitive disease resistance response. *Cell* **79**: 583-593.

Lin, C. H., S. L. Yang & K. R. Chung, (2009) The YAP1 homolog-mediated oxidative stress tolerance is crucial for pathogenicity of the necrotrophic fungus *Alternaria alternata* in citrus. *Molecular Plant-Microbe Interactions* **22**: 942-952.

Lledias, F., P. Rangel & W. Hansberg, (1999) Singlet oxygen is part of a hyperoxidant state generated during spore germination. *Free Radical Biology and Medicine* **26**: 1396-1404.

Luikenhuis, S., G. Perrone, I. W. Dawes & C. M. Grant, (1998) The yeast *Saccharomyces cerevisiae* contains two glutaredoxin genes that are required for protection against reactive oxygen species. *Molecular Biology of the Cell* **9**: 1081-1091.

Ma, L. H., C. L. Takanishi & M. J. Wood, (2007) Molecular mechanism of oxidative stress perception by the Orp1 protein. *Journal of Biological Chemistry* **282**: 31429-31436.

Maeta, K., S. Izawa, S. Okazaki, S. Kuge & Y. Inoue, (2004) Activity of the Yap1 transcription factor in *Saccharomyces cerevisiae* is modulated by methylglyoxal, a metabolite derived from glycolysis. *Molecular Cell Biology* **24**: 8753-8764.

Martinez-Pastor, M. T., G. Marchler, C. Schuller, A. Marchler-Bauer, H. Ruis & F. Estruch, (1996) The *Saccharomyces cerevisiae* zinc finger proteins Msn2p and Msn4p are required for transcriptional induction through the stress response element (STRE). *The EMBO Journal* **15**: 2227-2235.

Mattern, I. E., P. J. Punt & C. van den Hondel, (1988) A vector of *Aspergillus* transformation conferring phleomycin resistance. *Fungal Genetics Newsletter* **35**.

May, K. J., M. K. Bryant, X. Zhang, B. Ambrose & B. Scott, (2008) Patterns of expression of a lolitrem biosynthetic gene in the *Epichloë festucae*-perennial ryegrass symbiosis. *Molecular Plant-Microbe Interactions* **21**: 188-197.

Michalakis, Y., I. Olivieri, F. Renaud & M. Raymond, (1992) Pleiotropic action of parasites: How to be good for the host. *Trends in Ecology and Evolution* **7**: 59-62.

Miller, E. W., B. C. Dickinson & C. J. Chang, (2010) Aquaporin-3 mediates hydrogen peroxide uptake to regulate downstream intracellular signaling. *Proceedings of the National Academy of Sciences of the United States of America* **107**: 15681-15686.

Molina, L. & R. Kahmann, (2007) An *Ustilago maydis* gene involved in H_2O_2 detoxification is required for virulence. *Plant Cell* **19**: 2293-2309.

Moon, C. D., K. D. Craven, A. Leuchtmann, S. L. Clement & C. L. Schardl, (2004) Prevalence of interspecific hybrids amongst asexual fungal endophytes of grasses. *Molecular Ecology* **13**: 1455-1467.

Moon, C. D., B. A. Tapper & B. Scott, (1999) Identification of *Epichloë* endophytes in planta by a microsatellite-based PCR fingerprinting assay with automated analysis. *Applied and Environmental Microbiology* **65**: 1268-1279.

Morel, M., A. Kohler, F. Martin, E. Gelhaye & N. Rouhier, (2008) Comparison of the thiol-dependent antioxidant systems in the ectomycorrhizal *Laccaria bicolor* and the saprotrophic *Phanerochaete chrysosporium*. *New Phytologist* **180**: 391-407.

Morgan, B. A., G. R. Banks, W. M. Toone, D. Raitt, S. Kuge & L. H. Johnston, (1997) The Skn7 response regulator controls gene expression in the oxidative stress response of the budding yeast *Saccharomyces cerevisiae*. *Embo Journal* **16**: 1035-1044.

Motoyama, T., N. Ochiai, M. Morita, Y. Iida, R. Usami & T. Kudo, (2008) Involvement of putative response regulator genes of the rice blast fungus *Magnaporthe oryzae* in osmotic stress response, fungicide action, and pathogenicity. *Current Genetics* **54**: 185-195.

Moy, M., F. Belanger, R. Duncan, A. Freehoff, C. Leary, W. Meyer, R. Sullivan & T. White, (2000) Identification of epiphyllous mycelial nets on leaves of grasses infected by clavicipitaceous endophytes. *Symbiosis* **28**: 291-302.

Mulford, K. E. & J. S. Fassler, (2011) Association of the Skn7 and Yap1 Transcription Factors in the *Saccharomyces cerevisiae* Oxidative Stress Response. *Eukaryotic Cell* **10**: 761-769.

Mutoh, N., M. Kawabata & S. Kitajima, (2005) Effects of four oxidants, menadione, 1-chloro-2,4-dinitrobenzene, hydrogen peroxide and cumene hydroperoxide, on fission yeast *Schizosaccharmoyces pombe*. *Journal of Biochemistry* **138**: 797-804.

Namiki, F., M. Matsunaga, M. Okuda, I. Inoue, K. Nishi, Y. Fujita & T. Tsuge, (2001) Mutation of an arginine biosynthesis gene causes reduced pathogenicity in

Fusarium oxysporum f. sp. *melonis*. *Molecular Plant-Microbe Interactions* **14**: 580-584.

Navarro, R. E., M. A. Stringer, W. Hansberg, W. E. Timberlake & J. Aguirre, (1996) *catA*, a new *Aspergillus nidulans* gene encoding a developmentally regulated catalase. *Current Genetics* **29**: 352-359.

Nguyen, A. N., A. Lee, W. Place & K. Shiozaki, (2000) Multistep phosphorelay proteins transmit oxidative stress signals to the fission yeast stress-activated protein kinase. *Molecular Biology of the Cell* **11**: 1169-1181.

Noguera-Mazon, V., I. Krimm, O. Walker & J. M. Lancelin, (2006) Protein-protein interactions within peroxiredoxin systems. *Photosynthesis Research* **89**: 277-290.

Ogusucu, R., D. Rettori, D. C. Munhoz, L. E. Netto & O. Augusto, (2007) Reactions of yeast thioredoxin peroxidases I and II with hydrogen peroxide and peroxynitrite: rate constants by competitive kinetics. *Free Radical Biology and Medicine* **42**: 326-334.

Ohdate, T. & Y. Inoue, (2012) Involvement of glutathione peroxidase 1 in growth and peroxisome formation in *Saccharomyces cerevisiae* in oleic acid medium. *Biochimica et Biophysica Acta* **1821**: 1295-1305.

Ohdate, T., S. Izawa, K. Kita & Y. Inoue, (2010) Regulatory mechanism for expression of GPX1 in response to glucose starvation and Ca in *Saccharomyces cerevisiae*: involvement of Snf1 and Ras/cAMP pathway in Ca signaling. *Genes to Cells* **15**: 59-75.

Ohmiya, R., H. Yamada, C. Kato, H. Aiba & T. Mizuno, (2000) The Prr1 response regulator is essential for transcription of ste11(+) and for sexual development in fission yeast. *Molecular and General Genetics* **264**: 441-451.

Oide, S., J. Y. Liu, S. H. Yun, D. L. Wu, A. Michev, M. Y. Choi, B. A. Horwitz & B. G. Turgeon, (2010) Histidine kinase two-component response regulator proteins regulate reproductive development, virulence, and stress responses of the fungal cereal pathogens *Cochliobolus heterostrophus* and *Gibberella zeae*. *Eukaryotic Cell* **9**: 1867-1880.

Okazaki, S., A. Naganuma & S. Kuge, (2005) Peroxiredoxin-mediated redox regulation of the nuclear localization of Yap1, a transcription factor in budding yeast. *Antioxidants and Redox Signaling* **7**: 327-334.

Okazaki, S., T. Tachibana, A. Naganuma, N. Mano & S. Kuge, (2007) Multistep disulfide bond formation in Yap1 is required for sensing and transduction of H_2O_2 stress signal. *Molecular Cell* **27**: 675-688.

Orozco-Cardenas, M. & C. A. Ryan, (1999) Hydrogen peroxide is generated systemically in plant leaves by wounding and systemin via the octadecanoid pathway. *Proceedings of the National Academy of Sciences of the United States of America* **96**: 6553-6557.

Ouyang, X., Q. T. Tran, S. Goodwin, R. S. Wible, C. H. Sutter & T. R. Sutter, (2011) Yap1 activation by H_2O_2 or thiol-reactive chemicals elicits distinct adaptive gene responses. *Free Radical Biology and Medicine* **50**: 1-13.

Panadero, J., C. Pallotti, S. Rodriguez-Vargas, F. Randez-Gil & J. A. Prieto, (2006) A downshift in temperature activates the high osmolarity glycerol (HOG) pathway, which determines freeze tolerance in *Saccharomyces cerevisiae*. *Journal of Biological Chemistry* **281**: 4638-4645.

Pasquali, M., F. Giraud, J. P. Lasserre, S. Planchon, L. Hoffmann, T. Bohn & J. Renaut, (2010) Toxin induction and protein extraction from *Fusarium* spp. cultures for proteomic studies. *Journal of Visualized Experiments* **36:** 1690.

Peshenko, I. V. & H. Shichi, (2001) Oxidation of active center cysteine of bovine 1-Cys peroxiredoxin to the cysteine sulfenic acid form by peroxide and peroxynitrite. *Free Radical Biology and Medicine* **31**: 292-303.

Pocsi, I., M. Miskei, Z. Karanyi, T. Emri, P. Ayoubi, T. Pusztahelyi, G. Balla & R. A. Prade, (2005) Comparison of gene expression signatures of diamide, H_2O_2 and menadione exposed *Aspergillus nidulans* cultures - linking genome-wide transcriptional changes to cellular physiology. *BMC Genomics* **6**: 182.

Powis, G. & W. R. Montfort, (2001) Properties and biological activities of thioredoxins. *Annual Review of Pharmacology and Toxicology* **41**: 261-295.

Qiao, J. J., D. P. Kontoyiannis, R. Calderone, D. M. Li, Y. Ma, Z. Wan, R. Y. Li & W. Liu, (2008) Afyap1, encoding a bZip transcriptional factor of *Aspergillus fumigatus*, contributes to oxidative stress response but is not essential to the virulence of this pathogen in mice immunosuppressed by cyclophosphamide and triamcinolone. *Medical Mycology* **46**: 773-782.

Quinn, J., V. J. Findlay, K. Dawson, J. B. A. Millar, N. Jones, B. A. Morgan & W. M. Toone, (2002) Distinct regulatory proteins control the graded transcriptional response to increasing H_2O_2 levels in fission yeast *Schizosaccharomyces pombe*. *Molecular Biology of the Cell* **13**: 805-816.

Quinn, J., P. Malakasi, D. A. Smith, J. Cheetham, V. Buck, J. B. A. Millar & B. A. Morgan, (2011) Two-component mediated peroxide sensing and signal transduction in fission yeast. *Antioxidants & Redox Signaling* **15**: 153-165.

Reverberi, M., K. Gazzetti, F. Punelli, M. Scarpari, S. Zjalic, A. Ricelli, A. A. Fabbri & C. Fanelli, (2012) Aoyap1 regulates OTA synthesis by controlling cell redox balance in *Aspergillus ochraceus*. *Applied Microbiology and Biotechnology* **95**: 1293-1304.

Rhee, S. G., S. W. Kang, T. S. Chang, W. Jeong & K. Kim, (2001) Peroxiredoxin, a novel family of peroxidases. *IUBMB life* **52**: 35-41.

Rhee, S. G., K. H. Kim, H. Z. Chae, M. B. Yim, K. Uchida, L. E. Netto & E. R. Stadtman, (1994) Antioxidant defense mechanisms: a new thiol-specific antioxidant enzyme. *Annals of the New York Academy of Science* **738**: 86-92.

Rhee, S. G., H. A. Woo, I. S. Kil & S. H. Bae, (2012) Peroxiredoxin functions as a peroxidase and a regulator and sensor of local peroxides. *Journal of Biological Chemistry* **287**: 4403-4410.

Rouhier, N., E. Gelhaye & J. P. Jacquot, (2002) Glutaredoxin-dependent peroxiredoxin from poplar: protein-protein interaction and catalytic mechanism. *Journal of Biological Chemistry* **277**: 13609-13614.

Rouhier, N., A. Villarejo, M. Srivastava, E. Gelhaye, O. Keech, M. Droux, I. Finkemeier, G. Samuelsson, K. J. Dietz, J. P. Jacquot & G. Wingsle, (2005) Identification of plant glutaredoxin targets. *Antioxidants and Redox Signaling* **7**: 919-929.

Rowan, D., J. Dymock & M. Brimble, (1990) Effect of fungal metabolite peramine and analogs on feeding and development of argentine stem weevil (*Listronotus bonariensis*). *Journal of Chemical Ecology* **16**: 1683-1695.

Saikkonen, K., S. H. Faeth, M. Helander & T. J. Sullivan, (1998) Fungal endophytes: a continuum of interactions with host plants. *Annual Review of Ecology and Systematics* **29**: 319-343.

Schardl, C., R. Balestrini, S. Florea, D. Zhang & B. Scott, (2009) *Epichloë* endophytes: clavicipitaceous symbionts of grasses. In: Plant Relationships. H. Deising (ed). Springer Berlin Heidelberg, 275-306.

Schardl, C. L., (2010) The Epichloae, symbionts of the grass subfamily Poöideae. *Annals of the Missouri Botanical Garden* **97**: 646-665.

Schardl, C. L., R. B. Grossman, P. Nagabhyru, J. R. Faulkner & U. P. Mallik, (2007) Loline alkaloids: Currencies of mutualism. *Phytochemistry* **68**: 980-996.

Schardl, C. L., A. Leuchtmann & M. J. Spiering, (2004) Symbioses of grasses with seedborne fungal endophytes. *Annual Reviews of Plant Biology* **55**: 315-340.

Schardl, C. L., A. Leuchtmann, H. F. Tsai, M. A. Collett, D. M. Watt & D. B. Scott, (1994) Origin of a fungal symbiont of perennial ryegrass by interspecific hybridization of a mutualist with the ryegrass choke pathogen, *Epichloë typhina*. *Genetics* **136**: 1307-1317.

Schardl, C. L. & B. Scott, (2010) Recommendations for gene nomenclature for *Epichloë* species and related *Clavicipitaceae*. In: 7th International Symposium on Fungal Endophyte of Grasses. C. Young, G. Aiken, R. McCulley, J. Strickland & C. L. Schardl (eds). Lexington, Kentucky: The Samuel Roberts Noble Foundation, Ardmore, Oklahoma, 84-87.

Schnell, N., B. Krems & K. D. Entian, (1992) The Par1 (Yap1/Snq3) gene of *Saccharomyces cerevisiae*, a C-Jun homolog, is involved in oxygen-metabolism. *Current Genetics* **21**: 269-273.

Schrettl, M., N. Beckmann, J. Varga, T. Heinekamp, I. D. Jacobsen, C. Jochl, T. A. Moussa, S. Wang, F. Gsaller, M. Blatzer, E. R. Werner, W. C. Niermann, A. A. Brakhage & H. Haas, (2010) HapX-mediated adaption to iron starvation is crucial for virulence of *Aspergillus fumigatus*. *PLoS Pathogens* **6**: e1001124.

Scott, B. & C. J. Eaton, (2008) Role of reactive oxygen species in fungal cellular differentiations. *Current Opinion in Microbiology* **11**: 488-493.

Scott, B. & C. Schardl, (1993) Fungal symbionts of grasses: evolutionary insights and agricultural potential. *Trends in Microbiology* **1**: 196-200.

Segmuller, N., L. Kokkelink, S. Giesbert, D. Odinius, J. van Kan & P. Tudzynski, (2008) NADPH oxidases are involved in differentiation and pathogenicity in *Botrytis cinerea*. *Molecular Plant-Microbe Interactions* **21**: 808-819.

Semighini, C. P. & S. D. Harris, (2008) Regulation of apical dominance in *Aspergillus nidulans* hyphae by reactive oxygen species. *Genetics* **179**: 1919-1932.

Sharma, R., Y. Yang, A. Sharma, S. Awasthi & Y. C. Awasthi, (2004) Antioxidant role of glutathione S-transferases: Protection against oxidant toxicity and regulation of stress-mediated apoptosis. *Antioxidants and Redox Signaling* **6**: 289-300.

Singh, K. K., (2000) The *Saccharomyces cerevisiae* Sln1p-Ssk1p two-component system mediates response to oxidative stress and in an oxidant-specific fashion. *Free Radical Biology and Medicine* **29**: 1043-1050.

Singh, P., N. Chauhan, A. Ghosh, F. Dixon & R. Calderone, (2004) SKN7 of *Candida albicans*: Mutant construction and phenotype analysis. *Infection and Immunity* **72**: 2390-2394.

Sivaraman, T., T. K. S. Kumar, G. Jayaraman & C. Yu, (1997) The mechanism of 2,2,2-trichloroacetic acid-induced protein precipitation. *Journal of Protein Chemistry* **16**: 291-297.

Spiers, A. G. & D. H. Hopcroft, (1993) Black canker and leaf spot of Salix in New Zealand caused by *Glomerella miyabeana* (*Colletotrichum gloeosporioides*). *European Journal of Forest Pathology* **23**: 92-102.

Stevens, D. A., (1995) Coccidioidomycosis. *New England Journal of Medicine* **332**: 1077-1082.

Sumimoto, H., (2008) Structure, regulation and evolution of Nox-family NADPH oxidases that produce reactive oxygen species. *FEBS Journal* **275**: 3249-3277.

Sung, G. H., N. L. Hywel-Jones, J. M. Sung, J. J. Luangsa-Ard, B. Shrestha & J. W. Spatafora, (2007) Phylogenetic classification of Cordyceps and the clavicipitaceous fungi. *Studies in Mycology* **57:** 5-59.

Tachibana, T., S. Okazaki, A. Murayama, A. Naganuma, A. Nomoto & S. Kuge, (2009) A major peroxiredoxin-induced activation of Yap1 transcription factor Is mediated by reduction-sensitive disulfide bonds and reveals a low level of transcriptional activation. *Journal of Biological Chemistry* **284**: 4464-4472.

Takahashi, M., K. Yamashita, A. Shiozawa, A. Ichiishi, F. Fukumori & M. Fujimura, (2010) An AP-1-like transcription factor, NAP-1, regulates expression of the glutathione S-transferase and NADH:Flavin oxidoreductase genes in *Neurospora crassa*. *Bioscience Biotechnology and Biochemistry* **74**: 746-752.

Tanaka, A., M. J. Christensen, D. Takemoto, P. Park & B. Scott, (2006) Reactive oxygen species play a role in regulating a fungus-perennial ryegrass mutualistic interaction. *Plant Cell* **18**: 1052-1066.

Tanaka, A., B. A. Tapper, A. Popay, E. J. Parker & B. Scott, (2005a) A symbiosis expressed non-ribosomal peptide synthetase from a mutualistic fungal endophyte of perennial ryegrass confers protection to the symbiotum from insect herbivory. *Molecular Microbiology* **57**: 1036-1050.

Tanaka, T., S. Izawa & Y. Inoue, (2005b) GPX2, encoding a phospholipid hydroperoxide glutathione peroxidase homologue, codes for an atypical 2-Cys peroxiredoxin in *Saccharomyces cerevisiae*. *Journal of Biological Chemistry* **280**: 42078-42087.

Temme, N. & P. Tudzynski, (2009) Does *Botrytis cinerea* ignore H_2O_2-induced oxidative stress during infection? Characterization of *Botrytis* Activator Protein 1. *Molecular Plant-Microbe Interactions* **22**: 987-998.

Thorpe, G. W., C. S. Fong, N. Alic, V. J. Higgins & I. W. Dawes, (2004) Cells have distinct mechanisms to maintain protection against different reactive oxygen species: oxidative-stress-response genes. *Proceedings of the National Academy of Sciences of the United States of America* **101**: 6564-6569.

Thorsen, M., Y. Di, C. Tangemo, M. Morillas, D. Ahmadpour, C. Van der Does, A. Wagner, E. Johansson, J. Boman, F. Posas, R. Wysocki & M. J. Tamas, (2006) The MAPK Hog1p modulates Fps1p-dependent arsenite uptake and tolerance in yeast. *Molecular Biology of the Cell* **17**: 4400-4410.

Tian, C. G., J. Y. Li & N. L. Glass, (2011) Exploring the bZIP transcription factor regulatory network in *Neurospora crassa*. *Microbiology* **157**: 747-759.

Timmermann, B., S. Jarolim, H. Russmayer, M. Kerick, S. Michel, A. Kruger, K. Bluemlein, P. Laun, J. Grillari, H. Lehrach, M. Breitenbach & M. Ralser, (2010) A new dominant peroxiredoxin allele identified by whole-genome re-sequencing of random mutagenized yeast causes oxidant-resistance and premature aging. *Aging* **2**: 475-486.

Toews, M. W., J. Warmbold, S. Konzack, P. Rischitor, D. Veith, K. Vienken, C. Vinuesa, H. Wei & R. Fischer, (2004) Establishment of mRFP1 as a fluorescent marker in *Aspergillus nidulans* and construction of expression vectors for high-throughput protein tagging using recombination in vitro (GATEWAY). *Current Genetics* **45**: 383-389.

Toone, W. M., S. Kuge, M. Samuels, B. A. Morgan, T. Toda & N. Jones, (1998) Regulation of the fission yeast transcription factor Pap1 by oxidative stress: requirement for the nuclear export factor Crm1 (Exportin) and the stress-activated MAP kinase Styl/Spc1. *Genes and Development* **12**: 2650-2650.

Torres, M. A., J. D. Jones & J. L. Dangl, (2006) Reactive oxygen species signaling in response to pathogens. *Plant Physiology* **141**: 373-378.

Ukai, Y., T. Kishimoto, T. Ohdate, S. Izawa & Y. Inoue, (2011) Glutathione peroxidase 2 in *Saccharomyces cerevisiae* is distributed in mitochondria and involved in sporulation. *Biochemical and Biophysical Research Communications* **411**: 580-585.

Vanden Wymelenberg, A.J., D. Cullen, R.N. Spear, B. Schoenike & J. H. Andrews, (1997) Expression of green fluorescent protein in Aureobasidium pullulans and quantification of the fungus on leaf surfaces. *Biotechniques* **23**: 686-690.

Veal, E. A., V. J. Findlay, A. M. Day, S. M. Bozonet, J. M. Evans, J. Quinn & B. A. Morgan, (2004) A 2-Cys peroxiredoxin regulates peroxide-induced oxidation and activation of a stress-activated MAP kinase. *Molecular Cell* **15**: 129-139.

Veal, E. A., S. J. Ross, P. Malakasi, E. Peacock & B. A. Morgan, (2003) Ybp1 is required for the hydrogen peroxide-induced oxidation of the Yap1 transcription factor. *Journal of Biological Chemistry* **278**: 30896-30904.

Vivancos, A. P., E. A. Castillo, B. Biteau, C. Nicot, J. Ayte, M. B. Toledano & E. Hidalgo, (2005) A cysteine-sulfinic acid in peroxiredoxin regulates H_2O_2-sensing by the antioxidant Pap1 pathway. *Proceedings of the National Academy of Sciences of the United States of America* **102**: 8875-8880.

Vivancos, A. P., E. A. Castillo, N. Jones, J. Ayte & E. Hidalgo, (2004) Activation of the redox sensor Pap1 by hydrogen peroxide requires modulation of the intracellular oxidant concentration. *Molecular Microbiology* **52**: 1427-1435.

Walther, A. & J. Wendland, (2012) Yap1-dependent oxidative stress response provides a link to riboflavin production in *Ashbya gossypii*. *Fungal Genetics and Biology* **49**: 697-707.

Welinder, K. G., J. M. Mauro & L. Norskov-Lauritsen, (1992) Structure of plant and fungal peroxidases. *Biochemical Society Transactions* **20**: 337-340.

Whitmarsh, A. J. & R. J. Davis, (1996) Transcription factor AP-1 regulation by mitogen-activated protein kinase signal transduction pathways. *Journal of Molecular Medicine* **74**: 589-607.

Wilkinson, H. H., M. R. Siegel, J. D. Blankenship, A. C. Mallory, L. P. Bush & C. L. Schardl, (2000) Contribution of fungal loline alkaloids to protection from aphids

in a grass-endophyte mutualism. *Molecular Plant-Microbe Interactions* **13**: 1027-1033.

Wilkinson, M. G., M. Samuels, T. Takeda, W. M. Toone, J. C. Shieh, T. Toda, J. B. Millar & N. Jones, (1996) The Atf1 transcription factor is a target for the Sty1 stress-activated MAP kinase pathway in fission yeast. *Genes and Development* **10**: 2289-2301.

Winterbourn, C. C. & M. B. Hampton, (2008) Thiol chemistry and specificity in redox signaling. *Free Radical Biology and Medicine* **45**: 549-561.

Wolfe, K. H. & D. C. Shields, (1997) Molecular evidence for an ancient duplication of the entire yeast genome. *Nature* **387**: 708-713.

Woo, H. A., W. Jeong, T. S. Chang, K. J. Park, S. J. Park, J. S. Yang & S. G. Rhee, (2005) Reduction of cysteine sulfinic acid by sulfiredoxin is specific to 2-cys peroxiredoxins. *Journal of Biological Chemistry* **280**: 3125-3128.

Wood, M. J., E. C. Andrade & G. Storz, (2003a) The redox domain of the Yap1p transcription factor contains two disulfide bonds. *Biochemistry* **42**: 11982-11991.

Wood, M. J., G. Storz & N. Tjandra, (2004) Structural basis for redox regulation of Yap1 transcription factor localization. *Nature* **430**: 917-921.

Wood, Z. A., L. B. Poole & P. A. Karplus, (2003b) Peroxiredoxin evolution and the regulation of hydrogen peroxide signaling. *Science* **300**: 650-653.

Xanthoudakis, S. & T. Curran, (1992) Identification and characterization of Ref-1, a nuclear-protein that facilitates Ap-1 DNA-binding activity. *Embo Journal* **11**: 653-665.

Yan, C., L. H. Lee & L. I. Davis, (1998) Crm1p mediates regulated nuclear export of a yeast AP-1-like transcription factor. *EMBO Journal* **17**: 7416-7429.

Yazdanparast, S. A. & R. C. Barton, (2006) Arthroconidia production in *Trichophyton rubrum* and a new ex vivo model of onychomycosis. *Journal of Medical Microbiology* **55**: 1577-1581.

Yin, W. B., S. Amaike, D. J. Wohlbach, A. P. Gasch, Y. M. Chiang, C. C. Wang, J. W. Bok, M. Rohlfs & N. P. Keller, (2012) An *Aspergillus nidulans* bZIP response

pathway hardwired for defensive secondary metabolism operates through aflR. *Molecular Microbiology* **83**: 1024-1034.

Young, C., M. K. Bryant, M. J. Christensen, B. A. Tapper, G. T. Bryan & B. Scott, (2005) Molecular cloning and genetic analysis of a symbiosis-expressed gene cluster for lolitrem biosynthesis from a mutualistic endophyte of perennial ryegrass. *Molecular Genetics and Genomics* **274**: 13-29.

Young, C., Y. Itoh, R. Johnson, I. Garthwaite, C. O. Miles, S. C. Munday-Finch & B. Scott, (1998) Paxilline-negative mutants of *Penicillium paxilli* generated by heterologous and homologous plasmid integration. *Current Genetics* **33**: 368-377.

Zadzinski, R., A. Fortuniak, T. Bilinski, M. Grey & G Bartosz, (1998) Menadione toxicity in *Saccharomyces cerevisiae* cells: activation by conjugation with glutathione. *Biochemistry and Molecular Biology International* **44**: 747-759.

Zhang, N., S. Zhang, S. Borchert, K. Richardson & J. Schmid, (2011) High levels of a fungal superoxide dismutase and increased concentration of a PR-10 plant protein in associations between the endophytic fungus *Neotyphodium lolii* and ryegrass. *Molecular Plant-Microbe Interactions* **24**: 984-992.

Zhang, W. J., Y. X. He, Z. Yang, J. Yu, Y. Chen & C. Z. Zhou, (2008) Crystal structure of glutathione-dependent phospholipid peroxidase Hyr1 from the yeast *Saccharomyces cerevisiae*. *Proteins* **73**: 1058-1062.

Zhang, Z. G., D. B. Collinge & H. Thordal-Christensen, (1995) Germin-like oxalate oxidase, a H_2O_2-producing enzyme, accumulates in barley attacked by the powdery mildew fungus. *Plant Journal* **8**: 139-145.

Znaidi, S., K. S. Barker, S. Weber, A. M. Alarco, T. T. Liu, G. Boucher, P. D. Rogers & M. Raymond, (2009) Identification of the *Candida albicans* Cap1p regulon. *Eukaryotic Cell* **8**: 806-820.

8 Appendices

8.1 Supplementary figures

Figure 8.1 pYES2

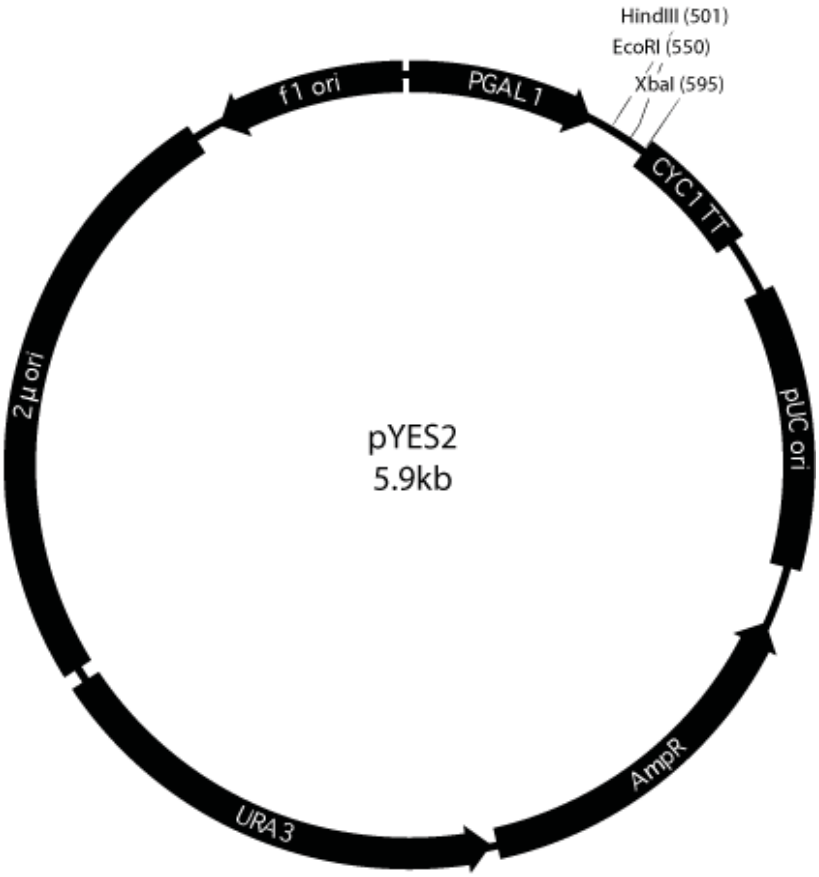

Figure 8.2 pGC5 *E. festucae gpxC*/pYES2

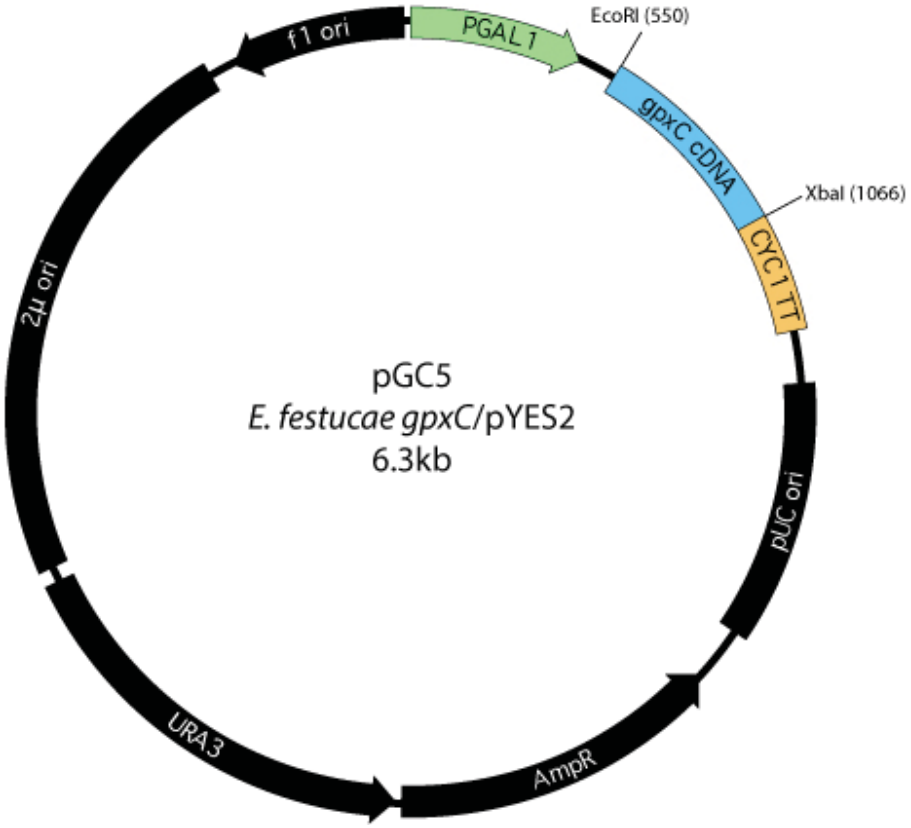

Figure 8.3 pGC6 *E. festucae yapA*/pYES2

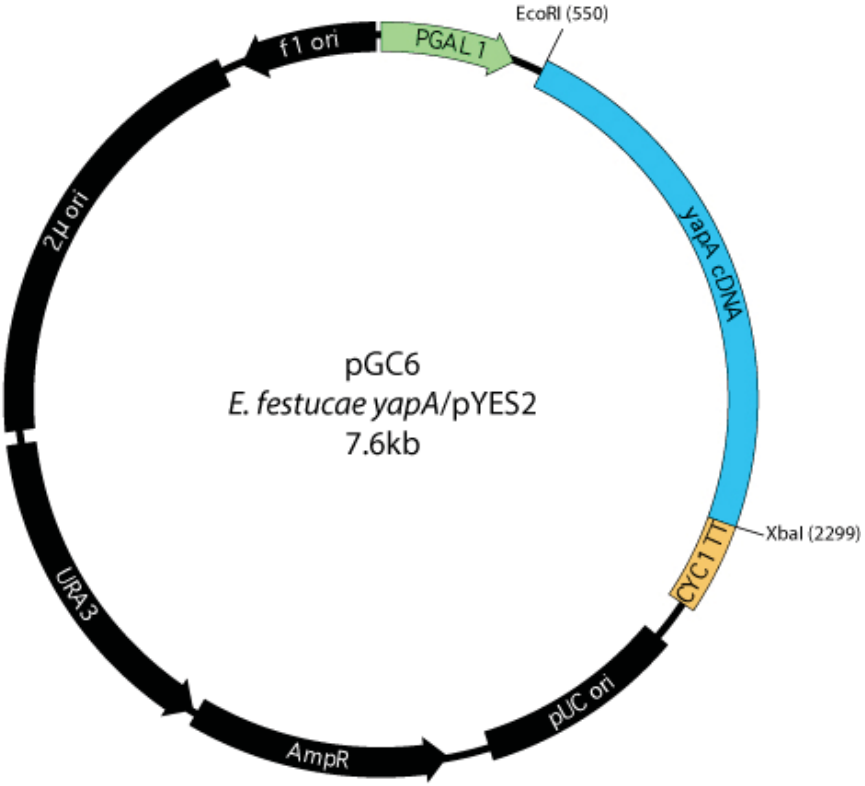

Figure 8.4 pGC7 *S. cerevisiae GPX3*/pYES2

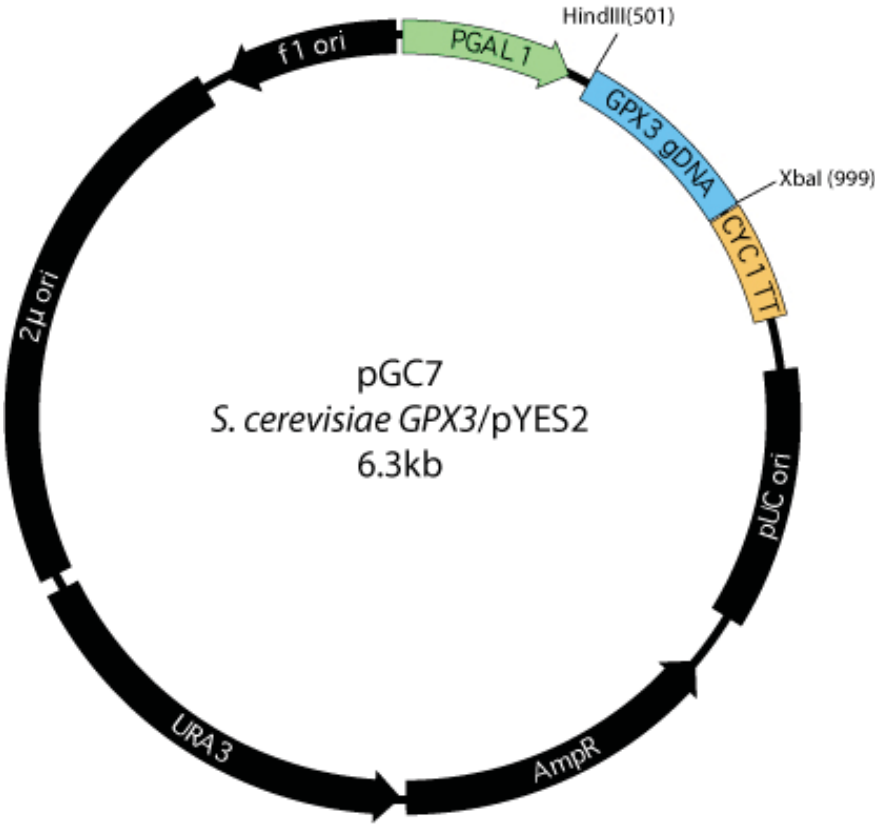

Figure 8.5 pGC8 *S. cerevisiae YAP1*/pYES2

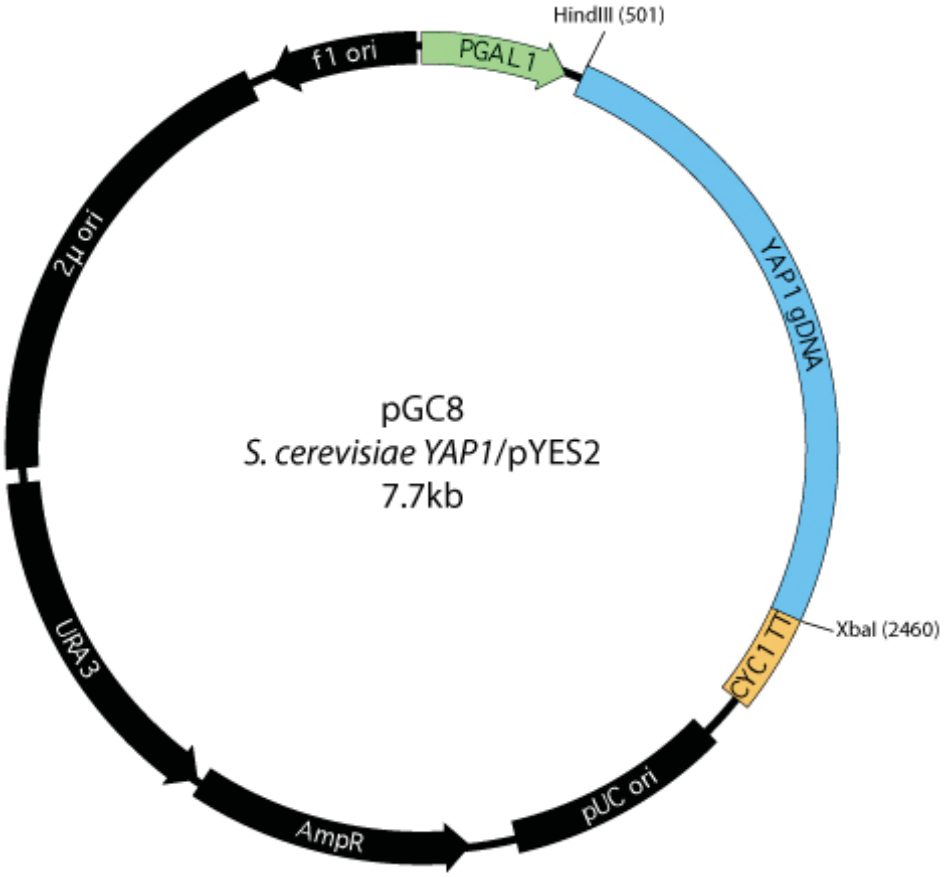

Figure 8.6 pSF15.15

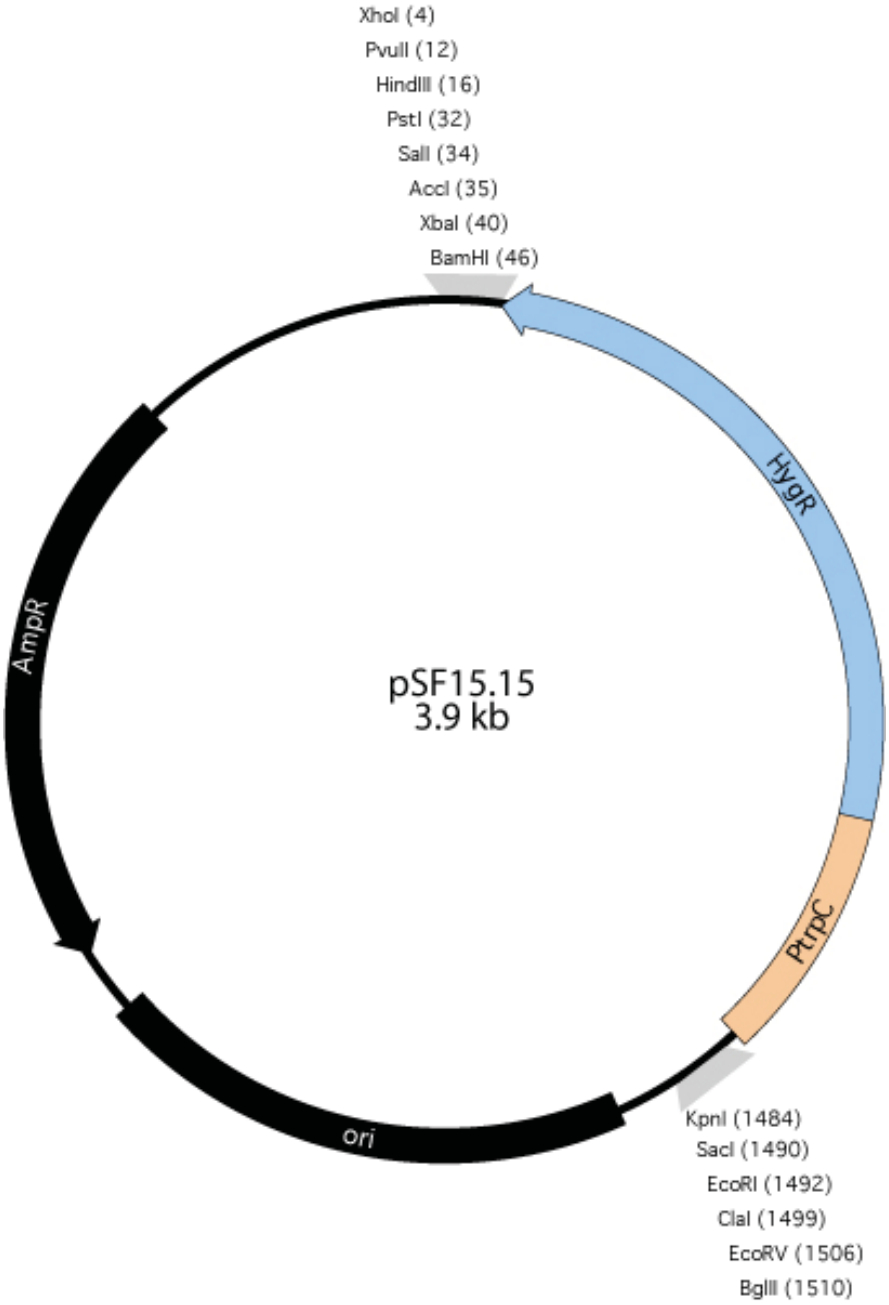

Figure 8.7 pGC2 *yapA* replacement construct

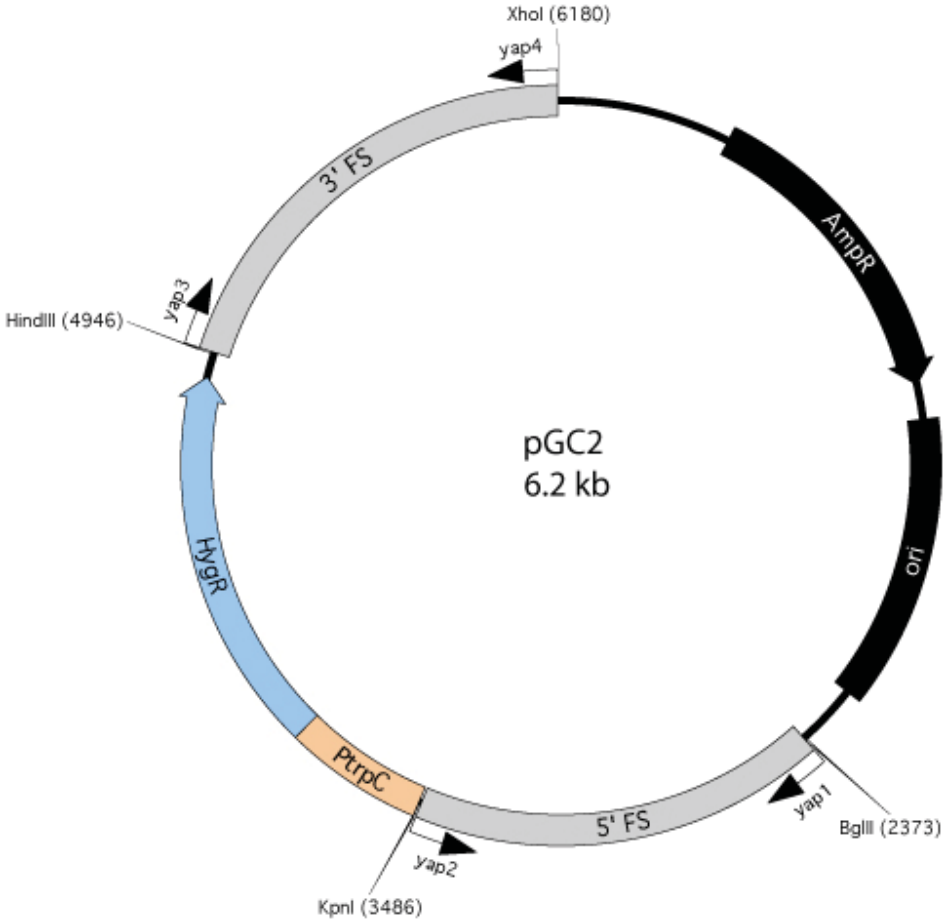

Figure 8.8 pSF17.8

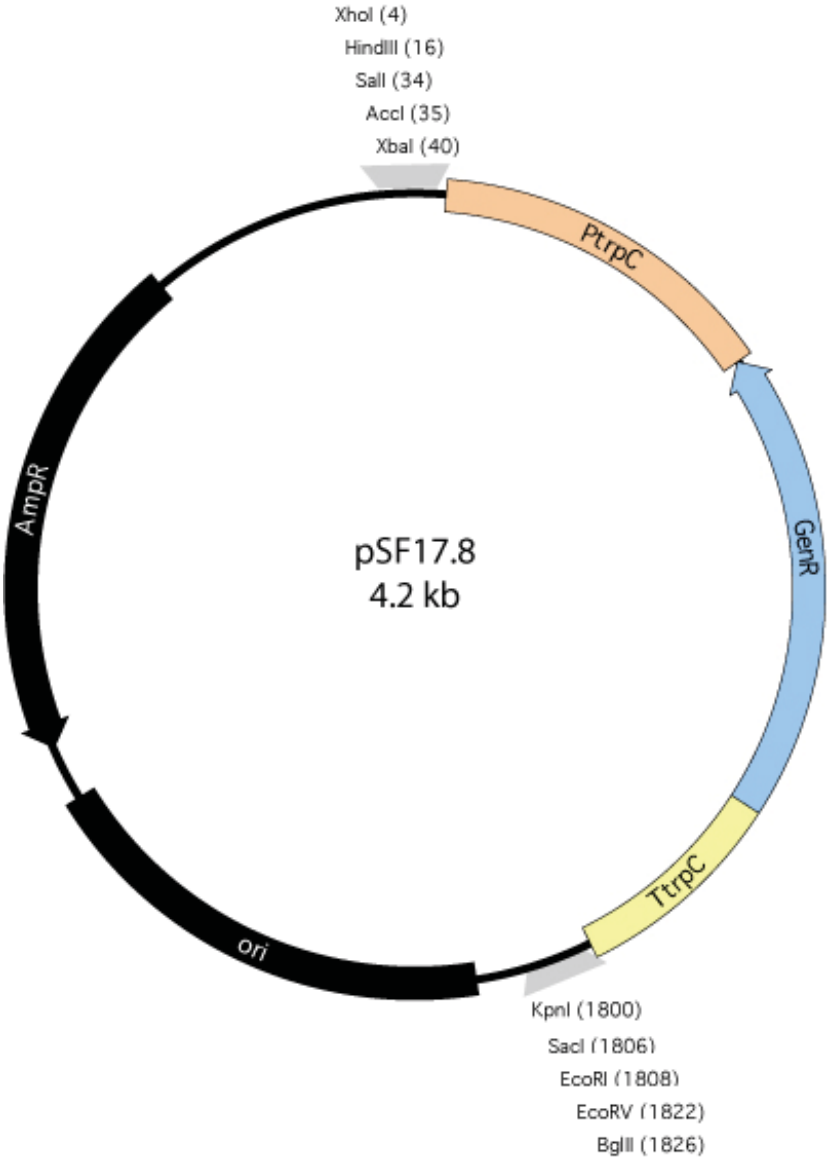

Figure 8.9 pGC4 *gpxC* replacement construct

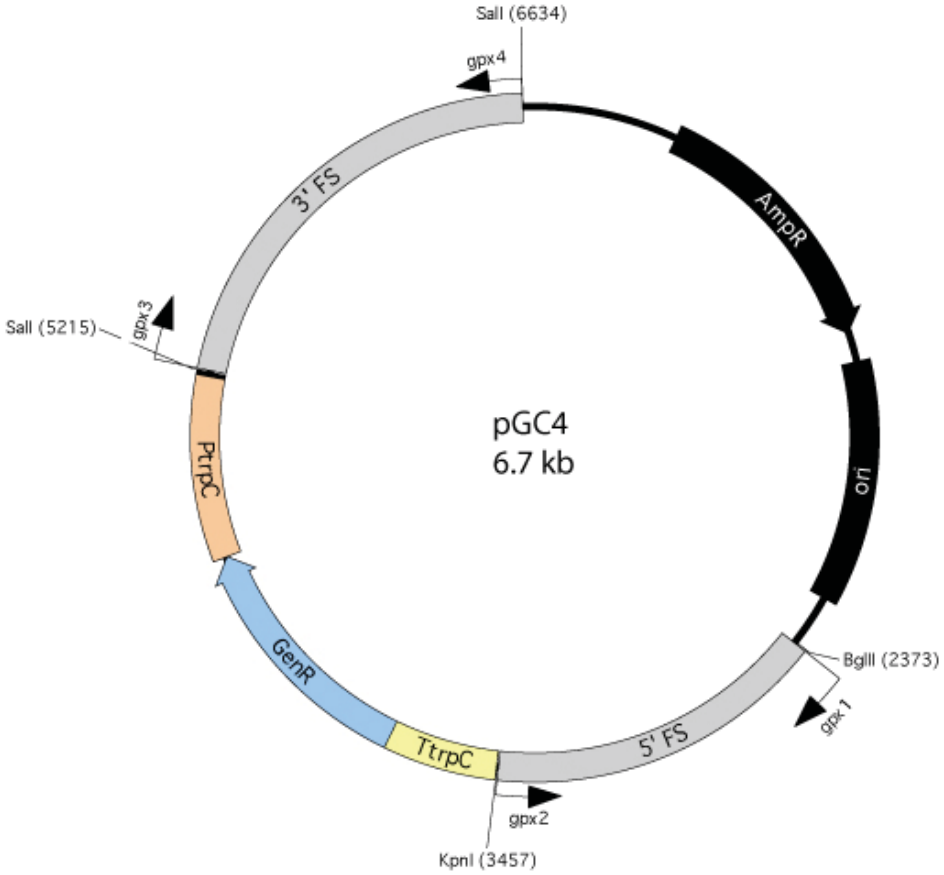

Figure 8.10 pGC12 *tpxA* replacement construct

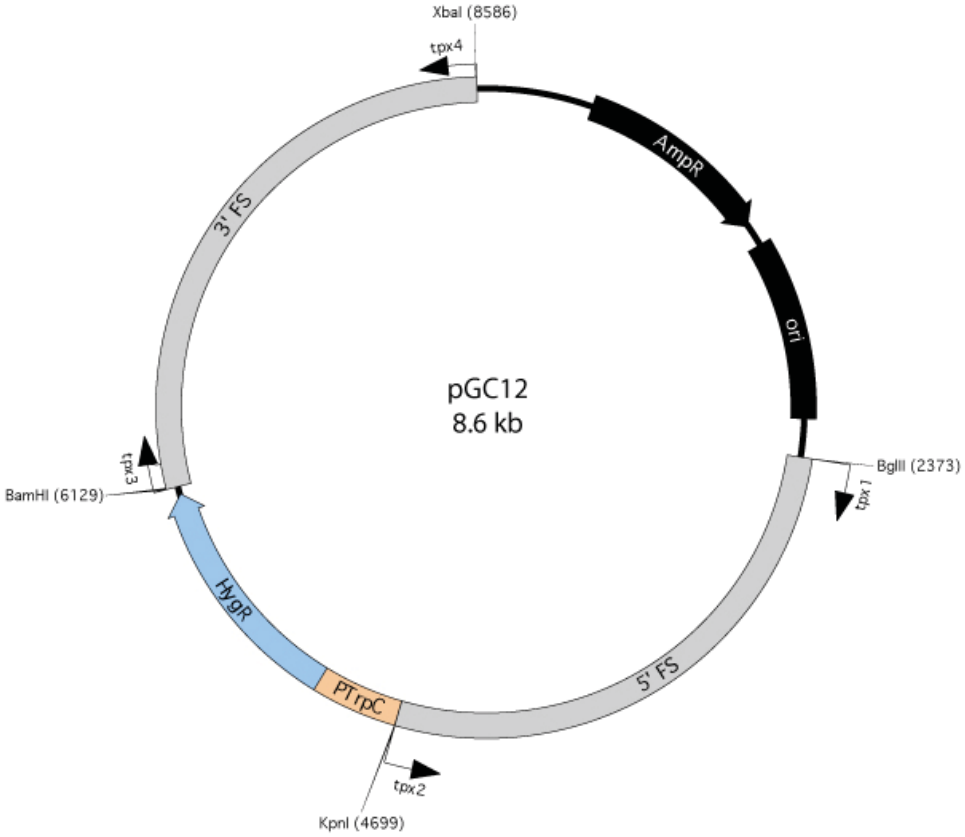

Figure 8.11 pPN94

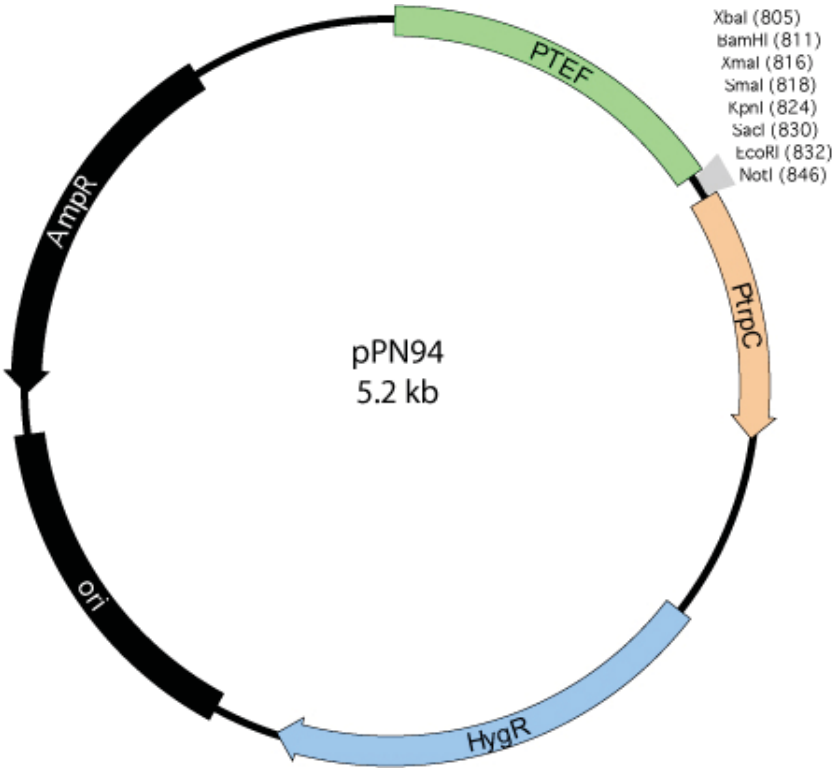

Figure 8.12 pGC9 *yapA-EGFP* fusion construct

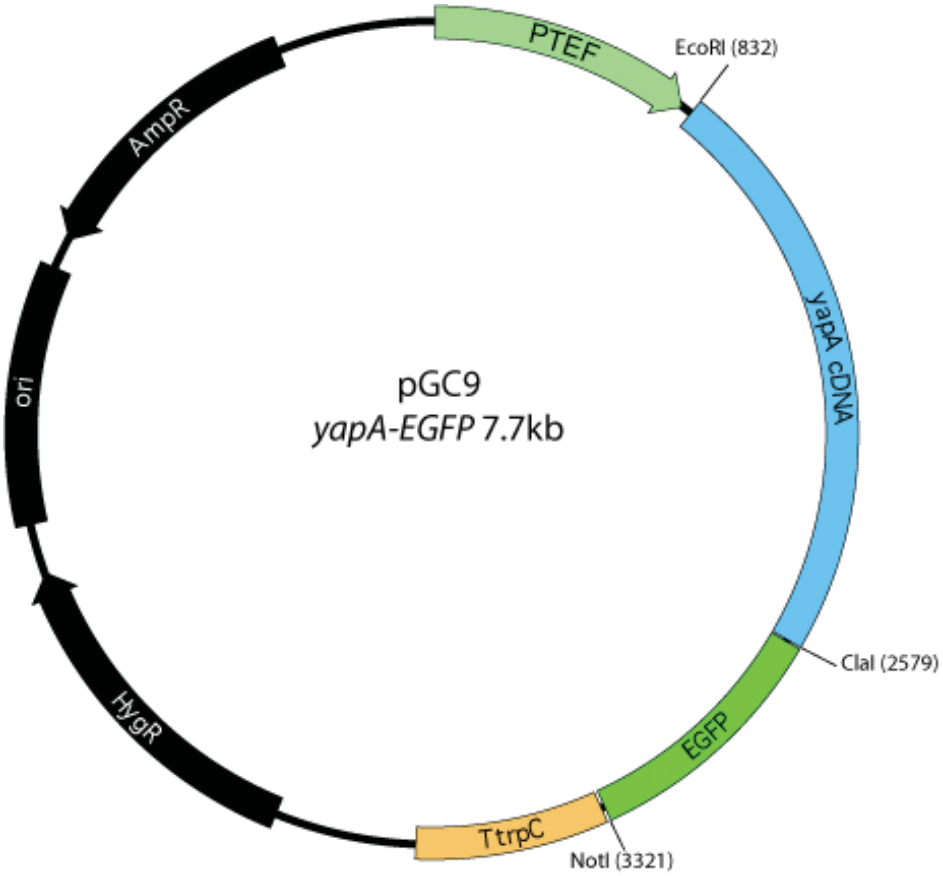

Figure 8.13 pGC10 *EGFP-yapA* fusion construct

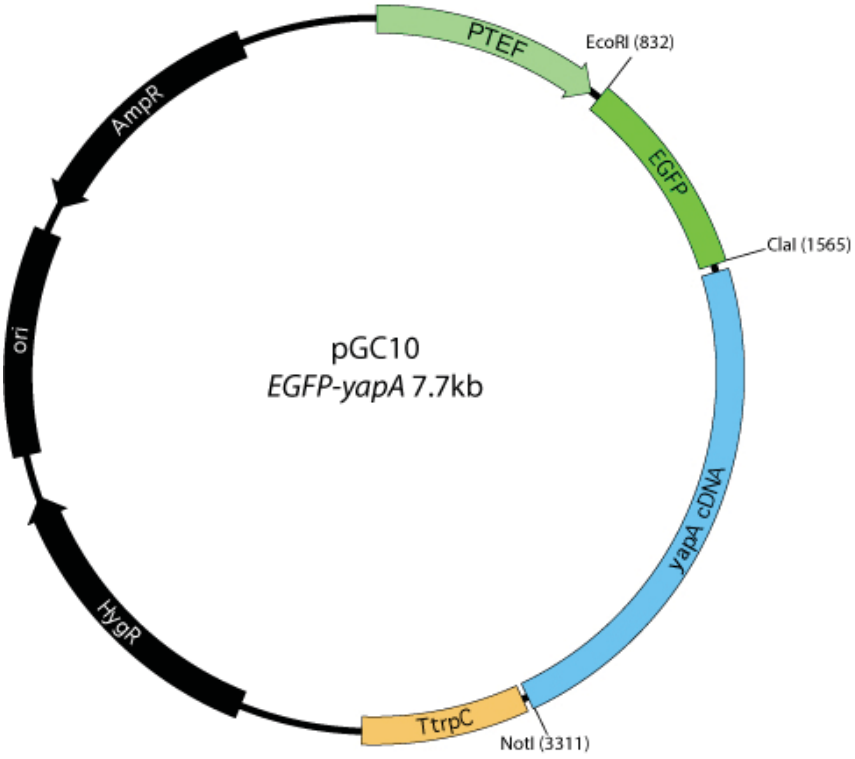

Figure 8.14 pGC18 Yap1-EGFP/pYES2 fusion construct

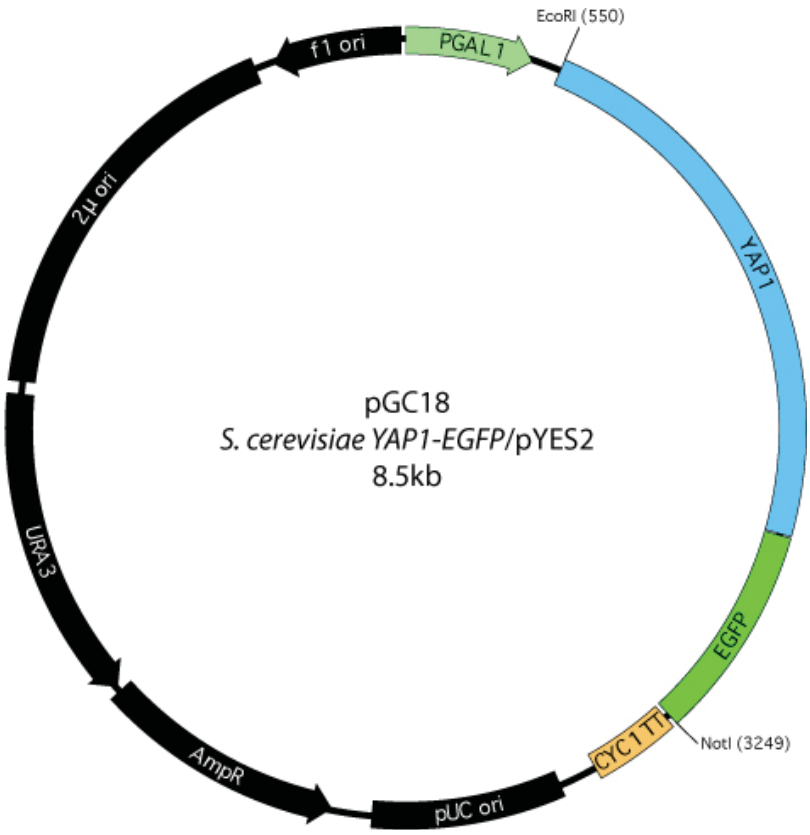

Figure 8.15 pGC19 Yap1-EGFP/pPN94 fusion construct

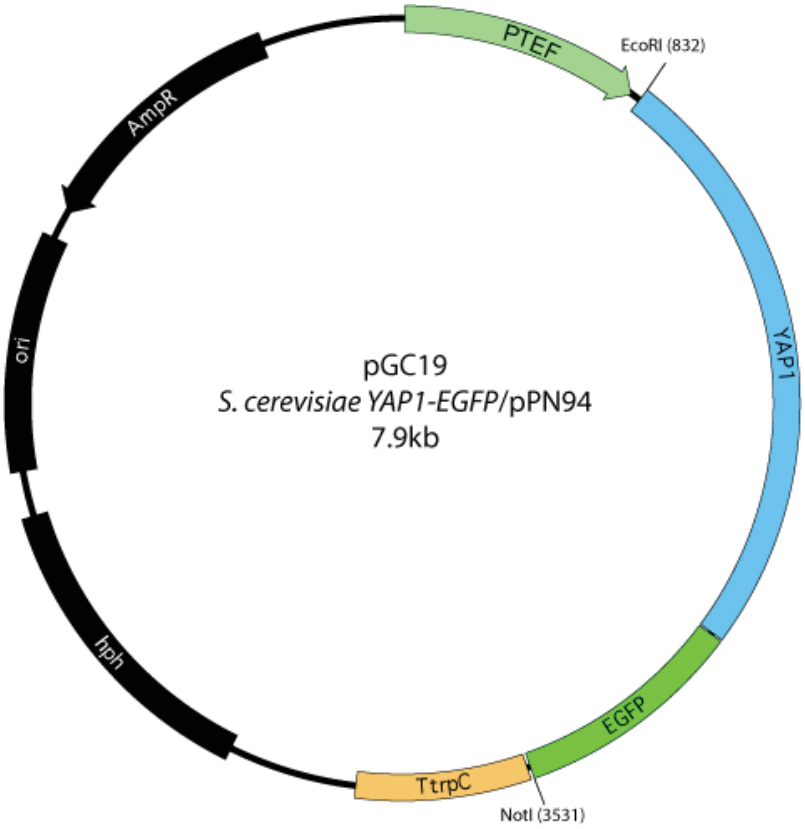

8.2 Supplementary tables

Table 8.1 YRE motif identification in *E. festucae* homologues of NcAp-1 targets.

N. crassa gene	*E. festucae* gene	Annotation	YRE Canonical	YRE Variant 1	YRE Variant 2
NCU00831	EfM2.021910	serine protease	No	No	No
NCU00847	EfM2.057370	7alpha-cephem-methoxylase P8 chain	No	TGACAAA	No
NCU00995	no homologue	hypothetical protein			
NCU01675	EfM2.049800	pre-rRNA processing protein	TTAGTAA	TTACAAA	No
NCU01720	contig 1071 A.2.318*	hypothetical protein	No	No	No
NCU02191	EfM2.025160	hypothetical protein	No	No	No
NCU02327	EfM2.066110	integral membrane protein	TTAGTTAA TTAGTAA	No	TGAGCTAA TGAGGAAA
NCU02627	EfM2.107250	integral membrane protein	No	TTACAAA TGACAAA	No
NCU02668	EfM2.077170	cell cycle regulation and aging protein	TTACCTAA TTATCTAA	No	No
NCU02904	EfM2.068040	hydrolase	No	No	TGAGGAAA TGAGCAAA TGACGAAA
NCU03355	no homologue	calpain			
NCU03776	EfM2.056890	multidrug resistance protein	TTATCTAA	No	No
NCU04109	EfM2.019890	glutathione s-transferase	TTACTAA	No	No
NCU04153	EfM2.090130	pseudouridine synthase	No	No	TGACTAA
NCU04197	EfM2.031850	hypothetical protein	No	No	No
NCU04236	EfM2.097870	hypothetical protein	No	No	No
NCU04452	EfM2.121350	NADPH2 dehydrogenase chain OYE2	TTAGTAA TTACTTAA TTATGTAA TTAGATAA	No	TGACCTAA
NCU04537	EfM2.114080	glucose transporter	No	No	No
NCU05079	EfM2.057180	peptide transport protein	No	No	No
NCU05134	no homologue	hypothetical protein			
NCU05164	EfM2.026760	protoporphyrin	No	No	TGAGGAAA

		ogen oxidase			
NCU05318	EfM2.092380	hypothetical protein	No	No	TGACGAAA TGAGAAA
NCU05319	contig 134 A.6.271*	hypothetical protein	No	No	TTAGCAAA
NCU05567	EfM2.026780	hypothetical protein	No	No	TGAGATAA
NCU05770	EfM2.069120	catalase	No	No	TGAGAAA
NCU05780	EfM2.013580	glutathione S-transferase	TTAGTAA	TTACAAA	No
NCU05826	EfM2.021200	hypothetical protein	No	No	No
NCU06323	no homologue	hypothetical protein			
NCU07017	EfM2.033390	hypothetical protein	TTACATAA TTACTAA	No	TTACTAAA
NCU07159	contig 1194 A.16.35*	endopeptidase K	No	No	TTACCAAA
NCU07200	EfM2.117480	metalloprotease MEP1	TTACTAA	No	No
NCU07452	EfM2.098650	flavin oxidoreductase	TTAGTAA	No	No
NCU07923	EfM2.080770	hypothetical protein	No	TTACAAA TGACAAA	TGACGAAA
NCU08188	no homologue	hypothetical protein			
NCU08229	EfM2.073820	hypothetical protein	TTACTAA	No	TTACTAAA
NCU08402	EfM2.055060	NADP-dependent alcohol dehydrogenase	No	No	No
NCU09040	EfM2.008340	reductase RED1	No	No	TGAGAAA TGACTAA
NCU09285	EfM2.067050	alcohol dehydrogenase	No	No	No
NCU09506	EfM2.057910	hypothetical protein	No	TTACAAA	TGAGATAA
NCU09507	no homologue	mutanase			
NCU09534	EfM2.018640	glutathione peroxidase	No	TTACAAA	No
NCU09774	no homologue	related to esterase D			
NCU09874	EfM2.083740	hypothetical protein	TTACATAA	No	No
NCU09992	EfM2.021910	hypothetical protein	No	No	TTAGAAA TTACTTAA
NCU10970	EfM2.110680	hypothetical protein	TTACTTAA	No	TTAGAAA

Homologues of NcAp-1-dependent, H_2O_2-responsive genes were identified in *E. festucae* (Tian *et al.*, 2011) and the promoters (1000 bp upstream of ATG start codon) examined for the presence of YRE motifs using the DNA Pattern Find analysis tool in the Sequence Manipulation Suite available at http://www.bioinformatics.org/sms2/dna_pattern.html. YRE Canonical (TTA(C/G)TAA, TTA(CG)(ATCG)TAA. YRE Variant 1 (TGACAAA, TGAGTAA, TTACAAA) experimentally confirmed by He & Fassler (2005). YRE Variant 2 (T(T/G)A(C/G)(A/T)AA, T(T/G)A(C/G)(C/G)(A/T)AA) not confirmed by He & Fassler (2005). * No M2 model available for FGenesh gene prediction.

Table 8.2 YRE motif identification in *E. festucae* control gene set.

***E. festucae* gene**	**Annotation**	**YRE Canonical**	**YRE Variant 1**	**YRE Variant 2**
EfM2.037020	adhesin protein Mad1	No	No	No
EfM2.037530	adhesin protein Mad2	No	No	No
EfM2.117690	ser/thr kinase	No	No	TTACCAAA
EfM2.069810	ser/thr kinase	No	No	No
EfM2.102240	ser/thr kinase	TTAGTAA TTAGTAA	No	TTAGTAAA TTAGTAAA
EfM2.111080	polysaccharide synthase	TTAGTAA TTACATAA TTACTTAA	No	No
EfM2.051660	phosphatidylinositol transfer protein	No	No	No
EfM2.012040	phosphatidylinositol transfer protein	No	No	No
EfM2.097180	cell wall protein	No	TTACAAA	No
EfM2.024830	unknown function	No	No	No
EfM2.091590	cystathionine beta-lyase	No	No	No
EfM2.065730	tetraspanin	No	No	No
EfM2.014640	ser/thr kinase	No	No	TGAGAAA
EfM2.047380	ser/thr kinase	No	No	No
EfM2.007460	ser/thr kinase	No	No	No
EfM2.089350	transcriptional corepressor	No	No	No
EfM2.051050	chromatin associated protein	No	No	TTAGAAA
EfM2.085040	putative transcriptional repressor	TTAGTAA TTAGTAA TTAGTAA TTACTTAA	No	TTAGAAA TTAGTAAA TTAGAAAA
EfM2.086340	non-ribosomal peptide synthetase	No	No	No
EfM2.092450	major facilitator superfamily transporter	No	No	No
EfM2.036990	Zn finger/ankyrin protein	No	No	No
EfM2.037030	Aspartic protease	No	TGACAAA	TGACTAA
EfM2.037040	Ankyrin repeat	No	No	TGACCAAA
EfM2.037500	3-isopropylmalate dehydrogenase	No	No	No
EfM2.037540	hypothetical protein	No	TGAGTAA	No
EfM2.037550	major facilitator superfamily protein	No	No	No
EfM2.110670	casein kinase 1	No	No	No
EfM2.110630	hypothetical protein	No	No	No
EfM2.069840	cyclin-like protein	No	No	No
EfM2.069830	NEFA-interacting nuclear protein NIP30	No	TTACAAA	No
EfM2.069820	mitochondrial import inner membrane translocase subunit	No	No	TGAGAAA TGAGAAAA

	tim-54			
EfM2.102270	FluG domain-containing protein	No	No	No
EfM2.102250	Multidrug resistance protein 1	No	No	No
EfM2.051630	hypothetical protein	No	No	No
EfM2.051650	dimethylaniline monooxygenase	No	No	TTACGAAA
EfM2.051680	hypothetical protein	No	No	TGAGAAA TGAGAAAA
EfM2.051710	RNA Helicase	No	No	TGAGATAA
EfM2.012030	hypothetical protein	No	No	No
EfM2.012050	endo/exonuclease/phosphata se family protein	TTACTAA	No	TGACTAA TGACTAA TGACTAA TTACTAAA
EfM2.012060	hypothetical protein	No	TTACAAA	TTAGAAA TTACGAAA
EfM2.012070	N-acetyltransferase	No	TTACAAA	No
EfM2.012080	duf1713 domain containing protein	No	No	No
EfM2.097160	hypothetical protein	No	No	TGAGGAAA
EfM2.097170	MFS transporter	No	TGACAAA	No
EfM2.107430	Cytochrome p450	No	No	TTAGCAAA
EfM2.107410	phosphorylcholine phosphatase	No	No	TGACGAAA TGACGAAA
EfM2.024850	pseudouridine synthase 3	No	No	No
EfM2.024840	phosphatidylinositol N-acetylglucosaminyltransferase	No	No	No
EfM2.091620	hypothetical protein	No	No	No
EfM2.091560	hypothetical protein	No	No	No
EfM2.091530	transducin family protein	No	No	No
EfM2.112380	MADS box protein	No	No	No
EfM2.065740	vacuolar ATP synthase subunit E	No	No	No
EfM2.014650	MSH3 protein	No	No	No
EfM2.014630	hypothetical protein	No	No	No
EfM2.014610	ThiF family protein	No	No	No
EfM2.047360	CAP1 capsule-associated protein	No	No	TGAGAAA
EfM2.007500	hypothetical protein	No	No	TGACTAA
EfM2.007470	WD repeat protein	No	No	TGACCTAA
EfM2.007450	GTPase	No	TGAGTAA TGACAAA	No
EfM2.007440	KH domain RNA-binding protein	No	No	TGAGGTAA
EfM2.089360	hypothetical protein	No	No	No
EfM2.089340	60S ribosomal protein L3	No	No	No
EfM2.089320	C6 transcription factor	No	TGACAAA	TGACAAAA
EfM2.051030	hypothetical protein	No	No	TGACTAA TTAGAAA

				TGACTAAA
EfM2.051060	hypothetical protein	TTAGGTAA	No	TGAGAAA
EfM2.051070	vacuolar amino acid transporter	TTACTAA TTACCTAA TTACATAA	No	No
EfM2.084980	hypothetical protein	No	No	No
EfM2.084950	small GTPase ypt1	No	No	No
EfM2.111060	NADP:D-xylose dehydrogenase)	No	No	TGACTAA TGACTAA TGACTAAA
EfM2.111070	FAD dependent oxidoreductase	No	No	No
EfM2.111090	hypothetical protein	TTAGGTAA TTAGCTAA	No	No

Promoters (1000 bp upstream of ATG start codon) of genes not previously shown to be YapA dependent or H_2O_2-responsive were examined for the presence of YRE motifs using the DNA Pattern Find analysis tool in the Sequence Manipulation Suite available at http://www.bioinformatics.org/sms2/dna_pattern.html. YRE Canonical (TTA(C/G)TAA, TTA(CG)(ATCG)TAA. YRE Variant 1 (TGACAAA, TGAGTAA, TTACAAA) experimentally confirmed by He & Fassler (2005). YRE Variant 2 (T(T/G)A(C/G)(A/T)AA, T(T/G)A(C/G)(C/G)(A/T)AA) not confirmed by He & Fassler (2005).

Table 8.3 YRE motif identification in putative YapA targets.

E. festucae gene	Annotation	YRE Canonical	YRE Variant 1	YRE Variant 2
EfM2.113210	thiol peroxidase	TTACCTAA TTAGATAA TTACTAA TTACTTAA TTACTAA	No	TTAGGAAA TGAGTTAA
EfM2.068360	thioredoxin 2	No	No	No
EfM2.109050	thioredoxin 1	No	TTACAAA	No
EfM2.077760	thioredoxin	No	No	No
EfM2.048560	glutathione reductase	No	No	TTACTTAA TTACTAAA TTAGGTAA
contig 455 A1.835*	CuZn-superoxide dismutase	No	No	No
EfM2.013840	Mn-superoxide dismutase	No	No	TGAGAAA
EfM2.083430	Mn-superoxide dismutase	No	No	No
EfM2.011370	superoxide dismutase copper chaperone	No	No	No
EfM2.015090	Fe-superoxide dismutase	TTACTTAA TTACTAA TTAGTAA TTAGTAA TTAGGTAA	No	TTAGAAA
EfM2.120580	CuZn superoxide dismutase	No	TGACAAA	No
EfM2.113330	CuZn superoxide dismutase	No	No	No

Putative YapA targets were selected based on homology to filamentous fungal proteins with functions in ROS detoxification and oxidative stress protection. The promoters (1000 bp upstream of ATG start codon) examined for the presence of YRE motifs using the DNA Pattern Find analysis tool in the Sequence Manipulation Suite available at http://www.bioinformatics.org/sms2/dna_pattern.html. YRE Canonical (TTA(C/G)TAA, TTA(CG)(ATCG)TAA. YRE Variant 1 (TGACAAA, TGAGTAA, TTACAAA) experimentally confirmed by He & Fassler (2005). YRE Variant 2 (T(T/G)A(C/G)(A/T)AA, T(T/G)A(C/G)(C/G)(A/T)AA) not confirmed by He & Fassler (2005). * No M2 model available for FGenesh gene prediction.